Syntheses and Characterizations of Cysteine-Derived Compounds and Polymers

By

Di Zhang

A thesis submitted to

the Faculty of Graduate Studies and Postdoctoral Affairs

in partial fulfillment of the requirements for the degree of

Doctor of Philosophy

Department of Chemistry

Carleton University

Ottawa, Ontario, Canada

April 2017

Table of Contents

Abstract

Driven by the increasing concerns on sustainability, environmental pollution and the advances in processing technology, research on new chemicals is gradually shifting from petroleum feedstock towards viable and renewable alternatives. L-cysteine is naturally abundant and has a great potential of becoming a valuable building block. In this thesis work, we intend to utilize the thiol group of L-cysteine in the thiol-ene click reaction or the reaction with aldehydes for functionalization. In addition, dimerization through the amino-acid group of L-cysteine leads to the formation of diketopiperazines (DKP). The structurally rigid DKPs are a class of naturally occurring cyclic amino acids and are explored as a new cyclic building block for various functional compounds and polymers is this thesis research.

The thesis outlines several synthetic routes to multifunctional compounds and polymers derived from L-cysteine. First, a series of cysteine-based DKP and DKP-containing polymers were synthesized from S-alkylated compounds under mild conditions and in high yields. The chiroptical activity of the obtained diastereomers was detected and present great potential as a high-selective, sensitive sensor for sensing silver ion in aqua system. Next, a series of DKP-containing difunctional monomers were synthesized from 4-thiazolidinecarboxylic acid derivatives. Based on the type of imported functional group, DKP-containing polymers including polyesters and polycarbonates were produced with high molecular weights. Last, linear and star-shaped macromolecules containing L-cysteine at the chain ends were prepared. Their surface tension, pH-sensitivity and self-assembling behaviors were studied. In addition, cyclodextrins and polysaccharides were functionalized with L-cysteine and their potential uses for detection and separation of chiral acids were investigated.

Acknowledgement

It is my great pleasure to express my deepest gratitude to the following people who helped me during my doctor study and made this thesis possible:

First of all, I would like to thank my supervisor Dr. Wayne Wang, for his guidance, patience, encouragement and motivation.

I would like to thank Dr. Jane Gao for her invaluable advices and guidance in lab, as well as help in daily life.

I would also like to thank all my colleagues: Duo Li, Wendy Hao, Saif Mia, Khama Rani Ghosh, Sukanta Kumar Saha, Yasaman Aghili, Luck Farmer, Haoyang Yu, Mirvat Sanaallah for their friendship and assistance.

To Jim Logan, Tony O'Neill, Keith Burke, Elena Montana, and Chantelle Gravelle: I would like to thank everyone for supporting instrument technology and guidance.

Finally, I would like to dedicate this thesis to my parents, who have raised me and give my endless love, and to my beloved husband, for his understanding and support in my study at Carleton University.

List of Figures

List of Schemes

List of Tables

List of Symbols and Abbreviations

Ala-Ala	Cyclic alanine
AIBN	2,2′-Azobis(2-methylpropionitrile)
BP	Benzophenone
BPA	Bisphenol A
CAC	Critical aggregate concentration
CD	Circular dichroism
ß-CD	ß–cylcodextrin
CDI	1,1'-carbonyldiimidazole
Cys-Cys	Cyclic cysteine
DCC	Dicyclohexylcarbodiimide
DIC	Diisopropylcarbodiimide
DIEA	*N*, *N*-diisopropylethylamine
DKP	Diketopiperazine
DMF	Dimethylformamide
DMPA	Dimethoxyphenylacetophenone
DPPA	Diphenylphosphoryl azide
GLC	Gas liquid chromatography
Gly-Gly	Cyclic glycine
GPC	Gel permeation chromatography
HBTU	O-benzotriazol-1-yl-tetramethyluronium
His-His	Cyclic histidine
IR	Infrared spectroscopy
Leu-Leu	Cyclic leucine
Lys-Lys	Cyclic lysince

MMA	Methyl methacrylate
NMP	N-methyl-2-pyrrolidone
NMR	Nuclear magnetic resonance
NOE	Nuclear Overhauser effect
PB	Polybutadiene
PBD-b-PEO	Polybutadiene-block-poly (ethylene oxide)
PC	Polycarbonate
PE	Polyester
PEG	Poly (ethylene glycol)
PDI	Polydispersity indices
PTMEG	Poly (tetrametheylene glycol)
TCA	4-Thiazolidinecarboxylic acid
TEC	Thiol-ene click
UV	Ultraviolet-visible
Val-Val	Cyclic valine

Chapter 1 Introduction

1.1 Green Chemistry

Organic chemicals play an important role in our daily lives. With the ultrafast and dramatic expansion of the organic world, the design of new chemicals in laboratory research has become increasingly "fancy", with rare starting materials, unusual catalysts, complex instruments and harsh experimental conditions. However, issues related to low reaction efficiency, high energy costs, the utilization of toxic reagents and the production of hazardous compounds, have been overlooked to some extent.[1] In fact, not only on the laboratory scale, the chemical industry also has these problems, which have led to severe threats to economic and social developments such as the greenhouse effect, the contamination of drinking water and the accumulation of chemical waste in landfills, especially the overexploitation of petroleum feedstock.[2,3] Fossil oil is the main material resource for chemical production, but it takes thousands of years to form and the regeneration amount lags far behind our needs. If this consumption continues at the current growth rate, it is estimated to run out by 2050.[4] All of these concerns in chemistry development are prompting researchers to develop a long-term, sustainable and environmentally friendly organic industry.[5,6]

In 1987, The World Commission for Environment and Development published a report, *Our Common Future.* In this report, scientists not only pointed out the problems during the process of chemical production, but also put forward many valuable suggestions. They strongly appealed to "meet the needs of the present without compromising the ability of future generations to meet their own needs".[7] In that case, the term "Green Chemistry" was then introduced by Anastas and his colleagues from the U.S. Environmental Protection Agency at the beginning of the 20th century.[8] Although it was the first time that this important part of modern chemistry was defined with a fixed and unified name, there were many previous studies that could also be described as being within the green chemistry realm.[1] The purpose of setting

up this chemistry branch is definitely meant to attract the world's attention and to ensure stable and sustainable progress on a world scale.

The key points of green chemistry include high reaction and atom efficiency, harmless and non-toxic chemical involvement, innocuous solvents or water, potentially degradable products, derivation prevention, *etc*.[9] Recently, Poliakoff et *al.* condensed the rules into 12 phrases, abbreviated to "PRODUCTIVELY, where P – Prevent wastes; R – Renewable materials; O – Omit derivatization steps; D – Degradable chemical products; U – Use of safe synthetic methods; C – Catalytic reagents; T – Temperature, Pressure ambient; I – In-Process monitoring; V – Very few auxiliary substrates; E – E-factor, maximize feed in product; L – Low toxicity of chemical products; Y – Yes, it is safe."[10] These 12 principles not only mention the adoption of renewable resources, but also emphasize the utilization of sustainable synthetic approaches to avoid hazardous substances, to use mild and eco-friendly conditions, to reduce the derivatization steps and to get rid of the catalyst involvements. Based on the numerous reviews on biopolymers presently, it is obvious that the green synthetic approaches are well under development and have already been applied to industrial synthesis, for example, neat reaction.[11,12] Neat reaction refers to the solvent-free condition and is a desired alternative to replace conventional solution reactions to minimize solvent wastes and reduce solvent expenses.

Today, the green concept has already received widespread attention and becomes one of the main tendency of current chemistry research. There is no doubt that, these rules have a profound impact both on chemical circles and on the chemical commodity industry. In conclusion, the dissemination and implementation of the green concept is our responsibility and objective towards the future.

1.2 Biomass

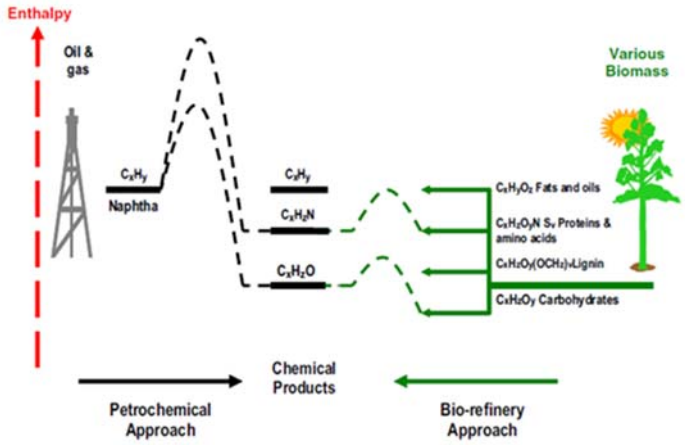

Figure 1.1 The use of biomass as an energy-efficient raw material. (Adapted from ref. 13)

Driven by the increasing concerns for sustainability, environmental pollution and the advances in processing technology, research on materials has been gradually shifted from petroleum feedstock towards viable and renewable alternatives, biomass (Fig. 1.1).[13-15] Biomass is the matter that has living organism origins, which could be derived from agricultural crops and forestry, from aquatic plants and microorganisms, and even from municipal waste.[16] As shown in Fig. 1.2, biomass-derived monomers have four categories according to the molar ratio of C/O.[17] The annual global production of biomass was estimated to exceed 150 trillion kilograms. However, the utilization rate is only 3.5%, while 5% of those are consumed for non-food purposes.[18] Definitely, there is huge potential for bio-based feedstock to share markets with their fossil counterparts.

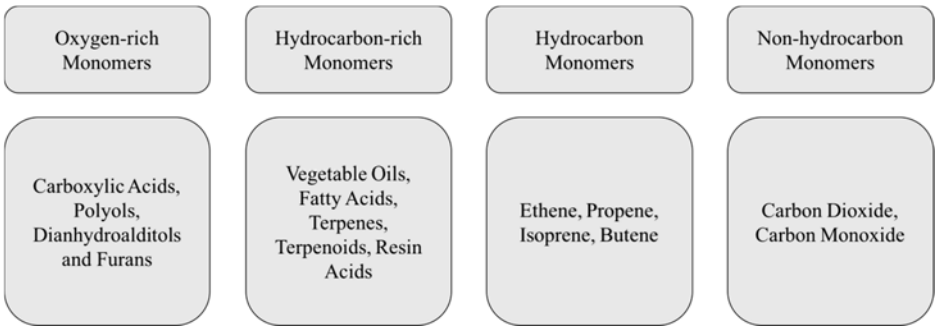

Figure 1.2 Four categories of biomass derived monomers.[17]

Indeed, biomass is sufficient to provide monomers and polymers that have the same structures or functions as that petroleum-derived counterparts.[19] Polyesters, for example, are definitely the most promising polymer family using biomass-based monomers, which are attributes to their extensive polymer properties for various applications, biodegradability and potential biocompatibility (Scheme 1.1). Furthermore, the biomass building blocks for polyesters are relatively easily accessible and inexpensive, from small molecules such as vegetable oil-based polyols and sugar-based diacids, to macromolecules such as poly(ethylene glycol) (PEG) and poly(tetrametheylene ether glycol) (PTMEG).[20-23] It has been reported that the production of green plastics was growing rapidly from less than 300,000 metric tons in 2009 to more than 1.0 million metric tons in 2011. Currently, several companies are commercializing biodegradable or partially renewable-based aromatic polyesters, such as, poly(ethylene terephthalate) which is composed of 30% plant-based material and poly(ethylene furanoate), and 100% natural poly(lactic acid) from the CornFlower.[23]

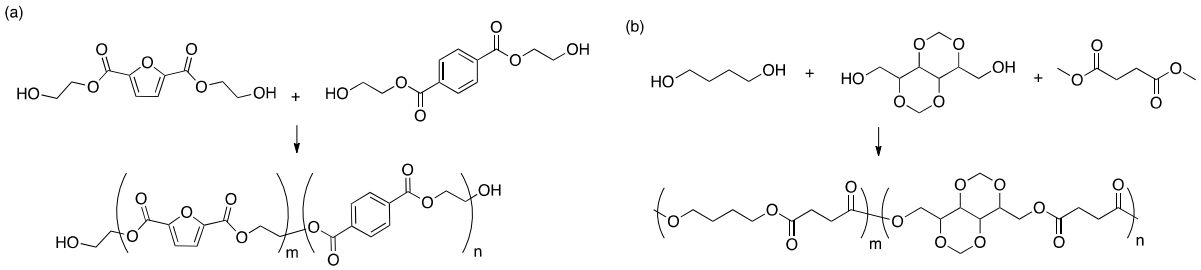

Scheme 1.1 Syntheses of renewable (a) aromatic polyester and (b) aliphatic polyester.[21,22]

Biomass is readily transformed to biofuels and raw chemicals through three pathways: thermo-chemical conversion, biological conversion and direct extraction.[24] The chemical route is conducted under high temperature and pressure with the assistance of a catalyst. However, the terrible side effects, low efficiency, significant volume of waste and the use of corrosive chemicals, are urging scientists to seek new techniques to solve these problems. Biological conversions refer to the fermentation processes that uses the biological enzymes or living

organisms to achieve the transformation of biomass. Due to its high yield and selectivity, it has been the most promising technique so far and attracts the most scientists' attention.[24] Many chemicals have been successfully made through yeast and bacterial fermentation processes and launched to market, for example, L-cysteine.[19,25,26] Indeed, the biological conversion is still at the early stage of its development. With great efforts devoted in future years, the process will become more efficient and more reliable. Compared to the thermal and biological route, direct extraction is cost-optimal without complicated operations and fewer chemicals are involved in the process.[27,28] For example, it is reported that vanillin could be selectively extracted with specific sorbents from various solutions.[24] With the rapid development of biorefinery, more and more chemicals are added to the biomass category. To promote the utilization of the biomass in practical production, in 2004, the U.S. Department of Energy selected 12 top value added biomass feedstock from more than 300 candidates. They are four carbon 1,4 diacids (succinic, fumaric and malic acids), 2,5-furan dicarboxylic acid, 3-hydroxy propionic acid, aspartic acid, glucaric acid, glutamic acid, itaconic acid, levulinic acid, glycerol, sorbitol, 3-hydroxybutyrolactone, xylitol/arabinitol. These compounds not only can be easily transformed from sugars but also convert to a variety of secondary chemicals or family derivatives.[29,30]

Protein is the primary component of cells and exists in nature in a variety of forms. With a relative high concentration of protein content in plants and animals, it is definitely a promising biomass resource (Table 1.1).[31] Some bio-based proteins have already been commercially available with a long history, including wheat proteins, soy proteins and milk proteins.[31] Complete protein refinery is required to get desirable platform chemicals from biomass feedstock. The first step is isolation and hydrolysis of the proteins into mixtures of amino acids. This is the fundamental step and conventionally achieved through chemical hydrolysis under acid or alkaline conditions.[34] For example, at 100^{o} C, 5N HCl/NaOH for 24 hours.[31] However, it is difficult to isolate the amino acids from the inorganic salt wastes and

some of the amino acids may decompose under such conditions. Thus, a mild and efficient alternative route is preferred through enzymatically treating with proteases.[34] Hydrolysis of the biomass substrates lead to a mixture of amino acids. To separate them individually, different techniques, including reactive extraction, electrodialysis and ion-exchange chromatography can be used. Finally, the purified amino acid can be converted to its desired structures for further usage.[31]

Table 1.1 Protein contents in different feedstocks.[31-33]

Feedstock	Protein content (%)	Feedstock	Protein content (%)
Microalgae	47	Sunflower	22.9
Soybean	40	Rice hull	2.3
Rapeseed	26.2	Rice straw	4.7

Amino acid is the basic element to construct proteins and plays an important role in physiological activities. Besides building up proteins and enzymes, amino acids also anticipate in a variety of biological activities as an energy source or intermediate in metabolic pathways, for example, in the biosynthesis of the neurotransmitter.[35,36] Thanks to its wide application in pharmaceutical, animal feed and the food industry, the extraction of amino acids from protein rich biomass has attracted great attention (Table 1.2).[37] It has been estimated that if 10% of transportation fuels were substituted by biofuels, it could generate 100 million tons of protein on an annual basis world wide. With around a 50% conversion rate, approximately 50 million tons of amino acid can be obtained.[38,39] Because only nine amino acids (lysine, leucine, isoleucine, threonine, methionine, histidine, tryptophan, phenylalanine, and valine) are used in the regular feed industry, the abundant production of amino acids could be used not only to meet the amino acids demand for human beings, but also supply rich crude materials for the chemical industry.[34,39]

Table 1.2 Amino acid compositions extracted from leaf protein (mg/g).[37]

Lysine	26.5	Glutamic acid	90.8
Histidine	11.2	Proline	9.2
Arginine	58.3	Glycine	19.9
Aspartic acid	4.1	Alanine	33.4
Threonine	17.2	Cysteine	6.4
Serine	23.2	Valine	24.8

1.3 L-Cysteine

L-cysteine with the formula $HO_2CCH(NH_2)CH_2SH$, is a unique amino acid among the 20 basic amino acids, as it contains both the amino acid group (-COOH and $–NH_2$) and the reactive thiol group (-SH). L-cysteine is a non-essential amino acid and its metabolism circle of cysteine is well defined. It can be synthesized from methionine in the human liver under normal physiological conditions or converted from serine in bacteria or plants.[40] In the cysteine industry, it is conventionally derived from the hydrolysis of poultry feathers or human hair, by boiling these substances with concentrated acid or base, followed by electrolysis. However, it requires huge energy consumption and noxious wastes are produced during the manufacturing process. Thus, the current method of preparation of L-cysteine is gradually being replaced by microbial fermentation of Escherichia coli.[41] L-cysteine is widely used in food, cosmetics and pharmaceutical products, as a common dough conditioner for breaking down gluten for bakery goods, as flavor enhancers and a precursor in some dietary supplements, as a radical scavenger in cosmetics, and as an expectorant in cough medicines.[41-45] It was reported that the global consumption for L-cysteine reached 12,000 t/year in 2012 and would increase at a fast rate.[44] Moreover, Wacker company recently released a statement on a larger-scale fermentation plant acquisition to meet the global demand.[45] It is clear that the importance of L-cysteine as a desirable biomass is being gradually recognized.

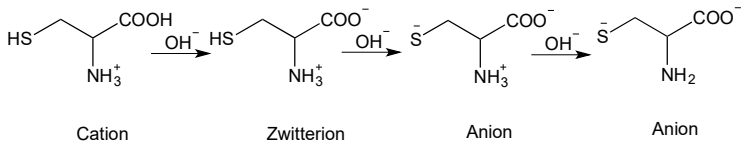

Figure 1.3 Various forms of L-cysteine under different pH values.

Like other amino acids, L-cysteine is an amphoteric compound, which can either function as an acid or a base in solution. As shown in Fig. 1.3, under acidic conditions, L-cysteine exists in cationic form. As the pH increases, the carboxylic acid releases its proton first to neutralize OH^-. When the environment pH reaches a certain point, which is defined as the isoelectric point, L-cysteine exists in its zwitterionic form and the molecule contains both negative and positive charges, but without a net charge. The isoelectric point of L-cysteine is reported around 5.05.[46] Moreover, if the pH keeps increasing, the thiol group will be gradually deprotonated and finally, L-cysteine with two negative charges becomes an anion. More and more researches on the utilization of L-cysteine zwitterion for surface modifications were reported in recent years.[47] For example, Huang and co-workers used a zwitterionic L-cysteine derivative in nanoshell modifications. The obtained material not only displayed good antifouling properties, but also contained better colloidal stability and photothermal stability at high temperature.[47]

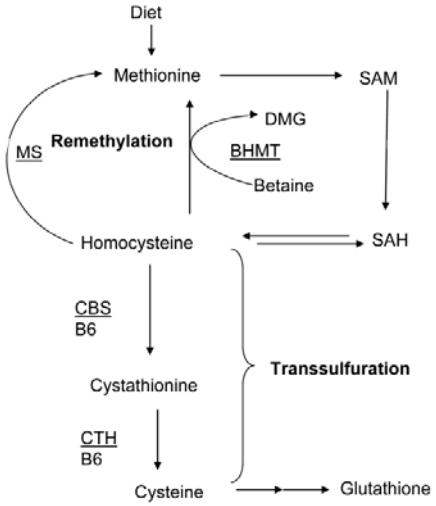

Figure 1.4 A path from protein-rich diet to cysteine.

L-cysteine could be taken from protein-rich foods and serves an important role in biological functions, which is mainly based on the nucleophilicity and redox activity of the thiol functional group (Fig. 1.4).[48] It is known that in cysteine, the S atom is at the oxidation state of -2. With a unique electron configuration, thiol is able to be oxidized with oxidation states ranging from -2 to +6. It was reported by Reddie and co-workers that cysteine had 10 different biological transformations in the human body and each of these states has their own stability, redox-behavior, nucleophilicity, and catalytic activity for different physiological functions.[49] For example, due to the ability of thiol to undergo redox reactions, cysteine has antioxidant property in the glutathione serving as a proton donor. Moreover, cysteine is the rate-limiting factor in cellular glutathione biosynthesis, which is capable of preventing damage to important cellular components caused by reactive oxygen species. Besides, the disulfide form is another important form with high physiological reactivity, which is easily formed through the oxidization of thiol group. Since the sulfide bond is a quite stable bond, it plays an important part in protein folding behavior and the maintenance of the protein framework. Meanwhile, because the S–S bond is susceptible to breaking up through reduction reactions or thiol-disulfide exchange, disulfide is readily to return back to the thiol format in the reducing cellular compartments for further applications (Scheme 1.2).[49-51]

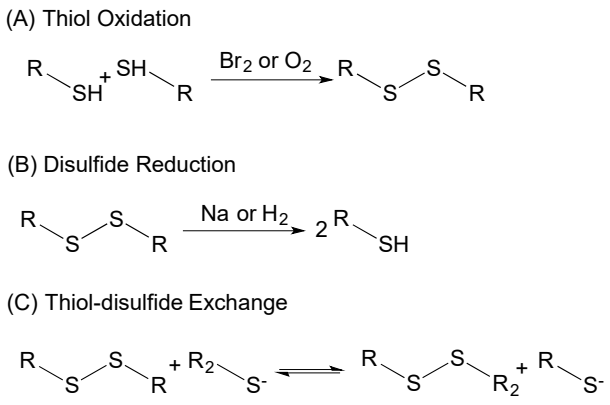

Scheme 1.2 Thiol related oxidation, reduction and thiol-disulfide exchange reactions.

Thiol oxidation-reduction reaction and thiol-disulfide exchange reaction are not only important for the normal maintenance of body metabolism, but also for the foundation of L-cysteine applications in the commodity market. For example, in bakery applications, the sulfhydryl groups tear apart the disulfide bonds of gluten which gives dough its softness.[44] In the laboratory, many oxidants can promote thiol oxidation, including air, iodine, bromine, singlet oxygen, and hydrogen peroxide. On the other hand, the reduction of disulfide could be promoted in the presence of hydride agents, for example, NaH, and alkali metals, as well as a reducing reagent, for example, H_2 (Scheme 1.2).[52,53]

L-cysteine containing the elements N, O, S can readily form the chelating complexes with silver, lead, copper and other metal ions. The formed metal–amino acid complex plays important roles in physiological activities, for example, forming alcohol dehydrogenase with Zn^{2+}.[54] In addition, the thiol group also has a high affinity for heavy metals such as Hg and Pd, which in turn, can improve the biochemical lesion causing the unusual high level of metal ions.[55] Owing to its metal chelating ability combined with its chiral feature, cysteine has been widely used in the design of chiroptical sensors. For example, Carney and co-workers reported the synthesis and utilization of (*R*)-*N*, *N*-bis(2-quinolylmethyl)-*S*-methyl cysteine as a chiroptical sensor (Fig. 1.5). Since it showed different chelating abilities with Hg^{2+} and gave a unique optical signal in circular dichroism (CD) measurements, it was capable being used as a chiroptical sensor with high selectivity for Hg^{2+}.[56] Another example is given by Nan and co-workers, where they found that with the addition of Hg^{2+}, the CD signal of an Ag-L-cysteine nanoparticle was completely changed due to the extraordinary chelating ability of L-cysteine with Hg^{2+} and the displacement of Ag^{+} in the chiral nanoparticles by Hg^{2+} (Fig 1.5).[57]

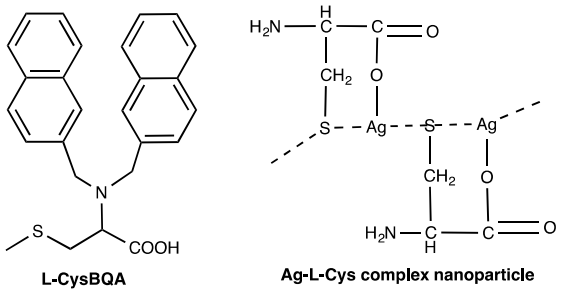

Figure 1.5 Examples of chiroptical sensors inspired by L-cysteine chiropitical property.[56,57]

L-cysteine with amino acid functional groups can anticipate in amino acid-related reactions, such as amide formation, esterification and alkylation. But most of the chemical information is concentrated on the reactivity of the thiol group, which can participate in thiol-click reactions. Since thiol-click reaction is widely used in molecular functionalization, L-cysteine is treated as an ideal graft molecule for molecular modifications. Moreover, by importing L-cysteine into molecule structures, the obtained compounds are granted with new properties, such as chiroptical property and self-assembling ability. For example, Geng et al. reported the successful modification of polybutadiene-block-poly (ethylene oxide) (PBD-b-PEO) block copolymers through the addition of cysteine derivatives on PBD segments and obtained an amphiphilic polymer with great self-assembling property, which was also able to tune the shape according to the hydrophobic–hydrophilic ratios in the structure as a smart polymer (Fig. 1.6). Furthermore, attributed to the hydrogen-bonding and chiral interactions from cysteine, a helical superstructure was observed in CD measurement (Fig. 1.6).[58] Another example is demonstrated by Passaglia and Donati. They reported the successful functionalization of styrene and butadiene random copolymers by L-cysteine ethyl esters and the grafted polymer was potentially optical active with chiral centers on side chains.[59]

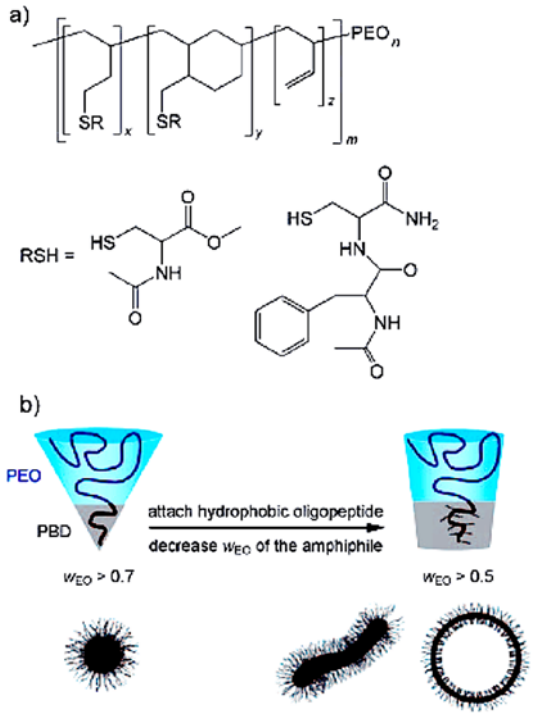

Figure 1.6 (a) PBD-b-PEO modified with cysteine derivatives; b) morphological changes of amphiphilic polymer. (Adapted from Ref. 58)

Amino acid is widely regarded as a valuable building block for the preparation of biodegradable or biocompatible materials with interesting properties. However, besides the molecular functionalization, cysteine is rarely directly used in material preparations, which is limited by the excess activity of its thiol group in most organic reactions that involves high temperatures and oxidative reagents. Therefore, the utilization of L-cysteine normally goes through complicated protection and deprotection procedures. For example, Fu and co-workers reported the synthesis of a poly (L-cysteine) containing material and the obtained polymer not only displayed reversible thermal-responsive property in water, but also was capable of working as a metal sensor. However, as shown in Scheme 1.3, to avoid the side reaction on the thiol group, the conventional thermal condensation reaction was replaced by the ring-opening strategy due to the involvement of high reaction temperature.[60] There are a lot of similar examples. It can be seen that the potential of L-cysteine in the preparations of cysteine-based

materials has been highly restricted and thus, is a valuable direction that is worth more study.

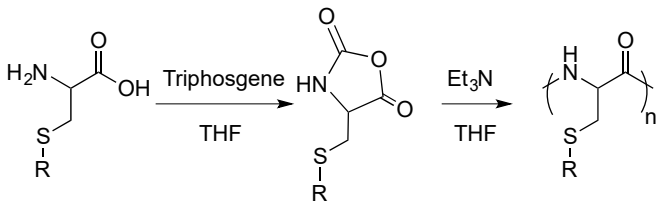

Scheme 1.3 Synthesis of poly (L-cysteine)-based material.[60]

1.4 Thiol-ene click reaction

Thiol-ene click reaction (TEC reaction) was first noted in the early 1900s and is famous for its modular process under mild reaction conditions with high yield and regioselectivity. The remarkable features of TEC reaction include its orthogonality to a wide range of functional groups such as esters, primary amines, carboxylic acids, alcohols and sugars groups, the compatibility of oxygen and the stability of thioether linkage under physiological conditions.[61] Since it satisfies most of the criteria of click-chemistry, it is assigned under the category of click reaction.[62]

As discussed above, due to the electronegativity of sulfur and relative weak S-H bond energy, the thiol functional group is prone to the reaction involved with nucleophilic thiolate anions and electrophilic thiol radical, such as thiol-Michael addition reaction and thiol-ene radical reaction.[61-63] According to the pK_a values, thiol compounds could be divided into four groups, alkyl thiols, thiolpropionate thiols, thiolacetate thiols and aromatic thiols. Since their pK_a have a big influence on the reactivity, the corresponding thiol reaction rate and efficiency are also affected. As shown in Fig. 1.7, with the increasing of thiol pK_a, the tendency of the nucleophilic reaction is strengthened, while the trend of electrophilic reaction is lowered. In fact, the toolbox of thiol-X click reaction is quite broad, including thiol-ene, thiol-alkyne, thiol-isocyanate, thiol-epoxy and thiol-halogen. But thiol-ene reactions, which satisfies most of the criteria of click-chemistry, attract most attention.[61]

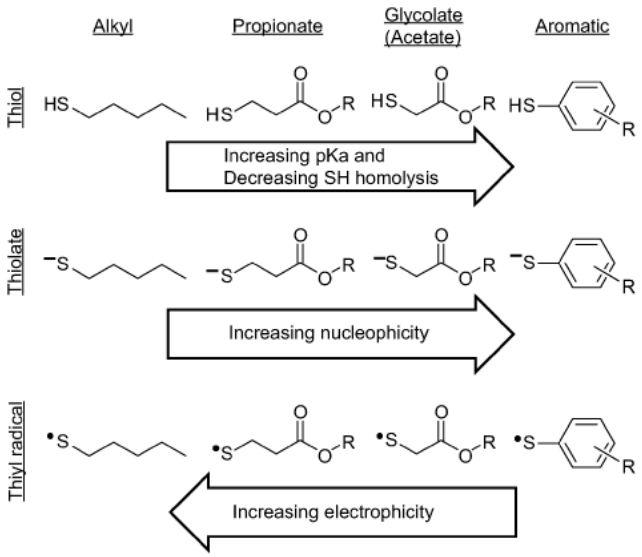

Figure 1.7 Categories of thiol compounds and their corresponding pK_a and reactivity. (Adapted from Ref. 61)

Though the thiol-ene system is quite powerful, it still has some drawbacks, such as the unpleasant odor of the thiols and the short shelf-life stability of some formulations.[61,64] Since lot of multifunctional thiols with less odor are now commercially available and the research on various stabilizers has also been conducted to eliminate the premature polymerization, (e.g. radical scavengers), the drawbacks of thiol odor and short shelf-life have been minimized to a large extent, which in turn broadens the scope of thiol reaction in synthetic chemistry.[61,64]

1.4.1 Thiol-Michael reaction

The study on thiol Michael reaction can be traced back to the 1940s.[65] It is defined as the addition reaction of thiols, in the presence of a catalyst, to an electron-deficient α,β - unsaturated carbonyl compound.[66] The reaction is traditionally initiated through activation the thiols by base. As shown in Scheme 1.4, the base B first abstracts a proton from the thiol creating a nucleophilic thiolate anion RS^- and a conjugate acid BH^+. Then the nucleophile RS^- attacks the electrophilic carbon of the C=C bond, producing the intermediate carbon-centered

anion. Finally, it abstracts a proton from the conjugate acid BH^+, yielding the thiol-Michael addition product.[61] The reaction efficiency was reported as being strongly affected by reaction solvent, basicity of the catalyst, pK_a of the thiol and the nature of the electron withdrawing group connected to the olefin bond.[67] Therefore, it was reported that the thiol-Michael reaction followed the order: maleimide > fumarates > maleates > acrylates/acrylamides > acrylonitrile > crotonate > cinnamate > methacrylates.[61] To increase the reaction efficiency, a variety of catalysts with significant functions were explored, including primary/secondary amine or alkyl phosphine, especially tertiary phosphine. It was proven that even in the Michael reaction with least reactive methacrylates, the phosphine-mediated catalyst could lead to a quantitative conversion of the reactants within less than an hour.[61,68] Beside the base catalysts, the reaction can also be catalyzed by metal catalysts or acids (e.g. boric acid) or some unusual catalysts (e.g. PEG).[67,69]

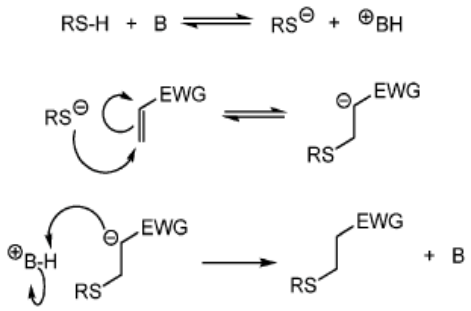

Scheme 1.4 Thiol-Michael reaction mechanism. (Adapted from Ref. 61)

1.4.2 Thiol radical reaction

TEC radical reaction is another versatile click reaction. It is a typical radical-chain process with initiation, propagation and termination steps (Scheme 1.5). The reaction starts from the generation of a sulfeneyl radical. Then, the radical attacks the electrophilic alkene substrate in an anti-Markovnikov form and creates a new carbon radical, which subsequently reacts with another thiol molecule to give a new sulfenyl radical and continues the radical circle.

Finally, the reaction is terminated through different recombination of free radicals.[70]

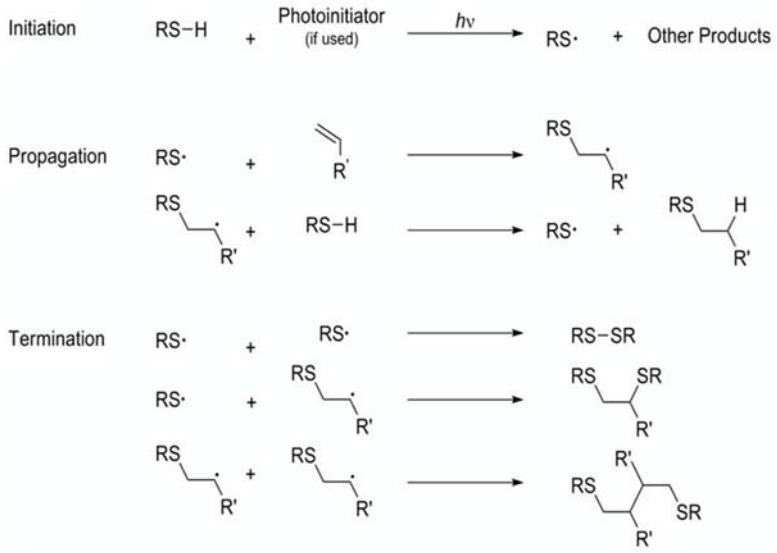

Scheme 1.5 Thiol-radical reaction mechanism. (Adapted from Ref. 61)

There are two feasible ways to initiate the reaction: heating or irradiation. Normally, a thermal-initiated reaction is conducted in solvent in the presence of a thermal radical initiator 2,2′-azobis(2-methylpropionitrile) (AIBN) at high reaction temperature, while a photo-coupling reaction could be triggered upon UV irradiation at 365 nm in the presence of classical photo-initiator such as benzophenone (BP) or dimethoxyphenylacetophenone (DMPA).[71] However, the presense of photo-catalysts is not necessary, which has been demonstrated by Cramer and co-workers who discovered that the reaction was able to be self-initiated in the presence of 254 nm UV-light without photoinitiator.[72] In some extreme cases, the reaction could be readily proceeded even upon exposure to unfocused sunlight.[61] For example, Fiore and co-workers successfully performed a reaction between glucosyl thiol and galactose-based ene under sunlight.[73] Moreover, it was reported that sunlight was able to induce thiol-ene polymerization between tetrathiol and trivinyl with extremely high efficiency.[74] Considering that some thiol-ene reactions could proceed in the absence of light, these discoveries may solve the yellowing problem induced from the degradation of the photo-initiator and contribute to

the formation of clear materials.[75] Generally, the photo-initiation reaction is more preferable than its thermal-initiation counterpart, due to its numerous advantages such as higher efficiency, shorter reaction time, more ambient reaction condition and higher tolerance to various functional groups.[65] Beside, the photo-initiation mechanism allows accurate spatial and temporal control by simply tuning the starting material ratio, light intensity, exposure time and range, or light wavelength.[68]

As mentioned above, the efficiency of thiol radical reaction can vary considerably based on the chemical structures of the ene and thiol components. Therefore, the order of C=C reactivity is reported in Lowe's review of TEC reaction to follow: vinylether > propenyl > alkene > vinylester > N-vinylamide > allylether > allyltriazine > allylisocyanurate > acrylate > N-substituted maleimide.[76] Meanwhile, they pointed out that the weakest reactivity of methacrylate was related to the high stability of its intermediate radicals, which led to difficulty of abstraction H from RS–H in the propagation step and the terminal enes were significantly more reactive towards hydrothiolation compared to internal enes.[76]

1.4.3 Applications of TEC reactions

As mentioned above, TEC click reaction has many advantages including mild reaction conditions, high yield, orthogonality to a wide range of functional groups and compatibility with water and oxygen. Therefore, TEC applications have been found in every aspects of the chemical industry, spanning from small molecules to macromolecules, from polymer syntheses to polymer modifications, from linear homopolymers to branched polymeric structures and from synthetic molecules to natural-occurring biomolecules.[61,77,78]

The primary application of TEC reaction is the post-polymerization with tailored functional groups. It offers a viable alternative for polymer modification to the traditional techniques involved in the ring opening or living radical polymerization, in which the

monomers are synthetic and the diversity of the functional groups is limited.[79] By employing target functional groups on alkene-containing polymers, the tailored polymers will contain interesting morphologies, physical properties and applications, especially serving as smart polymers for the pharmacological uses.[80] The pioneer work of TEC modification started from polybutadiene (PB) in the report by Serniuk and co-workers in 1948 (Scheme 1.6). However, the PB modification was limited by the competing reaction which resulted in an undesirable five or six-member ring and less than 100% conversion rate, even though excess thiol was used. This deficiency could be avoided by increasing the distance of neighbouring double bond.[81,82] For example, Gress and co-workers reported the grafting of poly[2-(3-butenyl)-2-oxazoline] by several types of mercaptans under moderate reaction conditions with complete conversion and the modified polymer exhibited different thermal properties compared to the starting materials.[81] Additionally, Lv and coworkers reported a thiol-ene modification corporate with amine-ene reaction. When a primary amine was reacted with olefin, the newly generated secondary amine could undergo spontaneous intra-molecular cyclization to form a five membered lactam. Thus the achieved polyesters had two degradation stages and one of them was self-degradation with controlled rate at room temperature.[82] TEC post-polymerization is also important in the synthesis of biohybrids which contain synthetic polymer backbones and biologically inspired side groups.[70] For example, Schlaad and co-workers successfully created several biohybrid polymers through polymer functionalization of PB with thiol compounds containing sugars, cholesterol and amino acid moieties.[83]

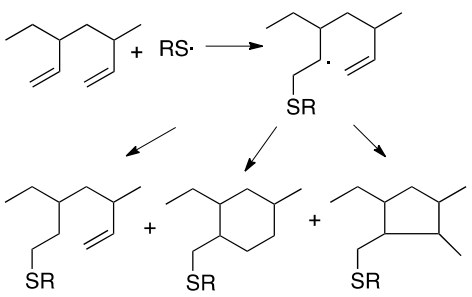

Scheme 1.6 PB post-polymerization via TEC reaction.[81]

Furthermore, TEC coupling is also widely employed in the dendrimer formations.[84,85] A dendrimer is a polymeric molecule composed of branched monomers from a central core. The first dendrimer molecule appeared in 1978 where amine Michael-addition reactions were repeatedly performed for dendron formation.[86] Dendrimer provides a perfect nanotechnology platform for numerous applications, particularly in pharmaceutics as drug delivery carrier, because of "its internal cavity for drug encapsulation, large numbers of surface functional groups for drug conjugations, the nanometric size for easy permeability into vasculature and high molecular weight for drug localization".[87] The dendrimer preparations required a series of reactions to form different generations. Thus, TEC reaction which is well-known for its high efficiency and orthogonality are ideal in dendrimer creations. For example, Hawker and co-workers reported the synthesis of a fourth generation dendrimer with 2,4,5-triallyloxy-1,3,5-triazine core through alternately repeating the TEC reaction and esterification reaction (Scheme 1.7).[88] Inspired by that, Ma and co-workers synthesized a series of dendrimers from asymmetrical monomers through simple and efficient TEC pathways. The synthesized polyester dendrimers have pendant methacrylate or amine groups exhibiting conjugation abilities to various drugs.[89] Beside the constitution of dendrimer scaffold, TEC coupling is capable of further modifying the peripheral units by grafting various structures. As shown in Scheme 1.7, the peripheral units of the dendrimer were further modified by grafting various structures to add extra functional end-groups.[86] Moreover, it was reported that glycodendrons could be prepared by importing thiogalactoside on dendrimer surface via TEC reactions.[90,91] The obtained glycodendrimer exhibited high affinity with the LecA lectin and efficiently served as potent anti-adhesive agents against bacterial infections and biofilm formation.[91]

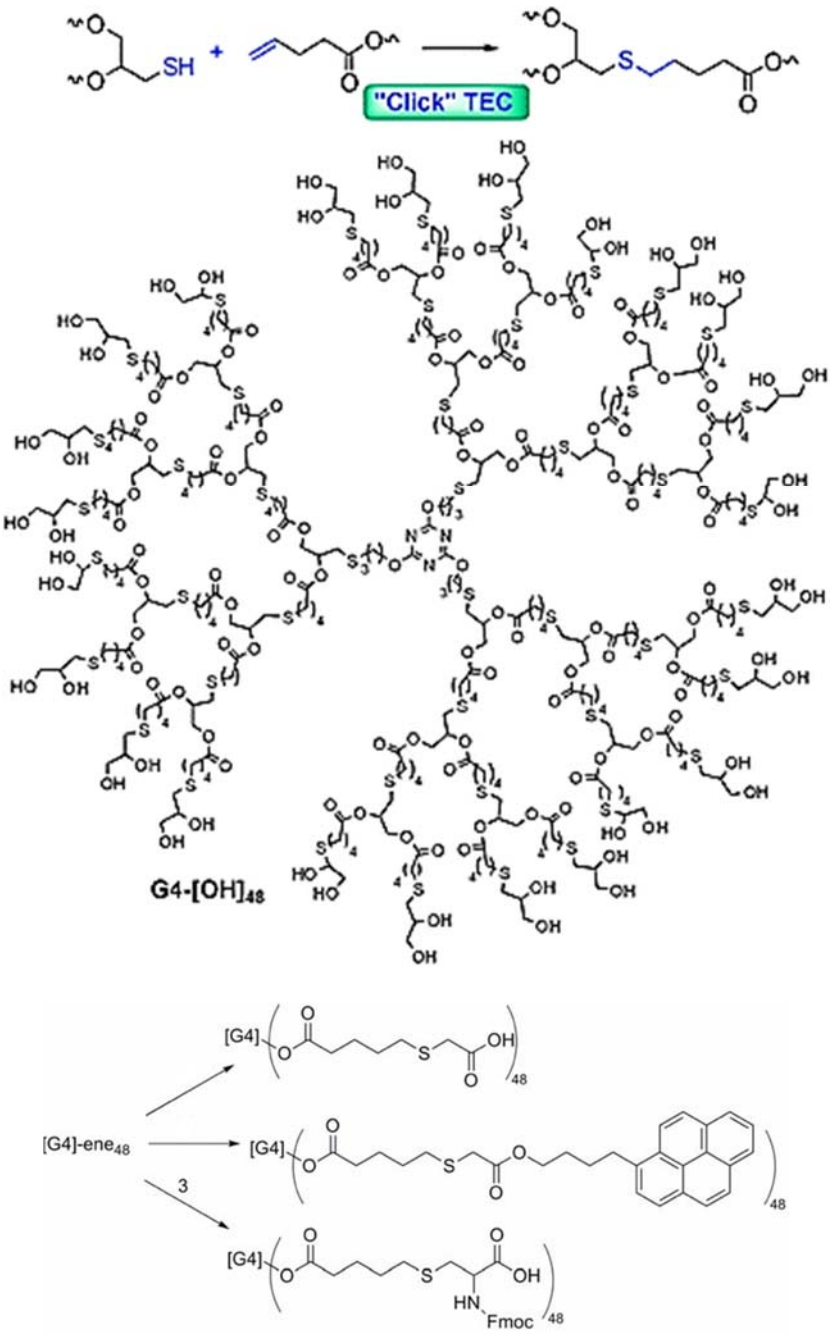

Scheme 1.7 TEC reaction in dendrimer synthesis. (Adapted from Ref. 88)

Both the applications of post-polymerizations and dendrimer preparations mainly depend on the TEC orthogonality nature, but the step-growth mechanism of TEC reaction has also been taken fully advantage of to form ultra-thin photo-curable materials with homogeneous and uniform properties, with dramatically increased capacity for mechanical energy absorption and significantly delayed gel point conversion, which enables the

polymerizing system to continue to flow for an extended period for better shrinkage accommodation[61,70,77] In addition, since TEC reactions are easily controlled spatially and temporally, they could be exploited to create materials with gradient or patterned chemical, physical and biological properties. For example, Harant and co-workers utilized this feature and made ultra-thin films from 1,6-hexanedithiol and triethylene glycol divinyl ether with various thickness that ranged from 0.1 nm to 9.6 nm through varying the monomer ratios.[92] Similarly, Khire and co-workers created bi-directional surface gradients with varying thickness through tuning the UV exposure time.[93]

1.5 2.5-Diketopiperazine

Diketopiperazine (DKP) is the smallest cyclic dipeptide containing a six-member ring that consists of two amide linkages. DKP has three different regioisomers which are distinguished by the location of two carbonyl group and nitrogen atoms (Fig. 1.8). These isomers present different physical and chemical properties for different applications and are synthesized by different synthesis approaches.[94] Among them, 2,5-DKP attracts the most attention due to its center symmetric and highly regulated structure that the two nitrogen atoms and the two carbonyls are at opposite positions in the ring.

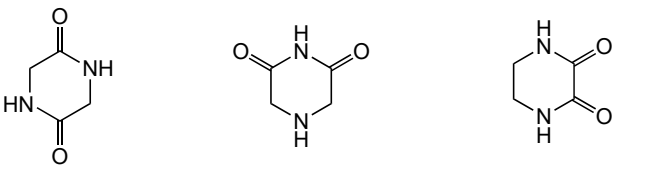

Figure 1.8 Three structural isomers of DKP.

DKPs are a class of naturally occurring compounds and exist abundantly in a variety of organisms like fungi, bacteria, plants and mammals. It is the secondary functional metabolites and is found as a side product of peptide degradation. DKP has very interesting properties, such

as remarkable stability in vivo as compared with their linear counterparts, resistance to proteolysis, dynamic stereochemistry, mimicking of peptide pharmacophoric groups, conformational rigidity and supramolecular structure formed through a hydrogen bond.[95] Therefore, DKPs recently have gained more and more interests in drug discovery and medical purposes as inhibitors of various enzymes, antitumor agents, antiviral agents, antifungal agents, antibacterial agents, anticancer agents and preparations for drug delivery capsules.[95,96]

1.5.1 Preparation of 2,5-DKP

With the increasing importance of DKPs in the pharmaceutical area, more and more DKPs that are prepared from both natural occurring and synthetic amino acids were reported in the literature since the late 19th century.[97] Based on the DKP structure, it is easily found that there are three possible cleavages: the amide bond (A), the *C–N* bond (B), and the *C–C* bond (C) (Fig. 1.9). Accordingly, Alan Borthwick classified DKP synthesis into four main groups with eleven approaches including a) amide bond formation (dipeptide formation and cyclization, Ugi chemistry, amino acid condensation and Aza-Wittig cyclization), b) N-alkylation (α-haloacyl derivatives of amino acids, Aza-Michael addition and Diels-Alder reaction), c) Tandem cyclization (N1-C2/C3-N4 bond formation and C2-N1-C6 bond formation) and d) C-acylation (enolate acylation and C-C cyclization radical-mediated).[98] Since amide bond formation is the most frequently used in DKP syntheses, we will focus on this method below.

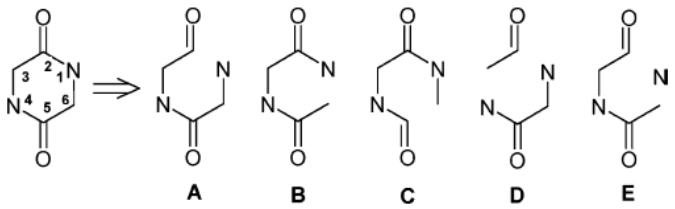

Figure 1.9 The possible bond cleavage sites in the retrosynthesis of 2,5-DKP. (Adapted from Ref. 98)

DKP preparation through dipeptide cyclization is the most commonly used approach, where the linear peptide is protected at both N-terminal and C-terminal (Scheme 1.8). The cyclization is able to proceed under acid, basic or thermal conditions.[98] In the early days, research was mainly focused on linear dipeptide cyclization for DKP synthesis and there were several famous synthesis methods.[99-102] In Nitecki's method, the Boc-protected dipeptide methyl ester was deprotected by HCOOH, subsequent refluxing of the ester formate in a mixture of s-BuOH and toluene.[99] With regard to Suzuki's method, DKP was achieved after the dipeptide ester was refluxed in acetic acid containing iso-butanol.[100] Fischer's design involves the aminolysis of dipeptide ester in ammonia saturated methanol.[101] However, these methods have some drawbacks such as complicated preparation of linear peptides, low yield or severe side reactions.[99-101]

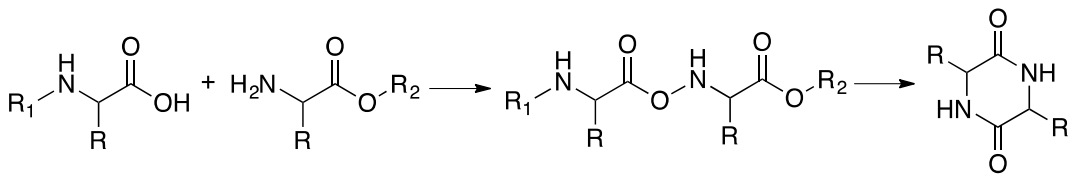

Scheme 1.8 DKP synthesis via dipeptide cyclization.[98]

In 1983, Toshihisa and co-workers integrated the advantages from the old methods and published an improved synthesis route, where DKP was formed by refluxing dipeptide methyl ester in methanol. Meanwhile, they pointed out that the type of protective groups, the solvent species and the side chains had big influences on the efficiency of DKP formations.[102] For example, it concluded that the larger the size of the side chain, the slower the reaction rate, which was consistent with the analysis from Naraoka and co-workers.[102,103] Finally, comprehensive information on naturally occurring amino acid-based DKPs was collected (Table 1.3).[100,102] However, there are still some DKPs that failed to be dimerized directly from linear dipeptide, for example, cysteine-based DKP.

Table 1.3 Melting points of natural-occurring amino acid-based DKPs.[100]

DKP	M.P. (°C)	DKP	M.P. (°C)
-Pro-Leu-	158-160	-Val-Leu-	259-261
-Leu-Pro-	157-159	-Val-Val-	269-271
-Pro-Val-	169-171	-Val-Leu-	259-261
-Leu-Leu-	273-274	-Val-Ala-	259-261
-Val-Ile-	276-278	-Ile-Ile-	259-262
-Gly-Ile-	249-251	-Gly-Phe-	247-250
-Met-Tyr-	273-277	-Tyr-His-	196-198
-Asp-Ala-	189-192	-Asn-Arg(NO_2)-	235-237

To improve the reaction efficiency for DKP preparation, a solid-phase approach was developed.[98] The solid-phase synthesis normally involves three steps, the preparation of linear peptide precursor on resin, cyclization, and cleavage from the resin. Based on the different orders of these procedures, this method could be divided into three categories: (i) cyclization first and then cleavage, (ii) cleavage of the precursor from the resin first and then cyclization, and (iii) cleavage and cyclization spontaneously in one step.[94,98] For example, Albericio and co-workers discovered a DKP synthesis route with nearly quantitative yield through the solid-phase method (i). As shown in the Scheme 1.9, the amino acid methyl ester was first attached to a functionalized resin. The second amino acid group was then connected via acylation and formed a linear dipeptide. The cyclization was conducted in the mixture of toluene and ethanol in the presence of a catalyst and finally the obtained DKP was cleaved from the solid support.[102] Although this method has been successfully used in many DKP synthesis, its selection on the type of functionalized resin is still time-consuming.[104]

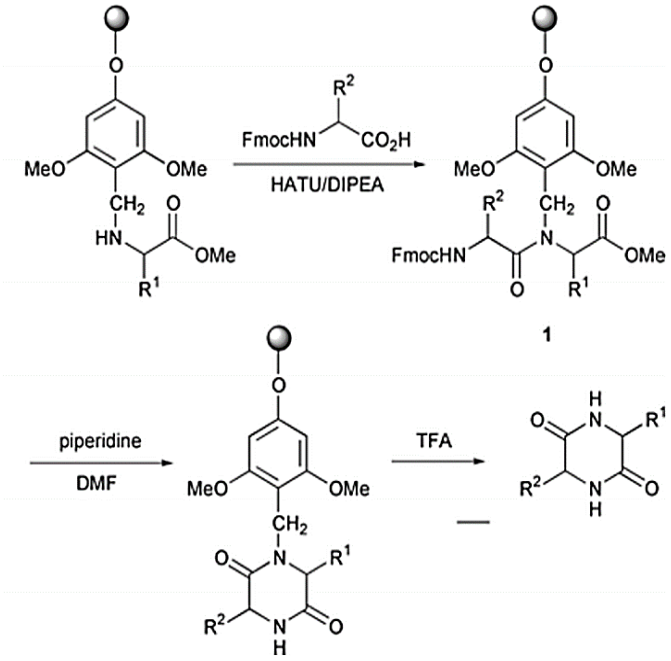

Scheme 1.9 Solid-phase synthesis of DKP. (Adapted from Ref. 104)

The simplest method for DKP synthesis is the direct self-condensation of two amino acids or esters by heating, which normally involves the intermolecular amide formation and intramolecular lactamization.[105,106] However, this method is normally reported with low yield or required harsh reaction conditions.[106,98] One of the common improvements is the addition of peptide coupling reagents, which are employed to activate the carboxyl groups by making an acid derivative with a more favorable leaving group (Fig. 1.10). Today, peptide coupling reagents are being developed from carbodiimide reagents (DIC, DCC) to triazolol reagents (HOBt, HOAt) to urea-based cationic reagents (HATU, HBTU, TBTU).[98,104,107] However, in every amino acid dimerization reaction, the use of a catalyst is not interchangeable or being substituted by another, which may lead to the failure of ring closure or the formation of macro cycles or oligomers containing more than two peptide bonds.

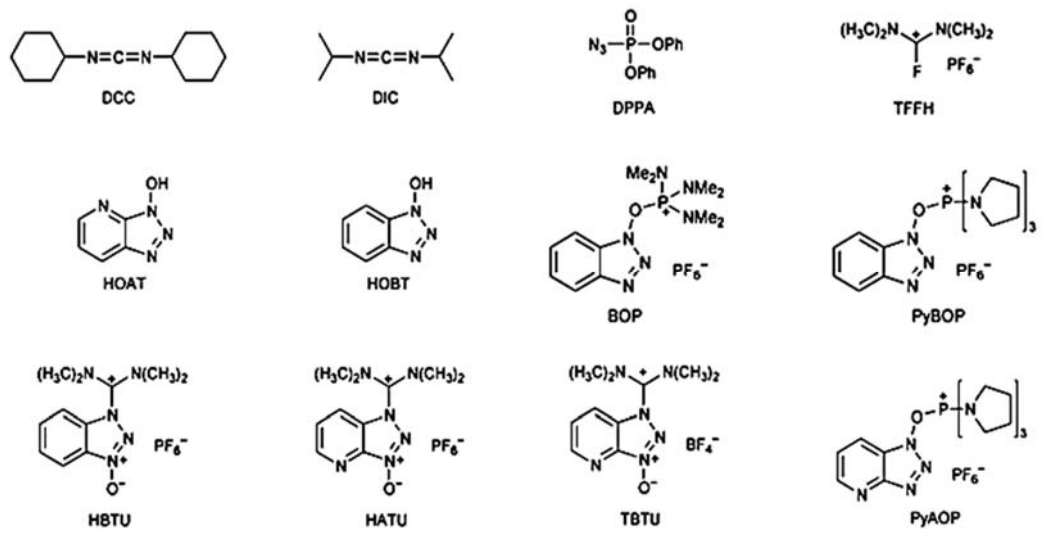

Figure 1.10 Common peptide coupling reagents.[104]

Compared to conventional dimerization methods, microwave-mediated DKP synthesis is definitely a hot topic, due to its short reaction time, high efficiency, catalyst-free process and simple purification.[98,108-110] For example, Perez-Picaso developed a microwave-assisted synthesis route with linear peptide as starting material and the DKP was achieved after irradiation for 10 minutes using water as the solvent.[109] Later, Nonappa and co-workers simplified the reaction by directly using amino acids as building blocks, where a series of DKPs were successfully obtained in nearly quantitative yields.[110] Undoubtedly, the microwave-mediated method is most promising for future DKP synthesis.

1.5.2 DKP diastereomers

It has been known that during the process of DKP formation, there are four possible isomers, L-L, D-L, D-D, L-D, for cyclic peptides and they are classified into cis-isomers, (L-L and D-D), and trans-isomers, (L-D). The ratios of cis/trans are affected by many factors including reaction methods, reaction temperatures, and the choice of catalysts.[103] Moreover, it has been reported that these isomers could be transformed to one another under alkaline

conditions (Fig. 1.11). As early as 1925, the phenomenon that DKP was racemized at a high rate under proper conditions had been observed.[111] Then in 1928, Levene and co-workers identified that when DKP was treated with dilute alkali, it showed an obvious racemization phenomenon, and when treated with concentrated alkali, the degree of racemization was minimized. Meanwhile, they mentioned that the racemization of linear dipeptides and polypeptides is not significant compared to their DKP counterparts.[112]

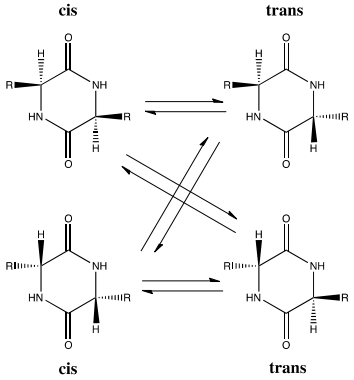

Figure 1.11 Four stereoisomers of 2,5-DKP.[111]

It has been known that DKP ring could exist in a flat or a slightly puckered boat or chair conformation, therefore though DKP diastereomers have exact same molecular weights and molecular formulas, the conformation of these isomers is quite different (Fig. 1.12). As reported, there were several factors affecting its conformation, for example, the substituted functional groups on the side-chain.[98] It has been found that the imidazole aromatic ring in cyclic histidine (His-His) tends to be stacked over the DKP ring due to the aromatic-amide interaction. Thus, the trans-isomer of His-His presents in a planar conformation and the cis-isomer is in a boat-shape.[112] Besides, the state of the matter and its environment are also determinants in DKP conformations.[98] It has been shown that the cyclic glycine (Gly-Gly) is in a planar conformation in solution and solid-state. But the molecule adopts a boat form in the gaseous state. The change is attributed to the boat conformer possessing the lowest energy at gas state and there is only few kcal/mol difference among the energies of different

conformations that the external forces from a crystal or solution environment is sufficient to keep a planar structure.[98]

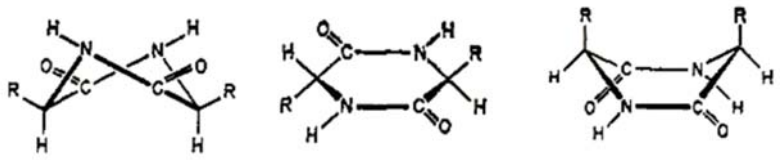

Figure 1.12 Twist-boat, planar and boat conformations of DKP.[111]

Various techniques have been applied to study the conformations of cyclic dipeptides including infrared absorption, nuclear magnetic resonance (NMR), vibrational circular dichroism, Raman optical activity, ultraviolet-visible absorption (UV-vis), electronic circular dichroism, X-ray diffraction and optical rotatory dispersion.[96,98,102,103] Among them, NMR is the most straightforward and most commonly used, for example, the DKP conformation could be identified by ^{3}J coupling constants of H-$^{\alpha}$C-N-H from the NMR analysis. Moreover, the chemical shift differences of the NH signal of different isomers could also be used, since in different conformers, the intermolecular hydrogen bonding effect of the DKP ring is different.[96,113] Based on the NMR methods, the conformation information of cyclic valine (Val-Val), cyclic leucine (Leu-Leu), cyclic alanine (Ala-Ala), Gly-Gly and other DKPs from synthetic amino acids were collected.[96,113]

Different stereoisomers play different roles in practical applications. For example, the diastereomers of cyclic leucine-histidine which carries a hydrophobic alkyl side chain and a nucleophilic side chain, exhibit different reaction activity in the hydrolysis of carboxylic acid *p*-nitrophenyl esters. It was demonstrated that only the trans-isomer was an effective catalyst and the cis-isomer was inactive on hydrolytic activities.[114] Therefore, under some circumstance, the separation of DKP isomers is necessary, especially for the high-selective application.

DKP diastereomers have been successfully separated by a variety of chromatographic techniques such as gas liquid chromatography (GLC) and high performance liquid

chromatography.[102,115] The first report on the successful separation of DKP diastereomers arose through the GLC technique in 1968. In the paper, retention times of various DKPs at two different temperatures were given and considered to be related to the molecular weights (Table 1.4).[115] It was clearly shown that the cyclic valine-proline and the cyclic isoleucine-proline, which had larger molecular weights, gave a high degree of diastereomeric resolution with the trans/cis ratio of 1.37, while the Val-Val isomers, which had a smaller molecular weight had very similar retention time. Moreover, the retention time was identified to be related to the temperature and side chain structures. It was found that the differences of the retention time for diastereomers were enlarged at a low temperature and the DKPs containing an aromatic ring required a higher temperature for GLC than the purely aliphatic ones.[115] However, until now, the research on separation of DKP diastereomers is still limited, since the accurate control of the racemization during the DKP synthesis is always first taken into consideration to obtain pure DKP isomers.

Table 1.4 The retention time (mins) of DKP diastereomers at different temperatures.[115]

DKP	206 °C	196 °C
cis-Val-Val	10.6	17.2
trans-Val-Val	9.6	15.4
Val-Pro	12.3	19.5
Val-Pro	16.7	26.8
Ileu-Pro	16.3	25.7
Ileu-Pro	21.8	35.2

DKP rings could self-assemble to supramolecular structures when the amide group form intermolecular hydrogen bonds (N−H···O) with adjacent molecules. For example, Gly-Gly crystalline represents as a linear tape structure, where the neighboring DKPs form a cyclic eight-membered ring involving two intermolecular hydrogen bonds (Fig. 1.13a). There are also

some DKPs, such as His-His and Ala-Ala, existing in the form of a large layer-type structure (Fig. 1.13b).[98,116] It was reported that the supramolecular structures have been utilized to position guest molecules with the desired intervals, sizes and shapes. Therefore, the properties of designed organic compounds could be tuned through controlling the structure of DKP supramolecular structures.[117]

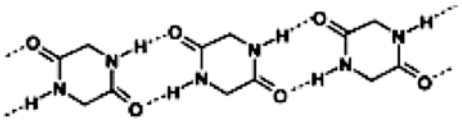

(a) Tape

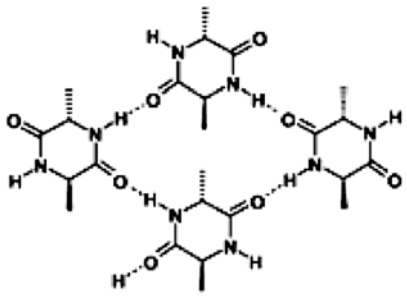

(b) Layer

Figure 1.13 Supermolecular structures of DKP. (Adapted from Ref. 98)

1.5.3 Applications of DKP

DKP has been widely applied in the preparation of polymeric materials for different applications, because DKP-related reactions could take place at up to six positions: on carbon (C-3 and C-6), on nitrogen and on carbonyl carbon (C-2 and C-5), and the rigidity of DKP can contribute to improve the polymer mechanical and thermal properties. The history of incorporating DKP in polymer preparation could be traced back to 1968 and now, the synthesis of DKP containing polymer is well developed.[118] A series of DKP-based polymers have been successfully produced such as aspartic DKP-containing polyesters, serine DKP-containing polyesters, lysine DKP-containing polyamides and lysine DKP-containing polyurethanes (Fig. 1.14).[118,119] It was reported that the DKP-containing polymers possessed good thermal and mechanical properties. Moreover, as one of the starting material was derived from natural

occurring amino acid, the obtained polymers were partially biodegradable and potentially biocompatible, which are suitable for biomedical applications.[118,119]

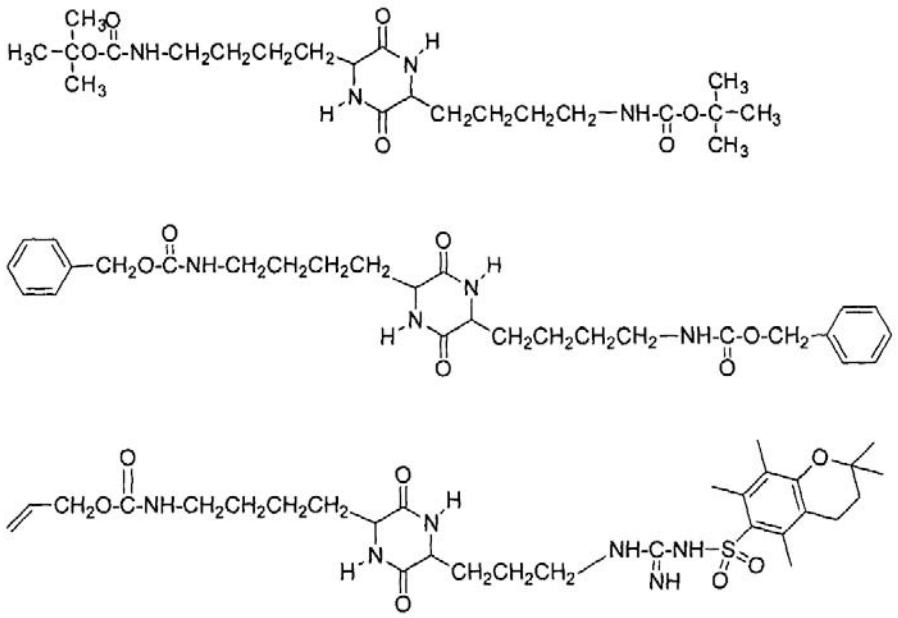

Figure 1.14 Urethanes containing the lysine-based DKP. (Adapted from Ref. 119)

As mentioned above, amino acid containing O, N and additional metal binding site could chelate with various metal ions to form a stable five membered complex. Thus, DKP which is derived from amino acid, is considered to present better chelating ability, due to its rigid conformation of the six-membered ring.[120-122] For example, in an intensive research performed by Gockel and co-workers, the binding behaviors of zinc with cysteine and histidine containing DKPs, including His-His, Gly-Cys, His-Cys and Cys-Cys, were extensively studied (Fig. 1.15). They not only demonstrated that thiol group in cysteine was a much better ligand for zinc than the imidazole in histidine, but also revealed that the two cysteine side chains were not positioned favorably for a zinc coordination.[120] Indeed, the researches on the binding ability of DKP with different metal ions are quite useful, since they are helpful in the protein conformation studies and have great potential to be applied in the design of the sensors with high-selectivity.[121,122]

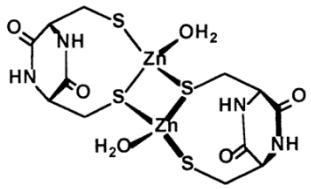

Figure 1.15 Proposed conformation of cyclic cysteine with zinc. (Adapted from Ref. 120)

The other important application of DKP is in drug delivery systems. It is known that the delivery of drugs has had some major problems for many years, especially the instability of the delivered drug which causes it to decompose or be consumed before it reaches the desired target.[123-125] Though a variety of enteric coatings have been developed, they can only ensure the drugs are undestroyed prior to the small intestine. Therefore, an improved drug carrier is preferred, which should not only be stable before reaching to the target, but also encapsulate the drug to deliver into the bloodstream. Several structures have been carefully examined from natural systems to synthetic polymers and finally it was demonstrated that DKPs with rigid conformation and self-assembling properties are the ideal structure for drug delivery applications.[123] The pioneering work on DKP drug delivery applications was claimed by Robert Feldstein and co-workers in 1992 in the US Patent 5352461 entitled "*Self Assembling Diketopiperazine Drug Delivery System*" (Scheme 1.10). In the patent, 2,4-diketo-3,6-di(4-succinylaminobutyl) piperazine was synthesized starting from a lysine building block and ending up with a DKP-containing diacid. Because the COOH functional group was reported to exhibit pH-dependent assembly-disassembly features, acid and base were added to encapsulate the drugs. The measurements on the effect of the new drug carrier were performed through an oral administration tests in rats. It was found that the DKP effectively took the drugs into rat body and received good healing results.[123] Inspired by that, the research on DKP-based drug cargos have sprung up since then.[124-126] For example, based on the structure in Scheme 1.10, a series of DKP-based drug encapsulation systems were designed, where the acid end-group was

replaced by basic groups or other functional groups through covalently coupling with functional segments such as PEG, proteins, peptides, oligosaccharides, carbohydrate and lipids. Thus the system could adhere to specific regions of the tissues or to certain cell targets.[123,124] Moreover, the symmetric DKP structure could be switched to asymmetric one with desired functional groups and the size or shape of the DKP cargos could be further tuned to ensure the drug can pass through certain tissues or organisms.[123,124] Since DKP nanoparticles are non-toxic, simple to prepare, available for further modification, and degradable under certain physiological conditions, it is definitely one of the most promising candidates for smart drug delivery in the future.

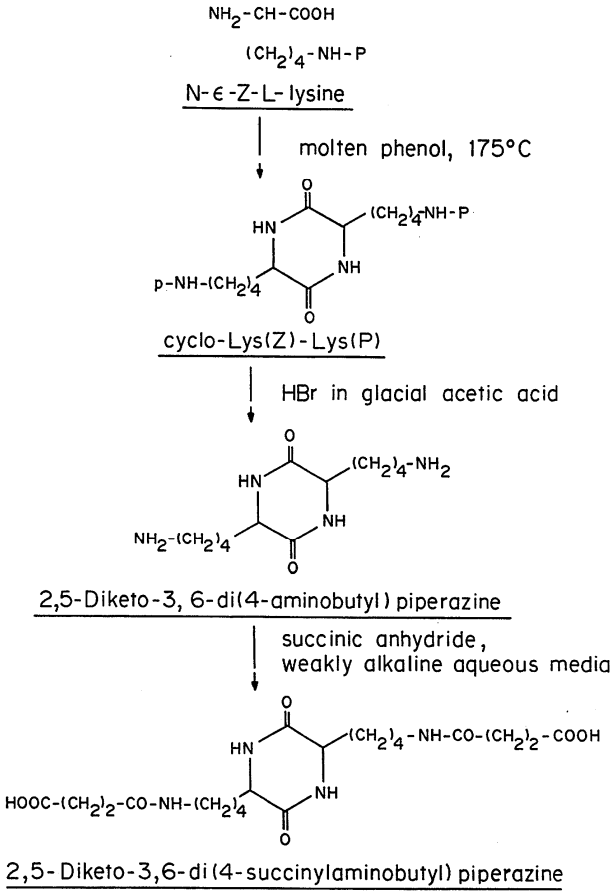

Scheme 1.10 Synthesis of lysine-based DKP for drug delivery. (Adapted from Ref. 123)

1.6 Rationale and Objectives

Organic chemicals are involved in every aspect of our lives and the use of fossil fuels

is still predominant in serving as the main raw material in chemical industries. However, there are increasingly concerns on the excess consumption of petroleum feedstock and environmental pollution, which in turn, spur the development of green chemistry with biomass-based chemicals as the starting material. L-cysteine is definitely one of the most promising renewable building blocks with great potential applications. It is commercially available in large scale through microbial fermentation and is predicted to have a wider market in the future. Thiol group of L-cysteine is famous for the modular thiol-ene click reactions including thiol-Michael reaction and thiol-radical reaction, which are preformed under mild conditions with numerous substrates. Besides, the thiol-ene coupling is well known for its high efficiency and orthogonality to place a variety of functional units on double bond. Therefore, L-cysteine has been applied in polymer modifications as an ideal graft molecule. Moreover, the amino acid functional group could be used to prepare DKP. DKPs are a class of naturally occurring cyclic amino acid and their structures are more rigid than linear amino acids, which can lead to the polymers with much improved properties and solvent resistance. Synthetic DKPs have been employed in the preparation of biodegradable polymers and in pharmacological field for drug delivery purposes. However, there is little research on cysteine-based DKP, due to the excess reactivity of the thiol group. Thus, the development and applications of L-cysteine based DKP derivatives are urgent and of great significance.

The overall objective of this thesis research is to develop versatile and robust routes to the value-added compounds from L-cysteine. The following are specific objectives for the thesis research:

(1) To explore suitable reaction conditions for the synthesis of cysteine-based DKPs and DKP-containing polymers. The thiol-Michael addition click reaction and thiol-ene free radical click reaction will be used to protect the thiol group and prepare S-alkylated intermediates.

(2) To synthesize cysteine-based DKPs from 4-thiazolidinecarboxylic acid derivatives, which can be prepared through the reaction between L-cysteine and aldehydes. By attaching the functional groups onto the DKP ring, the difunctional DKPs can be used as monomers for the synthesis of DKP containing polymers.

(3) To introduce L-cysteine into small molecules, linear macromolecules, star-shape macromolecules and polysaccharides, and study their self-assembling behaviors and the chiral recognition ability.

References

1. Sheldon, R. A.; *Chem. Soc. Rev.*, **2012**, *41,* 1437.
2. Gandini, A.; *Green Chem.,* **2011**, *13*, 1061.
3. Mathers, R. T. *J. Polym. Sci. Part A: Polym. Chem.,* **2012**, *50*, 1.
4. Dai, J.; Ma, S.; Wu, Y.; Han, L.; Zhang, L.; Zhu, J.; Liu, X. *Green Chem.,* **2015**, *17*, 2383.
5. Muñoz-Guerra, S.; Lavilla, C.; Japu, C.; Martínez de Ilarduya, A.; *Green Chem.,* **2014**, *16*, 1716.
6. Stevens, E. S. *Green Plastics: An Introduction to the New Science of Biodegradable Plastics*, Princeton University Press, Princeton, **2002.**
7. Brundtland, C. G. *Our Common Future, The World Commission on Environmental Development*, Oxford University Press, Oxford, **1987**.
8. Anastas, P. T.; Zimmerman, J. B. *Sustainability Science and Engineering Defining Principles*, ed. Abrahams, M. A. Elsevier, **2006**, 11.
9. Anastas, P. T.; Farris, C. A. *Benign by Design: Alternative Synthetic Design for Pollution Prevention*, ACS Symp. Ser. nr. 577, ed. American Chemical Society, Washington, DC, **1994.**
10. Tang, S. L. Y.; Smith, R. L.; Poliakoff, M. *Green Chem.*, **2005**, *7*, 761.
11. Kulshrestha, A. S.; Gao, W.; Gross, R. A. *Macromolecules*, **2005**, *38*, 3193.
12. Olsson, A.; Lindstro, M.; Iversen, T. *Biomacromolecules*, **2007**, *8*, 757.
13. Scott, E.; Peter, F.; Sanders, *J. Appl. Microbiol. Biotechnol.,* **2007,** *75,* 751.
14. Xiao, P. T.; Kirchhoff, M. *M. Acc. Chem. Res.,* **2002**, *35*, 686.
15. Huber, G. W.; Iborra, S.; Corma, A. *Chem. Rev,.* **2006**, *106*, 4044.
16. Crocker, M.; Crofcheck. C. *Energeia,* **2006**, *17*, 1.
17. Yao, K.; Tang, C., *Macromolecules*, **2013**, *46*, 1689.

18. Robertson, G. L. *Food Packaging: Principles and Practice, Third Edition.* CRC Press, **2016**.
19. Dodds, D. R.; Gross, R. A. *Science*, **2007**, *318*, 1250.
20. BASF. *BASF now offers biobased PolyTHF.,* 2015. http://biomassmagazine.com/articles/11670/basf-now-offers-biobased-polythf
21. Lavilla, C.; Alla, A.; Martınez de Ilarduya, A.; Munoz- Guerra, S. *Biomacromolecules*, **2013**, *14*, 781.
22. Sousa, A. F.; Matos, M.; Freire, C. S. R.; Silvestre, A. J. D.; Coelho, J. F. J. *Polymer*, **2013**, *54*, 513.
23. Vilela, C.; Sousa, A. F.; Fonseca, A. C.; Serra, A. C.; Coelho, J. F. J.; Freire, C. S. R.; Silvestre, A. J. D. *Polym. Chem.,* **2014**, *5*, 3119.
24. Xu, Y.; Hanna, M.A.; Isom, L. *The Open Agriculture Journal*, **2008**, *2*, 54.
25. Huang, L. P.; Jin, B.; Lant, P.; Zhou, J. *Biochem. Eng. J.,* **2005**, *23*, 265.
26. Atsushi, S.; Somsak, S.; Kohtaro, K.; Shoji, U. *J. Ferment. Bioeng.*, **1996**, *81*, 320.
27. Meier, M. A. R.; Metzger, J. O.; Schubert, U. S. *Chem. Soc. Rev.,* **2007**, *36*, 1788.
28. Mutlu, H.; Meier, M. A. R. *Eur. J. Lipid Sci. Technol.,* **2010**, *112*, 10.
29. Werpy, T.; Petersen, G. *Top Value Added Chemicals from Biomass*, U.S. Department of Energy, Oak Ridge, TN, USA, **2004**.
30. Hajian, H.; Yusoff, W. M. W. *Curr. Res. J. Biol. Sci*., **2015**, *7*, 37.
31. Proteins in Biomass streams. *A study commissioned by the Biorenewable Resources Platform, Energy Transition (Platform Groene Grondstoffen)*, Wageningen UR Food & Biobased Research, **2010**.
32. Friedman, M. *J. Agr. Food Chem.,* **2013**, *61*, 10626.
33. Naeem, M.; Rajput, N.; Li, Z.; Su, Z.; Rui, Y.; Tian, W. *Pak. J. Agric. Sci.,* **2014**, *51,* 229.

34. Sheldon, R. A. *Appl. Microbiol. Biotechnol.*, **2011**, *92*, 467.

35. Zhu, G.; Zhu, X.; Xiao, Z.; Zhou, R.; Feng, N.; Niu, Y. *Biomass Conv. Bioref.,* **2015**, 309.

36. Curis, E.; Nicolis, I.; Moinard, C.; Osowska, S.; Zerrouk, N.; Bénazeth, S.; Cynober, L. *Amino Acids*, **2005**, *29*, 177.

37. Adeyeye, E. I.; Omolayo, F. O. *Agric. Biol. J. N. Am.*, **2011**, *2*, 499.

38. Sanders, J.; Scott, E.; Weusthuis, R.; Mooibroek, H. *Macromol. Biosci.*, **2007**, *7,* 105.

39. Sheldon, R. A. *Green Chem*., **2014**, *16*, 950.

40. Hell, R. *Planta*, **1997***, 202,* 138.

41. *Discover a new dimension of pureness: vegetarian cysteine.* Wacker fermentation - grade cystine and cysteine, Wacker Chemie AG. http://www.brenntag.com/media/documents/bsi/product_data_sheets/life_science/wacker_amino_acids/cystine_cysteine_brochure.pdf

42. Huang, T.; Ho, C.; Hui, Y. H.; Nip, W.; Rogers, R. eds. Meat Science and Applications, ch. *Flavors of Meat Products*, CRC, **2001**.

43. *Food Ingredients and Colors*. U.S. Food and Drug Administration. 2004.

44. China L-cysteine Industry Analysis & 2018 Forcasts in New Market Research Report at MarketReports Online. com. **2017**. http://www.worldofchemicals.com/media/wacker-acquires-antibioticos-fermentation-plant-in-spain/10948.html

45. Wacker acquires Antibioticos' fernebtation plant in Spain. **2016.** http://www.worldofchemicals.com/media/wacker-acquires-antibioticos-fermentation-plant-in-spain/10948.html

46. *Table of pKa and pI values.* http://www.mhhe.com/physsci/chemistry/carey5e/Ch27/ch27-1-4-2.html

47. Huang, C.; Chu, S.; Li, C.; Lee, T. R. *Colloids Surf., B: Biointerfaces,* **2016***, 145,* 291**.**

48. Giles, N. M.; Watts, A. B.; Giles, G. I.; Fry, F. H.; Littlechild, J. A.; Jacob, C. *Chem. Bio.*, **2003**, *10*, 677.

49. Reddie, K. G.; Carroll, K. S. *Curr. Opin. Chem. Biol*., **2008**, *12*, 746.

50. Sevier, C. S.; Kaiser, C. A. *Nat. Rev. Mol. Cell Bio.,* **2002**, *3,* 836.

51. Rovira, I. I., Finkel, T., Masters, B. S., Dickman, M. B., Lee, J., Ragsdale, S. W.; Lee, C. C. *Redox Regulation of Physiological Processes*, eds Banerjee, R.; Becker, D. F.; Dickman, M. B.; Gladyshev, V. N.; Ragsdale, S. W. Redox Biochemistry, John Wiley & Sons, Inc., Hoboken, NJ, USA. **2007**.

52. Koval, I. V. *Russian Chemical Reivoews,* **1993**, *62*, 769.

53. Disulfide. https://en.wikipedia.org/wiki/Disulfide#cite_note-Sevier-2

54. Lippard, S. J.; Berg, J. M. *Principles of Bioinorganic Chemistry.* Mill Valley, CA: University Science Books, **1994.**

55. Baker.; D. H.; Czarnecki-Maulden, G. L. *J. Nutr.,* **1987,** *6*, 1003.

56. Carney, P.; Lopez, S.; Mickley, A.; Grinberg, K.; Zhang, W.; Dai, Z. *Chirality*, **2011**, *23*, 916.

57. Nan, J.; Yan, X. *Chem. Commun.*, **2010**, *46*, 4396.

58. Geng, Y.; Discher, D. E.; Justynska, J.; Schlaad, H. *Angew. Chem. Int. Ed.,* **2006**, *45*, 7578.

59. Passaglia, E.; Donati, F. *Polymer*, **2007**, *48*, 35.

60. Fu, X.; Shen, Y.; Fu, W.; Li, Z. *Macromolecules*, **2013**, *46*, 3753.

61. Hoyle, C. E.; Lowe, A. B.; Bowman, C. N. *Chem. Soc. Rev.*, **2010**, *39*, 1355.

62. Bowman, C. N.; Hoyle, C. E. *Angew. Chem. Int. Ed.,* **2010**, *49*, 1540.

63. Griesbaum, K. *Angew. Chem., Int. Ed. Engl.,* **1970***, 9*, 273.

64. Esfandiari, P. Ligon, S. C.; Lagref, J. J.; Frantz, R.; Cherkaoui, Z.; Liska, R. *J. Polym.*

Sci. A-Polym. Chem., **2013**, *51*, 4261.

65. Hurd, C. D.; Gershbein, L. L. *J. Am. Chem. Soc.*, **1947**, *69*, 2328.
66. Stewart, I. C.; Bergman, R. G.; Toste, F. D. *J. Am. Chem. Soc.*, **2003**, *125*, 8696.
67. Mather, B. D.; Viswanathan, K.; Miller, K. M.; Long, T. E. *Prog. Polym. Sci.,* **2006**, *31*, 487.
68. Li, G. Z.; Randev, R. K.; Soeriyadi, A. H.; Rees, G.; Boyer, C.; Tong, Z.; Davis, T. P.; Becer, C. R.; Haddleton, D. M. *Polym. Chem.,* **2010**, *1*, 1196.
69. Chaudhuri, M. K.; Hussain, S. *J. Mol. Catal. A-Chem.* **2007**, *269*, 214.
70. Kryger, M. *Applications of thiol- ene coupling,* http://www.chemistry.illinois.edu/research/organic/seminar_extracts/2008_2009/Matt_Kryger_Chem535_FA08_Abstract.pdf, **2008**.
71. Campos, L. M.; Killops, K. L.; Sakai, R.; Paulusse, J. M. J.; Damiron, D.; Drockenmuller, E.; Messmore, B. W.; Hawker, C. J. *Macromolecules.* **2008**, *41*, 7063.
72. Cramer, N. B.; Scott, J. P.; Bowman, C. N. *Macromolecules*, **2002**, *35*, 5361.
73. Fiore, M.; Marra, A.; Dondoni, A. *J. Org. Chem*., **2009**, *74*, 4422.
74. Brummelhuis, N.; Diehl, C.; Schlaad, H. *Macromolecules,* **2008**, *41*, 9946.
75. Klemm, E.; Sensfuß, S.; Holfter U.; Flammersheim, H. J. *Macromol. Mater. Eng.,* **1993**, *212*, 121.
76. Lowe, A. *Polym. Chem.*, **2010**, *1*, 17.
77. Nair, D. P.; Podgórski, M.; Chatani, S.; Gong, T.; Xi, W.; Fenoli, C. R.; Bowman, C. N. *Chem. Mater*., **2014**, *26*, 724.
78. Hoyle, C. E.; Lee, T. Y.; Roper, T. *J. Polym. Sci. Part A: Polym.,* **2004**, *42*, 5301.
79. David, R. L. A.; Kornfield, J. A. *Macromolecules*, **2008**, *41*, 4.
80. Serniuk, G. E.; Banes, F. W.; Swaney, M. W. *J. Am. Chem. Soc*., **1948**, *70*, 1804.

81. Gress, A.; Volkel, A.; Schlaad, H. *Macromolecules,* **2007**, *40*, 7928.

82. Lv, A.; Li, Z.; Du, F.; Li, Z. *Macromolecules,* **2014**, *47*, 7707.

83. Hordyjewicz, Z.; You, L.; Smarsky, B.; Sigel, R.; Shlaad, H. *Macromolecules,* **2007**, *40,* 3901.

84. Franc, G.; Kakkar, A. K. *Chem. Soc. Rev.*, **2010,** *39*, 1536.

85. Killops, K. L.; Campos, L. M.; Hawker, C. J. *J. Am. Chem. Soc.,* **2008**, *130*, 5062.

86. Shahi, S. R.; Kulkarni, M. S.; Karva, G. S.; Giram, P. S.; Gugulkar, R. R. *Int. J. Pharm. Sci. Rev. Res.,* **2015**, *33*, 187.

87. Nanjwadea, B. K.; Bechraa, H. M.; Derkara, G. K.; Manvia, F.V.; Nanjwade,V. K. *Eur. J. Pharm. Sci.,* **2009,** *38*, 185.

88. Killops, K. L.; Campos, L.M.; Hawker, C. *J. Am. Chem. Soc.,* **2008**, *16,* 5062.

89. Ma, X.; Tang, J.; Shen, Y.; Fan, M.; Tang, H.; Radosz, M. *J. Am. Chem. Soc.,* **2009**, *131*, 14795.

90. Heidecke, C. D.; Lindhorst, T. K. *Chem. Eur. J.,* **2007**, *13*, 9056.

91. Kottari, N.; Chabre, Y. M.; Shiao, T. C.; Rej, R.; Roy, R. *Chem. Commun*., **2014**, *50*, 1983.

92. Harant, A. W.; Khire, V. S.; Thibodaux, M. S.; Bowman, C. N. *Macromolecules*, **2006**, *39*, 1461.

93. Khire, V. S.; Benoit, D. S. W.; Anseth, K. S.; Bowman, C. N. *J. Polym. Sci. Part A: Polym. Chem.,* **2006**, *44*, 7027.

94. Dinsmore, C. J.; Beshore, D. C. *Tetrahedron,* **2002**, *58,* 3297.

95. Martins, M. B.; Carvalho, I. *Tetrahedron*, **2007**, *63*, 9923.

96. Li, X.; Hopmann, K. H.; Hudecová, J.; Isaksson, J.; Novotná, J.; Stensen, W.; Andrushchenko, V.; Urbanová, M.; Svendsen, J. S.; Bouř, P.; RuudJ, K. *Phys. Chem. A*., **2013**, *117*, 1721.

97. O'Neill, J. C.; Blackwell, H. E. *Comb. Chem. High Throughput Screening*, **2007,** *10,* 857.

98. Borthwick, A. D. *Chem. Rev.,* **2012**, *112*, 3641.

99. Nitecki, D. E.; Halpern, B.; Westley, J. W. *J. Org. Chem.*, **1968,** *33*, 864.

100. Suzuki, K.; Sasaki, Y.; Endo, N.; Mihara, Y. *Chem. Pharm. Bull.,* **1981**, *29*, 233.

101. Fischer, E. *Chem. Ber.,* **1906**, *39*, 2893.

102. Toshihisa, U.; Morinobu, S.; Tetsuo, K.; Nobuo, I. *Bull. Chem. Soc. Jpn*., **1983**, *56*, 568.

103. Naraoka, H.; Harada, K. *J. Chem. Soc. Perkin Trans. I*, **1986**, 1557.

104. Lambert, J. N.; Mitchell, J. P.; Roberts, K. D. *J. Chem. Soc., Perkin Trans. 1*, **2001**, 471.

105. Greenstein, J. P.; Winitz, M. *Chemistry of the Amino Acids*, Vol. 1, Wiley, New York, **1961**, *2*, 785.

106. Kobler, C.; Haeussner, T.; Weckbecker, C. *Cyclic dipeptides as feed additives.* US Patent 20110295006 A1, **2011.**

107. Peptide coupling reagent: http://www.thefullwiki.org/Peptide_coupling_reagent

108. Martins, M. B.; Carvalho, I. *Tetrahedron*, **2007**, *63*, 9923.

109. Pérez-Picaso, L.; Escalante, J.; Olivo, H. F.; Rios, M. Y. *Molecules,* **2009**, *14*, 2836.

110. Nonappa, Ahonen, K.; Lahtinen, M.; Kolehmainen, E. *Green Chem.,* **2011**, *13*, 1203.

111. Eguchi, C.; Kakuta, A. *J. Am. Chem. Soc.,* **1974***, 96,* 3985.

112. Prasad, C. *Peptides*, **1995**, *16*, 151.

113. Tanihara, M.; Hiza, T.; Imanishi, Y.; Higashimura, T. *Bull. Chem. Soc. Jpn.,* **1983**, *56*, 1155.

114. Kawaguchi, K.; Tanihara, M.; Imanishi, Y. *Polym. J.,* **1983**, *15*, 97.

115. Mauger, A. B. *J. Chromatogr.,* **1968**, *37*, 315.

116. MacDonald, J. C.; Whitesides, G. M. *Chem. Rev.,* **1994,** *94*, 2383.

117. Palmore, G. **T**. R.; Luo, T. J.; McBride-Wieser, M. T.; Picciotto, E. A.; Reynoso-Paz, C. M. *Chem. Mater.*, **1999**, *11,* 3315.

118. Akerlund, J.; Harmeier, S.; Pumphrey, J.; Timm, D. C.; Brand, J. I. *J. Appl. Polym. Sci.,* **2000**, *78*, 2213.

119. Gao, J. P. *Urethanes and ureas and processes*, WO Patent 2013142969 A1, **2013.**

120. Gockel, P.; Vogler, R.; Gelinsky, M.; Meißner, A.; Albrich, H.; Vahrenkamp, H.; *Inorganica Chimica Acta,* **2001***, 323*, 16.

121. Carolan, J. V.; Butler, S. J.; and Jolliffe, K. A. *J. Org. Chem.*, **2009**, *74*, 2992.

122. Balasubramanian, D.; Misra, B.C. *Biopolymers,* **1975***, 14,* 1019.

123. Feldstein, R.; Glass, J.; Steiner, S. S. *Self-assembling diketopiperazine drug delivery system,* US Patent 5352461 A, **1994.**

124. Kraft, K. S. *Substituted diketopiperazine analogs for use as drug delivery agents.* US Patent 8906926 B2, **2014.**

125. Steiner, S. S.; Rhodes, C. A.; Shen, G. S.; McCabe, R. T. *Method for making self-assembling diketopiperazine drug delivery system*, US Patent 5503852 A, **1996.**

126. Milstein, S. J. *Diketopiperazin-based delivery systems.* US Patent 5693338 A, **1994.**

Chapter 2 Syntheses and Characterizations of Cysteine-based DKP from S-alkylated derivatives.

2.1 Molecular design and synthetic approaches

L-cysteine is a promising feedstock for future biomass-based materials.[1] In particular, the compounds and polymers derived from cysteine-based DKPs become more attractive, due to its improved thermal mechanical properties.[2] Great efforts have been devoted to the synthesis of cysteine-based DKPs. One of the simple and useful cysteine-based DKPs is the thiol-containing derivative, Cys-Cys (Scheme 2.1). As reported by Greenstein and co-workers, its synthesis starts with the amide bond formation between dicarbobenzoxycystyl chloride and cysteine ethyl ester, followed by removal of the Cbz protecting group with phosphonium iodide (PH_4I) and the disulfide reduction in boiling water with H_2S gas (Scheme 2.1).[3] Since the main obstacle in the formation of Cys-Cys was the high reactivity of thiol functional group towards oxidization, this synthetic route was complicated, and required the use of toxic reagents.[4]

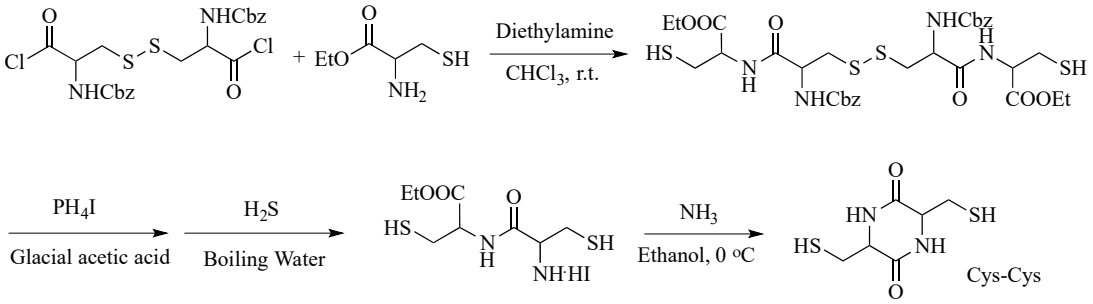

Scheme 2.1 Synthesis of cysteine-based DKP (Cys-Cys).[3]

The difunctional DKP compounds are useful building blocks or monomers for a variety of DKP-based compounds and polymers, such as dithiol-containing Cys-Cys, which would be an ideal monomer for making polymers through the thiol-ene reaction or other reactions such as the one with isocyanates. The preparation of Cys-Cys will be discussed in detail in Chapter 3. Herein, since the thiol group does not survive well during the DKP formation, we envision

a reverse sequence, in which the thiol group in cysteine is either protected first or reacts first before the dimerization of the amino acids to form the DKPs. This synthetic strategy can offer easy access to a variety of the DKP-containing small molecules and macromolecules, derived from L-cysteine (Scheme 2.2).

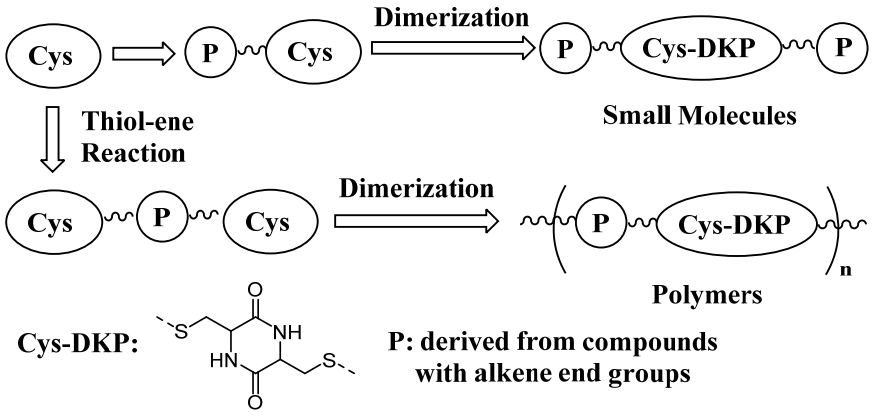

Scheme 2.2 Synthetic routes from L-cysteine for DKP-containing molecules and polymers.

Thiol-ene click (TEC) reactions have numerous advantages, such as high efficiency, high specificity and mild reaction conditions, and thus are ideal for use with L-cysteine.[5] The Michael addition reaction between L-cysteine and mono-acrylates is one of the TEC reactions and can be used to form the thiol-protected precursors to the DKPs. This reaction can be carried out in water, which is ideal for water-soluble cysteine. After dimerization, the products have a rigid six-member ring of DKP and two alkyl side chains. By varying the length of alkyl chains, the resulting DKPs are expected to have different properties. Moreover, the thiol-radical reaction with olefins provides another feasible "green" route to the DKP-based compounds and polymers, which is attributed to the commercial availability of biomass-based olefins and the benefits of thiol-ene radical click reaction.[5]

When using di-alkenes in the TEC reactions, the compounds with the two amino-acid groups can be obtained and can be used as a monomer for making polymers. Upon dimerization,

a series of DKP-containing polymers can be synthesized. The di-alkenes can be selected from either bis-acrylates or any compounds containing the two olefinic groups.

2.2 Results and discussion

2.2.1 Syntheses of S-alkylated cysteine derivatives

L-cysteine is soluble in water (0.112 mg/mL at 25 °C) and readily soluble in ethanol, acetic acid and acetone in acid condition.[6] A thiol-acrylate Micheal addition reaction was reported to proceed in water with almost 100 % yield.[7] Thus, in our work the reactions of L-cysteine with water-soluble acrylates were carried out in water at ambient temperature or in methanol at the elevated temperatures in the presence of boric acid as a catalyst (Scheme 2.3). The S-alkylated cysteine derivatives **1a-1e** were easily obtained in over 95% yields after removing the solvents and washing by acetone.

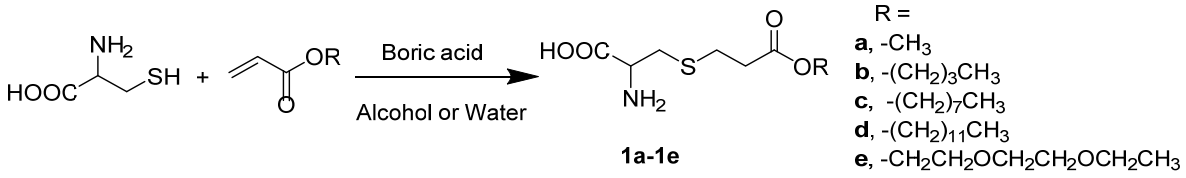

Scheme 2.3 Syntheses of S-alkylated L-cysteine derivatives **1a**-**1e**.

It is known that the pK_a values of a thiol group affect the reaction rate and the yield. The higher pKa value contributes to a stronger nucleophilicity of its corresponding thiolate towards the electron-deficient double bond (Fig. 2.1).[7] Therefore, L-cysteine with a moderate pKa of 8 is quite reactive in the Michael reaction with electron-deficient acrylates in water or alcohol. Comparing with maleimide, cinnamate, alkyne and methacrylate, acrylate is more reactive and easily accessible.[7] Many acrylates are commercially available and have relatively low toxicity. Therefore, acrylate is the best candidate in this thesis work for use in the reaction with L-cysteine.

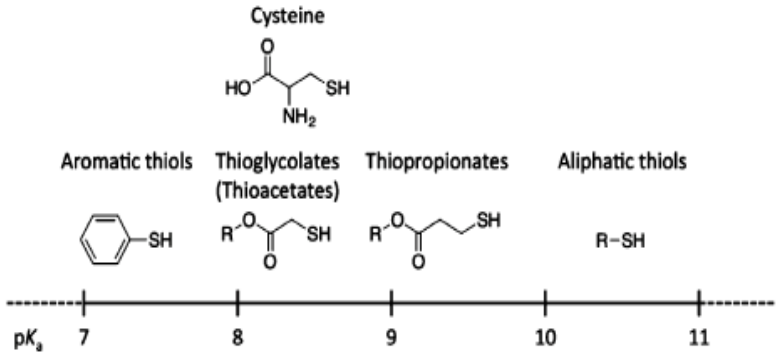

Figure 2.1 The pKa values for different thiol compounds. (Adapted from Ref. 7)

Normally, the thiol-Michael reaction is initiated with the assistance of a catalyst. Over the years, the development of catalysts has experienced steady changes from conventional bases (e.g., triethylamine) to nucleophiles (e.g., phosphines) and from metal catalysts to unusual catalysts (e.g., polyethylene glycol), leading to better efficiency and less undesired side reactions.[8] Although the bases and nucleophiles are the most commonly used catalysts, they are not suitable for use with cysteine. The carboxylic group in cysteine is acidic and can affect the efficiency of base and nucleophile catalysts.[7] In addition, the thiol group in cysteine becomes more labile towards air oxidation in the presence of a base. Therefore, a type of acid catalyst is the best choice. Boric acid is a widely used catalyst in trans-esterification, amide synthesis and esterification.[8,9] Boric acid in water or alcohol is able to generate a proton (H^+), according to the reaction of $B(OH)_3 + H_2O \rightleftharpoons B(OH)_4^- + H^+$ or $B(OH)_3 + ROH \rightarrow B(OH)_3(OR)^- + H^+$. The protonation of the carbonyl group of acrylate activates the substrate effectively for the thiol addition (Scheme 2.4).

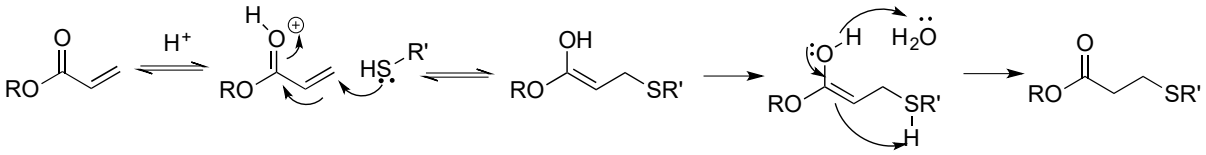

Scheme 2.4 Lewis-acid catalyzed thiol-Michael addition reaction.

The study by Chaudhuri *et al* indicates that boric acid is an effective catalyst for thiol Michael addition reaction of thiophenol with methyl acrylate in water and alcohols, in comparison with over 10 other catalysts including conventional base and metal catalysts.[8,9] By changing the solvents, amount of boric acid and reaction time, the optimal conditions (10 mol % of boric acid in water or alcohol) for the high-yield reaction were found (Table 2.1).

Table 2.1 Reactions of thiophenol with methyl acrylate under various conditions.[8]

Test Run	1	2	3	4	5	6	7
$B(OH)_3$ (mol%)	10	10	10	10	20	20	20
Solvent	MeOH	H_2O	EtOH	ACN	MeOH	H_2O	EtOH
Time (h)	3	4	4	8	2	3	3
Yield (%)	90	89	85	64	92	90	85

Accordingly, boric acid is a choice of catalyst in this thesis work. Using the optimal conditions above, the reaction of cysteine with water-soluble acrylates such as **1a**, **1b** and **1e** went smoothly in good yields. However, acrylates having long alkyl chains are less soluble in water and alcohols and as a result under the same reaction conditions, the reaction is difficult to go to completion and as well there is an increased tendency of self-polymerization at high concentration. By ^{1}H NMR analysis, in the reactions with octyl acrylate and dodecyl acrylate, a large amount of L-cysteine remained and only a trace amount of products **1c** and **1d** were formed.

A set of trial experiments were then carried out in order to optimize the reaction conditions for the synthesis of **1c** and **1d**. In particular, the variables include different solvents (methanol, ethanol, acetone, acetonitrile) or mixed solvents (water/methanol, water/ethanol, water/acetone and water/acetonitrile), different temperatures (ambient temperature, 30 °C, 50 °C and 80 °C) and addition of radical inhibitors (e.g., hydroquinone). The reactions were monitored and analyzed by ^{1} H NMR techniques. Finally, the catalyst-free reaction in methanol

at 50 °C was found to be the best and compounds **1c** and **1d** were successfully obtained with over 90% yield. In Table 2.2, the reaction conditions for the synthesis of S-alkylated L-cysteine derivatives **1a**-**1e** were summarized.

Table 2.2 Reaction conditions for the synthesis of compounds **1a-1e**.

Product	Catalyst	Solvent	Temperature	Yield (%)
1a, 1b, 1e	Boric acid	Water	r.t.	95
1c, 1d	Boric acid	Methanol	50 °C	90

The structures of compounds **1a-1e** were fully characterized by spectroscopic means (See experimental section). As an example, the ^{1}H NMR spectrum of **1a** in D_2O displays proton resonances (ppm) at 3.88-3.83 (m, 1H), 3.63 (s, 3H), 3.09-2.92 (m, 2H), 2.80-2.75 (m, 2H), 2.68-2.63 (m, 2H) (Fig. 2.2a). It could be found that the α-proton of the S-alkylated compound was shifted to 3.85 ppm in the higher field in comparison with the one in L-cysteine at 3.97 ppm. Moreover, the formation of the new peaks in the range of 2.63 ppm to 2.80 ppm, which are assigned to the protons belonging to the carbon from the alkene double bond and are characteristics for the successful addition of thiol on acrylates. In the ^{13}C NMR spectrum, carbon resonances (ppm) at 175.06, 172.71, 53.50, 52.32, 33.84, 32.07 and 26.32 were observed (Fig. 2.2b). The peaks for the two carbonyl carbons appear at 175.06 ppm and 172.71 ppm, which further confirmed the successful synthesis of S-alkylated cysteine derivative **1a**.

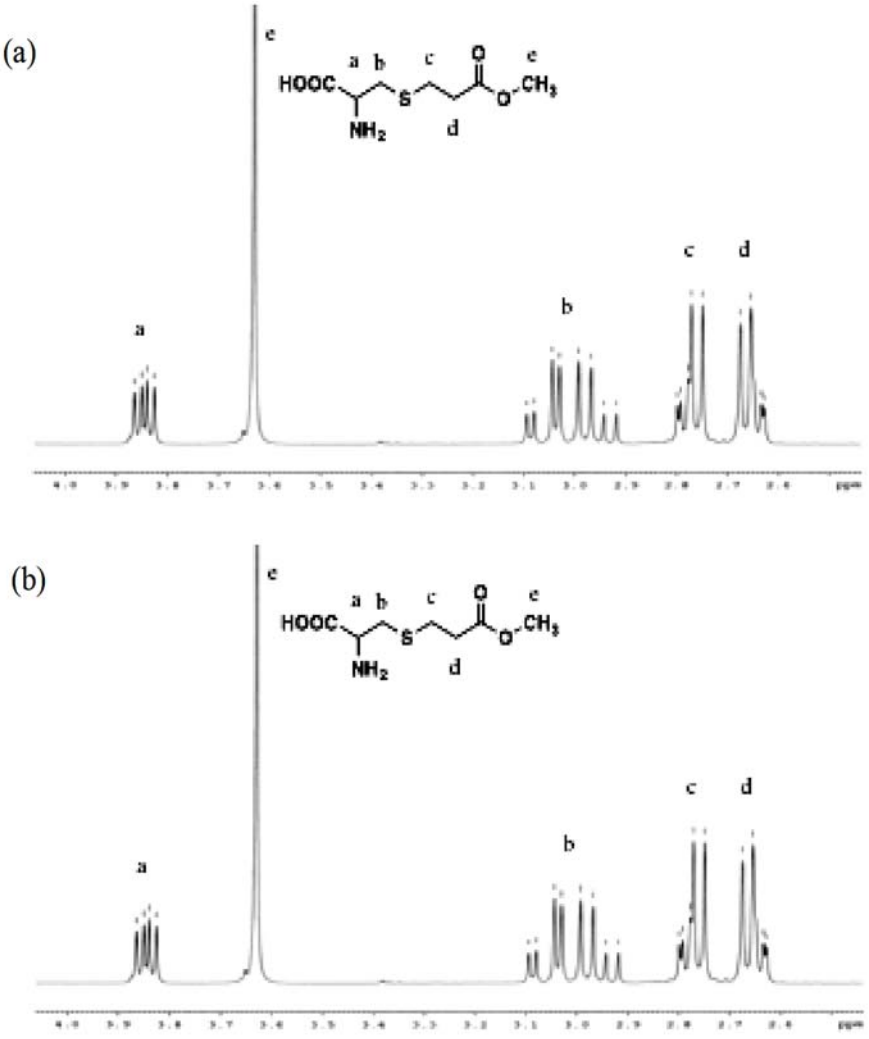

Figure 2.2 ^{1}H NMR (300 MHz, D_2O) and ^{13}C NMR (75 MHz, D_2O) spectra of **1a**.

All of the acrylates in Scheme 2.3 were directly purchased from commercial sources. But acrylates could also be synthesized by esterification of acrylic acid with an alcohol. Cholesterol is important for cell membrane and a precursor to a variety of biologically active substances.[10] If L-cysteine could be attached on cholesterol, the resulting compound would be of interest, for example, mimicking the activities of certain proteins. Therefore, the esterification between cholesterol and acrylic acid was done to yield the desired cholesterol acrylate.[11] However, the subsequent reaction with L-cysteine failed, possibly due to its large steric hindrance.

Moreover, methyl methacrylate (MMA) IS structurally similar to acrylate but less hazardous, so it was tested in our project. However, MMA is less reactive and requires an uncommon catalyst, for example, phosphine-mediated catalyst, in the thiol-Michael reaction. Furthermore, MMA tends to undergo a self-condensation reaction or even polymerization in the presence of a thiol compound.[12] Therefore, MMA was not used in our work.

Beside thiol-Michael addition reaction, the thiol-ene radical reaction is also applicable to L-cysteine and a variety of alkenes. The thiol-ene radical reaction is known for its click reaction features and has high tolerance to oxygen and water, as well as various functional groups.[5] The reactions of L-cysteine with some alkenes were fairly simple and straightforward (Scheme 2.5). L-cysteine was gradually dissolved in ethanol with the addition of HCl and then 10 % of the photoinitiator, dimethoxyphenylacetophenone (DMPA), was added. The mixture was irradiated under UV-lamp (λ = 365 nm) at room temperature for 3h. When large amounts of precipitates or turbidity were observed, the solvent was removed to give compounds **1f-1i** as light-yellow solids with over 98% yield.

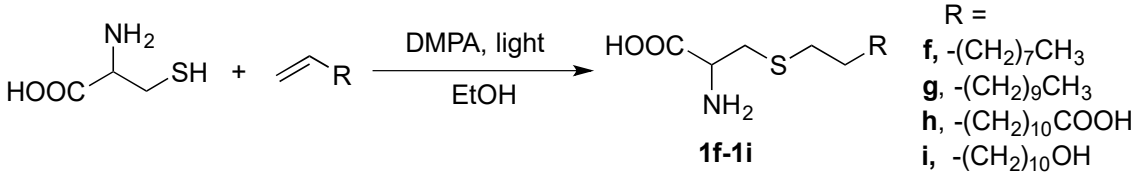

Scheme 2.5 Syntheses of L-cysteine derivatives **1f-1i** by thiol-ene radical reaction.

The structures of compounds **1f-1i** were characterized by spectroscopic means (See experimental section). As an example, the ^{1}H NMR spectrum of **1f** in DMSO-d_6 displayed proton resonances (ppm) at 4.11-4.06 (m, 1H), 3.02-3.01 (d, 2H), 2.58-2.53 (t, 2H), 1.54-1.44 (m, 2H), 1.28-1.23 (m, 14H), 0.86-0.82 (t, 3H) (Fig. 2.3). Compared with acrylate derivatives, the α-proton of amino acid in **1f** was shifted more significantly to 4.15 ppm due to the acidic

atmosphere in the ^{1}H NMR spectra. And the new peak appeared at 2.55 ppm further confirmed the successful addition of thiol group on carbon double bond.

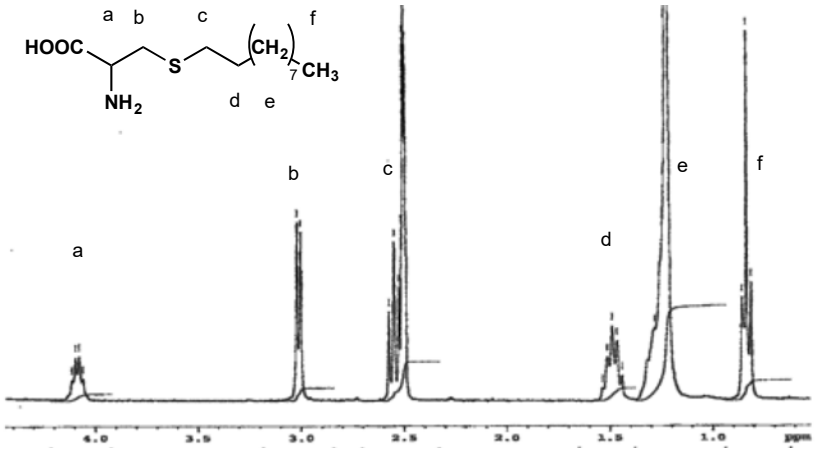

Figure 2.3 ^{1}H NMR spectrum (300 MHz, DMSO-d_6) of compound **1f**.

2.2.2 Syntheses of cysteine-based DKPs

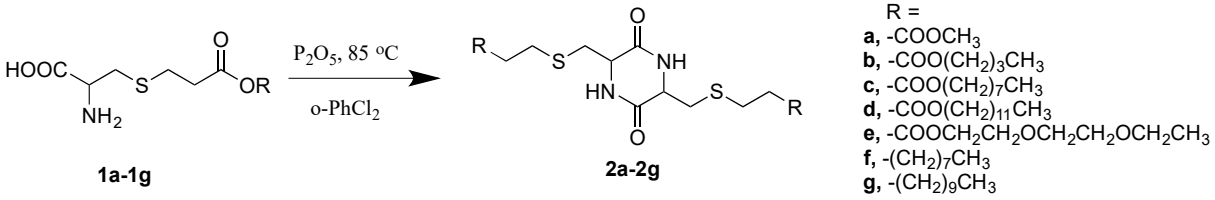

Scheme 2.6 Syntheses of cysteine-based DKPs **2a**-**2g**.

The synthesis of DKP **2a-2g** involves the dimerization of **1a-1g** through intermolecular amide formation and intramolecular lactamization (Scheme 2.6). The reaction was carried out in 1,2-dichlorobenzene in the presence of P_2O_5 as a catalyst and dehydrating reagent. The reaction was first run at temperatures from 40 to 140 °C. It was found that the reaction did not go to completion when the temperature was lower than 80 °C and at high temperatures the starting materials and final products tend to decompose. Thus, the reaction was best carried out at 80-110 °C.

The dimerization of **1h** and **1i** failed due to the interference from additional carboxylic acid groups and hydroxyl groups, which led to undesired side reactions. The obtained

compounds from the same reaction condition were the mixtures containing amino acid linear dipeptide, cyclic dipeptide and esters or amides. In fact, we tried to identify the structures by NMR and IR spectroscopy but failed to obtain any useful information on their structures due to severe peak overlapping.

As discussed in Chapter 1.5.1, peptide coupling reagents are necessary in the formation of DKPs in most cases. These agents react with one amino acid to form reactive intermediates which, in turn, react with the N-terminal amine of another amino acid to form a peptide.[13] Some of the known coupling reagents were tested in our work, including dicyclohexylcarbodiimide (DCC), diisopropylcarbodiimide (DIC), O-benzotriazol-1-yl-tetramethyluronium (HBTU), diphenylphosphoryl azide (DPPA) and Eaton's reagent. However, all of the tests failed. It was found that there was no reaction proceeding in the presence of HATU and HBTU. The reactions with DCC and DIC only afforded the linear dipeptides rather the desired cyclic DKPs. With DPPA, the reaction gave a complicated mixture containing a small amount of the DKP. And the starting material decomposed when Eaton's reagent was used.

Phosphorus pentoxide has been reported as an effective coupling reagent in the preparations of DKPs from glycine, alanine, leucine, isoleucine and phenylalanine.[14] In the case of "*Phosphorus pentoxide as a reagent in peptide synthesis*", it was described as a high-efficiency coupling reagent for making linear dipeptide from the protected amino acid.[15] Later in 2007, Stevenson and co-workers further revealed the remarkable efficiency of P_2O_5 in cyclo-condensation reaction of amino acids by comparing the catalyzed and unanalyzed DKP syntheses (Table 2.3). It was demonstrated that P_2O_5 could not only speed up the reaction rate, but also improve the yields significantly.[16] Therefore, P_2O_5 as an ideal catalyst with the features including simple, cost-effective, environmental-friendly, easy removal by water or methanol and high efficiency, was utilized in our work.

Table 2.3 Comparison of the catalyzed and uncatalyzed DKP synthesis.[16]

Catalyst	Temperature °C	Time (hours)	% Yield DKP
None	165	24-33	25-35
H_2SO_4	165	4	35
H_3PO_4	165	4	55
P_2O_5	165	1.5	60

In terms of the reaction solvent, the choice of 1,2-dichlorobenzene and NMP was not random. In fact, most of the common solvents available in laboratory were carefully examined, including m-cresol, acetonitrile, ethylene glycol, toluene, tetrahydrofuran, N,N-dimethylformamide (DMF), N-methyl-2-pyrrolidinone (NMP), chlorobenzene, dioxane, dimethylacetamide and dichlorobenzene. Several factors were taken into account when selecting a suitable solvent for this reaction: 1) Boiling points. Since the reactions proceed at relatively high temperatures, a solvent with a boiling point over 100 ºC is desirable. 2) Polarity. If the intermediate, a linear peptide, precipitates from the reaction medium, the subsequent cyclization is unlikely to proceed. Thus, a polar solvent is preferred to keep the intermediate in solution. 3) Nature of solvents. It has been proved by Jones *et al*. that the autoprotolysis equilibrium constants of the protic or protogenic solvents and solvent's proton affinity had significant effect on the reaction rate and efficiency. Protophilic solvents, which has a greater tendency to accept protons, are more conducive for dimerization.[17] Thus, 1,2-dichlorobenzene which is a polar, protophilic and high-boiling solvent, is the best choice for cyclization reaction.

Dehydration is the most important step in DKP formation, where water is the by-product in equilibrium with the DKP product. By removing water, the equilibrium reaction proceeds in favor of the formation of the target product. Thus, a stream of N_2 is purged continuously to remove water during the reaction. Otherwise, the reaction could not go to completion and afforded a mixture of linear and cyclic peptides that are extremely difficult to separate.

The course of the dimerization reaction could be monitored by the changes of the α-proton from amino acid by ^{1}H NMR spectroscopy. For example, after 1 hour of dimerization of **1a**, a new peak appeared at 4.15 ppm along with the peak at 3.8 ppm (spectrum b in Fig. 2.4), indicating a low degree of conversion at the early stage of reaction. The peak at 4.25 ppm gradually increases as the reaction proceeds (spectrum c in Fig. 2.4). After 6 hours, the ^{1}H NMR spectrum shows the presence of two intense peaks at 4.25 and 4.15 ppm and absence of the α-proton resonance at 3.8 ppm (spectrum d in Fig. 2.4).

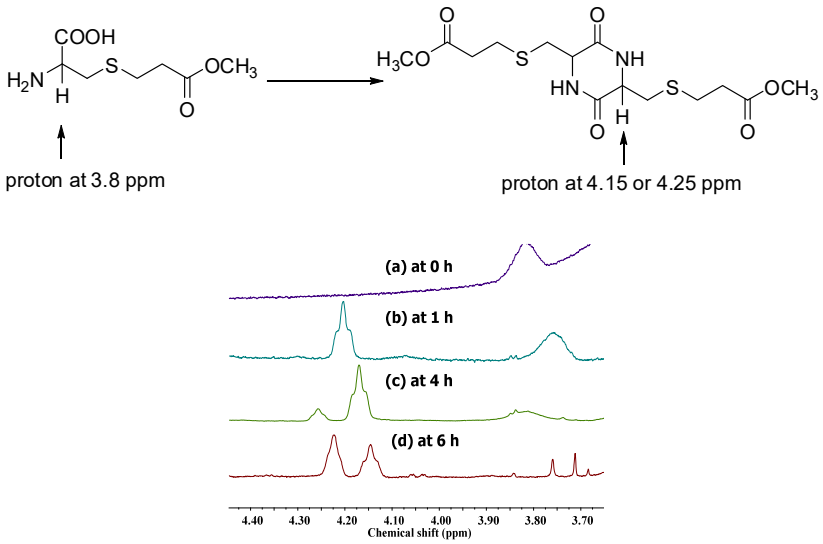

Figure 2.4 ^{1}H NMR spectra (300 MHz, DMSO-d_6) showing the progress of dimerization reaction of **1a** to form **2a** at different reaction times.

It is known that the dimerization of amino acid esters leads to the formation and isomerization of the cis/trans-DKP isomers, where the cis-DKP is C_2-symmetric and the trans-isomer is center-symmetric (Scheme 2.7). Moreover, the two diastereomers have the same molecular weights, but can be clearly distinguished by NMR methods.[18] It is assumed that the formation of diastereomers is resulted from the epimerization of the chiral α-proton at high temperature. Thus, at the beginning of reaction, the formation of LL-isomer was predominated because of the presence of a large amount of L-stereo isomeric precursor. As the dimerization

reaction proceeds, isomerization between the cis-isomer and the trans-isomer also takes place, leading to the formation of two diastereomers or LL-/DD- and LD-DKP. Therefore, the peak at 4.25 ppm can be assigned to trans-DKP **2a** and the one at 4.15 ppm is from the cis-isomer (Fig. 2.4).

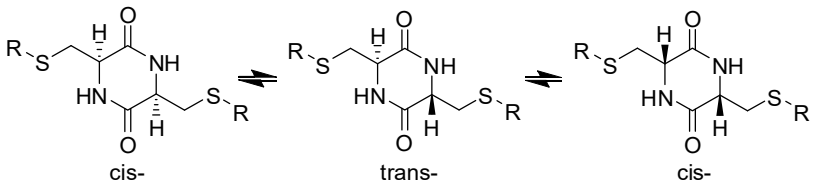

Scheme 2.7 Isomerization of cis- and trans-DKP isomers.

The assumption was supported by the results from other amino acid-based DKP research. In 1986, Naraoka and co-workers studied the stereochemistry of several DKPs made by self-condensation of amino acid esters (Table 2.4).[18] They clarified that the side groups not only influenced the reaction rates, but also determined the portion of diastereomers. The less bulky side group tends to drive the formation of trans-isomer at a faster reaction rate. But the more important finding was that little racemization took place in the beginning of the reaction where only cis-isomer presented, and with times went by, the ratio of cis/trans gradually decreased.[18] These views are consistent with the results from the work by Ueda *et al*.[19]

Table 2.4 Ratios of trans-DKP isomer in the mixture. (Adapted from Ref. 19)

Starting Material		Time (days)	Yield (%)	Trans:mixture ratio
DL-Ala-OMe	(1)	0.25	2.4	0.36
	(2)	0.5	10.0	0.43
	(3)	1	40.3	0.5
	(4)	2	64	0.53
DL-Ala-OEt	(1)	1	6.5	0.3
	(2)	1.5	15	0.36
	(3)	2	22.7	0.4
	(4)	3	44.1	0.45
DL-Leu-OMe	(1)	1	0.4	0.16
	(2)	2	3.2	0.27
	(3)	3	11.1	0.36
	(4)	4	25.5	0.43

DKPs derived from various amino acids were also investigated, which found that the α-proton of trans-DKP was normally located at the lower field region than that of cis-DKP in the ^{1}H NMR spectra. For example, in the study by Shoji and co-workers, the chemical shift of the $^{\alpha}$H signal for LL-Ala-Ala is located at 4.3 ppm and the signal of LD-isomer is at 4.7 ppm.[20] Tanihara *et al.* also confirmed the α-H signal of cis-Val-Val at 3.65 ppm and of trans-isomer at 3.68 ppm.[21] Additionally, Kopple and co-worker demonstrated that this phenomenon was observed in both symmetric and unsymmetrical DKPs, as well as the DKPs containing aromatic side chains.[22] Therefore, the assignments of peak at 4.25 ppm to trans-DKP **2a** and the one at 4.15 ppm to cis-isomer are reasonable.

Naraoka and coworkers also found that at the higher temperatures the dimerization is faster and the more racemization takes place.[19] The same observations were made in the preparations of cysteine-based DKPs. It was found that there were three possible factors that can influence the diastereomeric ratios, namely temperature, time and catalyst. Therefore, for a given reaction time of 6 hours, the effect of P_2O_5 catalyst and reaction temperature on the compositions of cis/trans isomers or diastereomers was investigated for the dimerization of **1a**. The ratios of cis and trans isomers were determined by the ^{1}H NMR method and listed in Table 2.5. It was clear that the temperature and catalyst concentration had a significant impact on the reaction outcomes. When increase in the temperature or catalyst concentration, the trans-isomer was formed more than the cis-isomer or the LD-diastereomeric DKP was a major product.

Table 2.5 Factors that influence the formation of cis/trans isomers of **2a**

Run	Time (h)	Catalyst (wt %)	Temperature (°C)	Cis: Trans Ratio
1	6 h	10	80	1:0.8
2	6 h	20	80	1:1.2
3	6 h	10	120	1:1.5

It is known that diastereomers have different physical and chemical properties, and thus are worth separation. Chromatography is the most popular method of separating diastereomers.[23,24] Because the DKPs from **2b** to **2g** are more soluble in organic solvents with the increase of the chain lengths, these compounds could be separated by column chromatography. For example, the cis- and trans-isomers of **2b** could be separated by column chromatography eluting with hexane/acetone at the ratio of 2:1 and 1:1, respectively.

It was observed that the diastereomeric isomers of DKP **2a** were also able to be separated by selective precipitation in methanol. Due to the different conformations of the rigid DKP rings and hydrogen bond interactions, the dominant isomer was prone to aggregate in methanol and precipitate afterwards. Thus, the desired pure isomer of DKP **2a** could be easily obtained through controlling the ratio of the diastereomers formed during the dimerization process, followed by a simple filtration work-up. For example, when the reaction stopped at the early stage, the cis-isomer of **2a** was the main product. Since it could self-aggregate and precipitate from methanol, the pure cis-isomer was successfully isolated by simple filtration. Likewise, when the trans-isomer became the major component, the product collected from methanol precipitation would be pure trans-isomer. It was found that the isomers of compound **2a** had an obvious difference in physical properties. For example, the cis-isomer has a melting point at 220 ^{o}C, which is slightly higher than its trans-counterpart. In addition, the solubility of trans-**2a** in dichloromethane is better than its cis-counterpart, which was attributed to the fact that cis-isomer has greater tendency in self-assembling through intermolecular hydrogen bonds (N−H···O) between adjacent molecules.

The structures of compounds **2a-2g** were fully characterized by spectroscopic means (See experimental section). Take the ^{1}H NMR spectra of cis- and trans-**2a** as an example, where the spectrum of trans-**2a** displays proton resonances (ppm) at 8.26 (s, 1H), 4.22 (s, 1H), 3.60 (s, 3H), 3.08-3.02 (m, 1H), 2.84-2.78 (m, 1H), 2.77-2.72 (m, 2H), 2.61-2.56 (m, 2H); those for

cis-**2a** locates at 8.20 (s, 1H), 4.15 (s, 1H), 3.60 (s, 3H), 3.02-2.96 (m, 1H), 2.91-2.85 (m, 1H), 2.78-2.73 (t, 2H), 2.62-2.57(t, 2H) (Fig. 2.5). A clear difference was observed from the signals of CH_2 in amino acid, where the peaks of cis-isomer was more narrow, which was attributed to the conformational differences of the cyclic rings and intramolecular hydrogen bonds. Therefore, to distinguish the diastereomers of cysteine-based DKPs, one could simply compare the specific data in ^{1}H NMR spectra.

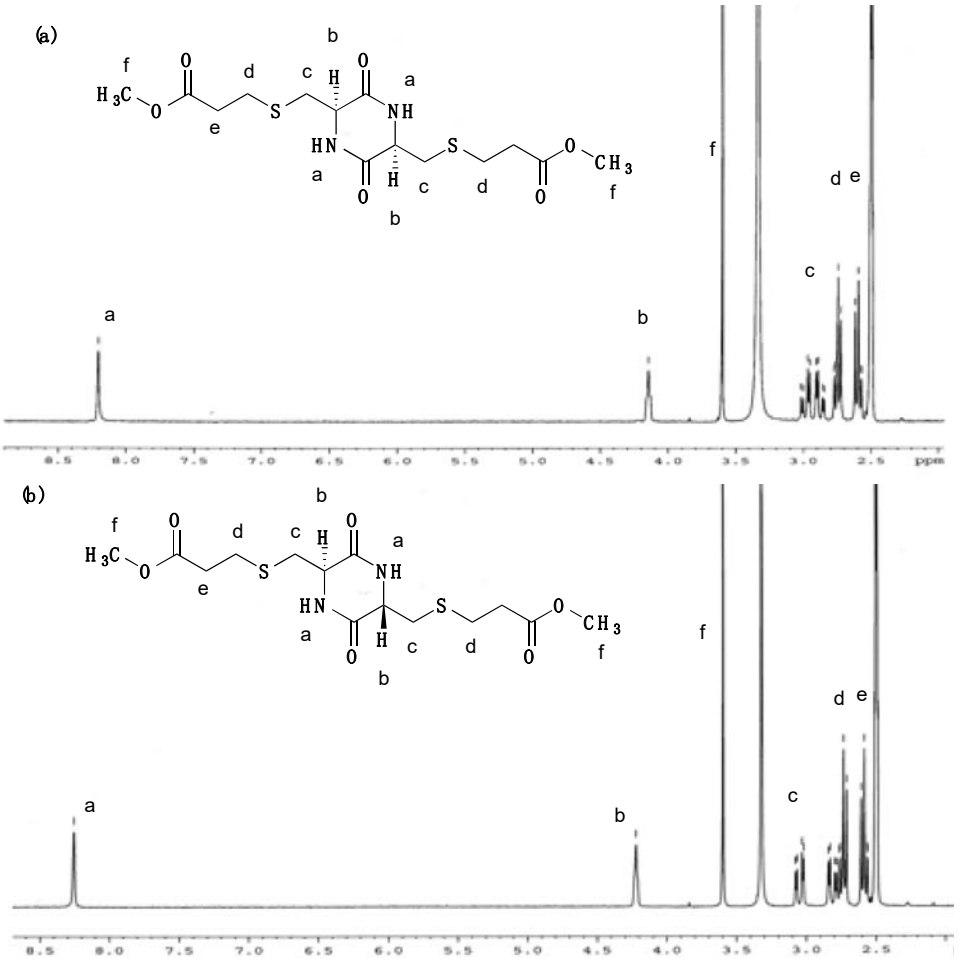

Figure 2.5 ^{1}H NMR (300 HMz, DMSO-d_6) spectra of (a) cis-**2a** and (b) trans-**2a**.

Studies on DKPs having aliphatic side chains revealed that the information on isomer structures could be obtained from the ^{3}J coupling constants of H-$^{\alpha}$C-$^{\beta}$C-H. In NMR analysis, cis-DKP normally has a larger coupling constant compared to the trans-isomer. For example, the coupling constants of cis-Val-Val is 3.31 Hz whereas the value of trans-isomer is 2.94 Hz.

In addition, cis-Leu-Leu has 8.46 Hz coupling constant which is larger than its *trans*-counterpart (7.35 Hz).[25] Thus, the ^{3}J coupling constants of H-$^{\alpha}$C-$^{\beta}$C-H of compound **2a**, 5.1 or 3.9 Hz for the cis-isomer and 3.3 or 3.6 Hz for the trans-isomer of cysteine-based DKPs, are consistent with previous assignments of LL- and LD-isomers. Additionally, the results from HSQC and COSY experiments drew the same conclusion on the assignment of cis- and trans-isomers (See Appendix A).

A library of studies on the conformations of cyclic dipeptides including infrared spectroscopy (IR), NMR, vibrational circular dichroism and X-ray diffraction, were punished .[26] Among them, nuclear Overhauser effect (NOE) test is a useful NMR experiment to aid the structure assignments and has been widely used to identify DKP conformations.[26,27] In our work, by irradiating the α-proton only, a 16.5% NOE on NH was observed for the cis isomer and 9.1% NOE was registered for the trans isomer by irradiating the α-proton only (See Appendix A). The observations were in accordance with the speculation that the cis-*i*somer was normally existing in boat or twist boat conformation, while trans-isomer prefers a planar ring.[28] Single crystals were also grown in various organic solvents for X-ray diffraction testing. Unfortunately, the single crystal was too small to be useful.

2.2.3 Attempted syntheses of DKPs by other methods

According to my knowledge on DKP synthesis, the commonly used methods are: solution method and microwave-mediated method nowadays.[13] The most conventional method is the solution method with the assistance of a coupling reagent. The reaction condition used in our work is under this category. Before it was determined, countless experiments were conducted to explore the right reaction method and conditions for the preparation of cysteine-based DKP.

Attracted by the high conversion rate, microwave synthesis was first implemented in this project.[29] Since the sample experiment we conducted on lysine was successfully converted to Lys-Lys, therefore the dimerization of the S-alkylated compound **1a** was conducted in the same reaction condition, where the starting material was mixed well with several drops of DMF first and then irradiated in microwave for 5-10 mins. However, a strong odor was given off from the microwave after the reaction stopped and the mixture surface turned to be complete black. Since the unpleasant smell and black surface were from the decomposition of S-containing compound, it was proved that the microwave technique was not suitable in cysteine-related reaction. Based on my experience from the utilization of microwave method in cysteine-based DKP syntheses, the microwave reaction has some drawbacks: 1) The system is completely closed, which may lead the reactor to deform or even explode, if the reaction creates high temperature and high pressure; 2) It is hard to measure the reaction temperature and could lead to significant side reactions; 3) The reactant amount is limited; 4) The heat is mainly concentrated at the bottom of tray or on the surface of the compound. Since the energy of the reaction system is uneven, the yield would be extremely low; 5) It prevents the organic synthesis which normally requires stirring, refluxing and dropping.

Keeping the essence of the microwave method, an oven method was developed, where the Ace pressure tube was used to avoid the interference from the air and oven was adopted to ensure a better control on the reaction temperature. The sample test was performed with histidine. At first, 1 g of histidine with 2-3 drops of water were placed at the bottom of the pressure tube and stirred vigorously after the addition of 10% acid such as HCl, H_2SO_4 or phosphoric acid. Then the tube was allowed to stand in the oven at 140 ^oC for around 4-8 hours. After the reaction finished, the target compound cyclic histidine was easily collected through simple purification in over 95% yield. The key step here was the adjustment of back-seal and front-seal cap. At the early stage of the reaction, when water was required to mix the starting

material and the acid catalyst, the front-seal cap was used to avoid water leaking. After the dimerization started for 1 h, the cap was replaced by a back-seal cap to allow the release of water and the equilibrium reaction would proceed in favor of the formation of the target product. This method was quiet effective and green, since only water and minimum amount of the acid were required, as well as the high yield. Though the reaction condition was well defined from sample experiments; unfortunately, it failed again to produce cysteine-based DKP due to the same decomposition problem.

2.2.4 Syntheses of DKP-containing polymers

DKP structure has been successfully incorporated into the preparation of green polymers, such as lysine-based DKP containing polyesters and polyurethanes. These DKP-containing polymers not only exhibit improved mechanical and thermal properties, due to the existence of rigid DKP ring, but also are potentially biodegradable and biocompatible since DKP is able to be hydrolyzed back into the corresponding amino acids.[2] However, there is no research on cysteine-based DKP containing polymer yet. Encouraged by the high yield of cysteine-based DKP formation in Chapter 2.2.2, the synthetic condition was feasible for the preparation of DKP containing polymers (Scheme 2.8).

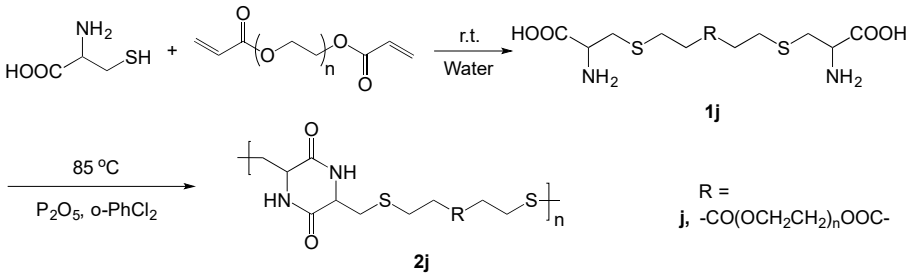

Scheme 2.8 Synthesis of DKP-containing polymer **2j.**

Considering the solubility influence on reaction efficiency in Scheme 2.1, water-soluble poly (ethylene glycol) diacrylate was chosen to prepare the corresponding polymer.

The reaction was carried out in water at room temperature to give **1j** in good yield and further dimerization led to a water-soluble polymer **2j** with high molecular weight. However, the obtained polymer was a viscous liquid that was soluble in a wide range of solvents from non-polar ethyl ether to polar DMSO solvent, and hard for purification. Thus, the polymer was purified through vigorous and repeated washing in hexane. The structure of compound **2j** was fully characterized by spectroscopic means (See experimental section). Polymer molecular weight and polydispersity indices (PDI) were determined by gel permeation chromatography (GPC) relative to polystyrene standards, where the number-average molecular weight of the obtained polymer was $3.03*10^5$ g/mol, the weight-average molecular weight was $5.03*10^5$ g/mol and the PDI was 1.48. Considering the high binding ability of L-cysteine with different metal ions, the water-soluble polymer is potentially applied in sewage treatments.

DKP-containing polymer with long alkyl chains is another type of desirable structure, in which DKP could pack through hydrogen bond to form hard block and the long alkyl chain was soft block. The synthetic polymer with alternative blocks was expected to show interesting features such as amphilicity for pharmaceutical applications or as an elastic polymer. Therefore, the diacrylates with long alkyl chains, 1,6-hexanediol diacrylate, was used in our work. However, due to its low solubility in aqueous solution and great tendency for self-polymerization at high temperature, only minimum acrylate was linked to L-cysteine and the target product was unable to be separated from the side products. To produce the polymer with alternative block, dialkene containing a long alkyl chain was then selected and reacted with L-cysteine through thiol-radical reaction to produce cysteine end-group compound **1k** for further dimerization (Scheme 2.9). However, in the second dimerization step, it was found that there were precipitates gradually formed after several hours of reaction, which was attributed to the poor solubility of the formed oligomer **2k**. Moreover, large amounts of starting material **1k**

were detected by ^{1}H NMR analysis. Thus, lack of efficient solvent, only oligomer **2k** was obtained without film-forming ability.

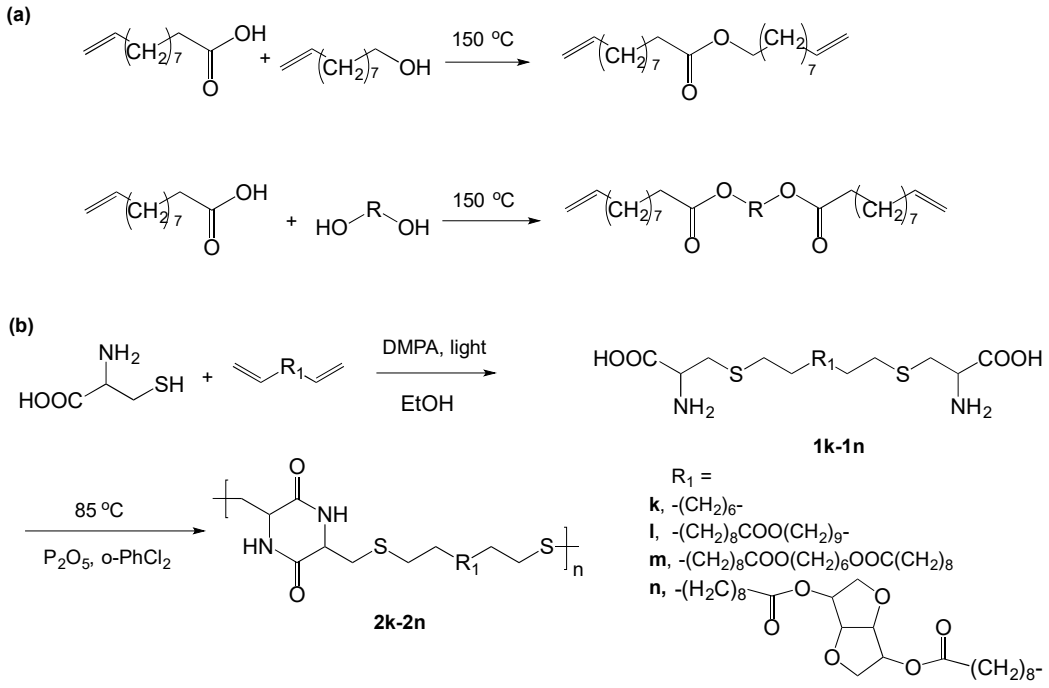

Scheme 2.9 Syntheses of (a) alkenes from undecenoic acid and diols and (b) DKP-containing polymers **2k-2n.**

Beside the commercially available diacrylates and diene, the substrates for thiol-ene reaction could also be synthesized in lab. Unlike the preparations of diacrylates which require specific catalyst and complicated work-ups for purification, the preparation of diene is easily achieved through simple esterification between an olefin containing acid and alcohol, and the product can be directly used for subsequent photoinitiated reaction without purification. Inspired by the successful synthesis of compounds **1h** where L-cysteine and undecenoic acid reacted smoothly without any side reactions, a series of bifunctional compounds with terminal olefins were produced through simply heating undecenoic acid and alcohol at 150 °C overnight (Scheme 2.9a). The reaction was not only a neat reaction, but also a green reaction due to its catalyst-free process, solvent-free system, water as the only byproduct, high yield, especially

the usage of biomass-based starting materials. In terms of the acid selection, undecenoic acid is an unsaturated fatty acid derived from castor oil, which has been widely used in the production of pharmaceuticals precursors, personal hygiene products, cosmetics and perfumes.[30] In terms of the selected diols in Scheme 2.10, they were also bio-based feedstock such as 1,6-haxane diol and isosorbide.[31,32] Indeed, a natural soybean oil without bio-refinery treatment and elucidated containing dihydroxyl groups was also used to prepare difunctional alkenes in our work.[33] As expected, the esterification was successful. But the subsequent thiol-ene reaction failed due to the existence of extra C=C or unknown functional groups in the polyol structure. In fact, we tried to identify the structures by NMR and IR methods but failed to obtain any useful information on the structures.

Followed the synthetic route in Scheme 2.9, a series of compounds with cysteine end-groups were successfully prepared for polymerization. The polymerization of monomer **2l** was successful and led to the desired polymer **2l**, which could form a thin film by casting. The structures of polymer **2l** was fully characterized by spectroscopic means and polymer molecular weight was determined by GPC measurements which was $5.29*10^4$ g/mol (See experimental section). However, the polymerization of monomers **1m** and **1n** failed due to their poor solubility in dichlorobenzene, which led to early precipitation of the oligomers after several hours of reaction. ~~I~~t is known that the degree of polymerization is closely related to the reaction conversion efficiency. Considering the low yield (85%) of dimerization of small molecule (Chapter 2.2.3), it is not surprised that the target polymers with high molecular weights could not be obtained.

2.3 Chiroptical property of cysteine-based DKP compound

L-cysteine contains a chiral carbon and is capable of producing chiral derivatives. Many L-cysteine derivatives are known to have chiroptical activity for metal sensing application.[34,35]

Therefore, the chiroptical property of the DKP-containing compounds were measured to explore their applications. CD spectroscopy was used herein as a primary signal detection technique, because it could provide useful information about the supra-molecular conformation and it can be used orthogonally to other spectroscopic techniques for sensing purposes.[36]

Compound **2a** with the simplest DKP structure was measured as an example. First, it was found that compound **1a** is chiral and optically active, as characterized by CD spectroscopy (Fig. 2.6). The CD spectra of compound **1a** shows a peak at 225 nm with a positive Cotton effect. This result is consistent with the point that there is no racemization detected during the synthesis of S-alkylated compound.[37]

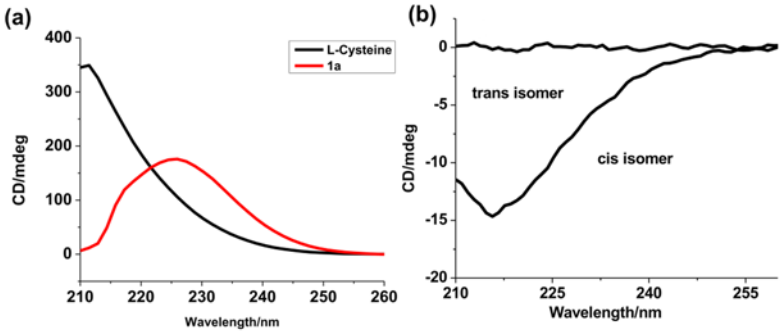

Figure 2.6 CD spectra of (a) L-cysteine and compound **1a** in water; (b) cis-**2a** and trans-**2a** in water.

Then, CD measurements on DKP diastereomers were performed. It is known that the C_2-symmetric cis-DKP is optically active and center-symmetric trans isomer is not optically active (Scheme 2.7). When the dimerization reaction of **1a** was terminated at the early stage where the cis-isomer was mainly produced, the isolated cis-isomer of **2a** was detected optically active with a specific optical rotation of -88° (C = 0.05, CH_3OH). Its CD spectrum displays a negative Cotton effect at 220 nm, which can be assigned to the n-π* transition of the amide group. The observation was consistent with reference to other known cyclic amino acids. For example, leucine-based DKP has a negative signal at 208 nm and valine-based DKP has a negative Cotton effect at 200 nm.[25] Moreover, as expected, the trans-isomer of **2a** showed no

optical activity. However, when the dimerization reaction went to nearly completion, the final products became totally optical inactive, indicating the complete racemization of each chiral isomer.

Cysteine-based DKP contains the amine (-NH), carbonyl (-COOH) and thiol (-SH) groups that are able to bind a number of metal ions through coordinate covalent bond.[38] If the metal binding is selective or specific and leads to a significant change in chiral property, the change of chiroptical activity could be used for sensing certain metal ions. The binding behavior of the isolated optically active cis-isomer of compound **2a** with different metal ions was studied by CD measurement. Solutions of various metal ions (Zn^{2+}, Cu^{+}, Pd^{2+}, Ni^{2+}, Mg^{2+}, Ca^{2+}, Ba^{2+}, Co^{2+}, Li^{+}, Mn^{2+}, Pb^{2+}, Na^{+} and Ag^{+}) were added and CD spectra were taken immediately afterwards (See experimental section). For the un-chelated ions, for example Pt^{2+}, there was no signal changing observed. For most of the chelated ions, chelation induced only slightly shift or decrease in CD signals, for example, Cu^{2+}. When Cu^{2+} was added, The CD band shifted from 217 nm to 233.7 nm accompanying a significant decrease (Fig. 2.7).

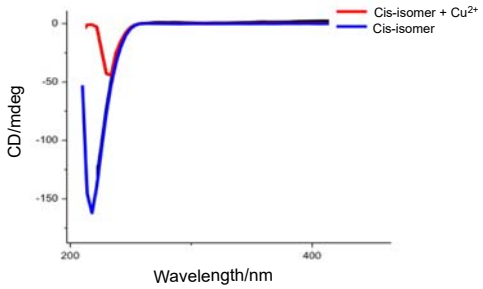

Figure 2.7 CD spectrum of cis-**2a** with Cu^{2+}.

But the chelation with silver ion induced a large change in CD spectra (Fig. 2.8a). As showed, upon addition of silver ion (1 x 10^{-5} M), a new CD band with an opposite sign appeared at 230 nm. By changing the molar ratios of Ag^{+} to the optically active cis-isomer of **2a**, the maximal binding ratio of 1:2 was found (Fig. 2.8b). The binding behavior of cysteine-based DKP with Ag^{+} was detected for the first time, but according to the conformations proposed

between Zn and Cys-Cys, the binding conformation of Ag^+ was also proposed (Fig. 2.9).

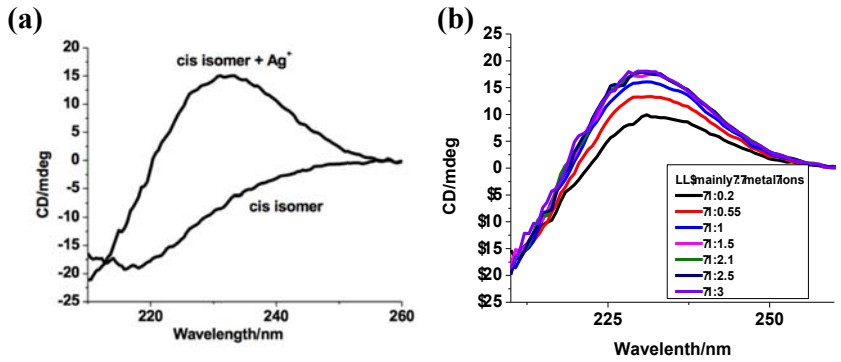

Figure 2.8 (a) CD spectra of cis-**2a** with Ag^+; (b) cis-**2a** with various molar ratios of Ag^+.

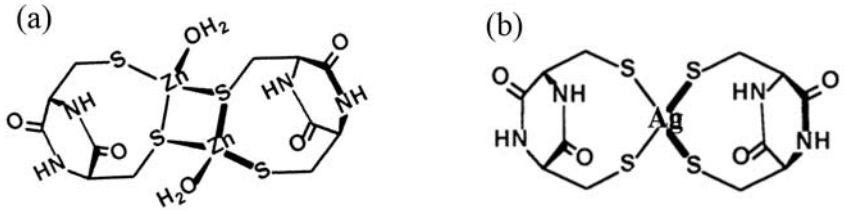

Figure 2.9 Proposed binding of L-cysteine-based molecules with metal ions. (Drawing (a) is adapted from Ref. 38)

Sensing and monitoring the silver ion become important as silver pollution in environment increasingly threatens a broad range of micro-organisms and marine invertebrate. Various chemo-sensors have been developed for Ag^+ detection in aqua system which are normally based on organic fluorophores and semiconductor quantum dots. However, these chemo-sensors have some drawbacks such as hard preparation, low water solubility, and/or poor selectivity toward Ag^+.[39] Thus, water-soluble, optically active cysteine-based DKP could be used as a sensitive CD probe for detection of silver ion in water with a concentration as low as 1 x 10^{-5} M. In addition, since the cysteine-based DKP compounds are potentially biodegradable, the DKP could also function as an environmental-friendly sensor.

The metal binding ability of cysteine-based DKP was also measured through surface tension methodology. It was found that the solution of cis-**2d** in water has a surface tension of 69 mN/m (1 x 10^{-4} mol/L), which was same as the aqueous solution of compound **2a** and similar

to water (73 mN/m). Surprisingly, in the presence of Cu^{2+}, surface tension decreased to 54 and 56 mN/m for the cis-isomer and cis/trans mixture of compound **2d**, respectively. In comparison, there was only a slight decrease in surface tension (65 mN/m) for cis-DKP **2a.** The significant decrease in surface tension was attributed to the amphiphilic structure of **2d** with lipophilic side chains and a hydrophilic DKP core. The hydrophilicity and amphiphilicity of the DKP core dramatically increases upon chelation with Cu^{2+} as a result of breaking up the intermolecular hydrogen-bonding, thus leading to different phenomenon compared with DKP **2a** with short alkyl side chains. Therefore, the DKP with long alkyl chains show specific metal ion-induced amphiphicility and find potential applications in micelles, surfactant and drug delivery.

2.4 Conclusion

Facile synthesis of cysteine-based DKP from thiol-protected precursors, mainly S-alkylated cysteine-derivatives, were demonstrated, where both thiol-acrylate Michael addition reaction and thiol-ene radical reaction were utilized to suppress the over-reactivity of thiol group. Accordingly, a series of DKP containing small molecules and polymers were successfully synthesized with the existence of diastereoisomers. The separations of DKP diastereoisomers were achieved in small molecules. Moreover, the chiroptical activity of the diastereoisomers combined with the isolated enantiomers of DKP compounds can be utilized for sensing silver ion in aqueous systems.

2.5 Experimental section

2.5.1 Materials

L-cysteine, methyl acrylate, butyl acrylate, lauryl acrylate, di(ethylene glycol) ethyl ether acrylate, phosphorous pentoxide, 1,2-dichlorobenzene, boric acid, 1-dodecene, 1-

undecene, undecenoic acid, 10-undecen-1-ol, poly (ethylene glycol) diacrylate (M*n*=700 g/mol), 1,9-decadiene, 1,6-hexanediol, isosorbide, methacrylate, cholesterol, acrylic acid and DMPA were purchased from Sigma Aldrich Chemicals Canada. Octyl acrylate was purchased from MP Biomedicals. Natural soybean oil was purchased from Argol compony. The water used in this work was purified using a Millipore™ Milli-Q™ Advantage A10 water purification system. Column chromatography was done using silica gel (Silicycle Chemical Division, 70–230 mesh) as the stationary phase.

2.5.2 Measurements

^{1}H, ^{13}C, COSY, NOESY, HSQC, NOE NMR spectra were measured on a Bruker Avance Digital 300 MHz spectrometer at ambient temperature using tetramethylsilane as an internal standard. Infrared measurements were recorded on a Varian 1000 FT-IR Scirinitar spectrophotometer in the regions of 4000–400 cm^{-1}. Mass spectra were performed with a Micromass Quattro LC ESI (EI). Fisher-Johns melting point apparatus was used to test the melting points (mp). Gel permeation chromatography (GPC) analysis was conducted on a PL-GPC 220 system with polystyrene as standard and tetrahydrofuran (THF) as eluent. CD spectrum was recorded on Olis Circular Dichroism Spectrophotometers and the wavelength starting from 210 nm. Specific rotation was performed on Autopol IV Automatic Polarmeter at 23 ºC in methanol. Surface tension was measured by Cenco-DuNouy Interfacial Tensiometer.

2.5.3 Synthesis

General procedure for cysteine reacting with acrylate:

Cysteine (1.21 g, 10.0 mmol) and boric acid (0.12 g, 10 wt%) were dissolved in 20 mL of distilled water or methanol in 50 mL round-bottom flask. Acrylate was then added under argon atmosphere. The mixture was stirred at ambient temperature or elevated temperature in the

dark for 10 h. After the reaction was completed, the solution was dropped into acetone with vigorous stirring and the product was collected by suction filtration.

1a: 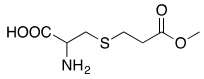

98% yield. ^{1}H NMR (300 MHz, D_2O): 3.87-3.83 (m, 1H), 3.63 (s, 3H), 3.09-2.92 (m, 2H), 2.80-2.75 (m, 2H), 2.68-2.63 (m, 2H); ^{13}C NMR (75 MHz, D_2O): 175.06, 172.71, 53.50, 52.32, 33.84, 32.07, 26.32; m.p.: 220 ºC.

1b: 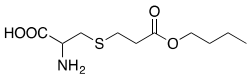

96% yield. ^{1}H NMR (300 MHz, D_2O + HCl): 4.13-4.09 (m, 1H), 3.92-3.88 (m, 2H), 3.04-2.86 (m, 2H), 2.66-2.61 (m, 2H), 2.61-2.46 (m, 2H), 1.42-1.33 (m, 2H), 1.17-1.05 (m, 2H), 0.64 (t, 3H); ^{13}C NMR (75 MHz, D_2O + HCl): 174.53, 170.13, 65.57, 51.97, 34.01, 31.03, 29.68, 26.54, 18.34, 12.76; m.p.: 220 ºC.

1c: 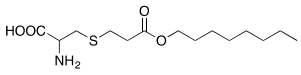

95% yield. ^{1}H NMR (300 MHz, DMSO-d_6+HCl): 4.10-4.08 (m, 1H), 3.97-3.87 (m, 2H), 3.09-2.91 (m, 2H), 2.77-2.73 (m, 2H), 2.62-2.57 (m, 2H), 1.52-1.46 (m, 1H), 1.32-1.21 (m, 8H), 0.85-0.78 (m, 6H); ^{13}C NMR (75 MHz, DMSO-d_6 + HCl): 171.90, 169.88, 66.58, 52.31, 38.52, 34.56, 31.60, 30.15, 28.72, 27.37, 23.60, 22.81, 14.36, 11.24; M.P.: 190 ºC; EI-MS calculated: 305.4, found 305.2.

1d: 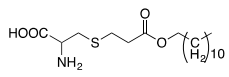

90% yield. ^{1}H NMR (300 MHz, DMSO-d_6 + HCl): 4.10-4.08 (m, 1H), 3.97-3.87 (m, 2H), 3.09-2.97 (m, 2H), 2.78-2.73 (m, 2H), 2.62-2.57 (m, 2H), 1.52-1.46 (m, 2H), 1.32-1.24 (m, 18H), 0.83 (t, 3H); ^{13}C NMR (75 MHz, DMSO-d_6 + HCl): 171.85, 169.93, 64.56, 52.32, 34.55, 31.73, 31.69, 29.50, 29.43, 29.40, 29.35, 29.14, 29.07, 28.52, 27.34, 25.77, 22.53, 14.41; M.P.: 185 ºC; EI-MS calculated for [M-EtO]: 360.2.

1e: 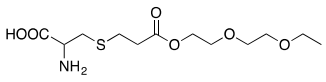

98% yield. ^{1}H NMR (300 MHz, D_2O): 4.23-2.20 (m, 2H), 3.88-3.84 (m, 1H), 3.71-3.47 (m, 8H), 3.10-2.93 (m, 2H), 2.82-2.77 (m, 2H), 2.71-2.55 (m, 2H), 1.10 (t, 3H); ^{13}C NMR (75 MHz, D_2O): 174.28, 172.64, 69.59, 68.82, 68.36, 66.58, 64.03, 53.48, 33.92, 32.08, 26.29, 14.06; M.P.: 195 ºC; EI-MS calculated for [M-EtO]: 264.1, found 264.1.

1j: 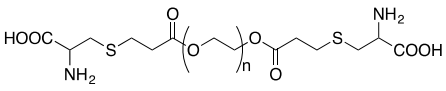

90% yield. ^{1}H NMR (300 MHz, D_2O): 4.22-4.19 (m, 2H), 3.86-3.82 (m, 1H), 3.71-3.68 (m, 2H), 3.65-3.60 (m, 22H), 3.09-2.91 (m, 2H), 2.80-2.75 (m, 2H), 2.69-2.65 (m, 2H); ^{13}C NMR (75 MHz, D_2O): 174.24, 172.60, 69.55, 68.40, 64.04, 53.46, 33.91, 32.08, 26.29; m.p.: 175 ºC.

General procedure for cysteine reacting with alkene:

Cysteine (1.21 g, 10.0 mmol) was added in 10 mL of ethanol in 50 mL Erlenmeyer flask. HCl was then added dropwise until cysteine completely dissolved. Alkene and DMPA (10 wt%) was added afterwards under argon atmosphere. The mixture was exposed to a UV-lamp (λ=365 nm) for several hours. After the reaction was completed, EtOH was removed by rotational evaporator and the mixture was washed with acetone. The final product was collected by suction filtration.

1f: 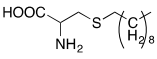

98%. ^{1}H NMR (300 MHz, DMSO-d_6 + HCl): 4.11-4.06 (m, 1H), 3.02-3.01 (d, 2H), 2.58-2.53 (t, 2H), 1.54-1.44 (m, 2H), 1.28-1.23 (m, 14H), 0.86-0.82 (t, 3H); ^{13}C NMR (75 MHz, DMSO-d_6 + HCl): 170.04, 52.34, 32.11, 31.73, 29.40, 29.32, 29.13, 29.03, 28.55, 22.54, 14.42.

1g: 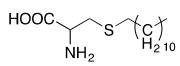

97%. ^{1}H NMR (300 MHz, DMSO-d_6 + HCl): 4.11-4.06 (m, 1H), 3.02-3.01 (d, 2H), 2.57-2.53 (t, 2H), 1.51-1.44 (m, 2H), 1.28-1.22 (m, 18H), 0.86-0.81 (t, 3H); ^{13}C NMR (75 MHz, DMSO-d_6 + HCl): 170.22, 52.31, 32.07, 31.76, 29.51, 29.48, 29.43, 29.28, 29.17, 29.06, 28.60, 22.56, 14.43.

1h: 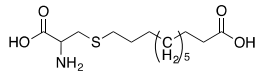

95%. ^{1}H NMR (300 MHz, $CDCl_3$): 5.89-5.75 (m, 1H), 5.04-4.92 (m, 2H), 2.36 (t, 2H), 2.09-2.02 (m, 2H), 1.69-1.60 (m, 2H), 1.43-1.32 (m, 10H).

1i: 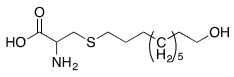

92%. ^{1}H NMR (300 MHz, DMSO-d_6): 4.13-4.07 (m, 1H), 3.35 (t, 2H), 3.02-3.00 (d, 2H), 2.55 (t, 2H), 1.54-1.45 (m, 2H), 1.40-1.24 (m, 13H).

1k: 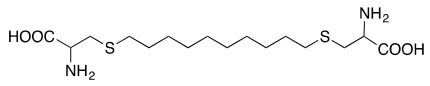

89%. ^{1}H NMR (300 MHz, DMSO-d_6 + HCl) 4.10-4.05 (m, 2H), 3.02-3.00 (d, 4H), 2.54 (t, 4H), 1.53-1.44 (m, 4H), 1.31-1.23 (m, 12H).

General procedure for cysteine reacting with synthetic dienes:

10-Undecenoic acid (1.84g, 10.0 mmol) and diols were added into a Schlenk flask and mixed well through vigorously stirring. Then, the temperature was gradually increased to 150 ºC and stirred for several hours. The pressure-release valve was adjusted to release the water produced and the process was monitored by ^{1}H NMR. When the reaction was complete, the mixtures containing dienes, were dissolved in ethanol for further use. Cysteine (1.21 g, 10.0 mmol) was mixed with 10 mL of ethanol in 50 mL Erlenmeyer flask. HCl was then added dropwise until cysteine completely dissolved. The mixtures and DMPA (10 wt%) were then added afterwards under argon atmosphere and exposed to a UV-lamp (λ=365 nm) for 6 h. After the reaction was

completed, EtOH was removed by rotary evaporator and the mixture was washed by acetone. The final product was collected by suction filtration.

1l: 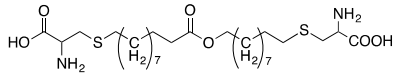

95 % yield. ^{1}H NMR (300 MHz, DMSO-d_6 + HCl): 4.08-4.06 (m, 1H), 3.98-3.94 (t, 1H), 3.01-2.99 (d, 2H), 2.56-2.50 (t, 2H), 2.25-2.20 (t, 1H), 1.49-1.42 (m, 4H), 1.30-1.21 (m, 14H). ^{13}C NMR (75 MHz, DMSO-d_6 + HCl): 173.48, 170.0, 64.08, 52.33, 33.99, 32.10, 31.67, 29.31, 29.26, 29.07, 29.02, 28.83, 28.53, 25.80, 24.94.

1m: 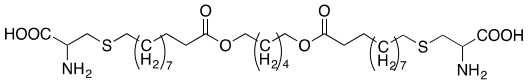

^{1}H NMR (300 MHz, DMSO-d_6 + HCl): 4.15 (s, 2H), 3.99 (t, 4H), 2.99-2.97 (t, 4H), 2.56 (t, 4H), 2.27 (t, 4H), 1.57-1.46 (m, 10H), 1.33-1.24 (m, 24H).

1n: 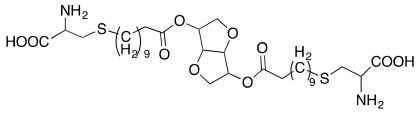

80%.^{1}H NMR (300 MHz, DMSO-d_6 + HCl): 5.03-4.95 (m, 2H), 4.67 (t, 1H), 4.29-4.27 (d, 1H), 4.02-4.01 (d, 2H), 3.77-3.63 (m, 4H), 2.97-2.95 (d, 4H), 2.48 (t, 4H), 2.23-2.19 (m, 4H), 1.42 (m, 8H), 1.15 (s, 24H).

General procedure for the preparation of cysteine-based DKP small molecules and polymers:

In a two-neck, round-bottom flask, a suspension of cysteine precursor (0.5 g) in 5 mL of 1,2-dichlorobenzene or NMP was stirred at room temperature and purged with nitrogen for 10 min. P_2O_5 (0.05 g, 10 wt%) was then added and the mixture was stirred for another 30 min at ambient temperature and then at 85 ^{o}C overnight. A sticky compound was obtained after o-dichlorobenzene was removed.

2a: 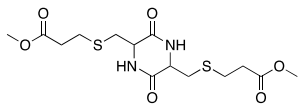

Methanol (10 mL) was added into the flask, **2a** was collected as precipitates by suction filtration (88% yield). ^{1}H NMR (300 MHz, DMSO-d_6): (Trans-) 8.26 (s, 1H), 4.22 (s, 1H), 3.60 (s, 3H), 3.08-3.02 (m, 1H), 2.84-2.78 (m, 1H), 2.77-2.72 (m, 2H), 2.61-2.56 (m, 2H); (Cis-) 8.20 (m, 1H), 4.15 (s, 1H), 3.60 (s, 3H), 3.02-2.96 (m, 1H), 2.91-2.85 (m, 1H), 2.78-2.73 (m, 2H), 2.62-2.57(m, 2H); ^{13}C NMR (75 MHz, DMSO-d_6): (Trans-) 172.30, 166.94, 55.19, 51.84, 36.17, 34.77, 28.11; (Cis-) 172.36, 166.47, 55.04, 51.89, 35.64, 34.62, 27.80. ES^{+}-MS calculated: 378.1, found 401.1 for [M+Na^{+}].

2b: 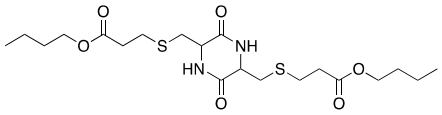

Cis- and trans isomers of **2b** were obtained in a total yield of 88% after column chromatography eluting with hexane – acetone (2:1 v/v) and hexane – acetone (1:1 v/v), respectively. ^{1}H NMR (300 MHz, DMSO-d_6): (Trans-) 8.25 (s, 1H), 4.22 (s, 1H), 4.02 (t, 2H), 3.08-3.02 (m, 1H), 2.84-2.79 (m, 1H), 2.76-2.71 (m, 2H), 2.60-2.55 (m, 2H), 1.60-1.50 (m, 2H), 1.39-1.26 (m, 2H), 0.89 (t, 3H); (Cis-) 8.20 (s, 1H), 4.13 (s, 1H), 4.02 (t, 2H), 3.02-2.85 (m, 2H), 2.77-2.71 (m, 2H), 2.60-2.55 (m, 2H), 1.60-1.50 (m, 2H), 1.39-1.27 (m, 2H), 0.88 (t, 3H); ^{13}C NMR (75 MHz, DMSO-d_6): (Trans-) 171.87, 166.94, 64.17, 55.20, 36.17, 34.98, 30.63, 28.20, 19.06, 14.01; (Cis-) 171.90, 166.46, 64.17, 55.05, 35.67, 34.80, 30.63, 27.84, 19.06, 14.01.ES^{+}-MS calculated: 462.2, found 485.2.

2c: 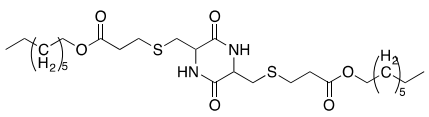

Cis- and trans isomer of **2c** were obtained in a total yield of 88% after column chromatography eluting with hexane – acetone (2:1 v/v) and hexane – acetone (1:1 v/v), respectively. ^{1}H NMR (300 MHz, DMSO-d_6): (Cis-) 8.20 (s, 1H), 4.14 (s, 1H), 3.99-3.91 (m, 2H), 3.02-2.95 (m, 1H),

2.791-2.85 (m, 1H), 2.77-2.71 (m, 2H), 2.60-2.56 (m, 2H), 1.54-1.50 (m, 1H), 1.35-1.24 (m, 8H), 0.88-0.81 (m, 6H); ^{13}C NMR (75 MHz, DMSO-d_6): (Cis-) 171.92, 166.45, 66.51, 55.04, 38.58, 35.68, 34.80, 31.13, 30.21, 28.77, 27.91, 23.65, 22.85, 14.35, 11.24; ES$^+$-MS calculated: 574.3, found 597.4.

2d: 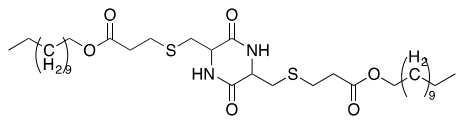

By adding 10 mL of methanol to the residue, **2d** precipitated out and was collected by suction filtration (80% yield). ^{1}H NMR (300 MHz, DMSO-d_6): (*Cis*-) 8.21 (s, 1H), 4.14 (s, 1H), 4.00 (t, 2H), 3.02-2.84 (m, 2H), 2.77-2.72 (m, 2H), 2.59-2.55 (m, 2H), 1.55 (t, 2H), 1.24 (s, 18H), 0.85 (t, 3H); ^{13}C NMR (75 MHz, DMSO-d_6): (Cis-) 171.87, 166.42, 64.46, 55.08, 35.74, 34.81, 31.77, 29.48, 29.18, 29.12, 28.57, 27.91, 25.81, 22.56, 14.41; (Trans-) 171.86, 166.93, 64.46, 55.21, 36.17, 34.97, 31.77, 28.57, 25.82, 22.57, 14.42. ES$^+$-MS calculated: 684.4, found 709.5.

2e: 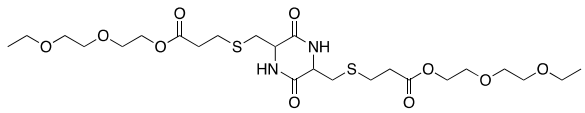

After addition of 10 mL of methanol into the flask, **2e** was collected as precipitates by suction filtration (82% yield). ^{1}H NMR (300 MHz, DMSO-d_6): (Cis-) 8.20 (s, 1H), 4.13 (m, 3H), 3.61-3.39 (m, 8H), 3.02-2.86 (m, 2H), 2.77-2.71 (m, 2H), 2.63-2.58 (m, 2H), 1.10 (m, 3H); (Trans-) 8.25 (s, 1H), 4.23 (s, 1H), 4.15-4.12 (m, 2H), 3.61-3.39 (m, 8H), 3.08-3.02 (m, 1H), 2.85-2.79 (m, 1H), 2.76-2.72 (m, 2H), 2.62-2.57 (m, 2H). 1.10 (m, 3H); ^{13}C NMR (75 MHz, DMSO-d_6): (Cis-)*:* 171.91, 166.47, 70.28, 79.62, 68.69, 66.02, 63.89, 55.02, 35.67, 34.72, 27.74, 15.56; (Trans-): 171.85, 166.93, 70.28, 69.62, 68.69, 66.01, 63.89, 55.19, 36.18, 34.91, 28.08, 15.58.

2f: 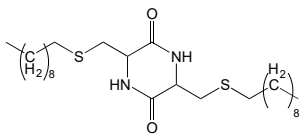

70% yield**. 2f** was collected after roughly washing by acetone. ^{1}H NMR (300 MHz, $CDCl_3$): (Cis-) 4.14-4.10 (m, 1H), 3.32-3.26 (m, 1H), 2.87-2.79 (m, 1H), 2.58-2.56 (t, 2H), 1.66-1.53

(m, 2H), 1.40-1.28 (m, 14H), 0.92-0.88 (t, 3H); (Trans-) 4.19-4.10 (m, 1H), 3.32-3.20 (m, 1H), 2.87-2.77 (m, 1H), 2.58-2.53 (m, 2H), 1.65-1.56 (m, 2H), 1.40-1.28 (m, 14H), 0.92-0.88 (t, 3H); ^{13}C NMR (75 MHz, $CDCl_3$): *(*Cis-*)* 166.04, 53.66, 36.53, 32.36, 31.89, 29.58, 29.50, 29.30, 29.18, 28.79, 22.68, 14.12. (Trans-) 166.38, 54.08, 37.03, 32.55, 31.89, 29.60, 29.54, 29.30, 29.18, 28.78, 22.68, 14.12.

2g: 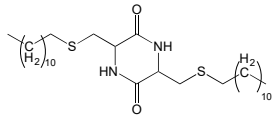

2g was collected after roughly washing by acetone. (70% yield). ^{1}H NMR (300 MHz, $CDCl_3$): 4.19-4.11 (m, 1H), 3.31-3.20 (m, 1H), 2.87-2.77 (m, 1H), 2.60-2.53 (m, 2H), 1.65-1.36 (m, 18H), 0.92-0.88 (t, 3H); ^{13}C NMR (75 MHz, $CDCl_3$): (Cis) 166.07, 53.70, 36.55, 32.38, 31.92, 29.59, 29.51, 29.35, 29.19, 28.92, 28.79, 22.70, 14.12; (Trans) 166.43, 54.10, 37.02, 32.57, 31.92, 29.64, 29.51, 29.35, 29.19, 28.92, 28.79, 22.70, 14.12.

2j: 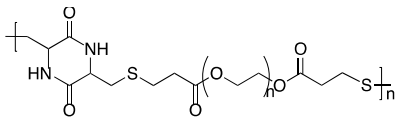

2j was collected after roughly washing by hexane. ^{1}H NMR (300 MHz, DMSO-d_6): 8.26-8.20 (d), 4.22 (s), 4.15-4.11 (t), 3.62-3.59 (t), 3.52-3.39 (m), 3.07-2.68 (m), 2.63-2.60 (m); ^{13}C NMR (75 MHz, DMSO-d_6): 171.92, 166.95, 166.48, 70.24, 68.69, 63.95, 63.89, 55.20,55.02, 53.18, 36.19, 35.66, 34.90, 34.72, 34.50, 28.08, 27.72, 26.96.

2k: 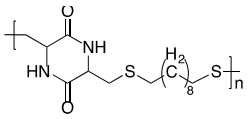

^{1}H NMR (300 MHz, DMSO-d_6): 4.58-4.51 (m), 4.45-4.38 (m), 3.67 (s), 2,96-2.66 (m), 2.53-2.48 (m), 1.53-1.44 (m), 1.33-1.24 (m).

2l: 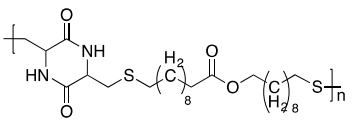

^{1}H NMR (300 MHz, DMSO-d_6): 4.19 (s), 4.10 (s), 3.99 (t), 3.05-2.66 (m), 2.51 (t), 2.29-2.16 (m), 1.51-1.48 (d), 1.24 (s); ^{13}C NMR (75 MHz, DMSO-d_6): 173.41, 166.39, 64.06, 55.28, 36.23, 34.12, 34.01, 33.01, 29.65, 29.39, 29.09, 28.90, 28.70, 28.59, 25.85, 24.98.

2.5.4 Preparation of detection solutions

Stock solutions (0.2 M) of different metal ions, including Pb^{2+}, Co^{2+}, Ni^{+}, Ca^{2+}, Mg^{2+}, Hg^{2+}, Mn^{2+}, Zn^{2+}, Cu^{2+}, Na^{+}, Li^{+}, Ba^{2+}, K^{+} and Ag^{+}, were prepared in de-ionized water. The detection solution was prepared by adding 0.01 mL of metal ion solution to 4 mL of **2a** (0.0005 M), respectively.

References

1. *Discover a new dimension of pureness: vegetarian cysteine.* Wacker fermentation - grade cystine and cysteine, Wacker Chemie AG. http://www.brenntag.com/media/documents/bsi/product_data_sheets/life_science/wacker_amino_acids/cystine_cysteine_brochure.pdf
2. Gao, J. P. *Urethanes and ureas and processes*, WO Patent 2013142969 A1, **2013**.
3. Greenstein, J. P. *J. Biol. Chem.* **1937**, *118*, 321.
4. Banerjee, R.; Becker, D. F.; Dickman, M. B.; Gladyshev, V. N.; Ragsdale, S. W. *Redox Biochemistry*, John Wiley & Sons, Inc., Hoboken, NJ, USA, **2008**.
5. Hoyle, C. E.; Lowe, A. B.; Bowman, C. N. *Chem. Soc. Rev.,* **2010**, *39*, 1355.
6. Ralph, T. R.; Hitchman, M. L.; Millington, J. P.; Walsh, F. C.; *J. Electroanal. Chem,.* **1994**, *375*, 1.
7. Krishnaveni, N. S.; Surendra, K.; Rao, K. R. *Chem. Commun.*, **2005**, *5*, 669.
8. Chaudhuri, M. K.; Hussain, S. *J. Mol. Catal. A-Chem.,* **2007**, *269*, 214.
9. Chaudhuri, M. K.; Hussain, S.; Kanram, M. L.; Neelima, B. *Tetrahedron Lett.,* **2005**, *46,* 8329.
10. *Cholesterol metabolism*. https://en.wikipedia.org/wiki/Cholesterol
11. Xu, J.; Cui, Y.; Wang, C. *Tianjin Huagong*, **2011**, *25*, 42.
12. Xia, P.; Cheng, H.; Yan, D. *J. Appl. Polym. Sci.,* **1992**, *45*, 579
13. Borthwick, A. D. *Chem. Rev.,* **2012**, *112*, 3641.
14. Erlanger, B.; Kokowsky, K. *J. Org. Chem.,* **1961**, *26*, 2534.
15. Galinsky, A. M.; Gearien, J. E.; Smissman, E. E. *J. Am. Pharm. Assoc.,* **1957**, *46,* 391.
16. Stevenson, J. J.; Moye-Sherman, D. *Phosphorus pentoxide as a reagent in peptide synthesis*, EP Patent 1786784 B1, **2007**.

17. Jones, G. S., Savage, S. A.; Ivy, S.; Benitez, P. L.; Ramirez, A. *J. Org. Chem*., **2011**, *76*, 10332.

18. Naraoka, H.; Harada, K. *J. Chem. Soc. Perkin Trans. I*, **1986**, 1557.

19. Ueda, T.; Saito, M.; Izumiya, N. *Bull. Chem. Soc. Jpn*, **1983,** *56*, 568.

20. Shoji, A.; Kimura, H.; Ozaki, T.; Sugisawa, H.; Deguchi, K. *J. Am. Chem. Soc*., **1996,** *118*, 7604.

21. Kopple, K.D.; Marr. D. *J. Am. Chem. Soc.,* **1967**, *89*, 6193.

22. Kawaguchi, K.; Tanihara, M.; Imanishi, Y. *Polym. J.,* **1983**, *15*, 97.

23. Mauger, A. B. *J. Chromatogr.,* **1968**, *37*, 315.

24. Toshihisa, U.; Morinobu, S.; Tetsuo, K.; Nobuo, I. *Bull. Chem. Soc. Jpn*., **1983**, *56*, 568.

25. Li, X.; Hopmann, K. H.; Hudecová, J.; Isaksson, J.; Novotná, J.; Stensen, W.; Andrushchenko, V.; Urbanová, M.; Svendsen, J. S.; Bouř, P.; RuudJ, K. *Phys. Chem. A*. **2013**, *117*, 1721.

26. Porzi, G.; Sandri, S. *Tetrahedron: Asymmetry,* **1994**, *5,* 454.

27. Prasad, C. *Peptides*, **1995**, *16*, 151.

28. Pérez-Picaso, L.; Escalante, J.; Olivo, H. F.; Rios, M. Y. *Molecules,* **2009**, *14*, 2836.

29. Van der Steen, M.; Stevens, C.V. *ChemSusChem*, **2009**, *2*, 692,

30. Muñoz-Guerra, S.; Lavilla, C.; Japu, C.; Martínez de Ilarduya, A.; *Green Chem.,* **2014**, *16*, 1716.

31. Allgeier, A. M.; DeSilva, N.; Korovessi, E.; Menning, C. A.; Ritter, J. C.; Sengupta, S. K. *Process for preparing 1, 6-hexanediol,* US Patent 20130172629 A1, **2013.**

32. Luo, N.; Qian, J.; Cupps, J.; Wang, Y.; Zhou B.; Armberuster, L.; Frenkel, P. *Natural Oil Polyol of High Reactivity for Rigid Polyurethanes,* Biobased Technologies, LLC, **2008**.

33. *Benefits of Agrol.* 2010-2016 BioBased Technologies, http://www.agrolinside.com/benefits.html

34. Carney, P.; Lopez, S.; Mickley, A.; Grinberg, K.; Zhang, W.; Dai, Z. *Chirality*, **2011**, *23*, 916.

35. Nan, J.; Yan, X. *Chem. Commun.,* **2010**, *46*, 4396.

36. Caricato, M.; Leza, N. J.; Roy, K.; Dondi, D.; Gattuso, G.; Shimizu, L. S.; Griend, D. A. V.; Pasini, D. *Eur. J. Org. Chem.,* **2013**, *27,* 6078.

37. Triola, G.; Brunsveld, L.; Waldmann, H. *J. Org. Chem.,* **2008**, *73*, 3646.

38. Gockel, P.; Vogler, R.; Gelinsky, M.; Meißner, A.; Albrich, H.; Vahrenkamp, H.; *Inorganica Chimica. Acta.,* **2001***, 323*, 16.

39. Singha, S.; Kim, D.; Seo, H.; Cho, S. W.; Ahn, K. H. *Chem. Soc. Rev.,* **2015**, *44*, 4367.

Chapter 3 Syntheses and Characterizations of Cysteine-based DKP from 4-thiazolidinecarboxylic Acid Derivatives

3.1 Molecular design and synthetic approaches

Beside thiol-ene click reaction, aldehydes can be used to protect the thiol group in L-cysteine by forming stable 4-thiazolidinecarboxylic acid (TCA) derivatives. In fact, the reaction between aldehyde and cysteine takes place every day when the biogenic aldehydes metabolize in the human body.[1] It is such an important reaction that has been reported by Schubert and co-workers as early as 1935.[2] Since then, the reaction between cysteine and aldehydes, was largely expanded by adopting different aldehyde species by Woodward, Soloway, Schmolka and their colleagues, respectively (Table 3.1).[3] The TCA derivatives not only show biocompatibility and biological reactivity in physiological activities, for example as antioxidants to quench hydroxyl and nitric oxide radicals effectively, but also have been widely used in the synthesis of drug precursors.[1,4]

Table 3.1 Reported 4-thiazolidinecarboxylic acid and its derivatives. (Adapted from Ref. 5)

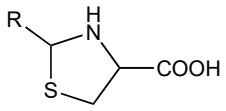

R	M.P. (°C)	R	M.P. (°C)
n-Pentyl	64	3',4'-Dichlorophenyl	83
n-Hcptyl	75	2',6'-Dichlorophenyl	89
n-Octyl	45	2'-Hydroxy-5'-chlorophenyl	77
n-Nonyl	46	2'-Nitrophenyl	76
n-Decyl	57	3'-Nitrophenyl	83
n-Undecyl	72	4'-Nitrophenyl	73
n-Tridecyl	75	1'-Naphthyl	68
n-Hexadecyl	76	4'-Dimethylaminophenyl	73
2'-Chlorophenyl	77	2'-Hydroxy-3'-methoxylphenyl	33
4'-Chlorophenyl	83	3'-Ethoxy-4'-hydroxyphenyl	88

TCA contains the amino acid functional group and is able to dimerize to form a DKP compound. Iannotta and co-workers have already reported the successful synthesis of cysteine-based DKP by dimerization of TCA using *O*-benzotriazol-1-yl-tetramethyluronium (HBTU) and *N*,*N*-diisopropylethylamine (DIPEA) at room temperature with a yield greater than 78% (Scheme 3.1).[6]

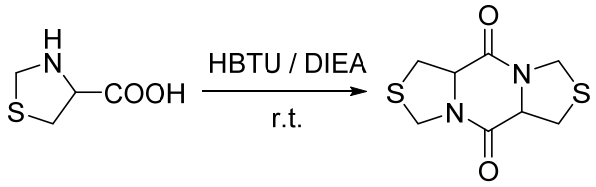

Scheme 3.1 A reported synthesis of a DKP compound.[6]

This synthetic route is feasible for other TCA derivatives and thus allows for the preparation of functionalized DKPs, especially the difunctional compounds as monomers for making DKP-containing polymers. By design, the DKPs containing the SH, Br and OH groups can be prepared using appropriate aldehydes (Scheme 3.2). The di-thiol monomers can be used to react with the diisocyanate monomers to form DKP-containing poly(thio-urethane)s and divinyl monomers to form the DKP-containing sulfide polymers. The dibromide monomers are expected to react with aryl diobronic acid monomers by the Suzuki cross-coupling reaction to afford the DKP-containing polymers. Finally, the diol is typically used to form a polyester and a polycarbonate. Many other DKP-containing polymers could be envisioned by utilization of a variety of reactions of the thiols, alcohols and bromides.

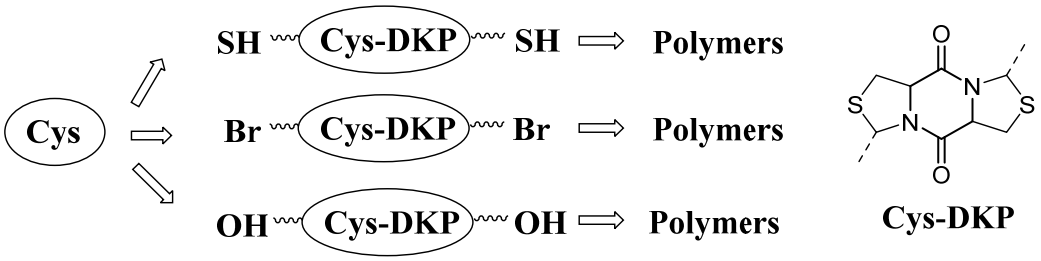

Scheme 3.2 Synthetic routes from L-cysteine to DKP-containing polymers.

3.2 Syntheses and characterizations of TCA derivatives

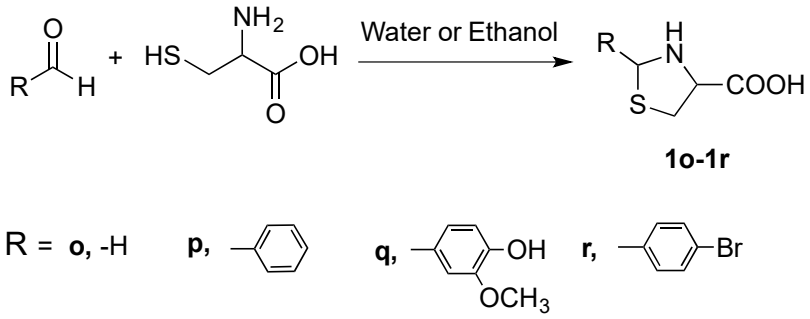

Scheme 3.3 Syntheses of cysteine derivatives **1o-1r** from aldehydes.

The cyclo-condensation reactions of L-cysteine and aldehydes were carried out in water or water/ethanol at room temperature overnight and afforded the TCA derivatives **1o-1r** with a yield greater than 90% (Scheme 3.3). Compared to a reported synthesis of the same compound (**1p**) from cysteine and N-(phenylmethylene)

benzenamine in the presence of potassium acetate with only 57% yield,[7] our synthetic route is definitely "green", mild and high yield. The reaction is affected by reaction temperature, solution concentration, the pH, reaction time and catalyst (e.g., acetate), and racemization take places readily during the cyclization process which could be partially diminished in the presence of a specific base, as revealed by Sun and co-workers.[9]

The reaction conditions for the preparation of TCA derivatives from L-cysteine are mild enough to tolerate a variety of functional groups and a range of aliphatic, aromatic and natural-occurring aldehydes can be used.[3] Nowadays, aldehyde is a biomass feedstock with abundant natural resources in living systems and plants. The natural occurring aldehydes have already been used in foods, fragrance and medicines as flavor additives (Fig. 3.1).[10] In our work, we chose acetophenone, which can be found in apple, cheese, beef and banana, and vanillin, which is the main flavor compound in vanilla, from the list below. Other aldehydes containing different functional groups are also applicable in our synthetic route to produce

DKP-containing difunctional compounds, for example, using jasmone to produce DKP-containing diene.

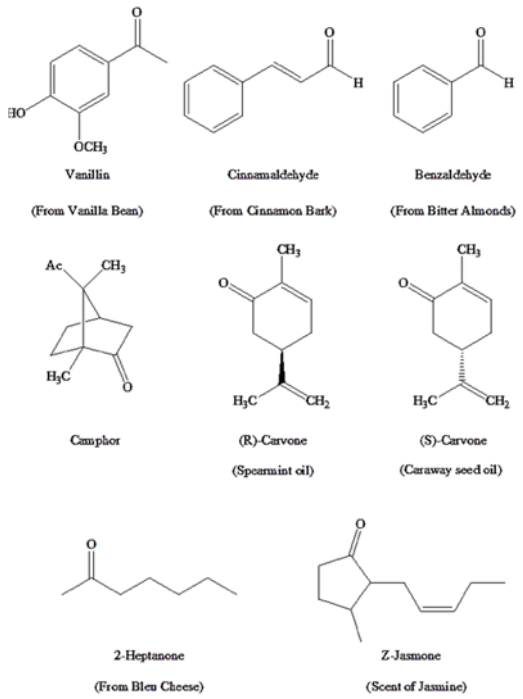

Figure 3.1 Naturally occurring aldehydes. (Adapted from Ref. 10)

However, it was found that not all of the aldehydes could be used in this reaction, for example, α,β-unsaturated aldehydes cinnamaldehyde and carvone.[5] It has been proposed that the TCA formation first goes through a hemi-mercaptal formation, followed by dehydration and cyclization reaction (Scheme 3.4).[11] In the case of α,β-unsaturated aldehydes, the existence of a resonance structure results in a low concentration of the activated aldehyde and the nucleophilic thiol prefers to attack at the β-carbon of α,β-unsaturated aldehyde, which in turn hampers the formation of hemi-mercaptals.[5] There is another reaction mechanism proposed by Wtodek *et al*., where an imine is considered an intermediate, followed by intramolecular nucleophilic attack from the thiol. One proof was provided by Karpiuski *et al.* that an amide product was detected in the decomposition study of TCA.[12]

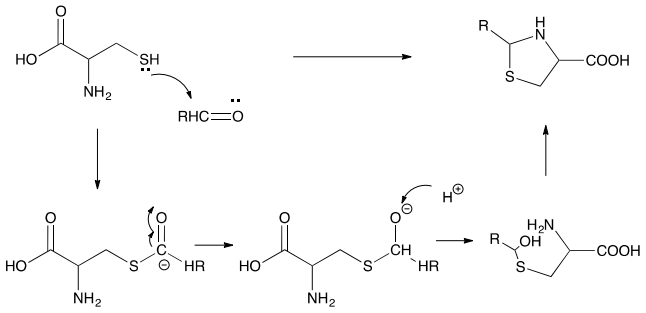

Scheme 3.4 Proposed reaction mechanism for the synthesis of TCA derivatives.[11]

TCA derivatives are not only biocompatible, but also potentially biodegradable, since they can be easily hydrolyzed back into L-cysteine under both acid and basic conditions. The advantage of TCA biodegradability is applicable for the preparation of environmental-friendly materials, for example, as urease inhibitors to reduce volatilization of urea based fertilizers in normal agricultural practices.[13]

The structures of compounds **1o-1r** were fully characterized by spectroscopic means (See experimental section). Take **1p** as an example, where the ^{1}H NMR spectrum of **1p** displays proton resonances (ppm) at 7.54-7.27 (m, 5H), 5.67/5.51 (s, 1H), 4.26-4.22/3.93-3.88 (m, 1H), 3.41-3.05 (m, 2H) (Fig. 3.2). Clearly, the diastereomers are formed during the cyclization. The peaks at 5.67 ppm and 5.51 ppm are assigned to the proton on the newly formed chiral carbon in the ring, indicating the almost 1:1 ratio between the two isomers. But the ratio of the diastereomers varies according to the reaction temperatures and times.

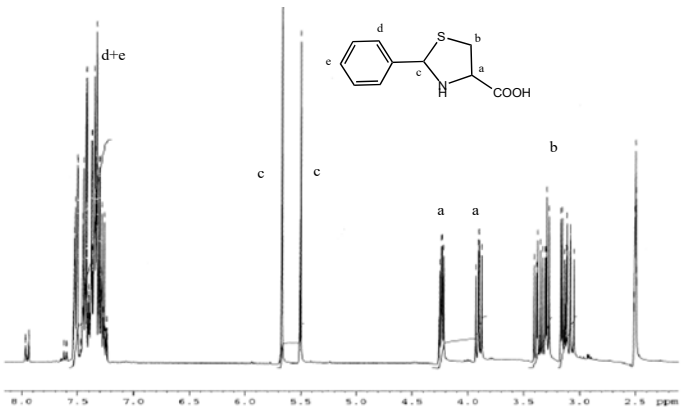

Figure 3.2 ^{1}H NMR spectrum (300 MHz, DMSO-d_6) of compound **1p**.

3.3 Synthesis of DKP-containing dithiol

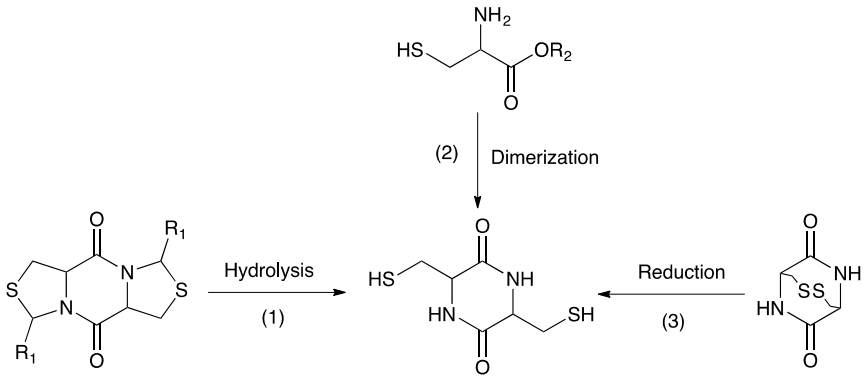

Scheme 3.5 Three routes to the preparation of Cys-Cys.

As shown in Scheme 3.5, based on the different starting materials, there are three pathways for the preparation of a potentially very useful Cys-Cys: (1) hydrolysis of a DKP intermediate, (2) direct dimerization from cysteine and (3) reduction of a DKP disulfide. The first pathway was claimed by Iannotta and co-workers in 2010 for the successful synthesis of Cys-Cys by hydrolysis of a DKP intermediate (Scheme 3.6).[6] Attracted by the huge potential of the dithol compounds in polymer preparations, this synthetic route was repeated.

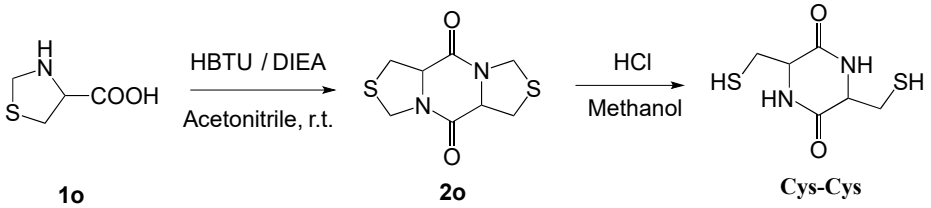

Scheme 3.6 A reported synthesis of Cys-Cys.[6]

As reported, the dimerization of TCA **1o** was carried out in acetonitrile in the presence of HBTU and DIEA at room temperature overnight and afforded the target compounds **2o** with the yields over 80%. HBTU is a well-known peptide coupling reagent and works by activating the carboxylic acid and forming a favorable leaving group (Scheme 3.7).[14,15] The carboxylate anion first attacks HBTU to form the unstable O-acyl(tetramethyl)isouronium salt. Then the anion rapidly attacks the isouronium salt, affording an aza derivative, whose stability

significantly contributes to the high conversion efficiency of the reaction. Finally, amine attacks the ester to form an amide. DIPEA is necessary to deprotonate function and together with HBTU, the racemization is diminished, especially in the synthesis of cysteine-based peptide which is prone to racemization.[14,15]

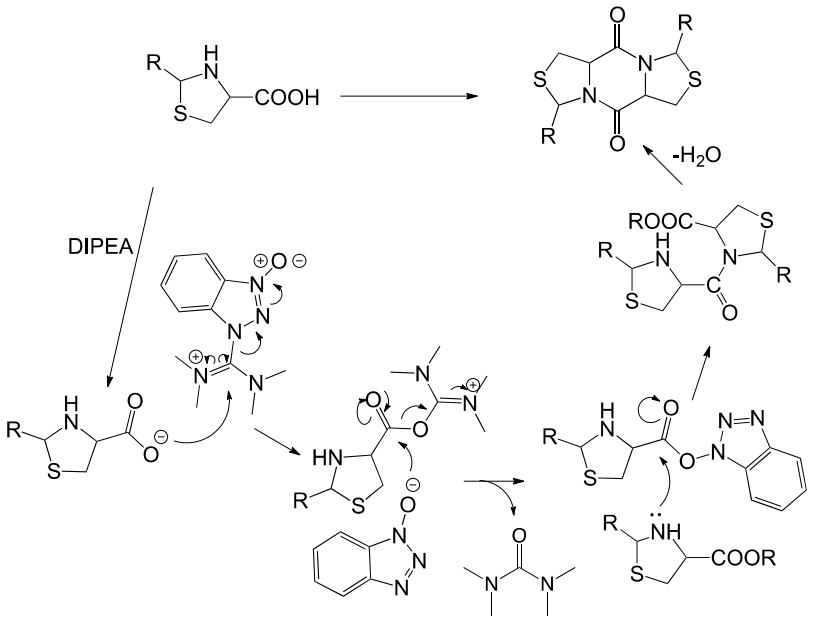

Scheme 3.7 A plausible mechanism for the HBTU/DIEA catalyzed reaction to form DKP.

However, the utilization of HBTU also has some drawbacks. Since HBTU is highly sensitive to moisture, the reaction efficiency is adversely affected by the water present. Therefore, solvent distillation prior to the reaction is required. Moreover, an excess of HBTU could result in a low reaction yield due to the formation of guanidine side product.[14,15] Thus, the actual amount of HBTU is necessary to guarantee the efficiency. Considering the high expense of HBTU, alternative coupling reagents, DCC was tested in our work and the course of the reaction was monitored by ^{1}H NMR method. Though DCC was effective to catalyze the DKP formation from TCA derivatives, it was difficult to separate the target product from the dicyclohexylurea by-product. In addition, encouraged by the successful dimerization of pyroglutamic acid which has similar structure as TCA, its reaction condition, where acetic acid

and pyridine was used as catalysts at 110 ºC was tried in our work. However, due to the lack of a strong electrophilic carbonyl group in TCA structure, the test failed.[15]

The structure of compound **2o** was fully characterized by ^{1}H NMR, which gave identical result as reported by Iannotta.[6] In the ^{1}H NMR spectrum, the spectrum displays proton resonances (ppm) at 4.83 (d, 1H), 4.54-4.49 (m, 2H), 3.49-3.37 (m, 2H) (Figure 3.3).

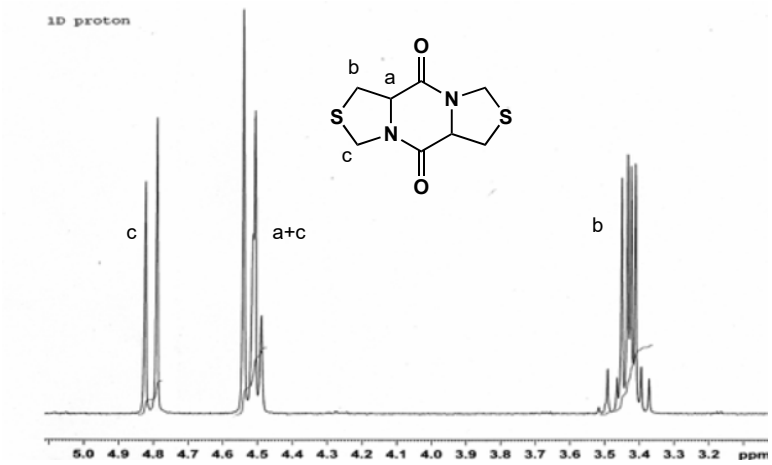

Figure 3.3 ^{1}H NMR spectrum (300 MHz, $CDCl_3$) of compound **2o**.

The subsequent hydrolysis of **2o** was reported to be done in methanol containing 0.2 M HCl and afforded the desired Cys-Cys with 78% yield (Scheme 3.6).[6] However, we attempted the same hydrolysis many times but failed. In order to break the five-member ring, many trial experiments were performed with different reaction conditions, such as with increased HCl concentration, using stronger acid H_2SO, elevating the reaction temperatures and even changing the substituted group (Scheme 3.8). However, the reported result was still not reproducible. Considering that Warner and co-workers also reported a failure of repeating the same hydrolysis reaction, the first approach to prepare DKP-containing dithiols failed.[17]

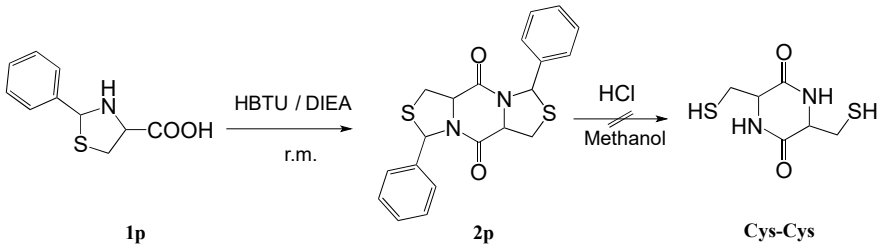

Scheme 3.8 Attempted synthesis of Cys-Cys by hydrolysis of compound **2p**.

In the second approach to preparation of the DKP-containing dithiol, cysteine and cysteine ester are directly used as the starting material. It was reported that DKP could be formed directly from amino acid methyl esters, such as methionine and lysine based DKPs.[18] Thus, a modified synthesis approach was developed. A solution of cysteine methyl ester hydrochloride in methanol with sodium methoxide was stirred at 50 °C for 2 h. Then the temperature was gradually increased to 150 °C and stirred at that temperature for several hours in a water jet vacuum (Scheme 3.9). Unfortunately, the obtained compound was identified as the disulfide. To prevent the disulfide formation, different reducing reagents, such as Na, Ni and H_2 gas, was added during the reaction.[19,20] However, all the attempts failed and the in-situ disulfide reduction was not effective.

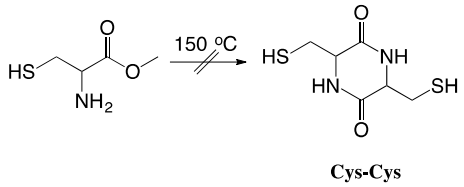

Scheme 3.9 Attempted synthesis of Cys-Cys from L-cysteine methyl ester.

Considering the difficulty in avoiding the disulfide formation during the dimerization reaction, cystine was designed to directly use as starting material. Thus, in the third approach, the dimerization would take place first, followed by the reduction of the disulfide bond (Scheme 3.10). However, due to the poor solubility of cystine in organic solvents and lack of effective coupling reagents, the reaction failed to prepare the corresponding DKP.

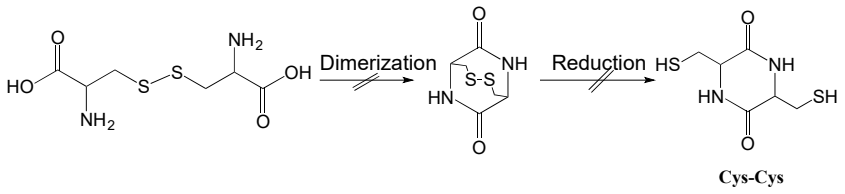

Scheme 3.10 Attempted synthesis of DKP from cystine.

Since a different type of thiol-protective intermediate was synthesized, the feasibility of using oven method in dimerization step was tested again followed by the procedure described in Chapter 2.2.3. Unfortunately, the decomposition of TCA derivatives or cystine, was always prior to the desired dimerization reaction and led to the failure in DKP synthesis. In conclusion, after countless trial experiments, the preparation of DKP containing dithiol was failed.

3.4 Syntheses of polymers from DKP-containing dibromide

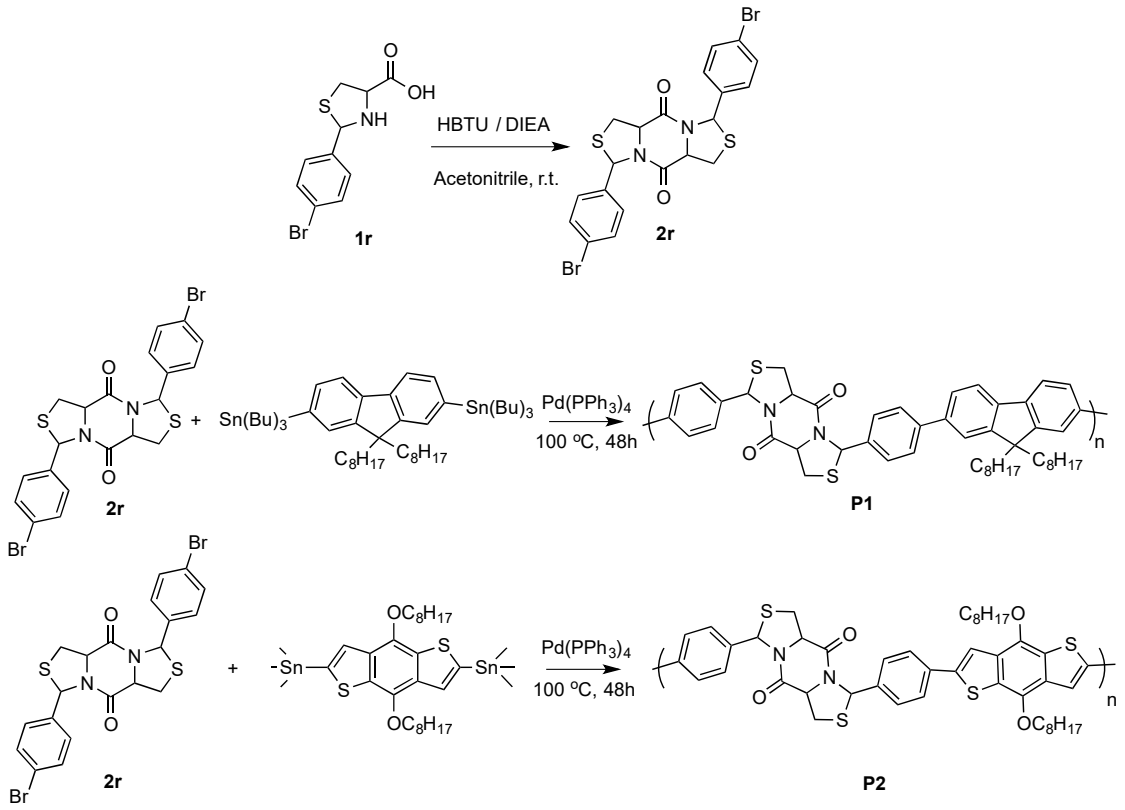

Scheme 3.11 Syntheses of dibromide monomer **2r** and DKP-containing polymers **P1-P2**.

The reaction between L-cysteine and 4-bromobenzaldehyde affords compound **1r**, which could undergo dimerization to give the DKP-containing dibromide monomer **2r** (Scheme 3.11). The reaction was carried out in acetonitrile in the presence of HBTU and DIEA at room temperature overnight. Compound **2r** was easily obtained with the yield over 80%. Its structure was fully characterized by spectroscopic means (See experimental section). The ^{1}H NMR spectrum of **2r** in $CDCl_3$ displays the peaks at 7.46 (d, 2H), 7.06 (d, 2H), 6.16 (s, 1H), 4.84-4.78 (m, 1H), 3.53-3.32 (m, 2H) (Fig. 3.4). There were two diastereomers of **2r** formed during the reaction, as revealed by the NMR method. However, only the predominant isomer was left after purification, as confirmed by the single peak at 6.16 ppm in ^{1}H NMR spectrum.

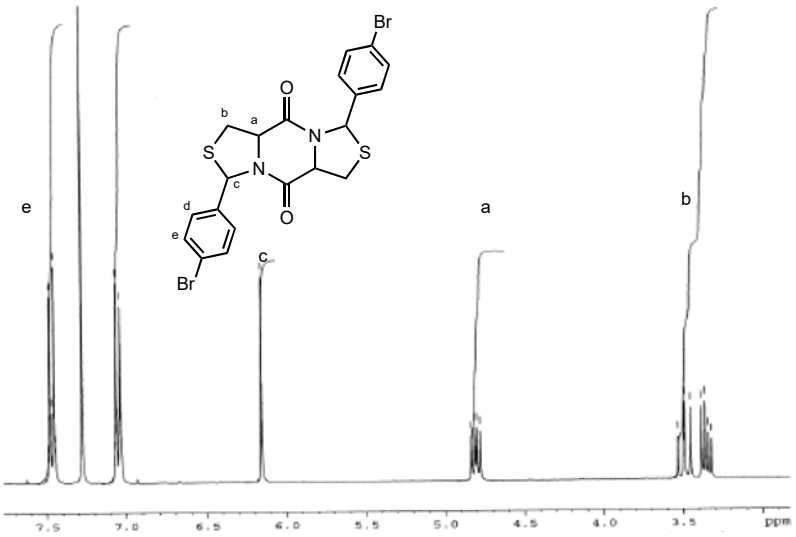

Figure 3.4 ^{1}H NMR spectrum (300 MHz, $CDCl_3$) of compound **2r**.

The obtained aromatic dibromides are routinely used in the Stille and Suzuki cross-coupling reactions to make polymers, such as 1,4-dibromo-2,5-dimethoxybenzene. However, the Suzuki reaction failed, possibly due to the hydrolysis of DKP under basic conditions. Then, the Stille cross-coupling reaction was conducted in chlorobenzene at 100 ^{o}C for 2 days using (4,8-Bis(octyloxy)benzo[1,2-b:4,5-b']dithiophene-2,6-diyl) bis(trimethylstannane) and 2,7-bis(trimethylstannane)-9,9-dioctyl fluorene as co-monomers (Scheme 3.11).[21] The original idea of adopting these conjugated monomers was to obtain DKP containing conjugated

polymer. Clearly, the π-conjugation in **P1** and **P2** were interrupted by the TCA and DKP rings. To increase the conjugation degree, a method from Credico's report was employed on **2r** (Scheme 3.12).[9] The reaction was also carried out in solution in the presence of pyridine and 25-fold excess of MnO_2. However, according to the NMR analysis, there was no target products obtained. Therefore, the design of DKP-containing conjugated polymer failed.

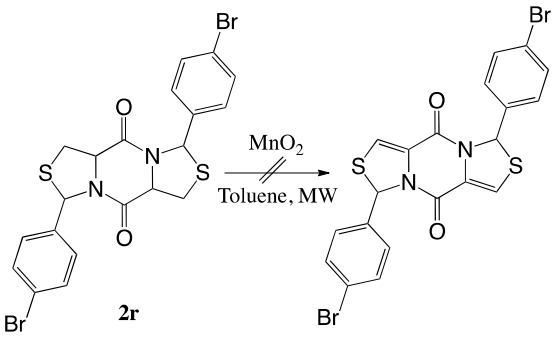

Scheme 3.12 Attempted conversion of compound **2r** to a conjugated analog.

Since polymers **P1** and **P2** have extremely poor solubility in all of the common organic solvents, polymers **P1** and **P2** were mainly characterized by the changes of optical properties such as absorptions and emissions, due to the existence of π-conjugated segments in these polymers. It was found that there was almost no absorption above 300 nm for monomer **2r** in DMF. In comparison, polymer **P1** had strong UV-absorption in the range of 260 nm to 550 nm and polymer **P2** had absorption below 350 nm (Fig 3.5a). In the fluorescence emission test, monomer **2r** showed a moderate fluorescent signal at 350 nm, while the fluorescent signal for polymer **P1** appeared at 480 nm and at 424 nm for polymer **P2** (Fig. 3.5b).

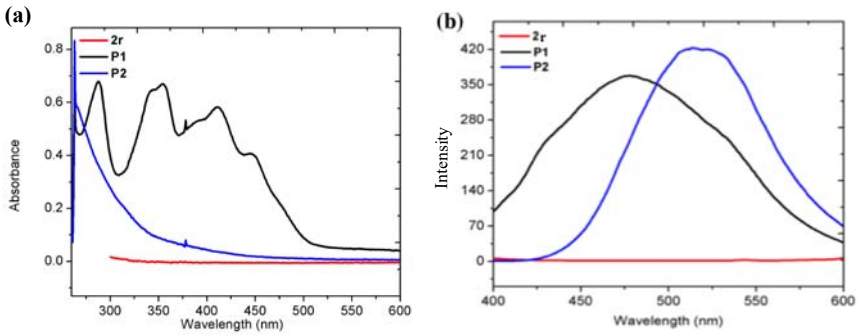

Figure 3.5 UV-Vis and PL spectra of monomer **2r,** polymers **P1** and **P2**.

Since cysteine-based DKPs have a binding ability with different metal ion, solutions of various metal ions (Zn^{2+}, Cu^{+}, Cd^{2+}, Ni^{2+}, Mg^{2+}, K^{+}, Ba^{2+}, Co^{2+}, Hg^{2+}, Li^{+}, Pb^{2+}, Na^{+} and Ag^{+}) were added to DKP **2r**, then UV and PL tests were taken immediately afterwards. It was found that for most of the chelated ions, there was no significant change induced by chelation effects. But when binding with Cu^{2+} ions, a slight increase or shift of the signal in UV spectra was detected (Fig. 3.6a). Similarly, upon addition of Cu^{2+} ions, a significant quenching of fluorescence intensity was observed (Fig. 3.6b).

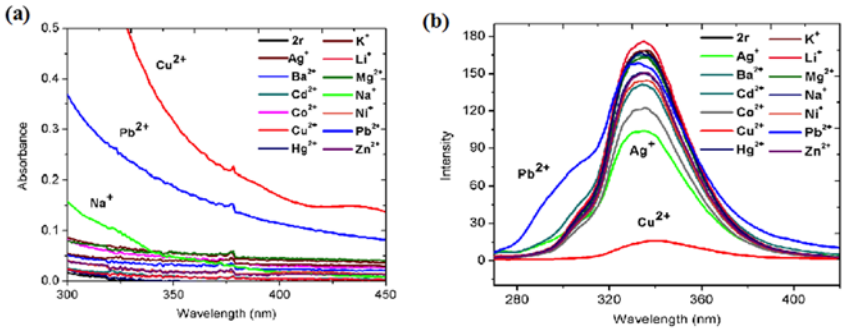

Figure 3.6 (a) UV-Vis absorption spectrum of compound **2r** with metal ions, (b) PL spectrum of compound **2r** with metal ions.

According to the CD studies on the DKPs in Chapter 2, it has been proved that DKPs synthesized from S-alkylated compounds have an ability to bind with metal ions and their chiroptical properties with Ag^{+} can induce a significant change in CD signal. Therefore, the

same experiment was performed with compound **2r**. However, there was no CD signal change in CD measurement. The reason might be due to the inhibited binding ability of sulfur in this large DKP compound.

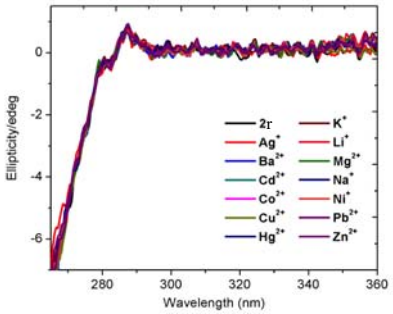

Figure 3.7 CD spectrum of compound **2r** with metal ions.

Then, the metal binding ability of DKP containing polymer **P1** was assessed with the assist from UV-absorption and fluorescence emission techniques. It was found that there was no obvious difference on UV-absorption upon addition of these metal ions (Fig. 3.8a). When chelated with Li, a significant increased signal with a slightly blue-shift was observed (Fig. 3.8b). However, lack of visible color changes and obvious signal differences, it is not sufficient to demonstrate the ability of **P1** as a metal sensor. On the other hand, when these metal ions were added into polymer **P2** solution, there was no significant signal change induced from chelation effect (See Appendix B).

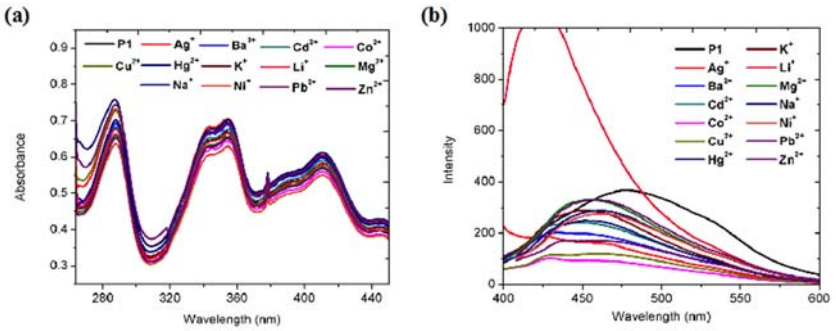

Figure 3.8 (a) UV-vis absorption spectrum of polymer **P1** with metal ions; (b) PL spectrum of polymer **P1** with different metal ions.

Moreover, because N atom in polymer may be protonated, which may cause the changes on UV-absorption and fluorescence emissions, the halochromic property of polymer **P1** was tested. At first, **P1** was dissolved into a water soluble solvent such as DMF or THF, the PL spectra were measured after adding HCl. However, there was no halochromic effects observed, even varying the concentration of HCl and increasing the system temperatures. It was assumed that the tertiary amine is too steric hindered to be protonated. Then, Lewis acid and electron acceptor were tested to add into the polymer solution, including $AlCl_3$, BF_3, tetracyanoquinodimethane, tetracyanoethylene, trifluoromethanesulfonic acid and 2,3-dichloro-5,6-dicyano-1,4-benzoquinone, because it was considered that the electron-rich amine was able to form a charge transfer complex with an electron acceptor, which could effectively quench the fluorescence by electron transfer. It was found that: 1) with the addition of $AlCl_3$ and trifluoromethanesulfonic acid, the intensity of fluorescence of **P1** decreased, but not completely quenched; 2) with the addition of electron acceptors, the fluorescence completely quenched at the beginning. There was no fluorescence turn-on that could be observed after heating; 3) with the addition of BF_3, the fluorescence is completely quenched at the beginning. Though fluorescence turned on after heating, it was not reversible. Because the intensity of PL was not recovered to original extent and was not quenched again after cooling down. It was concluded that though there was fluorescence quenching observed, they were not good halo-chromic and thermo-chromic dyes due to the failure to switch colors many times and having a high color contrast.

3.5 Syntheses of polymers from DKP-containing bisphenol

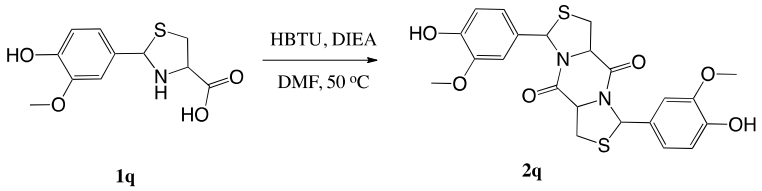

1q 2q

Scheme 3.13 Synthesis of DKP bisphenol **2q**.

The reaction between L-cysteine and vanillin affords compound **1q**, which undergoes dimerization to give a DKP bisphenol **2q** (Scheme 3.13). The reaction was carried out in DMF in the presence of HBTU and DIEA at 50 °C overnight. Acetonitrile is a good solvent for DKP preparation. However, due to poor solubility of **1q**, it is necessary to replace acetonitrile by DMF. Recrystallization of **2q** could be done in DMF, propylene carbonate and cyclohexanone. Since the isolated yield was relatively low (<20%) from DMF and cyclohexanone, propylene carbonate was finally selected to recrystallize compound **2q**.

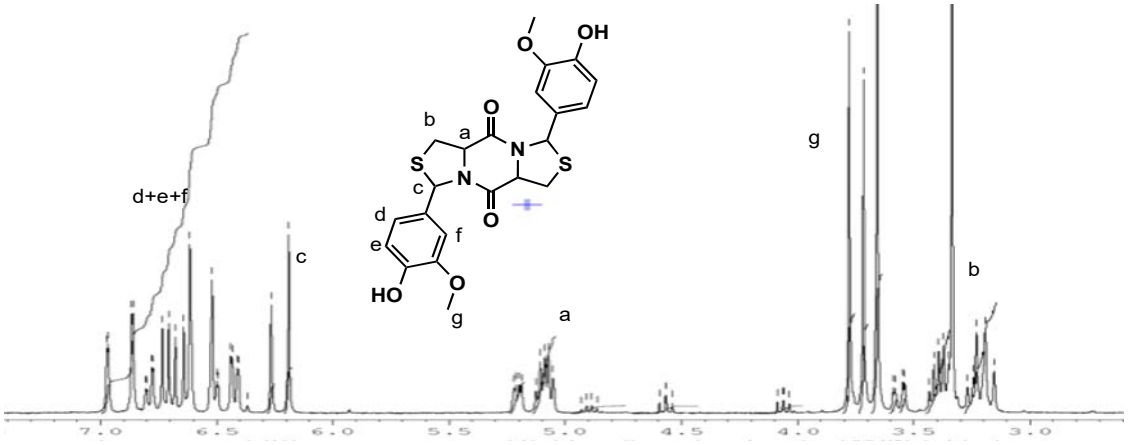

Figure 3.9 ^{1}H NMR spectrum (300 MHz, DMSO-d_6) of compound **2q.**

The structure of compound **2q** was fully characterized by spectroscopic means (See experimental section). As shown in Fig. 3.9, the ^{1}H NMR spectrum of **2q** in DMSO-d_6 displays proton resonances (ppm) at 6.97-6.37 (m, 3H), 6.27/6.19 (s, 1H), 5.22-5.19/5.13-5.50 (m, 1H), 3.78/3.72/3.66 (s, 1H), 3.59-3.16 (m, 2H). The other peaks belong to the residual of propylene

carbonate. As expected, the obtained product is a mixture of three stereoisomers and the ratio of isomers varied when reaction temperature was changed (Fig. 3.10). The peaks at 3.66 ppm, 3.72 ppm and 3.78 ppm are assigned to the O-CH_3 protons from three different isomers. Therefore, the ratio of three isomers can be determined by simple integration to be 1:0.64:0.72. Unfortunately, with many attempts, the separation of three isomers by chromatography was unsuccessful.

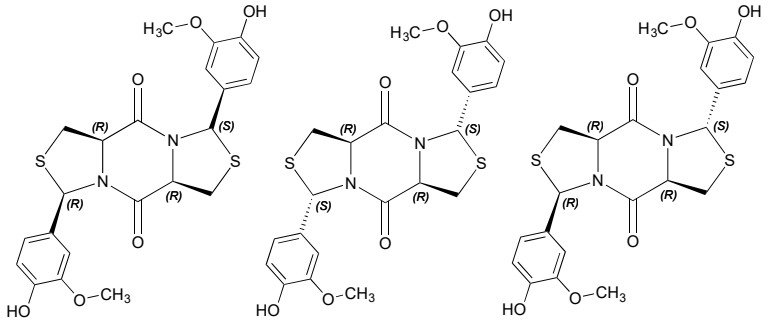

Figure 3.10 Three possible stereoisomers of DKP bisphenol **2q.**

Compound **2q** consists of a rigid tricyclic ring and two phenyl groups. It resembles bisphenol A (BPA) and thus can be used as a monomer for making polyesters (PE), polycarbonates (PC) and other specialty polymers. BPA is an important monomer for polycarbonate and engineering thermoplastic such as polysulfones.[22] Since BPA has recently been restricted for use in the products that are in contact with infants, it is desirable to develop an alternative to replace BPA.[23] Thus, bio-based compound **2q** is a potentially biocompatible monomer for polymers such as PC and PE.

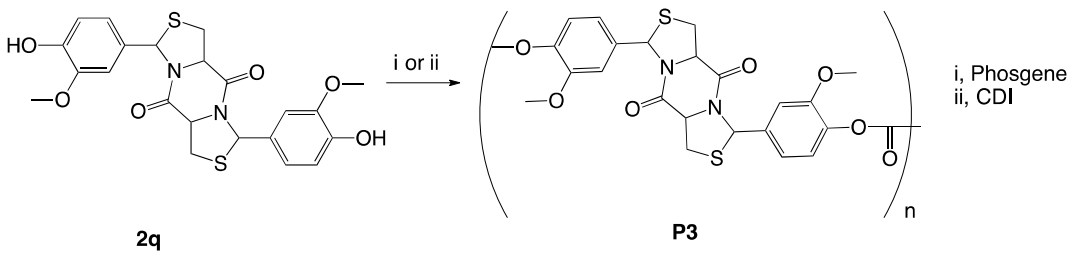

Scheme 3.14 Synthesis of polycarbonate from DKP bisphenol monomer **2q.**

DKP bisphenol **2q** was first tested in PC preparation. There are two common methods for polymerization: interfacial polymerization (water, organic solvent and alkaline base) and melt polymerization (ester trans-esterification). Since **2q** tends to decompose under the alkaline conditions and at high temperatures, both methods are not suitable for **2q** in polymerization. Therefore, a solution method using phosgene was attempted (Scheme 3.14). To find the optimal reaction conditions for polymerization of **2q**, a model reaction with BPA was done first. A stoichiometric amount of BPA and triphosgene was added in pyridine. The polycarbonate was obtained in high molecular weight, as it could form a tough thin film by casting. Thus, the same reaction condition was applied to the polymerization of **2q**, but polymerization failed. Since phosgene is known to react with the amide solvents to give undesirable side products, a failure in polymerization is likely due to the side reaction involving the lactam group in **2q** with phosgene or triphosgene.[24,25]

Then 1,1'-carbonyldiimidazole (CDI) was considered to replace phosgene or triphosgene in polymerization (Scheme 3.14). Similarly, a model reaction using BPA and CDI was performed in NMP at 50 ºC overnight. Once again, the high molecular weight PC was obtained. However, the polymerization of **2q** and CDI afforded only low molecular weight product. When the reaction temperature increased, a decomposition reaction was observed. Finally, polymer **P3** without good film-forming ability was obtained and characterized (Experimental Section). Take the IR spectrum as an example, where exhibits a band at 1777 cm^{-1} being characteristic for the carbonate group or polycarbonate and the band at 1678 cm^{-1} is for the DKP amide group (Fig. 3.11).

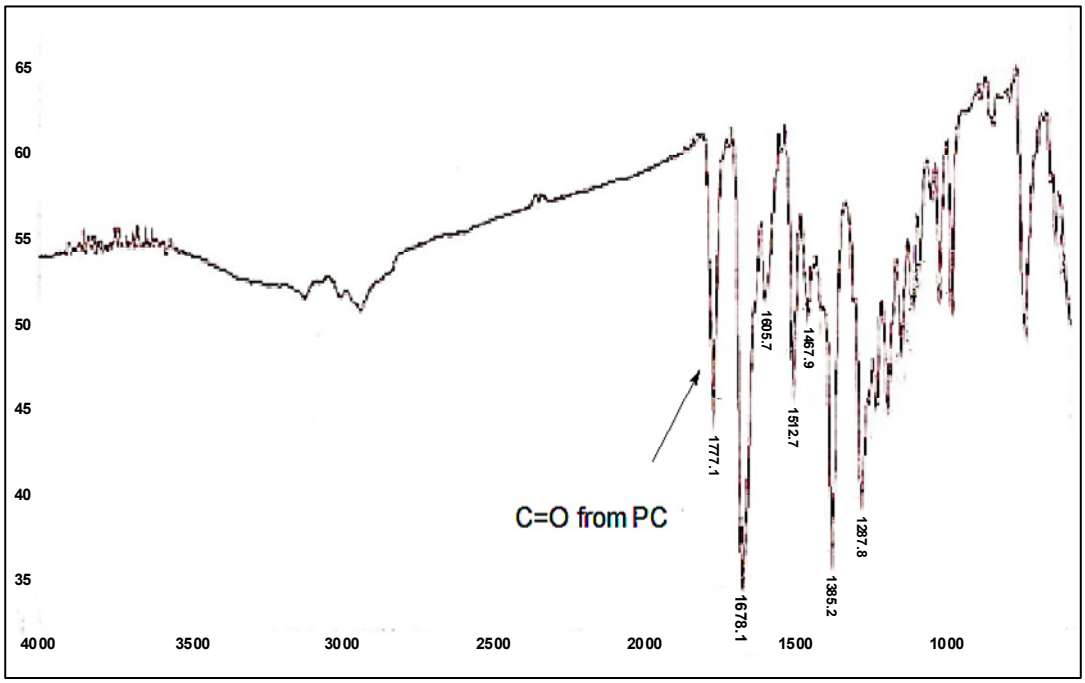

Figure 3.11 IR spectrum of polymer **P3.**

To circumvent the problem associated with the use of phosgene and CDI for polymerization of bisphenol **2q**, an alternative route was designed, where a bischloroformate was used as monomer to replace phosgene (Scheme 3.15). First, bischloroformates **1s** and **1t** were synthesized from isosorbitol and hexanediol with phosgene, respectively. The diol in dichloromethane was cooled to 0 ºC and a stream of phosgene was bubbled continuously into the solution. When phosgenation was complete, compound **1s** and **1t** were obtained after removal of the solvents. The polymerization with bisphenol **2q** and **1s** or **1t** was conducted in NMP in the presence of pyridine. But the polymerizations still failed with a lot of monomer **2q** left unreacted. It seems that these bischloroformate monomers tend to decompose or undergo side reactions under the polymerization conditions. Observation of significant color changes during the polymerization indicates side reactions of the bischloroformates. In comparison with the model reactions using BPA bischloroformate, the monomer stability is a key to successful polymerization, which implies that the DKP-containing chloroformate is relatively unstable.[22]

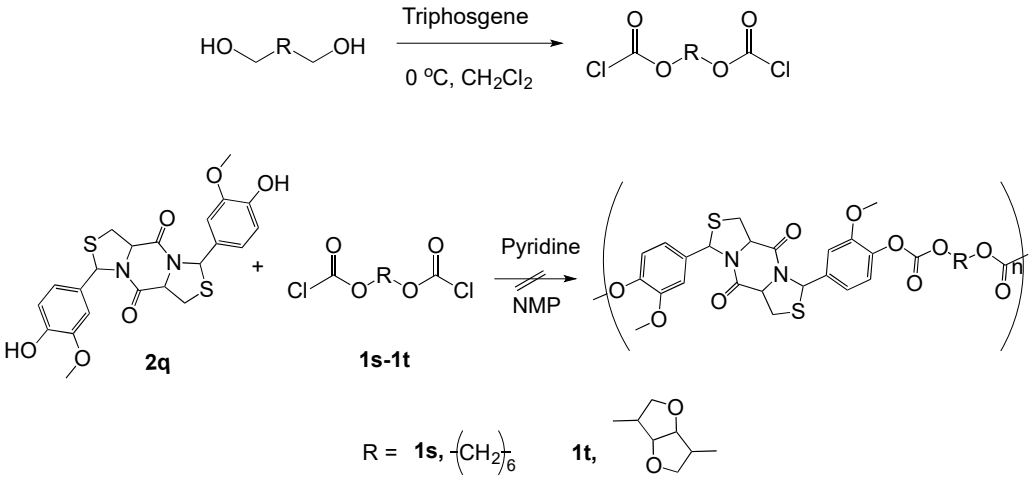

Scheme 3.15 Attempted polymerization of bischloroformates **1s** and **1t** with bisphenol **2q.**

DKP bisphenol **2q** can also be utilized to make DKP-containing polyesters. Therefore, a sample reaction between **2q** and decanoyl chloride was performed to identify the feasibility of the designed esterification reaction. It was identified that the reaction could proceed in acetonitrile with DIEA as a base at room temperature (Scheme 3.16). Through IR spectrum, it was easily to identify the formed ester structure through the formation of a new characteristic carbonyl peaks and the disappearance of hydroxyl peaks. As shown in Fig. 3.12, there was no signal 3000 cm^{-1}, indicating the complete reaction on hydroxyl group and the band at 1682 cm^{-1} belongs to the amide group of DKP. The new peak at 1762 cm^{-1} was assigned to the new carbonyl group and was used as the characteristic peak in the subsequent polymer synthesis.

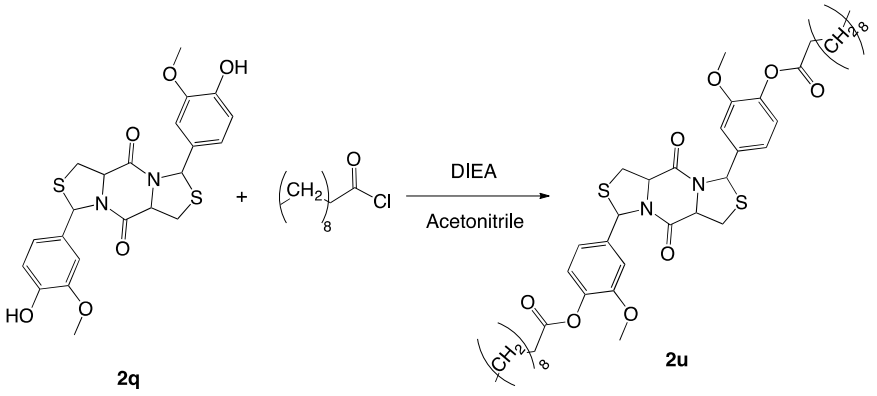

Scheme 3.16 Syntheses of DKP-containing ester **2u** from bisphenol **2q**.

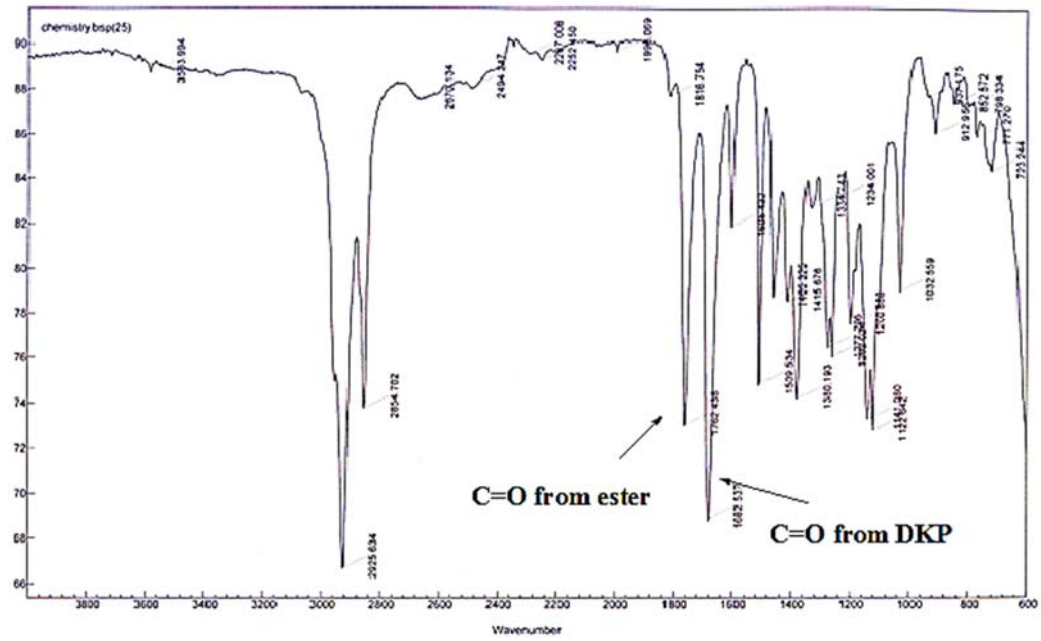

Figure 3.12 IR spectrum of compound **2u.**

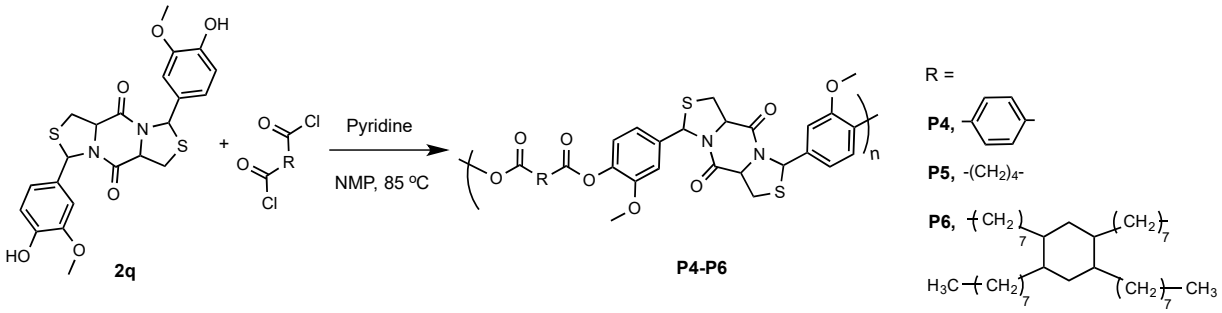

Scheme 3.17 Syntheses of polyesters **P4-P6** from monomer **2q**.

Then, a series of polyesters were synthesized from various acid chlorides with bisphenol **2r** (Scheme 3.17). To find the optimum solvent and base for polymerization, reactions in different solvent combinations of DMF, pyridine and NMP were performed and clarified that the condition with NMP as solvent and pyridine as base gave the highest efficiency. Thus, the polymerization reaction between bisphenol **2q** with dichlorides were carried out in NMP with the addition of pyridine as base at 85 ºC overnight. Finally, DKP-containing polyesters were successfully obtained in high molecular weights (Table 3.2), as they could form a free-standing thin film by drop casting.

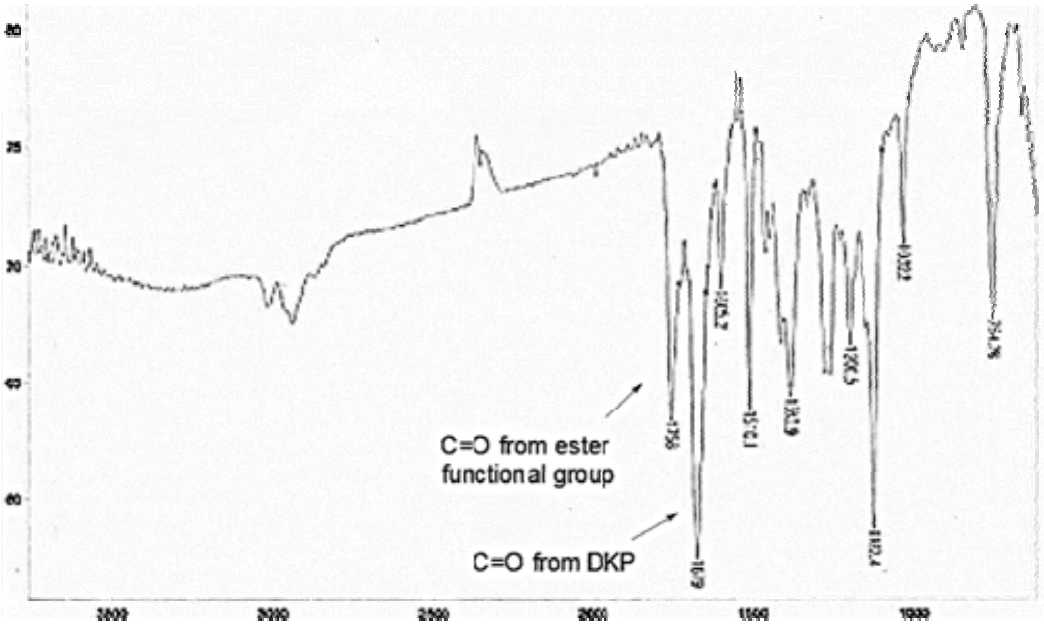

Figure 3.13 IR spectrum of polymer **P5.**

The structures of the obtained polymers were characterized by spectroscopic means (See experimental section). Take the IR spectrum of polymer **P5** as an example (Fig. 3.13). The IR spectrum exhibits a signal at 1758 cm^{-1}, being characteristic for the ester group in polymers, at 1679 cm^{-1} for DKP amide group and the complete disappearance of signals at 3000 cm^{-1} further confirming the successful achievement of polymers. Moreover, the molecular weights and PDI of these polymers were determined by GPC measurement relative to polystyrene standards (Table 3.2).

Table 3.2 Molecular weights and PDIs of polymers **P4-P6**.

Polymer	**M*n* (g/mol)**	**M*w* (g/mol)**	**PDI**
P4	$2.98*10^5$	$4.11*10^5$	1.38
P5	$2.25*10^5$	$2.88*10^5$	1.28
P6	$2.03*10^5$	$4.39*10^5$	2.16

3.6 Conclusion

A series of TCA derivatives with functional groups were synthesized from L-cysteine and aldehydes in water or ethanol at room temperatures with high yields. After dimerization in acetonitrile or DMF in the presence of HBTU and DIEA, a series of DKP-containing difunctional monomers were achieved with great potential for further polymerization. Based on the imported functional groups, different polymers were successfully synthesized. These polymers containing DKP structure have a great biodegradable potential.

3.7 Experimental section

3.7.1 Materials

L-Cysteine, formaldehyde, benzaldehyde, vanillin, 4-bromobenzaldehyde, HBTU, DIEA and cystine, L-cysteine methyl ester hydrochloride, pyridine, manganese dioxide, DCC, $AlCl_3$, BF_3, TCNQ, trifluortomethanesulfonic acid, tetracyanoquinodimethane, tetracyanoethylene, and 2,3-dichloro-5,6-dicyano-1,4-benzoquinone, CDI, 1,6-hexanediol, isosorbide, decanoyl chloride, adipoyl chloride and terephthaloyl chloride were purchased from Aldrich Canada. Dimer acid was purchased from China. The water used in this work was purified using a Millipore™ Milli-Q™ Advantage A10 water purification system. (4,8-Bis(octyloxy)benzo[1,2-b:4,5-b']dithiophene-2,6-diyl)bis(trimethylstannane) and 2,7-bis(trimethylstannane)-9,9-dioctyl fluorene were synthesized by Saif Mia in lab.

3.7.2 Measurements

^{1}H and ^{13}C NMR spectra were measured on a Bruker Avance Digital 300 MHz spectrometer at ambient temperature using tetramethylsilane as an internal standard. Resonances were quoted on the δ scale relative to tetramethylsilane (TMS, δ = 0) as an internal standard. Infrared measurements were recorded on a Varian 1000 FT-IR Scirinitar

spectrophotometer in the regions of 4000–400 cm^{-1}. Mass spectra were performed with a Micromass Quattro LC ESI (EI). Fisher-Johns melting point apparatus was used to test the melting points (mp). Gel permeation chromatography (GPC) analysis was conducted on a PL-GPC 220 system with polystyrene as standard and tetrahydrofuran (THF) as eluent. CD spectrum was recorded on Olis Circular Dichrosim Spectrophotometers and the wavelength starting from 210 nm. Decomposition temperature was measured on a thermogravimetric analyzer TGA 2950 CE at a heating rate of 10 ºC/min in nitrogen. The UV-absorption spectra were recorded using a UV-Vis Lambda 900 spectrophotometer and the fluorescence emission spectra were recorded on Shimadzu RF-1501 spectrofluorophotometer using 1 cm quartz cell.

3.7.3 Synthesis

General procedure for cysteine reacting with aldehyde:

Cysteine (1.21 g, 10.0 mmol) was dissolved in 20 mL of distilled water in 50 mL round-bottom flask. Aldehyde was then added under argon atmosphere. The mixture was stirred at ambient temperature or refluxing in dark overnight. After the reaction was completed, the target compound was collected by suction filtration and washed with water and ethanol.

1o: 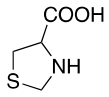

98%. ^{1}H NMR (300 MHz, DMSO-d_6): 4.23-4.20 (d, 1H), 4.04-4.01 (d, 1H), 3.83 (t, 1H), 3.10-2.78 (m, 2H).

1p: 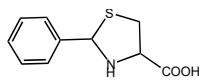

96%. ^{1}H NMR (300 MHz, DMSO-d_6+HCl): 7.55-7.27 (m, 5H), 5.68/5.55 (s, 1H), 4.3/4.9 (t, 1H), 3.53-3.08 (m, 2H); ^{13}C NMR (75 MHz, DMSO-d_6+HCl): 173.46, 172.70, 141.68, 139.40, 129.03, 128.77, 128.71, 128.06, 127.75, 127.40, 72.23, 71.56, 65.92, 65.36, 38.91, 38.45. M.P.: 174 ºC.

1q: 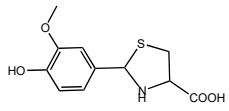

90%. ^{1}H NMR (300 MHz, DMSO-d_6+HCl): 7.15-6.70 (m, 3H), 5.40/5.55 (s, 1H), 4.30/3.85 (t, 1H), 3.75 (s, 3H), 3.0-3.2 (m, 2H). ^{13}C NMR (75 MHz, DMSO-d_6+HCl): 173.65, 172.71, 147.95, 147.82, 147.07, 146.61, 131.67, 129.90, 120.41, 120.13, 115.56, 115.41, 111.90, 111.69, 72.62, 72.04, 65.86, 65.23, 56.09, 56.05, 38.84, 38.24.

1r: 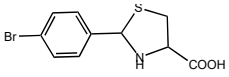

90%. ^{1}H NMR (300 MHz, DMSO-d_6+HCl): 7.56-7.38 (m, 4H), 5.67/5.50 (s, 1H), 4.19-3.88 (m, 1H), 3.89-3.05 (m, 2H). ^{13}C NMR (75 MHz, DMSO-d_6+HCl): 173.28, 172.52, 141.65, 139.12, 131.80, 131.56, 130.07, 129.60, 121.69, 120.95, 71.28, 70.59, 66.04, 65.29, 38.75, 38.49.

General procedure for the preparation of bischloroformate:

Diol was dissolved in dichloromethane in a round-bottom flask and cooled to 0 ^{o}C by using an iced bath. Then a stream of phosgene was bubbled continuously into the solution. When phosgenation was complete, target bischloroformate was obtained after removal of the solvents.

1s: 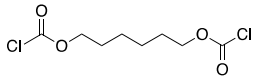

^{1}H NMR (300 MHz, $CDCl_3$): 4.34 (t, 2H), 1.80-67 (m, 2H), 1.51-1.46 (m, 2H).

1t: 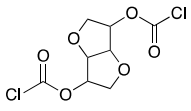

^{1}H NMR (300 MHz, $CDCl_3$): 5.30 (s, 2H), 5.00 (s, 1H), 4.60 (s, 1H), 4.24 (d, 1H), 4.05 (t, 2H), 3.92-3.89 (d, 1H).

General procedure for DKP formation from TCA derivatives:

TCA derivative (0.50 g) and HBTU were dissolved in dry acetonitrile or DMF in a round

bottom flask, then base DIEA was added dropwise. The reaction mixture was stirred under argon overnight at room temperature or elevated temperature. When the reaction complete, acetonitrile or DMF was removed and the obtained mixture was dissolved in ethyl acetate again, followed by washing with 1N HCl solution, 5% $NaHCO_3$ and brine. Target compound was obtained from organic phase after removal the solvent.

2o: 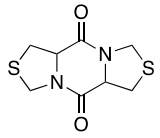

90%. ^{1}H NMR (300 MHz, $CDCl_3$) 4.83 (d, 1H), 4.54-4.49 (m, 2H), 3.49-3.37 (m, 2H).

2p: 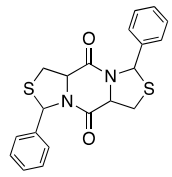

80%. ^{1}H NMR (300 MHz, $CDCl_3$): 7.42-7.15 (m, 10H), 6.62/6.53/6.28 (s, 1H), 4.81-4.75 (m, 1H), 2.71- 3.31 (m, 2H); ^{13}C NMR (75 MHz, $CDCl_3$): 164.32, 163.93, 162.37, 140.91, 138.90, 138.74, 128.93, 128.70, 128.63, 128.52, 128.22, 126.78, 126.44, 124.81, 65.68, 65.39, 64.95, 64.51, 63.70, 62.66, 33.29, 32.44, 30.26. M.P.:170 ºC.

2q: 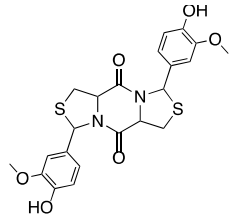

70%. ^{1}H NMR (300 MHz, DMSO-d_6): 6.97-6.37 (m, 3H), 6.27/6.19 (s, 1H), 5.22-5.19/5.13-5.50 (m, 1H), 3.78/3.72/3.66 (s, 1H), 3.59-3.16 (m, 2H).; ^{13}C NMR (75 MHz, DMSO-d_6): 165.27, 165.08, 164.82, 148.16, 147.97, 147.76, 146.72, 146.32, 134.24, 131.35, 118.47, 116.75, 115.67, 115.30, 115.22, 110.84, 110.39, 109.25, 65.20, 65.08, 64.17, 63.84, 63.74, 63.61, 56.17, 55.98, 55.89, 30.74, 29.50, 29.42.

2r: 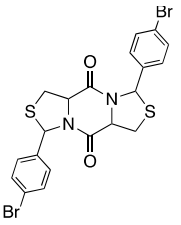

70%. ^{1}H NMR (300MHz, $CDCl_3$): 7.49-7.04 (m, 8H), 6.16 (s, 2H), 4.84-4.78 (m, 2H), 3.53-3.32 (m, 4H); ^{13}C NMR (75MHz, $CDCl_3$): 165. 36, 142.61, 132.01, 131.83, 127.39, 121.26, 65.20, 63.01, 29.70.

2u: 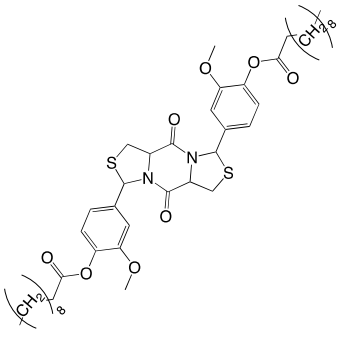

Bisphenol **2q** (0.25 g) was dissolved in 10 mL acetonitrile solvent in a two neck round bottom flask. Then 2.3 equivalent DIPEA was added dropwise. After 10 min stirring, 1.1 equivalent decanoyl chloride was added and stirred overnight. After the reaction completed, acetonitrile was evaporated and washed with ether. The filtrate was finally purified by column chromatography with hexane: acetone = 2:1 v/v.

^{1}H NMR (300MHz, $CDCl_3$): 7.14- 6.17 (m, 8H), 4.84-4.65 (m, 2H), 3.85/3.81/3.69 (s, 6H), 3.76-3.31 (m, 4H), 2.61-2.54 (m, 4H), 1.75 (t, 4H), 1.45-1.22 (m, 28H), 0.89 (t, 6H).

General procedure for synthesis of polymer P1-P2:

In a flame-dried 25-mL round-bottom flask under an argon atmosphere, organotin monomer and monomer **2r** in 1:1 mole ratio were dissolved in 8 mL of chlorobenzene. The solution was bubbled with argon for 30 min and then 10 mol % of $Pd(PPh_3)_4$ was added and solution was heated to 100 ºC and stirred for 48 hours. After cooling, the polymer was precipitated out in methanol and filtered. The polymer was purified via Soxhlet extraction (hexane and acetone)

to give dark solid.

P3: 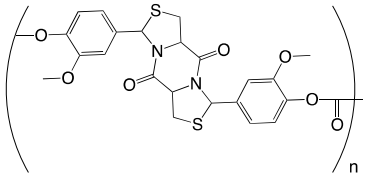

In a flame-dried 25-mL round-bottom flask under an argon atmosphere, monomer **2q** (0.5g, 0.84 mmol) was dissolved in 5 mL of NMP at 50 ºC. Then the solution of CDI (0.15g, 0.9 mmol) in NMP was added dropwise and the reaction was stirred at 50 ºC overnight. After cooling, the polymer was precipitated out in water and filtered.

^{1}H NMR (300 MHz, DMSO-d_6): 6.97-6.50 (m), 6.52 (s), 6.27 (s), 6.19 (s), 5.21-5.20 (m), 5. 13-5.07 (m), 3.84 (s), 3.78 (s), 3.72 (s), 3.66 (s), 3.59-3.16 (m). ^{13}C NMR (75 MHz, DMSO-d_6): 165.08, 164.81, 147.98, 147.77, 146.74, 146.34, 133.24, 131.35, 127.74, 122.14, 118.47, 117.50, 115.68, 115.23, 114.00, 110/84, 109.35, 65.09, 63.85, 63.75, 56.17, 55.90, 48.94, 30.75, 30.57, 29.42, 17.68. Molecular weight: $2.02*10^4$ g/mol with PDI of 5.91.

General procedure for synthesis of polyester P4-P6:

Bisphenol **2q** (0.1 g, 0.00022 mol) and dilute acid chloride (0. 033 mL, 0.00022 mol) were dissolved in NMP (1 mL) at room temperature. After stirring for 10 mins, the dilute pyridine in chloroform was added dropwise. Then the reaction was stirred at 40- 50 ºC for two days. IR were tested to monitor the reaction process. After cooling, the polymer was precipitated out in methanol and filtered.

P4: 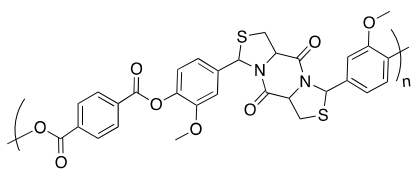

^{1}H NMR (300 MHz, DMSO-d_6): 8.24-13 (m), 7.29-6.29 (m), 5.38-5.11 (m), 3.85-3.72 (m), 3.58-3.22 (m).

P5: 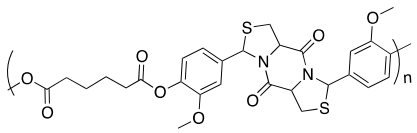

^{1}H NMR (300MHz, $CDCl_3$): 7.28 (s), 7.16 (s), 7.11 (s), 6.69 (s), 6.59 (s), 6.25 (s), 4.76 (s), 4.69 (s), 4.15-4.08 (m), 3.87-3.31 (m), 2.57 (d), 2.33 (t), 1.75 (s), 1.62-1.60 (d), 1.31-1.23(m).

P6: 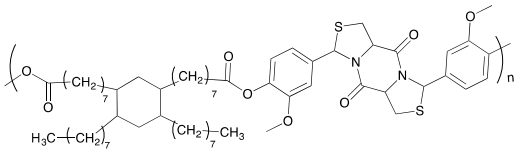

^{1}H NMR (300MHz, $CDCl_3$): 7.03 (s), 6.72 (m), 6.29 (s), 4.75 (s), 3.84-3.36 (m), 2.58-1.30 (m), 0.92 (s).

References

1. Helander, A.; Tottmar, O. *Alcohol Alcohol Suppl*., **1987**, *1*, 193.
2. Schubert, M. *J. Biol. Chem.,* **1935,** *111*, 671.
3. Wang, C.; Zheng, X.; Zhang, Q.; Liu, Q. *Chin. J. Org. Chem*., **2010,** *30,* 1441.
4. Iwao, J.; Chiba, T.; Oya, M.; Iso, T.; Baba, T. *Antihypertensive 4-thiazolidinecarboxylic acids.* CA Patent 1127157 A, **1982.**
5. Schmolka, I.; Spoerri, P. *J. Org. Chem.,* **1957,** *22*, 943.
6. Iannotta, D.; Castellucci, N.; Monari, M.; Tomasini, C. *Tetrahedron Lett*., **2010**, *51,* 4558.
7. Markovic, R.; Rajkovic, B. *J. Serbian Chem. Soc.*, **1997**, *62*, 957.
8. Qiu, T.; Hao, C. *Chemical reagents,* **2008**, *3.*
9. Credico, B. D.; Reginato, G.; Gonsalvi, L.; Peruzzini, M.; Rossin, A. *Tetrahedron* **2011**, *67*, 267.
10. Chemistry LibreTexts. *Natural Occurrence of Aldehydes and Ketones* https://chem.libretexts.org/?title=Core/Organic_Chemistry/Aldehydes_and_Ketones/Properties_of_Aldehydes_%26_Ketones/Natural_Occurrence_of_Aldehydes_and_Ketones
11. Schmolka, L. R.; Sperri, P. E. *J. Org. Chem.*, **1975**, *22*, 943.
12. Karpiuski, Z. J.; Kamy, M.; Kublii, Z.; *J. Electroanal.,* **1990,** *288*, **129**.
13. Khan, K. M.; Ullah, Z.; Ali, M.; Choudhary, M.; Rahman, A.; Haq, Z. *Mol. Divers,* **2006**, *10*, 223.
14. Peptide coupling reagent: Wikis http://www.thefullwiki.org/Peptide_coupling_reagent
15. El-Faham, A.; Albericio, F. *Chem. Rev.,* **2011**, *111*, 6557.
16. Parrish, D. A.; Mathias, L. J. *J. Org. Chem.*, **2002**, *67*, 1820.
17. Warner, D. S.; Limberg, C.; Mebs, S.; Anorg. Z. *Allg. Chem.,* **2013**, *639*, 1577.

18. Kobler, C.; Haeussner, T.; Weckbecker, C. *Cyclic dipeptides as feed additives.* US Patent 20110295006 A1, **2011**.

19. Koval, I. V. *Russian Chemical Reivoews,* **1993**, *62*, 769.

20. Disulfide. https://en.wikipedia.org/wiki/Disulfide#cite_note-Sevier-2

21. Saif M. *Development of low bandgap donor-acceptor polymers for use in optoelectronic*, PhD thesis, **2016**.

22. Boyles, D. A. Bendler, J. T. *Monomers containing at least one biaryl unit and polymers and derivatives prepared therefrom,* US 2004/0254327 A1, **2004.**

23. Romano, R. J.; Schmidt, D. F. *High Performance Bisphenol A (BPA) Free Epoxy Resins*. Toxics Use Reduction Institute, **2013**.

24. Marson, C. M. *Tetrahedron,* **1992**, *48*, 3659.

25. Mancuso, A. J.; Swern, D. *Synthesis,* **1981**, 165.

Chapter 4 Molecular modification with L-cysteine

4.1 Molecular design and synthetic approaches

The application of cysteine in polymer modification has a long history, especially in the creation of smart polymers for pharmaceutical uses. The modified polymer not only inherits the properties from the original structure, but also contains unique features from the amino acid, such as the chiroptical property.[1,2] In Chapter 2.2.2, L-cysteine has already been successfully attached to a series of small molecule diols by using undecenoic acid as a link, which has the alkene bonds for the thiol-ene reaction (TEC) and carboxylic acid for esterification. Inspired by this success, we intended to incorporate L-cysteine into macromolecules (Scheme 4.1).

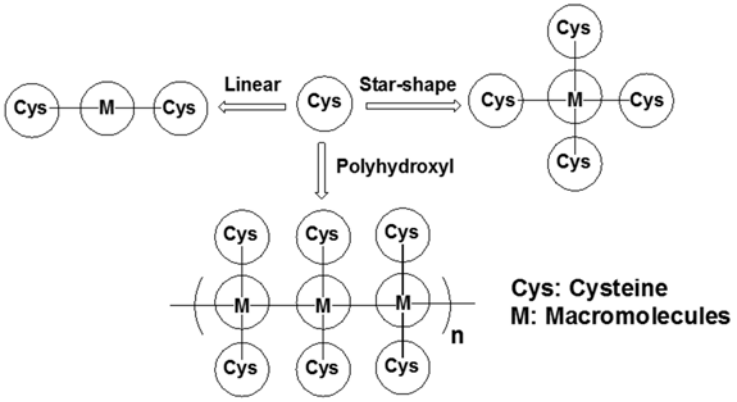

Scheme 4.1 Synthetic routes from L-cysteine to cysteine modified macromolecules.

First of all, if L-cysteine is attached to a linear macromolecules PEG and PTMEG, one can obtain a linear polyether with the end groups of L-cysteine. Since PEG and PTMEG with molecular weights ranging from 600 to a few thousand are commercially available, a variety of L-cysteine end-modified polyethers can be made available that may have interesting properties owing to the end groups of amino acid.

Moreover, by using a star-shape polyol, one could make cysteine-modified star-shape macromolecules. The star-shape macromolecules are expected to have a range of structural diversity, morphologies and functions and potential applications in surfactants, drug delivery,

sensors, molecular probes and membranes.[3,4] The star-shape polyols, such as glycerol, di(trimethylolpropane), ribitol and dipentaerythrito, are selected in our work as the core to build up a few examples of start-shaped macromolecules containing L-cysteine on the periphery.

Furthermore, L-cysteine can be introduced to polysaccharides. Polysaccharides are one of the most abundant natural-occurring macromolecules and currently used for applications such as coatings, drug delivery and biomedical materials.[5-7] The L-cysteine modified polysaccharide may possess some interesting properties and offer an opportunity for new applications for example, chiral recognition. Therefore, ß-glucan and ß-cyclodextirin were selected in our work.

4.2 Syntheses of L-cysteine-modified linear macromolecules

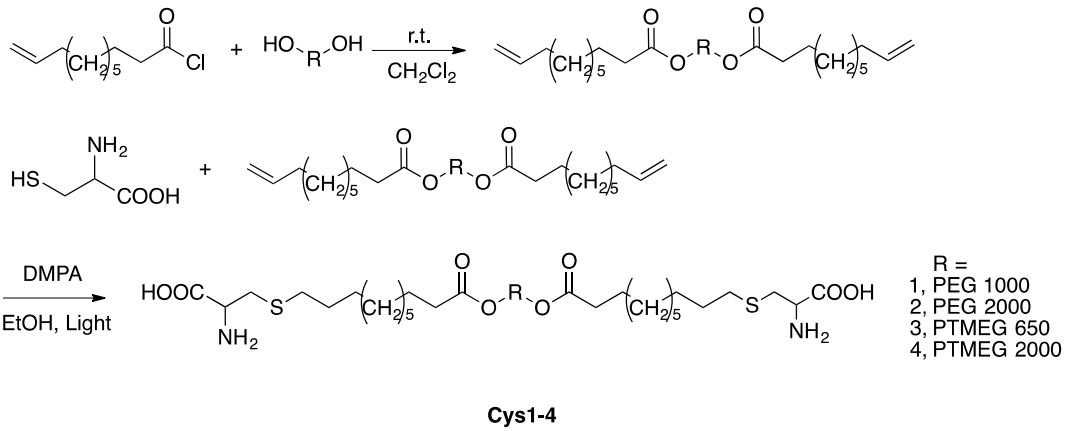

Scheme 4.2 Syntheses of cysteine-modified linear macromolecules **Cys1-4**.

The synthetic route to the preparation of cysteine-modified linear macromolecules involves a two-step process, esterification between undecenoic acid chloride and PEG or PTMEG, followed by a thiol-ene radical click reaction (Scheme 4.2). First, the esterification reaction was done in dichloromethane at room temperature overnight with almost 100% yield. After removal of the solvents, the alkene-functionalized polyethers were used in the subsequent thiol-ene reactions without purification. As discussed in Chapter 2.2.1, the thiol-radical

reaction was initiated with photoinitiator DMPA. Thus, the desired compounds **Cys1-4** were obtained after irritating for 6h.

However, an undesired side esterification between L-cysteine and the reaction solvent ethanol was observed when modifying PEG. It was the first time that a side reaction took place in the TEC reaction in my work. Since PEG with high molecular weight could fold and twist into coil in solution, it was assumed that PEG chain would wrap L-cysteine and ethanol together with an increased reaction concentration, which in turn accelerating the side reactions.[8,9] However, it leads to some difficulties in the separation of the target acid product from the ester side product. To obtain pure product, column chromatography and recrystallization were used and the reaction variables were changed, including temperatures, solvents, acid catalysts, addition of water, reaction times, which are summarized in Table 4.1. It was found that only the small-scale reaction gave the best result, since there was no side reaction took place before the reaction completion. The obtained **Cys1-2** was further recrystallized in 2-methyl-2 butanol. Unlike the purification of **Cys1-2**, the work-up for compound **Cys3-4** was quite simple, only involving removal of the solvents and washing with water and acetone.

Table 4.1 Attempted syntheses of L-cysteine end-modified PEG under various conditions.

<table>
<tr><th colspan="2">Variable</th><th>Observation</th></tr>
<tr><td rowspan="2">Temp.</td><td>0 °C</td><td>No reaction</td></tr>
<tr><td>10 °C</td><td>Slow reaction, resulting in more esterification</td></tr>
<tr><td rowspan="2">Acid</td><td>Acetic acid</td><td>Less than 30% conversion</td></tr>
<tr><td>No acid</td><td>Less than 30% conversion</td></tr>
<tr><td rowspan="5">Solvent</td><td>Acetone</td><td rowspan="5">No reaction or less than 30% conversion or ester group derived from undecenoic acid hydrolyzed</td></tr>
<tr><td>THF</td></tr>
<tr><td>Toluene</td></tr>
<tr><td>Dioxane</td></tr>
<tr><td>Mixed Solvents</td></tr>
<tr><td rowspan="2">Water</td><td>With HCl</td><td rowspan="2">Ester group derived from undecenoic acid hydrolyzed</td></tr>
<tr><td>Without HCl</td></tr>
</table>

Time	Stopped at the early stage	Impossible to separate the product from the starting materials
	Small-scale reaction with complete conversion within 1h	Product obtained

The structures of compounds **Cys1-4** were fully characterized by spectroscopic means (See experimental section). Take the ^{1}H NMR spectrum of **Cys2** as an example, where the spectrum displays proton resonances (ppm) at 4.15-4.10 (m, 6H), 3.60-3.37 (m, 200H), 2.98 (t, 4H), 2.54 (t, 4H), 2.29 (t, 4H), 1.46-1.55 (m, 8H) and 1.34-1.25 (m, 24H) (Fig. 4.1). The triplet split peak appeared at 2.54 ppm is the characteristic protons of CH_2, confirming the successful addition of cysteine onto the olefin-containing PEG.

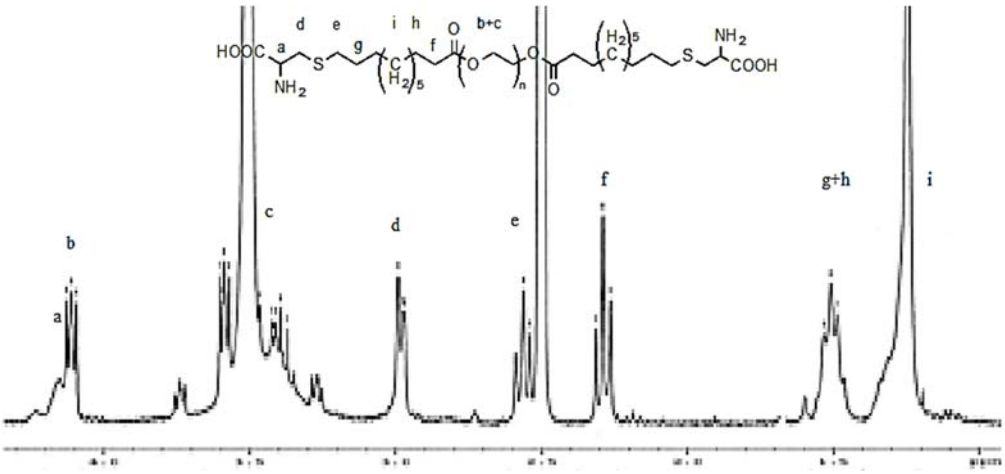

Figure 4.1 ^{1}H NMR (300 HMz, DMSO-d_6) spectrum of **Cys2.**

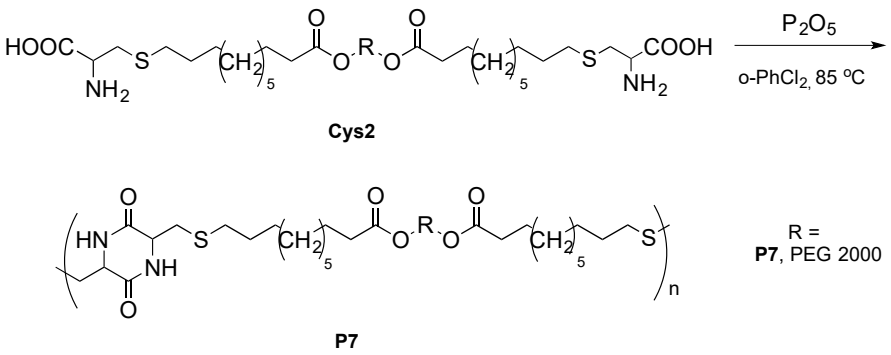

Scheme 4.3 Synthesis of polymer **P7** from **Cys2.**

Linear macromolecules with cysteine end-groups can be used as monomers for the production of DKP-containing polymers. However, restricted by the poor solubility of **Cys3-4** in organic solvents, only PEG derived **Cys1-2** were utilized in polymerization. As discussed in Chapter 2.2.1, the dimerization of cysteine derivatives was best carried out in 1, 2-dichlorobenzene in the presence of P_2O_5 as a catalyst and dehydrating reagent at 85 ºC for two days. When using **Cys1**, even at a higher reaction temperature over a long time, there was no significant change in solution viscosity, indicating the formation of low molecular weight polymer. When **Cys2** was used, after polymerization for one day, the reaction solution became viscous. The ^{1}H NMR analysis indicated the successful formation of the DKP-containing polymer **P7**, along with less than 40% of **Cys2** left. Further extension of reaction time after one day caused complete gelation. Polymer **P7** was isolated as a light-yellow gel and was insoluble in all the organic solvents we tested, such as DMSO, DMF, ethanol, benzonitrile, cyclohexaneone and acetic acid. Moreover, slight swelling was observed when placing **P7** into water. Thus, it can be concluded that **P7** is physically and slightly chemically cross-linked.

Polymer **P7** contains the hard-segment (rigid DKP ring) and soft-segment (PEG chain), and thus could be elastic. The polymer was then placed in a mold and left on preheated hot plate (110 ºC) and the mold was compressed for 3 mins. The mold was then cooled down and the specimen was an elastomer, as it could be stretched to twice of its original length and recover back to its original shape without permanent deformation (Fig. 4.2). More importantly, the polymer became fluid again at 150 ºC and was able to be reshaped at that temperature over and over again. The melting behavior strongly indicates no or a very slow degree of chemical crosslinking in **P7**.

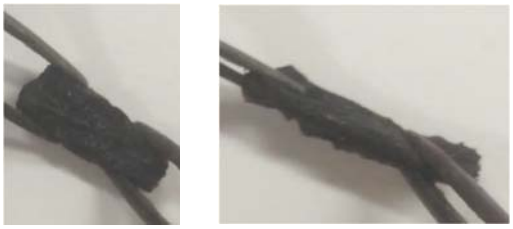

Figure 4.2 Photos of the molded part of polymer **P7** before and after stretching.

The molded **P7** in Figure 4.2 are black. The coloring is due to thermal decomposition of the trapped phosphoric acid and 1,2-dichlorobenzene in polymer. Therefore, many attempts were made to prevent physical crosslinking during the polymerization. The polymerization concentration and temperatures varied; benzoic acid, acetic acid and T3P were tried; acid-free condition with different concentrations of monomer and solvent-free polymerization in a sealed tube were attempted; inorganic salt (e.g., LiCl and $CaCl_2$) was to prevent the gelation. Unfortunately, none of them was successful. [10]

4.3 Syntheses of Star-shape macromolecules

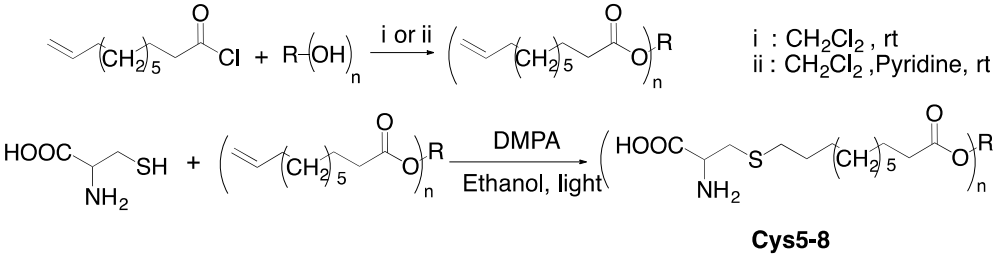

Cys5-8

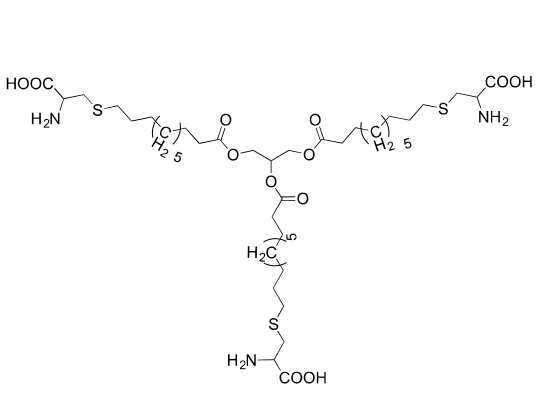

Cys5

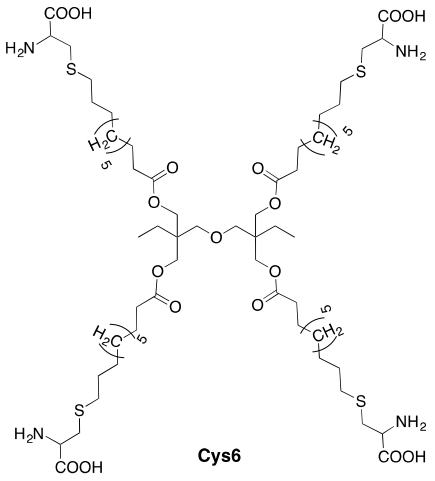

Cys6

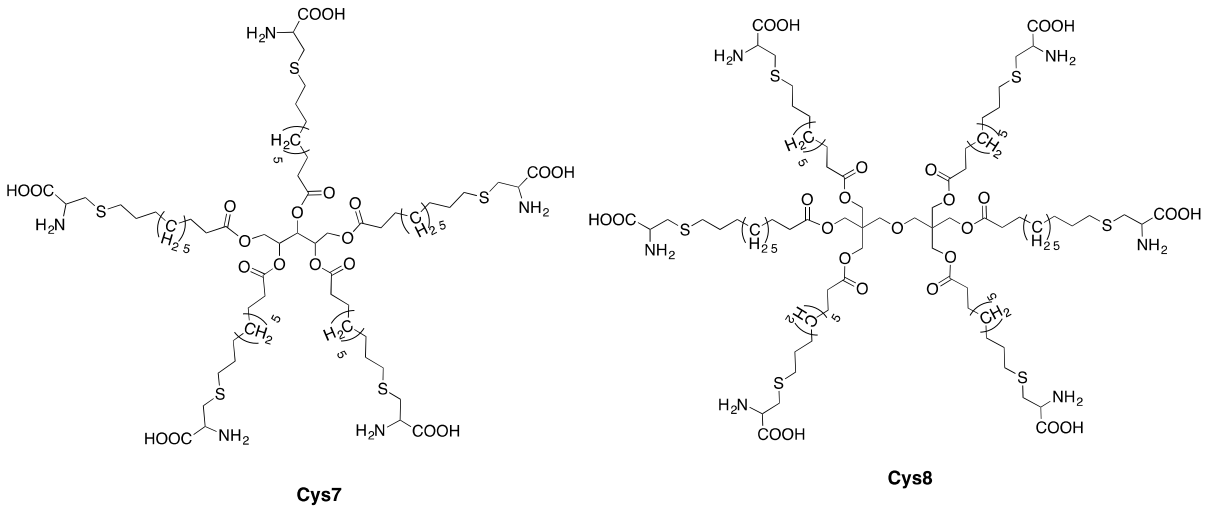

Scheme 4.4 Syntheses of cysteine-modified star-shape macromolecules **Cys5-8**.

The synthetic route to the preparation of cysteine-modified star-shape macromolecules is similar to the one for making linear-macromolecules, which involves a simple two-step process, esterification between undecenoic acid chloride and polyols, followed by a thiol-radical click reaction. Using the reaction condition in Scheme 4.2, L-cysteine modified **Cys6** and **Cys8** were obtained smoothly. In the case of glycerol and ribitol which have both primary and secondary alcohols, the reaction was carried out at elevated temperatures in the presence of a base and a nucleophilic acylation catalyst of 4-dimethylaminopyridine. In addition, column chromatography was required to purify the diene intermediates due to the existence of side products.

The structures of **Cys5-8** were fully characterized by spectroscopic means (See experimental section). Take the ^{1}H NMR spectra of **Cys6** as an example, where the spectrum displays proton resonances (ppm) at 4.09-4.04 (m, 4H), 3.86 (s, 8H), 3.19 (s, 4H), 3.01-2.99 (d, 8H), 2.53 (t, 8H), 2.23 (t, 8H), 1.47 (t, 16H), 1.32-1.20 (m, 52H), 0.75 (t, 6H). The peak appearing at 2.53 ppm is characteristic protons of CH_2 from alkene functional group which confirm the successful formation of the sulfide.

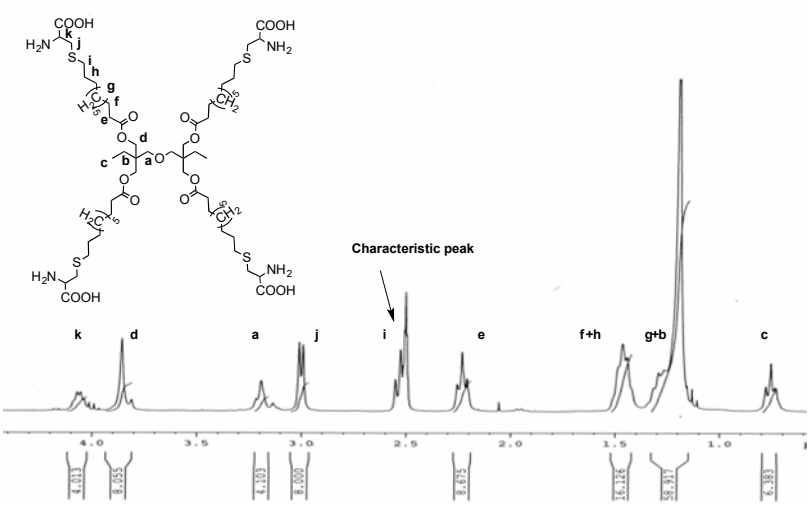

Figure 4.3 ^{1}H NMR spectrum (300 MHz, DMSO-d_6) of **Cys6.**

4.4 Self-assembling properties of L-cysteine modified macromolecules

The fact that cysteine is a type of hydrophobic amino acid has been proved, since it was reported to participate in the hydrophobic interactions in a prepared micelle and was associated with the hydrophobic area of proteins.[11,12] Since the cysteine end-group connected with long alkyl chains may also be hydrophobic, **Cys1-2** may be amphiphilic macromolecules with hydrophilic PEG block and should self-assemble in aqueous solution. The self-assembling feature is quite important for surfactants or drug delivery.[13] Considering that **Cys1-2** are almost monodispersed with a known molecular weight and easily produced from biomass-based feedstock, their self-assembling property deserves investigation.

To study the self-assembling behavior, the critical aggregate concentrations (CAC), above which the formation of aggregates could be detected, is usually measured first. Different methods could be applied to determine the CAC value, including fluorescent method using pyrene as a probe and dye micellization method. But the most classic and popular method is to measure the surface tension of the solutions with a tensiometer, which was used in our work.[14,15] Moreover, since the amino acid end groups may exist in different forms under different pH environment, for example, cation, anion and zwitterion, the self-assembling

behaviors at different pH were tested. In the experiments, 5 mL of the solutions **Cys1-2** at pH 2 with different concentrations were first prepared, and then sodium bicarbonate was added to increase pH gradually to 6.5-6.8 and further to 10. A pH meter was used to read the pH values. Each solution was sonicated for 20 mins and left in standing for 10 mins before the measurements. A plot of surface tension vs. the logarithm of the solution concentration was made to obtain the CAC value (See experimental section).

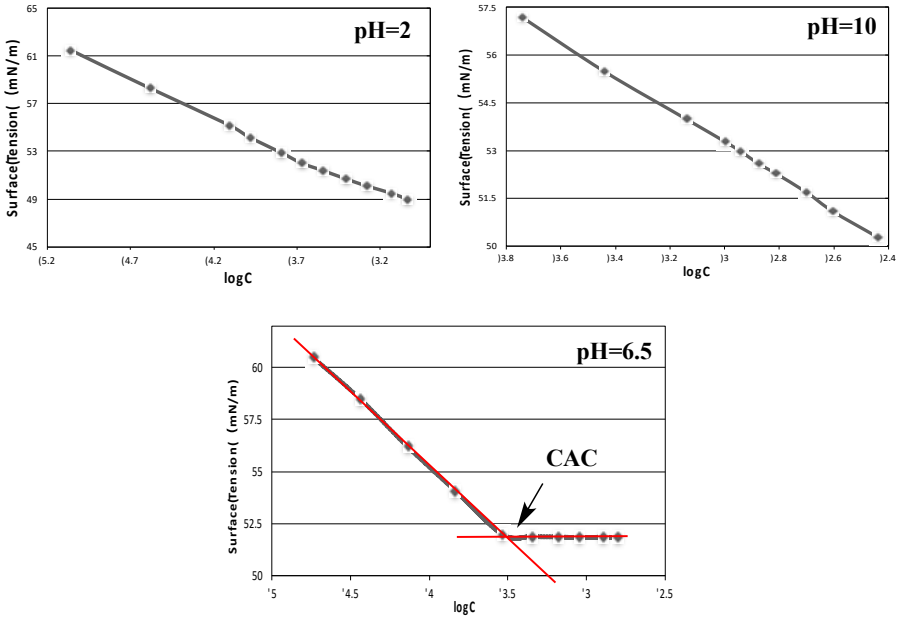

Figure 4.4 Surface tension of **Cys2** in water under different pH values.

Take the results of **Cys2** as an example. As shown in Fig. 4.4 (a) and (b), with the increase of solution concentrations, the surface tensions of the solution gradually decreased, being consistent with the fact that the surface tension for most organic molecules is concentration dependent, such as alcohols, esters and aldehydes.[16] At pH 6.5, cysteine exists in a zwitterionic form without net charges. Since a significant decrease in solubility of the **Cys2** was observed, it was assumed that the cysteine end group is hydrophobic at pH 6.5. Thus, an amphiphilic molecule is formed. The data in the Fig 4.4 (c) confirms the formation of surfactant molecules, since the surface tension decreases rapidly in dilute solutions, but becomes constant

after reaching to a certain concentration. Therefore, the CAC of **Cys2** was determined to be 0.0003 mol/L with a surface tension of 52 mN/m. Similarly, **Cys1** also shows the self-assembling feasture at 6.5 with the CAC of 0.00005 mol/L (Fig. 4.5a).

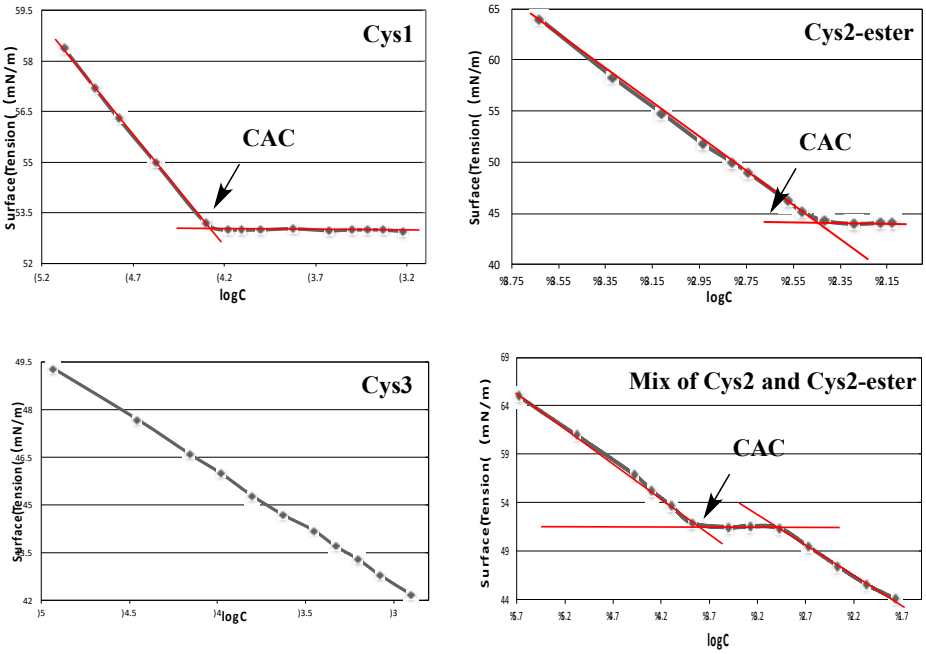

Figure 4.5 CAC values of **Cys1, Cys3** and **Cys2-ester** (pH=6.5).

However, due to the poor solubility of **Cys3-4** in neutral charge form, there was no self-assembling property that could be detected (Fig 4.5b). The ethyl ester of **Cys2** (**Cys2-ester**) was isolated as a by-product from the synthesis of **Cys2** (Fig. 4.6). Without the acid function, **Cys2-ester** is more hydrophobic than **Cys2** and should exhibit better self-assembling behavior. Indeed, it exhibited good surfactant property with a lower surface tension (44 mN/m) at the CAC of 0.0035 mol/L (Fig. 4.5c). In addition, it was found that the surface tension for the mixture of **Cys2** and **Cys2-ester** with 1:1 ratio was around 52 mN/m at the CAC, close to that of **Cys2**, which may be attributed to the leading role of **Cys2** during aggregation (Fig. 4.5d). And the second decrease on surface tension after reaching to the CAC, indicates the state change of aggregates in the water.

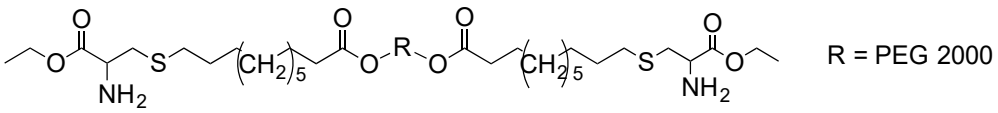

Figure 4.6 Structure of **Cys2-ester.**

Dynamic light scattering (DLS) investigations were further performed to determine the size distributions of the self-assembled **Cys1-2**. It was found that in acid or basic solutions, there was no signals that could be detected from DLS measurements, indicating no aggregates formed under such conditions. But for the solution of **Cys2** at 0.0003 mol/L, two different particle distributions were found: one with a mean particle size of 94.56 nm (45.9% intensity) and another with a size of 598.9 nm (54.1% intensity) (Fig. 4.7). The first peak was designated to the aggregates of **Cys2** and the second may be the induced form the agglomeration of those aggregates. Because at the CAC, **Cys1-2** are in the zwitterionic form, the electronic force between the adjacent molecules could lead to the agglomeration and even sedimentation which was indeed observed in sample solution one hour after preparation. Moreover, the DLS measurements on **Cys1** and **Cys2-ester** were also done (Fig. 4.7). For **Cys1** at 0.00005 mol/L, the particle sizes of 71.52 nm with 31.9% intensity and 713.1 nm with 68.1% intensity of aggregates were found. The relatively smaller size of **Cys1** aggregates was attributed to the low molecular weight of **Cys1** compared to **Cys2.** For **Cys2-eater** at the CAC, a 39.89 nm of particle size with intensity contribution of 100% was detected. The particle size of **Cys2-ester** is not only smaller than their acid counterparts, but also is homogeneous without further agglomeration. However, most of these measurements gave a large PDI around 0.8, which indicates the uneven distribution and instability of those aggregates.

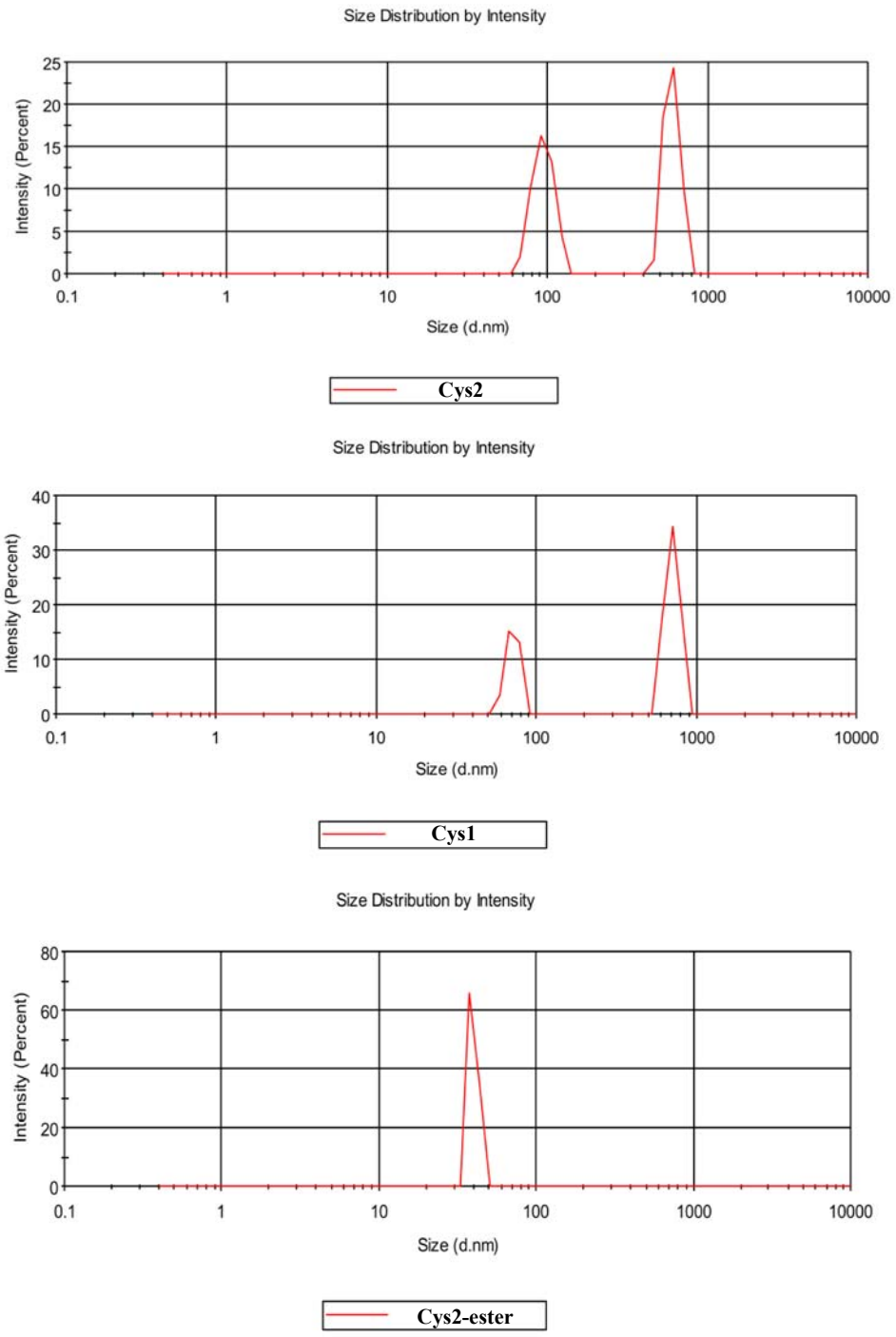

Figure 4.7 DLS measurements for **Cys2**, **Cys1** and **Cys2-ester**.

The morphologies of **Cys1-2** aggregates were further observed by transmission electron microscopy (TEM) (See experimental section). For example, **Cys2** is self assembled into spherical-like aggregates in water with a diameter ranging from about 80 nm to 120 nm, in agreement with the DLS results (94.56 mm) (Fig. 4.8a and b). The image of the aggregates

taken after 3h (Fig. 4.8c), clearly showed that the aggregates gradually agglomerated in solution.

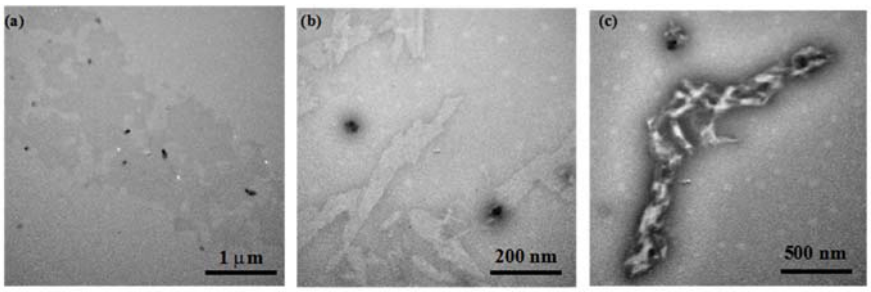

Figure 4.8 TEM images of (a and b) **Cys2** at CAC after 0.5h, (c) **Cys2** at CAC after 3h.

Beside the linear macromolecules, the star-shaped macromolecules were also studied for the self-assembling properties. Unlike the linear ones which tend to aggregate at pH 6.5, the star-shape macromolecules should self-assemble in acid or basic conditions due to their hydrophobic cores. Thus, the surface tensions of **Cys5-8** were measured at pH 2 and pH 10. However, only **Cys6** showed a possible self-assembling at pH 2. As shown in Fig (a), at the concentration of 0.00025 mol/L in water, **Cys6** showed a self-assembling behavior. For others under different pH values, they either had poor solubility in water or had no sign of aggregation.

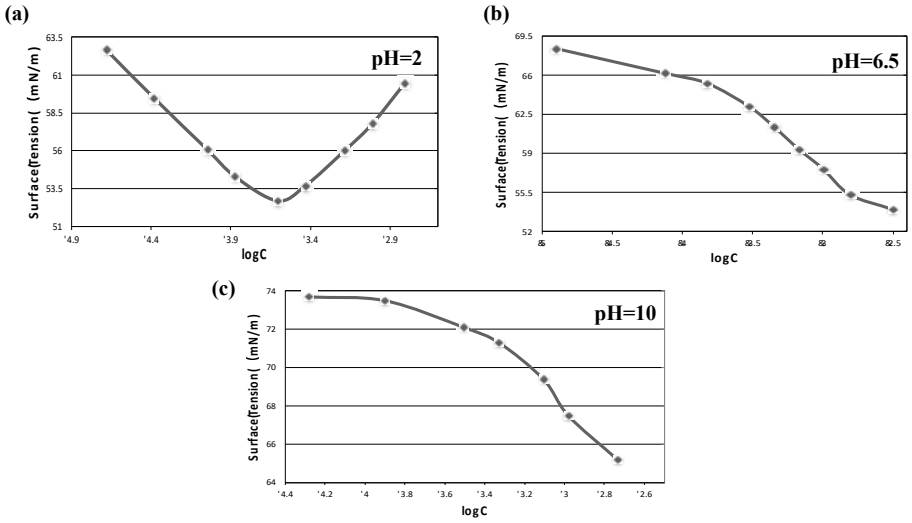

Figure 4.9 Surface tension of **Cys6** under different pH values.

4.5 Syntheses of cysteine-modified polysaccharides

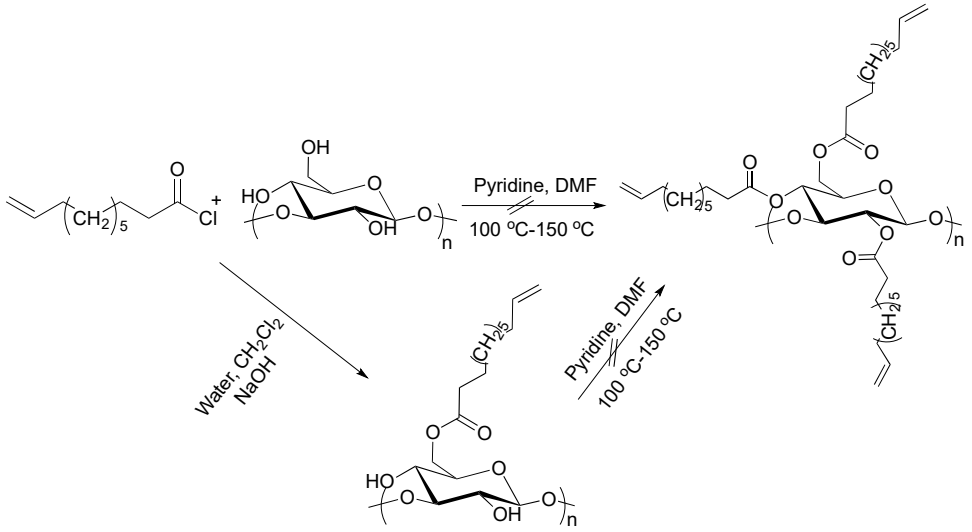

Scheme 4.5 Syntheses of L-cysteine modified ß-glucan.

ß-glucan is the major component of yeast cell walls, which maintains cells stability in physiological activities through self-assembling into helical superstructures. Moreover, ß-glucan has remarkable immunomodulatory function due to its ability to bind with the receptor Dectin-1 on macrophages which in turn, stimulates the immune system.[17,18] However, its application in biomaterials was restricted by its poor processability and solubility in water. Therefore, we intended to modify it with L-cysteine in order to alter its solubility and introduce some new properties, such as chiroptical property.[18] As shown in Scheme 4.5, the first trial experiment was conducted in organic solvent DMF, but failed due to the poor solubility of ß-glucan even under high temperatures and for prolonged reaction time. Then a two-step synthetic route was designed, in which a heterogeneous esterification reaction is done only at the primary hydroxyl group to increase the solubility of the intermediate product in organic solvent. Thus, the interfacial reaction was carried out in water and dichloromethane, and the intermediate was obtained after purification. However, the intermediate did not show an improved solubility in organic solvents as hoped. The reason is probably due to the incomplete esterification of primary hydroxyl groups in ß-glucan. Therefore, the formylation of the

primary hydroxyl group and the esterification of the rest hydroxyl function groups were then attempted.

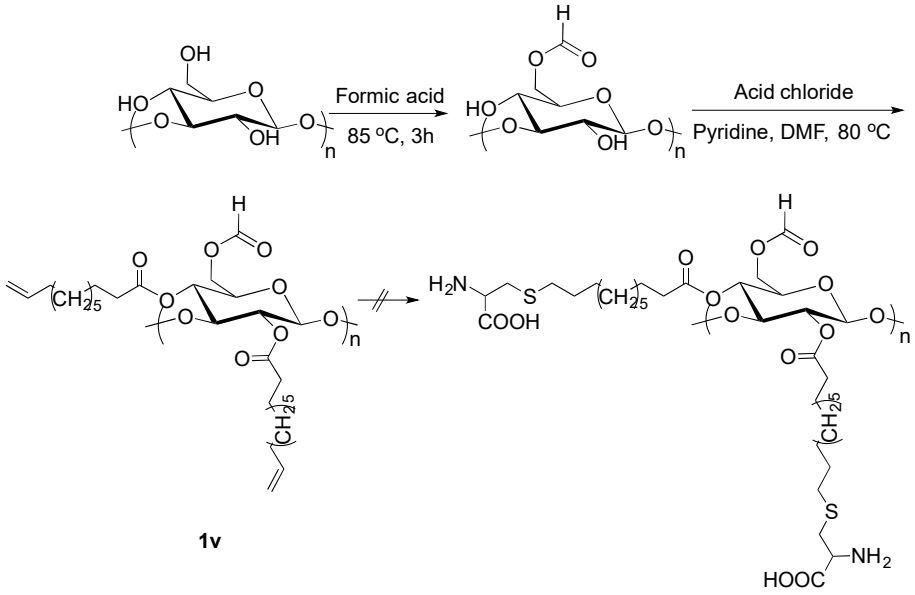

Scheme 4.6 Synthesis of cysteine modified ß-glucan.

Compound **1v** was successfully obtained and showed an improved solubility. The structure of compound **1v** was fully characterized by spectroscopic means (See experimental section). The IR spectrum confirms the presence of the carbonyl groups at 1740 cm^{-1} and the double bond at 1640 cm^{-1}.

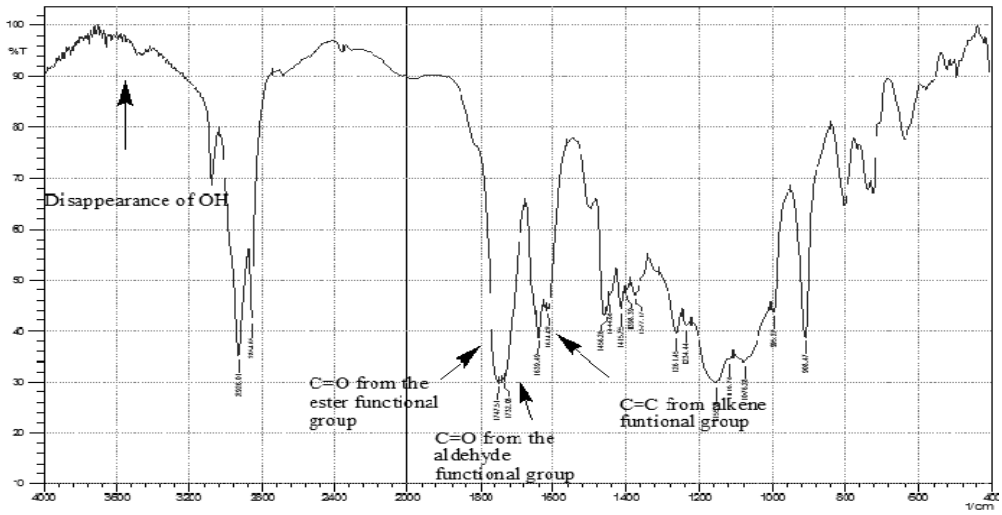

Figure 4.10 IR spectrum of compound **1v**.

However, the subsequent thiol-ene radical reaction between L-cysteine and compound **1v** failed, because the double-bond signal and glycosidic bond signals in the ^{1}H NMR spectrum were completely disappeared. The reason may be due to the acid-catalyzed deformylation in ethanol, which could lead to the complete decomposition of the compound **1v**.

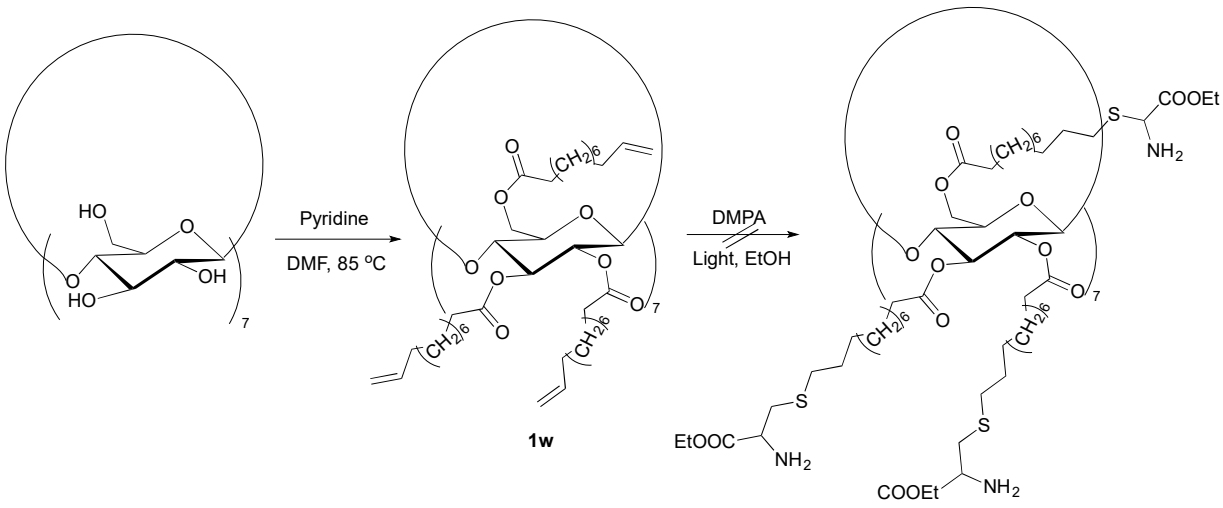

Scheme 4.7 Modification of ß-CD by esterification.

Another polysaccharide, ß–cyclodextrin (ß–CD), with a better solubility in organic solvents was then selected in our work. The synthesis began with the esterification by the reaction of undecenoic acid chloride (Scheme 4.7). The reaction was carried out in DMF with pyridine as a base at 85 ºC overnight. Compound **1w** was obtained after purification by column chromatography. The structure of compound **1w** was fully characterized by spectroscopic means (See experimental section). The IR spectrum displays no bands above 3200 cm^{-1}, indicating the absence of the hydroxyl groups and the new peak at 1641 cm^{-1} for the double bond, and the carbonyl peak at 1745 cm^{-1} for the ester (Fig. 4.10).

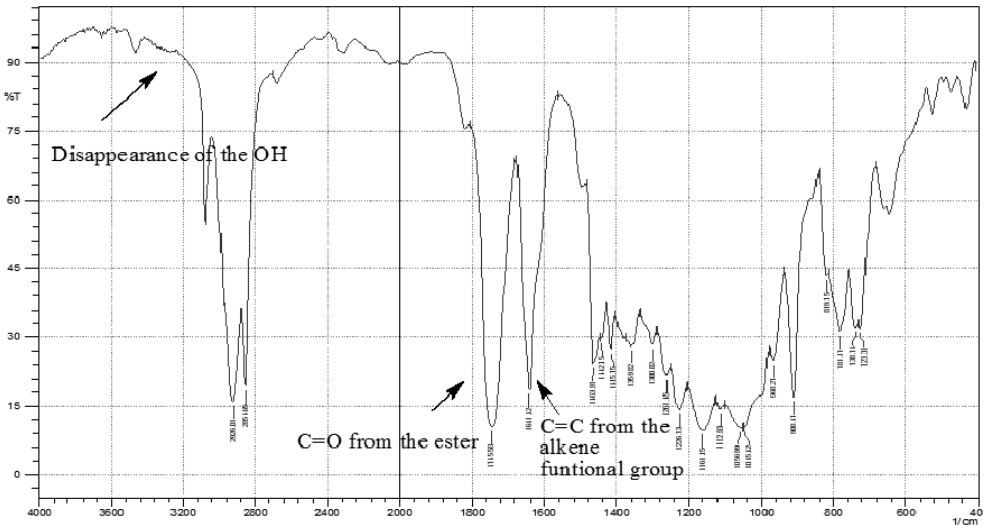

Figure 4.11 IR spectrum of compound **1w**.

Then thiol-ene radical reaction between L-cysteine and compound **1w** was carried out in the presence of a photo-initiator (DMPA) in ethanol. However, the undesired esterification between L-cysteine and ethanol was detected. Thus, cysteine ethyl ester was selected for CD modification in the same reaction condition. After irritation for 10h, the double-bond signal in the ^{1}H NMR spectrum was almost completely disappeared. Many attempts with different conditions (e.g., time, photoinitiator and light wavelength) proved futile. Under this thiol-ene reaction condition, the preferred reaction is the free radical polymerization or crosslinking of the vinyl units in compound **1w** that has a high content of double bonds per molecule.

Then thiol-ene radical reaction between L-cysteine and compound **1w** was carried out in the presence of a photo-initiator (DMPA) in ethanol. However, the undesired esterification between L-cysteine and ethanol was detected. Thus, cysteine ethyl ester was selected for CD modification in the same reaction condition. After irritation for 10h, the double-bond signal in the ^{1}H NMR spectrum was almost completely disappeared. Many attempts with different conditions (e.g., time, photoinitiator and light wavelength) proved futile. Under this thiol-ene reaction condition, the preferred reaction is the free radical polymerization or crosslinking of the vinyl units in compound **1w** that has a high content of double bonds per molecule.

4.6 Study on the chiral recognition of cysteine-based polyamine

ß–CD has a toroidal shape with hydrophilic surface and hydrophobic interior is an ideal host molecule to include hydrophobic guest molecules into its cavity. It has been known ß–CD could selectively include an enantiomer of a racemic complex into the cavity and give a different signal compared to its outside counterpart. Beside, ß–CD and its derivatives are able to form interactions with guest molecules through hydrogen bonding, Coulomb force, charge transfer and coordination bond.[19-22] Therefore, ß–CD is commonly treated as an ideal molecule for chiral recognition and is modified to tune its property for different guest molecules in this field, for example the amino modified ß–CD (NH_2-β-CD). The application of NH2-β-CD as a chiral recognition host has been studied for a long time, which is attributed to its protonated potential and viability to produce poly(NH_2-β-CD).[19, 22] Thus, if cysteine ethyl ester could be attached on compound **1v** in our work**,** we would obtain polyamine **1x** with a great potential in chiral recognition application.

To obtain polyamine **1x** before crosslinking took place, the thiol-radical reaction between L-cysteine ethyl ester and compound **1v** was stopped after light irradiation for 3h, where a larger amount of cysteine starting material could be detected from ^{1}H NMR spectrum. Then the obtained compound was dissolved in isopropanol for recrystallization two times. The structure of compound **1x** was characterized by spectroscopic means. Take IR as an example, as shown in Figure 4.12, a new band at 3000 cm^{-1} appeared indicating the presence of NH functional group and the peak at 1641 cm^{-1} indicates the existence of C=C functional group.

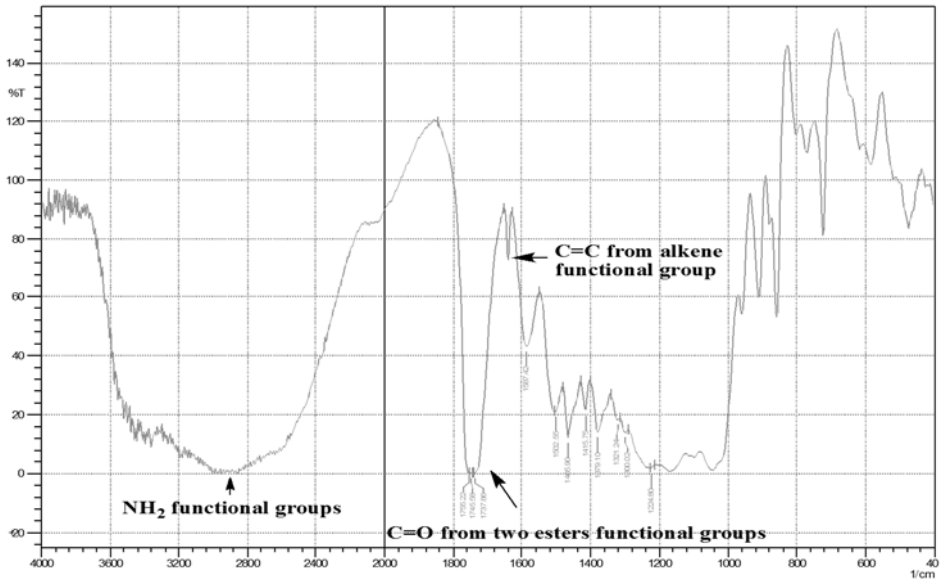

Figure 4.12 IR spectrum of polyamine **1x.**

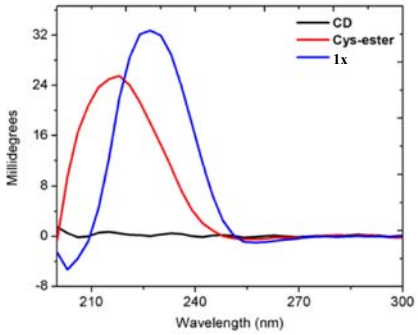

Figure 4.13 CD-spectra of ß–CD, L-cysteine ethyl ester and polyamine **1x** in water.

Beside the regular characterization by spectroscopic means, polyamine **1x** was also characterized by the changes of optical property such as circular dichroism (CD) spectroscopy due to the imported chiroptical characteristic from L-cysteine ethyl ester. As shown in Fig. 4.12, ß–CD has no optical activity and cysteine ethyl ester shows a CD-signal at 215 nm with a positive Cotton effect. However, an obvious signal shift to 227 nm was observed from the product isolated from the modification reaction, indicating the successful addition of L-cysteine ethyl ester on compound **1w**. Based on the data collected above, it was concluded that the polyamine **1x** was obtained.

Table 4.2 Chiral acids selected for chiral recognition study.

No.	Name	Enantiomer	
1	Di-*p*-toluoyl-tartaric acid	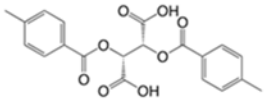	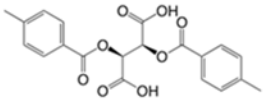
2	10-Camphorsulfonic acid	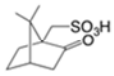	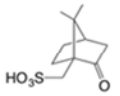
3	Tartaric acid	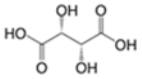	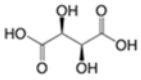
4	Mandelic acid	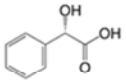	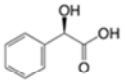
5	Methoxyphenylacetic acid	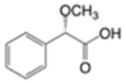	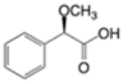
6	*O*-Acetylmandelic acid	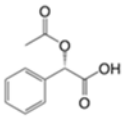	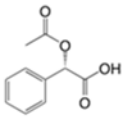

The chiral recognition of polyamine **1x** with different chiral acids was studied by CD measurement (Table 4.2). Solution of racemic chiral acids were prepared, then added to **1x** solution and the CD spectra were taken shortly after mixing. The pH of the polyamine **1x** in water was around 5, thus the amino group was protonated in acidic condition. It was reported that CD containing the NH_3^+ groups has a poor ability for chiral acid recognition, which is attributed to the decrease of hydrophobic interaction of the CD cavity.[21-22] Therefore, there was no CD signal change observed (Fig. 4.13a).

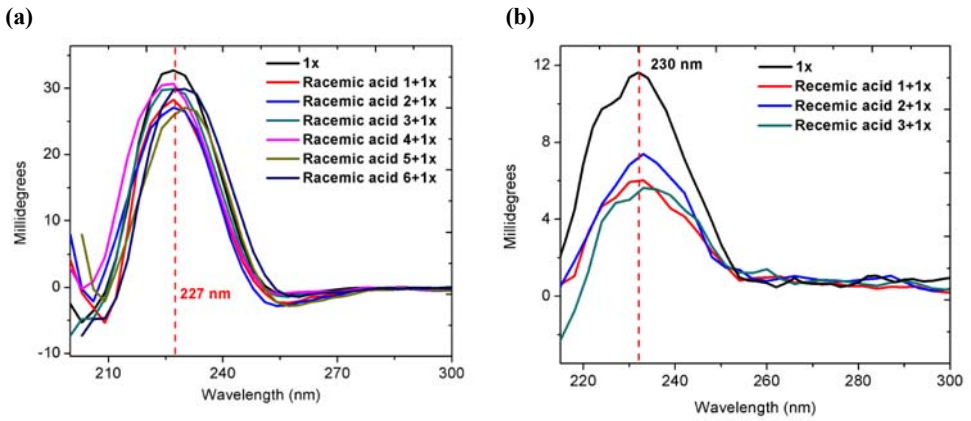

Figure 4.14 CD spectra of polyamine **1x** with various racemic acids (a) at pH 5; (b) at pH 7.5.

To enable the chiral recognition ability, sodium carbonate was then added to **1x** solution to deprotonate the ammonium group, which in turn could both increase the Coulomb forces between carboxylic acids and amines, and increase the hydrophobicity of CD cavity at same time. It was found that when solution pH was neutralized to pH 7.5, the CD signal of polyamine **1x** shifted from 227 nm to 230 nm. Moreover, when racemic chiral acids 1-3 (Table 4.2) were added, for example tartaric acid, no change in CD signal could be detected (Fig. 4.13b).

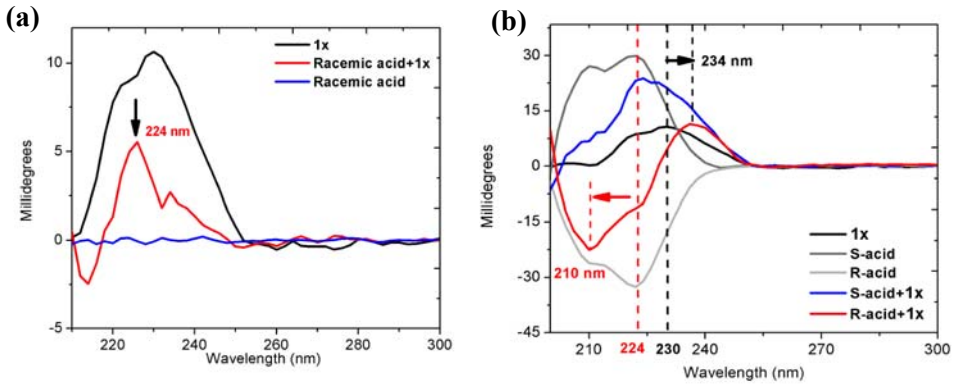

Figure 4.15 CD spectra of polyamine **1x** with (a) racemic acetylmandelic acid, (b) acetylmandelic acid enantiomers.

However, the addition of racemic acetylmandelic acid to **1x** solution induced an obvious change of CD bands. As shown in Fig. 4.14a, it exhibits a negative CD band at 210

nm and two positive CD bands at 224 nm and 234 nm, respectively. Because the CD band at 224 nm is same as the one of S-acetylmandelic acid, it was assumed that the polyamine **1x** selectively interacted with R-acetylmandelic acid and released out its S-enantiomer. To confirm this assumption, CD measurements for polyamine **1x** with each of the enantiomers were done. As shown in Fig. 14b, S-acetylmandelic acid has a positive CD-signal at 224 nm and its R-enantiomer gives an opposite signal at the same wavelength. When S-acid was added into **1x** solution, the spectra showed both the CD bands for polyamine **1x** at 230 nm and S-acid at 224 nm with positive Cotton effect, which indicating the absence of interaction between S-enantiomer and **1x**. But a significant signal change was induced when using R-acid, where the negative signal was shifted from 224 nm to 210 nm, a new positive CD band appeared at 234 nm and the CD-signal for polyamine **1x** disappeared. Because these induced signal changes were identical with the observation of CD-signals in Fig. 4.14a, it can be concluded that polyamine **1x** is enantioselective for R-acetylmandelic acid. Similar CD-signal changes were observed with the addition of racemic mandelic acid, where the signal of S-mandelic acid appeared at 226 nm and a shifted negative CD band at 208 nm were observed (Fig. 4.15a). These changes are consistent with the CD observations when adding R-mandelic acid in **1x** solution (See Appendix C). Moreover, the measurements on mixed methoxyphenylacetic acid gave the same result, where polyamine **1x** effectively discriminates methoxyphenylacetic acid (Fig. 4.15b). By the CD measurements with these three racemic chiral acids, polyamine **1x** successfully demonstrated its high-elective chiral recognition ability towards some of R-enantiomeric acid, which could be potentially applied in chemical-, biochemical- and pharmaceutical area.[23,24]

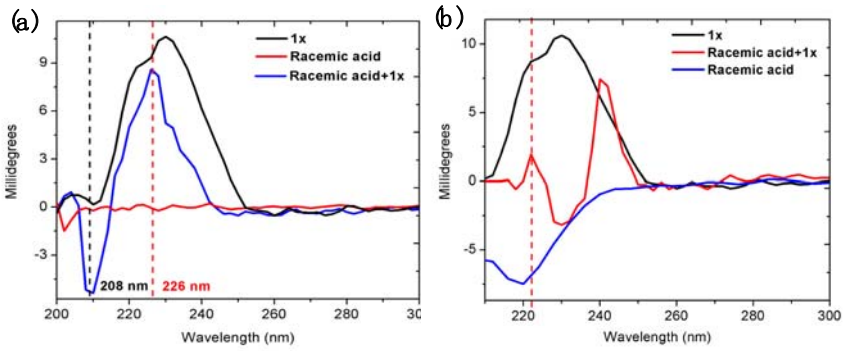

Figure 4.16 CD spectra of polyamine **1x** with (a) racemic mandelic acid and (b) mixed methoxyphenylacetic acid.

4.7 Conclusion

A series of linear and star-shaped macromolecules containing cysteine at the chain ends were prepared through simple esterification between undecenoic acid chloride and selected polyols, followed by thiol-radical click reaction. Their surface tension, pH-sensitivity and self-assembling behaviors of the amphiphiliac molecules studied by CAC, DLS and TEM measurements. Besides, cyclodextrins and polysaccharides were functionalized with L-cysteine and its derivative. The obtained polyamine compounds demonstrated great chiral recognitions on R-acid guest and could potentially develop to a high sensitive, selective and low-cost sensor to distinguish acid stereoisomers.

4.8 Experimental section

4.8.1 Materials

L-Cysteine, PEG 1000, PEG 2000, PTMEG 650, PTMEG 2000, HBTU, undecenoic acid, DIEA, L-cysteine ethyl ester hydrochloride, glycerol, di(trimethylolpropane), ribitol, dipentaerythritol, methoxyphenylacetic acid, *O*-A=acetymandelic acid, 4-dimethylaminopyridine and pyridine were purchased from Aldrich Canada. ß-glucan, ß-CD, Di-p-toluoyl-tartaric acid, 10-camphorsulfonic acid, tartaric acid and mandelic acid were

purchased from China. The water used in this work was purified using a Millipore™ Milli-Q™ Advantage A10 water purification system.

4.8.2 Measurements

^{1}H and ^{13}C NMR spectra were measured on a Bruker Avance Digital 300 MHz spectrometer at ambient temperature using tetramethylsilane (TMS) as an internal standard. Resonances were quoted on the δ scale relative to TMS (δ = 0) as an internal standard. Infrared measurements were recorded on a Varian 1000 FT-IR Scirinitar spectrophotometer in the regions of 4000–400 cm^{-1}. Mass spectra were performed with a Micromass Quattro LC ESI (EI). Fisher-Johns melting point apparatus was used to test the melting points. Gel permeation chromatography (GPC) analysis was conducted on a PL-GPC 220 system with polystyrene as standard and tetrahydrofuran (THF) as eluent. CD spectrum was recorded on Olis Circular Dichrosim Spectrophotometers and the wavelength starting from 210 nm. The UV-absorption spectra were recorded using a UV-Vis Lambda 900 spectrophotometer and the fluorescence emission spectra were recorded on Shimadzu RF-1501 spectrofluorophotometer using 1 cm quartz cell. A pH meter, PHS-3C was used to read the pH values. Surface tension measurements were tested with QBZY Series Automatic surface tension meter. DLS results were recorded on Malvern Zetasizer Nano. TEM photos were taken from JEOL JEM-1011 transmission electron microscope.

4.8.3 Synthesis

General procedure for cysteine reacting with alkenes with even numbered C=C:

Undecenoic acid chloride (2g) and polyols were dissolved in 20 mL of dichloromethane in 50 mL round-bottom flask. The mixture was stirred at ambient temperature overnight. After the reaction was completed, the solvent was removed and re-dissolved in ethanol for further use.

Cysteine (1.21 g, 10.0 mmol) was added in 10 mL of ethanol in 50 mL Erlenmeyer flask. HCl was then added dropwise until cysteine completely dissolved. The alkene mixture from previous step and DMPA (10 wt%) was added afterwards under argon atmosphere. The mixture was exposed to a UV-lamp (λ=365 nm) for several hours. After the reaction was completed, EtOH was removed by rotational evaporator and the mixture was washed by acetone. The final product was collected by suction filtration.

Cys1: 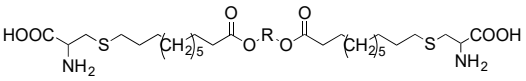 R=PEG 1000

^{1}H NMR (300 MHz, DMSO-d_6): 4.14-4.10 (m, 6H), 3.60-3.39 (m, 104 H), 3.00-2.99 (d, 4H), 2.56 (t, 4H), 2.29 (t, 4H), 1.55-1.46 (m, 8H), 1.34-1.25 (m, 24H); ^{13}C NMR (75 MHz, DMSO-d_6): 173.39, 170.18, 72.79, 70.24, 68.77, 63.50, 60.66, 52.31, 33.87, 32.09, 31.84, 29.36, 29.29, 29.15, 29.04, 28.88, 28.58. 25.00.

Cys2: 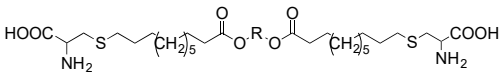 R=PEG 2000

^{1}H NMR (300 MHz, DMSO-d_6): 4.15-4.10 (m, 6H), 3.60-3.39 (m, 200H), 3.00-2.99 (d, 4H), 2.29 (t, 4H), 1.55-1.46 (m, 8H), 1.34-1.25 (m, 24H); ^{13}C NMR (75 MHz, DMSO-d_6): 173.37, 170.19, 72.81, 78.24, 68.77, 63.50, 60.65, 52.30, 33.86, 32.08, 31.82, 29.38, 29.31, 29.16, 29.05, 28.89, 28.60, 24.91.

Cys3: 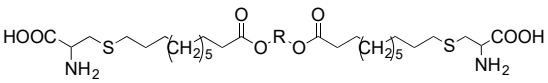 R=PTMEG 650

^{1}H NMR (300 MHz, DMSO-d_6): 4.09-4.04 (m, 2H), 3.97 (t, 4H), 3.36-3.29 (m, 34H), 3.01-2.99 (d, 4H), 2.53 (t, 4H), 2.23 (t, 4H), 1.58-1.42 (m, 44H), 1.29-1.20 (m, 24H); ^{13}C NMR (75 MHz, DMSO-d_6): 173.42, 169.97, 70.12, 69.83, 63.98, 60.95, 52.32, 33.94, 32.09, 31.65, 29.30, 29.08, 29.01, 28.85, 28.53, 26.15, 25.60, 24.91.

Cys4: 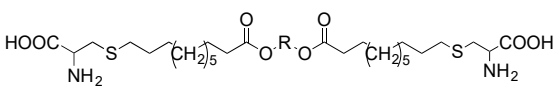 R=PTMEG 2000

^{1}H NMR (300 MHz, DMSO-d_6): 4.09-4.04 (m, 2H), 3.97 (t, 4H), 3.33-3.24 (m, 64H), 3.00-2.99 (d, 4H), 2.53 (t, 4H), 2.23 (t, 4H), 1.58-1.45 (m, 76H), 1.21 (m, 24H). ^{13}C NMR (75 MHz, DMSO-d_6): 173.43, 169.99, 70.13, 69.83, 63.99, 60.95, 52.32, 33.94, 32.08, 31.65, 29.64, 29.28, 29.09, 29.01, 28.85, 28.54, 26.48, 26.15, 25.60, 24.91.

Cys6:

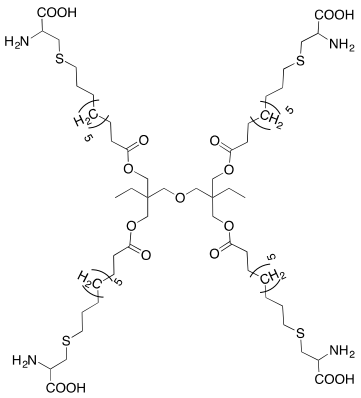

^{1}H NMR (300 MHz, DMSO-d_6+HCl): 4.09-4.04 (m, 4H), 3.86 (s, 8H), 3.19 (s, 4H), 3.01-2.99 (d, 2H), 2.53 (t, 8H), 2.23 (t, 8H), 1.47 (t, 16H), 1.32-1.20 (m, 52H), 0.75 (t, 6H); ^{13}C NMR (75 MHz, DMSO-d_6+HCl): 173.03, 169.98, 70.90, 63.94, 52.33, 41.58, 33.93, 32.10, 31.66, 29.39, 29.34, 29.15, 29.07, 28.90, 28.57, 24.91, 23.08, 7.69.

Cys8:

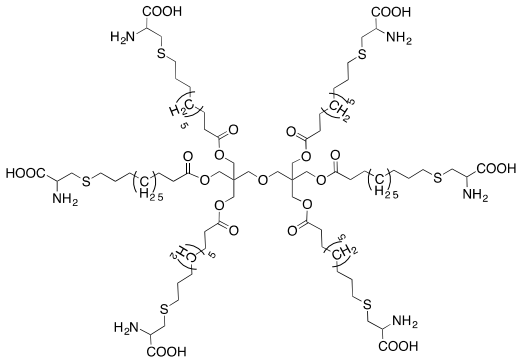

^{1}H NMR (300 MHz, DMSO-d_6+HCl): 4.09-4.05 (m, 6H), 3.97 (s, 12H), 3.32 (s, 4H), 3.02-3.00 (d, 12H), 2.53 (t, 12H), 2.24 (t, 12H), 1.52-.43 (m, 20H), 1.30-1.20 (m, 60H); ^{13}C NMR (75 MHz, DMSO-d_6+HCl): 172.87, 169.93, 69.83, 62.54, 52.33, 42.87, 33.82, 32.09, 31.62, 29.40, 29.33, 29.17, 29.08, 28.90, 28.56, 24.83.

General procedure for cysteine reacting with alkenes with odd numbered C=C:

Undecenoic acid chloride (2g), 4-dimethylaminopyridine**,** and polyols were dissolved in 20 mL of dichloromethane in 50 mL round-bottom flask. Then pyridine was added dropwise. The mixture was stirred at ambient temperature overnight. After the reaction was completed, the solvent was removed and purified through column chromatography. Cysteine (1.21 g, 10.0 mmol) was added in 10 mL of ethanol in 50 mL Erlenmeyer flask. HCl was then added dropwise until cysteine completely dissolved. The alkene mixture from previous step and DMPA (10 wt%) was added afterwards under argon atmosphere. The mixture was exposed to a UV-lamp (λ=365 nm) for several hours. After the reaction was completed, EtOH was removed by rotational evaporator and the mixture was washed by acetone. The final product was collected by suction filtration.

Cys5:

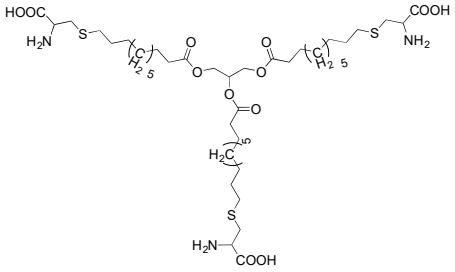

^{1}H NMR (300 MHz, DMSO-d_6+HCl): 5.18-5.11 (m, 1H), 4.25-4.20 (m, 2H), 4.12-4.04 (m, 5H), 3.01-3.00 (d, 6H), 2.53 (t, 6H), 2.26-2.20 (m, 6H), 1.51-1.42 (m, 12H), 1.29-1.20 (m, 36H). ^{13}C NMR (75 MHz, DMSO-d_6+HCl): 173.01, 169.97, 69.12, 62.21, 52.33, 33.93, 33.77, 32.10, 31.65, 29.32, 29.14, 29.06, 28.82, 28.56, 24.82.

Cys7:

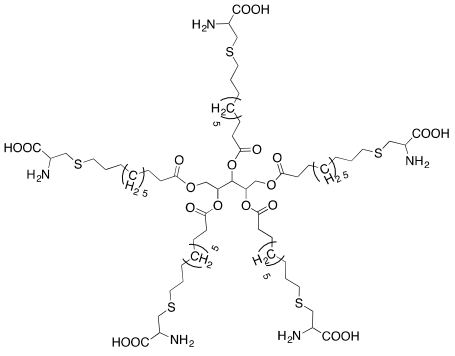

^{1}H NMR (300 MHz, DMSO-d_6+HCl): 5.27-5.17 (m, 3H), 4.34-4.30 (d, 2H), 4.12-4.06 (m, 7H), 3.01-3.00 (d, 10H), 2.54 (d, 10H), 2.34-2.22 (m, 10H), 1.53-1.46 (m, 20H), 1.31-1.24 (m, 60H);

^{13}C NMR (75 MHz, DMSO-d_6+HCl): 172.34, 172.07, 170.16, 69.46, 69.39, 52.37, 33.91, 33.77, 32.10, 31.81, 29.49, 29.39, 29.24, 29.16, 28.92, 28.85, 28.67, 24.79.

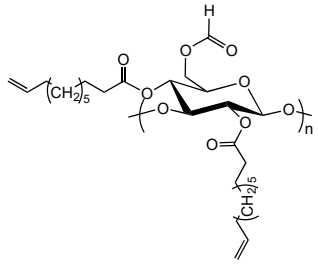

1v:

ß-glucan (1g, 0.002 mol) was dissolved in 20 mL formic acid in a 50 mL round bottom flask and the mixture was stirred at 85 ºC for 3h. After the reaction was completed and the solvent was removed by rotational evaporator, the obtained compound was washed with acetone and dissolve in DMF for next step. The system was then cooled to 0 ºC by using an ice bath and pyridine and acid chloride were added in turn dropwise. The reaction temperature was then increased to 85 ºC and the mixture was stirrred for 2 days. When the reaction was completed, DMF solvent was removed under vaccumn and the obtained mixture was dissolved in ethyl acetate again, followed by washing with 1N HCl solution, 5% $NaHCO_3$ and brine. Target compound was obtained from organic phase after removal the solvent and purified by column chromatography (hexane:ethyl acetate=10:1).

^{1}H NMR (300 MHz, DMSO-d_6): 5.86-5.76 (m), 5.37 (s), 5.03-4.90 (m), 4.81 (s), 4.54 (s), 4.18 (s), 4.02 (s), 2.28 (s), 1.56-1.40 (m), 1.30-1.27 (d).

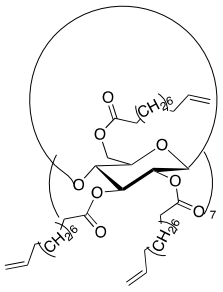

1w:

ß-CD (1g) was dissolved in 20 mL DMF in a 50 mL two-neck round bottom flask and the

system was then cooled to 0 ºC by using an ice bath. Then pyridine and acid chloride were added dropwise and stirred for 0.5h. Next, the reaction temperature was increased to 85 ºC and the mixture was stirrred for 2 days. When the reaction was completed, DMF solvent was removed under vaccumn and the obtained mixture was dissolved in ethyl acetate again, followed by washing with 1N HCl solution, 5% $NaHCO_3$ and brine. Target compound was obtained from organic phase after removal the solvent and purified by column chromatography (hexane:ethyl acetate=10:1).

^{1}H NMR (300 MHz, DMSO-d_6): 5.85-5.75 (m, 21H), 5.34 (s, 7H), 5.01-4.92 (m, 42H), 4.70 (s, 7H), 4.54 (s, 7H), 4.30 (s, 7H), 3.98 (s, 7H), 3.73 (s, 7H), 2.34 (s, 42H), 1.60 (s, 42H), 1.37-1.26 (m, 126H).

References

1. Geng, Y.; Itscher, D. E.; Justynska, J.; Schlaad, H. *Angew. Chem. Int. Ed.,* **2006**, *45*, 7578.
2. Passaglia, E.; Donati, F. *Polymer*, **2007**, *48*, 35.
3. Khanna, K.; Varshney, S.; Kakkar, A. *Polym. Chem.,* **2010**, *1*, 1171.
4. Yan, Q.; Sui, X.; Yuan, J. *Progress in Chemistry*, **2008**, *20*, 1562.
5. Huang, C.; Miao, M.; Janaswamy, S.; Hamaker, B. R.; Li, X.; Jiang, B. *J. Agric. Food Chem*., **2015**, *63*, 6450.
6. Li, S.; Xiong, Q.; Lai, X.; Wan, M.; Zhang, J.; Yan, Y.; Cao, M.; Lu, L.; Guan, J.; Zhang, D.; Lin, Y. *Comprehensive reviews in food science and food safety*, **2016**, *15*, 237.
7. Meng, X.; Edgar, K. J. *Prog. Polym. Sci*., **2016**, *53*, 52.
8. Sauvagnat, B.; Lamaty, F. *Tetrahedron Lett.* **1998***, 39,* 821.
9. Jin, S.; Huang, X. *J. Mol. Sci.;* **1985**, *2*, 159.
10. Phookan, S. *International Journal of Innovate research and development*, **2014**, *3*, 37.
11. Nagano, N.; Ota, M.; Nishikawa, K. *FEBS Lett.* **1999**, *458*, 69.
12. Heitmann, P. *Eur. J. Biochem*. **1968,** *3,* 346.
13. Tian, F.; Wu, J.; Huang, N.; Guo, T.; Mao, C. *SAR QSAR Environ. Res.,* **2013**, *24*, 89.
14. Ananthapadmananbhan, K. P.; Goddard, E. D.; Turro, N. J.; Kuo, P. L. *Langmuir*, **1985**, *1*, 352.
15. Patist, A., Bhagwat, S.S., Penfield, K.W.; Shah, D. O. *J. Surfact. Deterg.,* **2000**, *3*, 53.
16. Habradova, K.; Hovorka, S.; Bartovska, L. *J. Chem. Eng. Data*., **2004**, *49*, 1003.
17. Wu, Z. *Esterification of β-Glucan: self-assembly and its application as wound dressing*, Master thesis, **2015.**

18. Wang, Q.; Sheng, X.; Shi, A.; Hu, H.; Yang, Y.; Liu, L.; Fei, L.; Liu, H. *Molecules,* **2017**, *22*, 257.

19. Kano, K. *J. Phys. Org. Chem.,* **1997**, *10*, 286.

20. Tiwari, G.; Tiwari, R.; Rai, A. W. *J. Pharm. Bioallied. Sci*., **2010**, *2*, 72.

21. Brown, S. E.; Coates, J. H.; Duckworth, P. A.; Lincoln, S. F.; Easton, C. J.; May, B. L. *J. Chem. Soc*. *Faraday Trans.* **1993**, *89*, 1035.

22. Kitae, T.; Nakayama, T.; Kano, K. *J. Chem. Soc. Perkin Trans*., **1998**, *2,* 207.

23. Xie, G.; Tian, W.; Wen, L.; Xiao, K.; Zhang, Z.; Liu, Q.; Hou, G.; Li, P.; Tian, Y.; Jiang, L. Chem. Commun*.,* **2015**, ***51***, 3135.

24. Lu, H.; Guo, Y. *J. Am. Soc. Mass. Spectrom*., **2003**, *14*, 571.

Contribution to Knowledge

1. L-cysteine, especially its DKP form, is a desirable building block to prepare high-performance and functional materials. However, there is limited research on cysteine-based DKP. In our work, we carefully explored a feasible synthetic route to cysteine-based DKP, through thiol group protection followed by a dimerization reaction. Based on it, a serious of cysteine-based DKP small molecules and polymers were designed and synthesized.
2. To protect the thiol group, thiol-ene click reaction, both thiol-Michael addition and thiol-radical reaction were first adopted. The reactions between L-cysteine and various alkene containing compounds were conducted under mild reaction condition with high yield. In the subsequent cyclic dimerization, the reaction was conducted in dichlorobenzene in the presence of a catalyst P_2O_5 at elevated temperature with high yield.
3. Besides, the reaction between cysteine and aldehyde containing compounds which forming 4-thiazolidinecarboxylic acid was utilized to create stable S-precursors. In the subsequent cyclic dimerization, the reaction was conducted in a solvent in the presence of a coupling reagent HBTU at elevated temperature with high yield.
4. A series of linear- (PEG and PTMEG) and star-shape (three-, four-, five- and six-branched) macromolecules, as well as polysaccharides (ß-glucan and ß-CD) with L-cysteine end-group were designed and synthesized.
5. In our work, the compounds derived from L-cysteine have different properties that could be used in various applications, such as the chiroptical activity for sensing silver ion in aqueous systems, the chiral recognition ability for racemic acid separation, the self‒assembling property for drug delivery system and the degradability for the preparations of green materials.

APPENDIX A

Spectra of compounds and polymers in Chapter 2

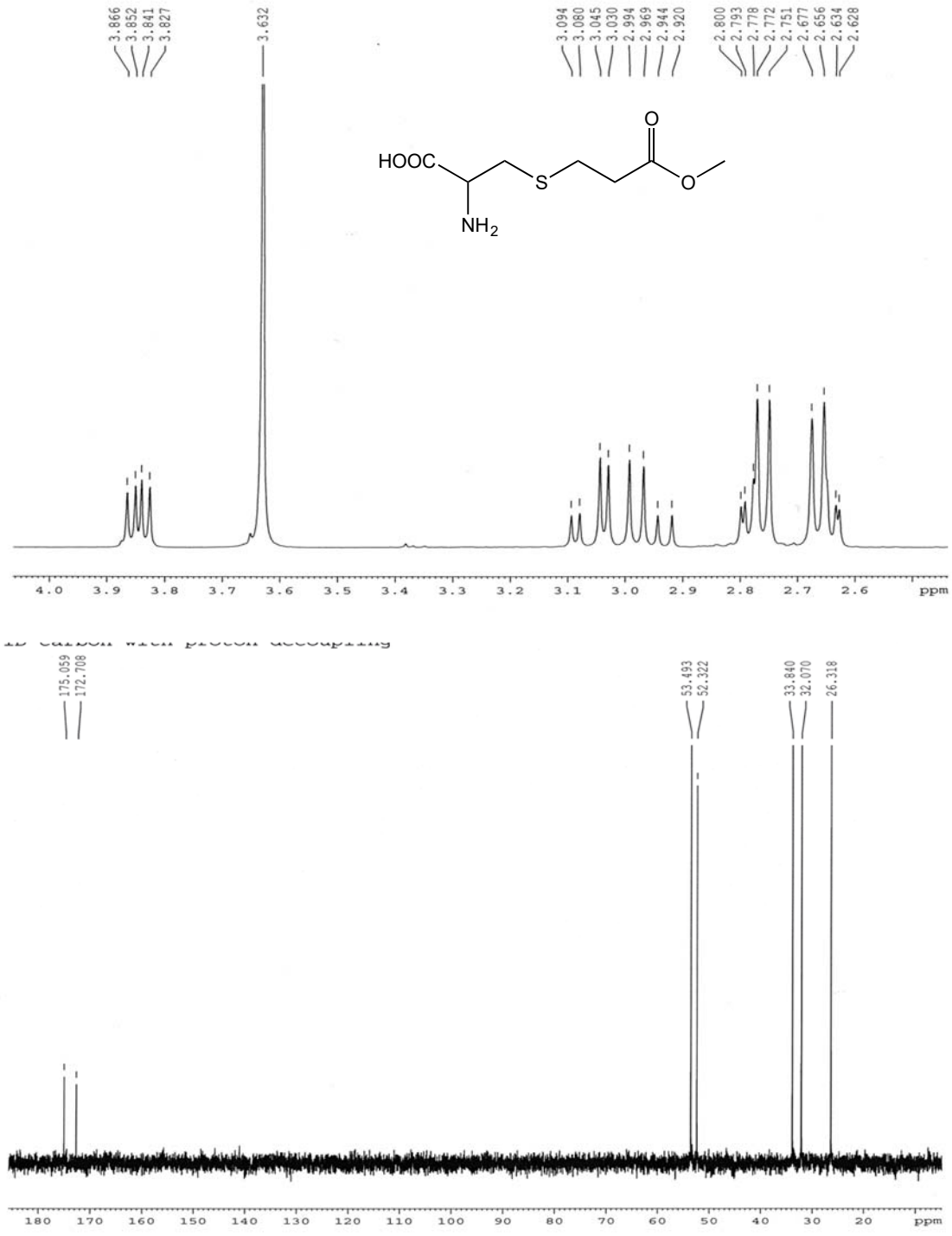

Figure A.1 ^{1}H NMR (300 MHz, D_2O) and ^{13}C NMR (75 MHz, D_2O) spectra of compound **1a.**

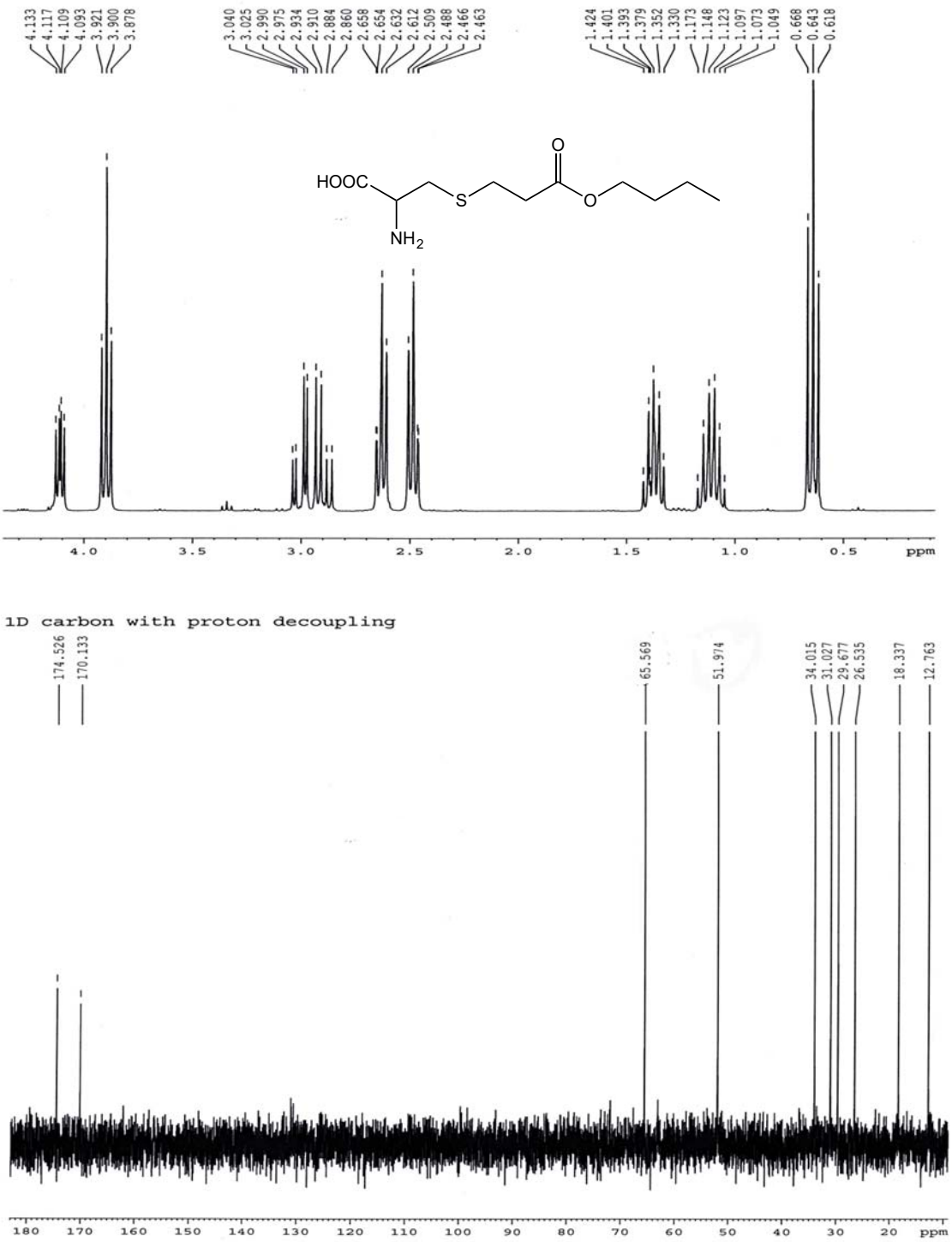

Figure A.2 ^{1}H NMR (300 MHz, D_2O+HCl) and ^{13}C NMR (75 MHz, D_2O+HCl) spectra of compound **1b.**

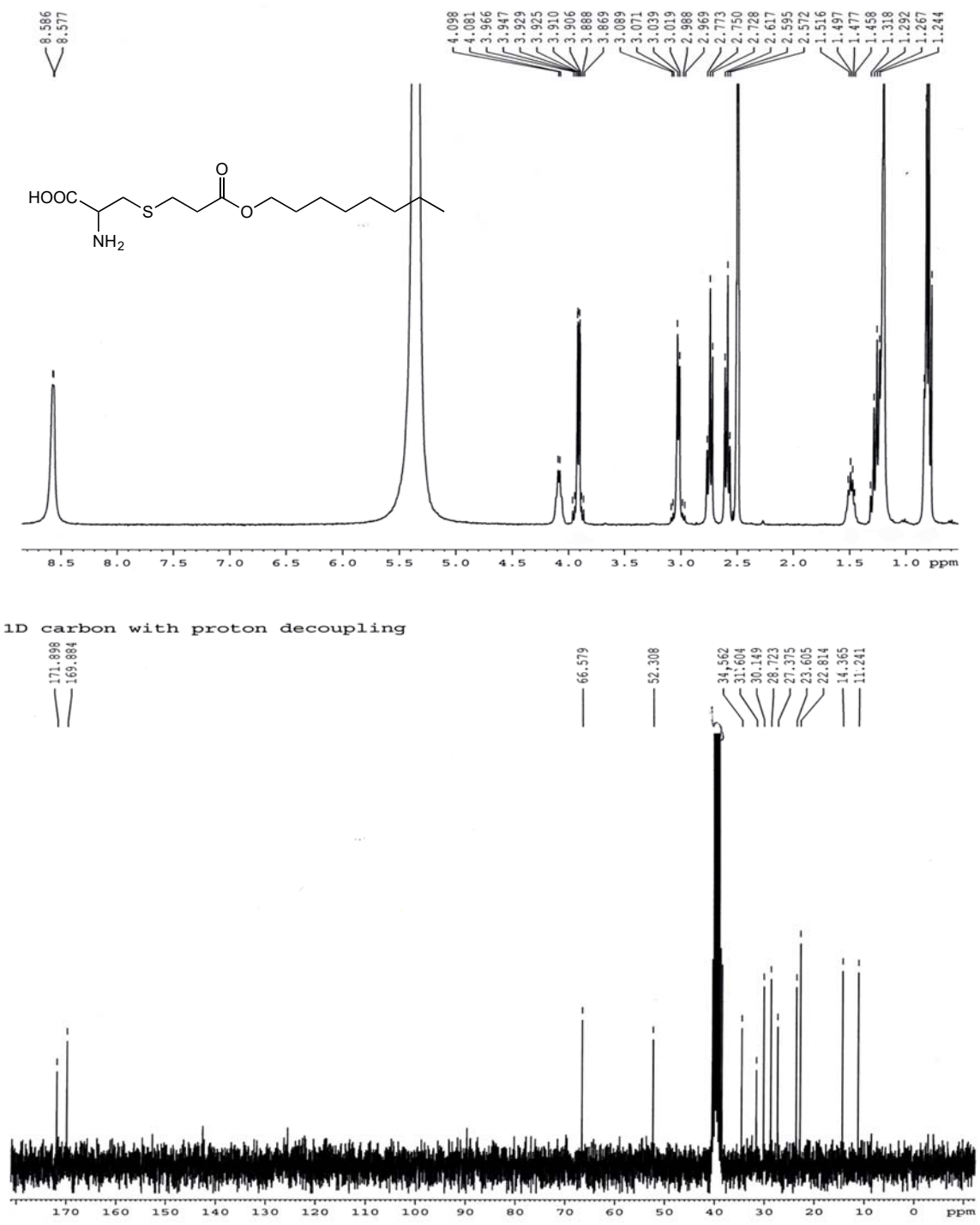

Figure A.3 ^{1}H NMR (300 MHz, DMSO-d_6) and ^{13}C NMR (75 MHz, DMSO-d_6) spectra of compound **1c.**

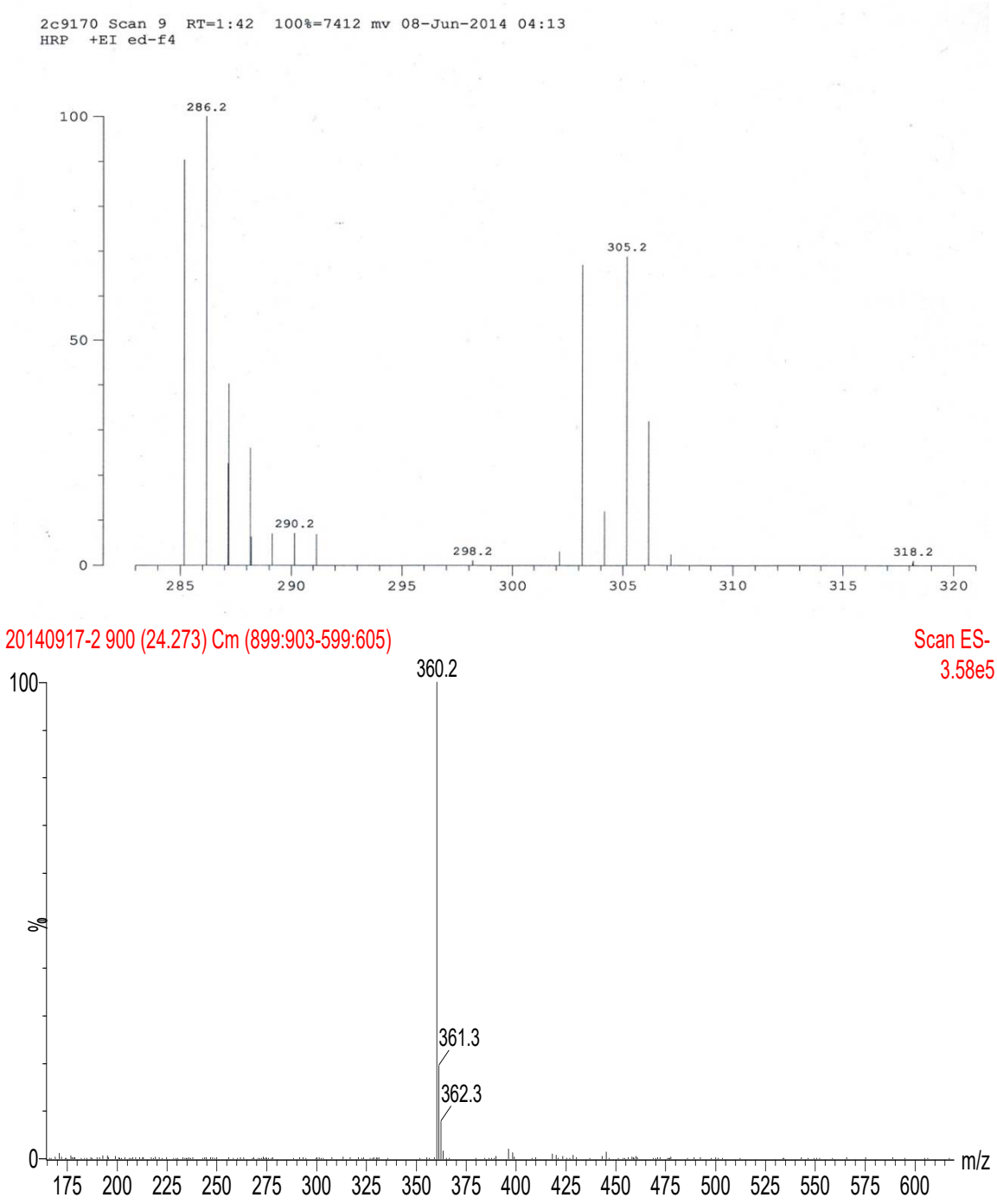

Figure A.4 Mass spectra of compounds **1c** and **1d.**

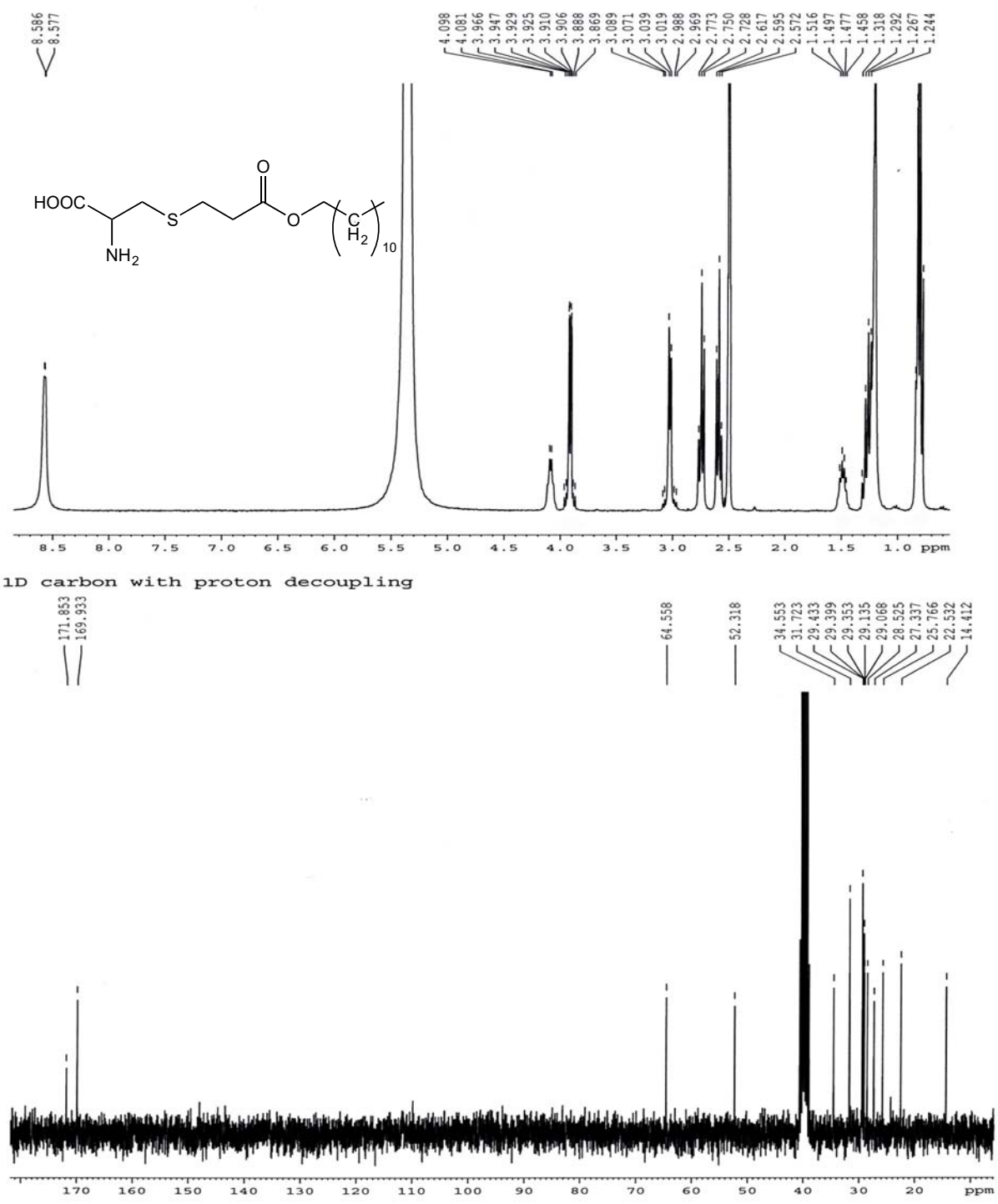

Figure A.5 ^{1}H NMR (300 MHz, DMSO-d_6+HCl) and ^{13}C NMR (75 MHz, DMSO-d_6+HCl) spectra of compound **1d.**

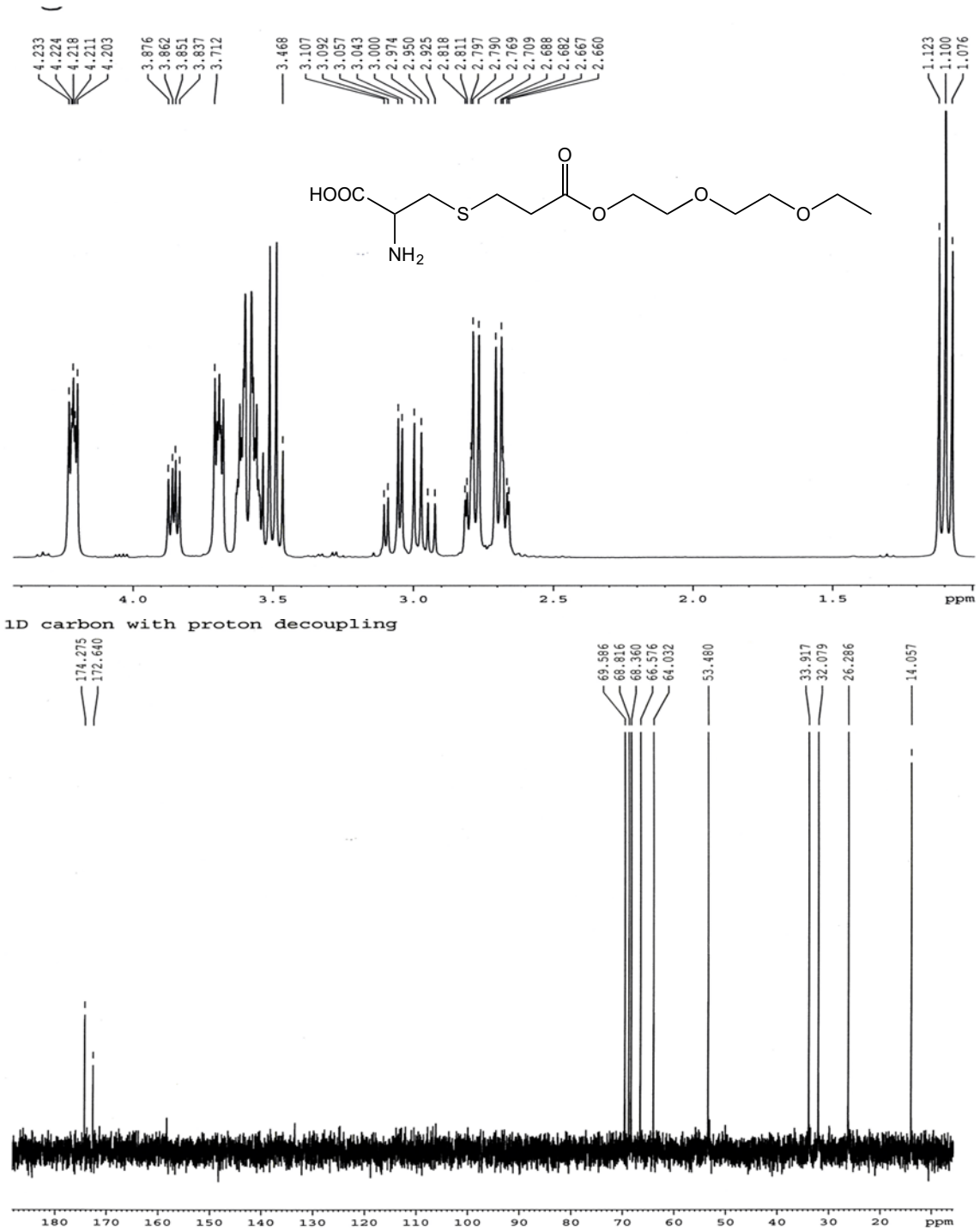

Figure A.6 ^{1}H NMR (300 MHz, D_2O) and ^{13}C NMR (75 MHz, D_2O) of compound **1e.**

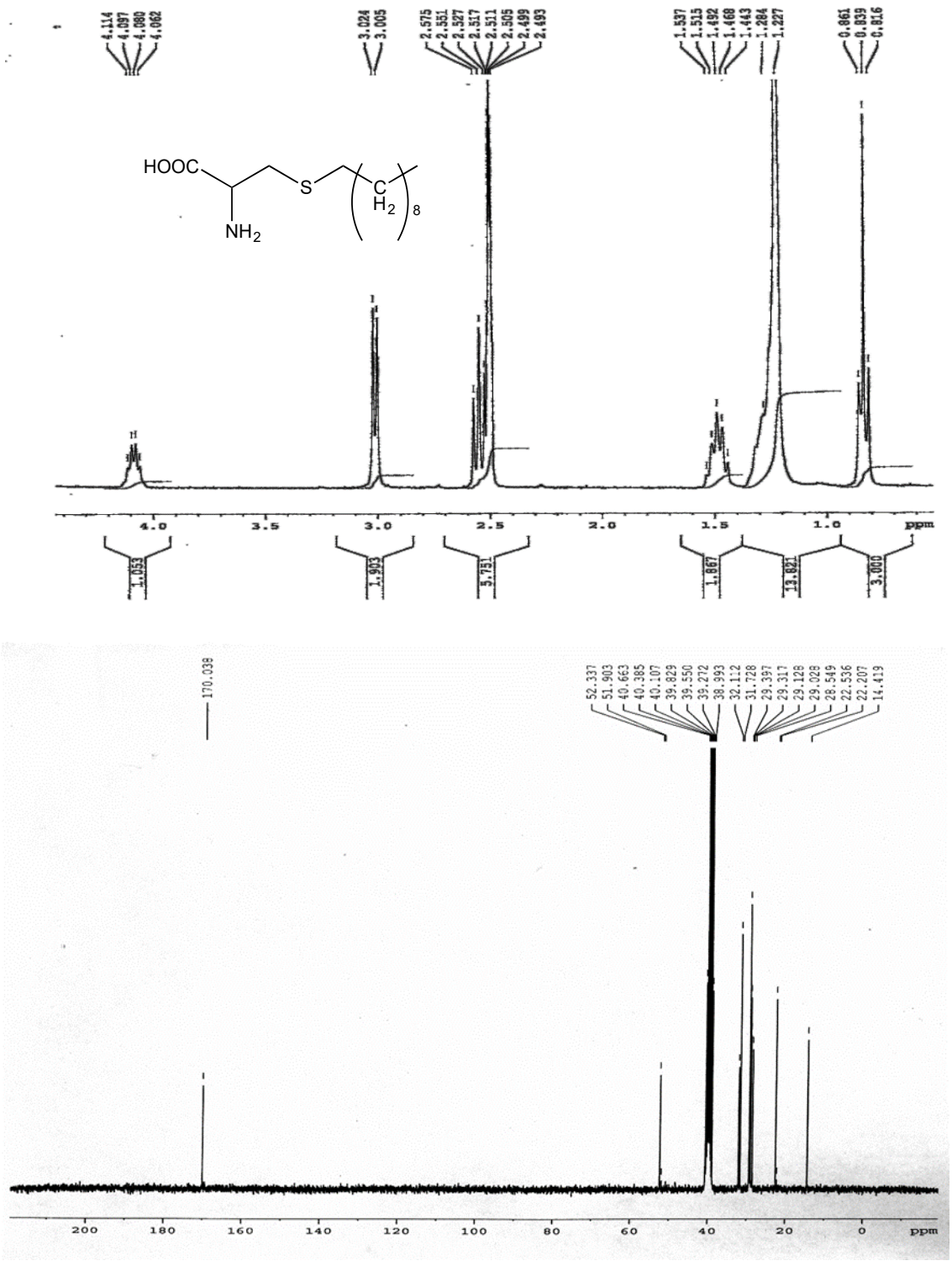

Figure A.7 ^{1}H NMR (300 MHz, DMSO-d_6) and ^{13}C NMR (75 MHz, DMSO-d_6) spectra of compound **1f.**

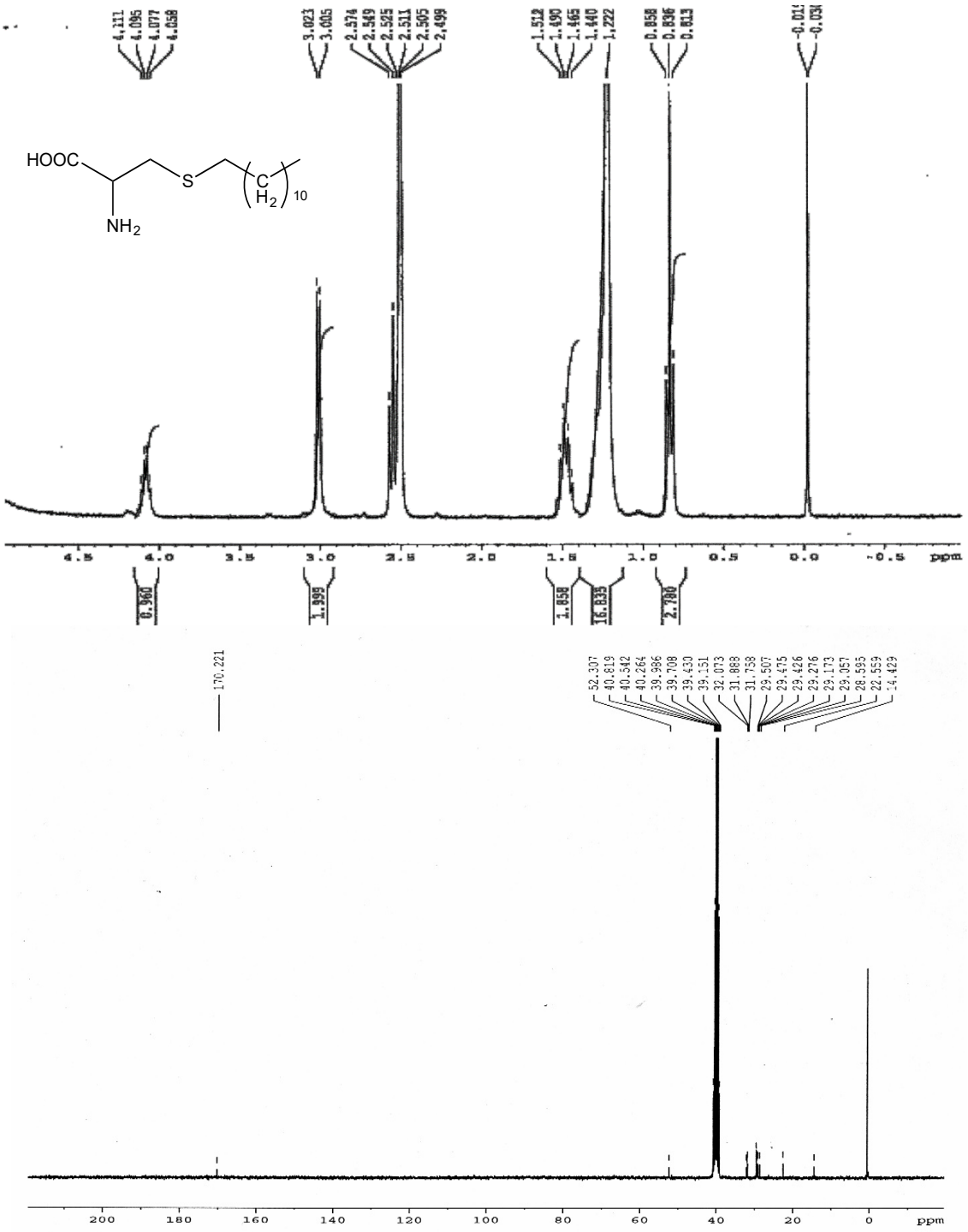

Figure A.8 ^{1}H NMR (300 MHz, DMSO-d_6) and ^{13}C NMR (75 MHz, DMSO-d_6) spectra of compound **1g.**

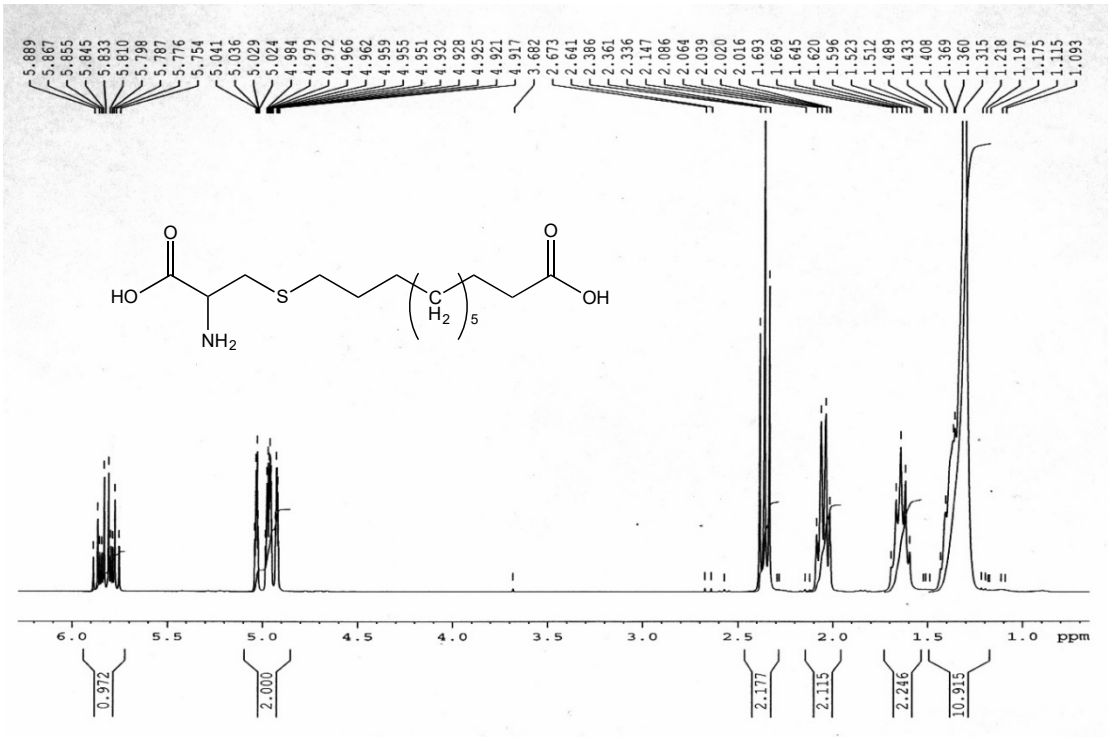

Figure A.9 ^{1}H NMR (300 MHz, DMSO-d_6) spectrum of compound **1h.**

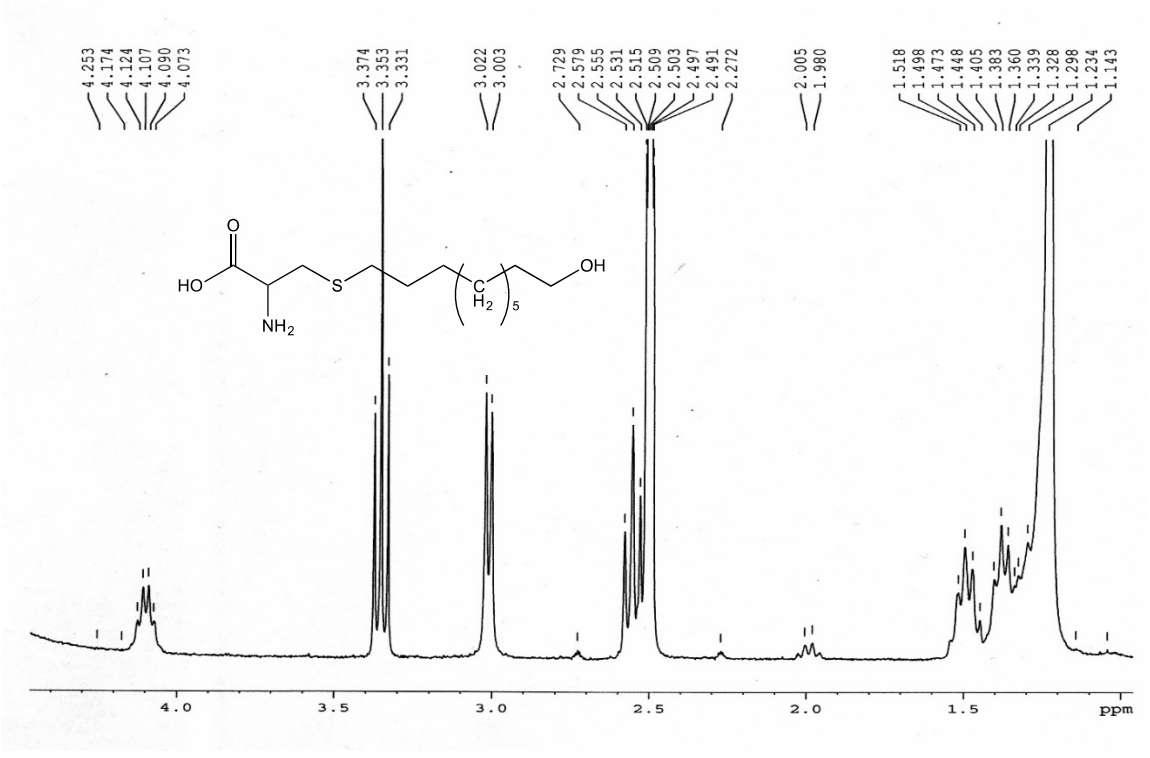

Figure A.10 ^{1}H NMR (300 MHz, DMSO-d_6) spectrum of compound **1i**.

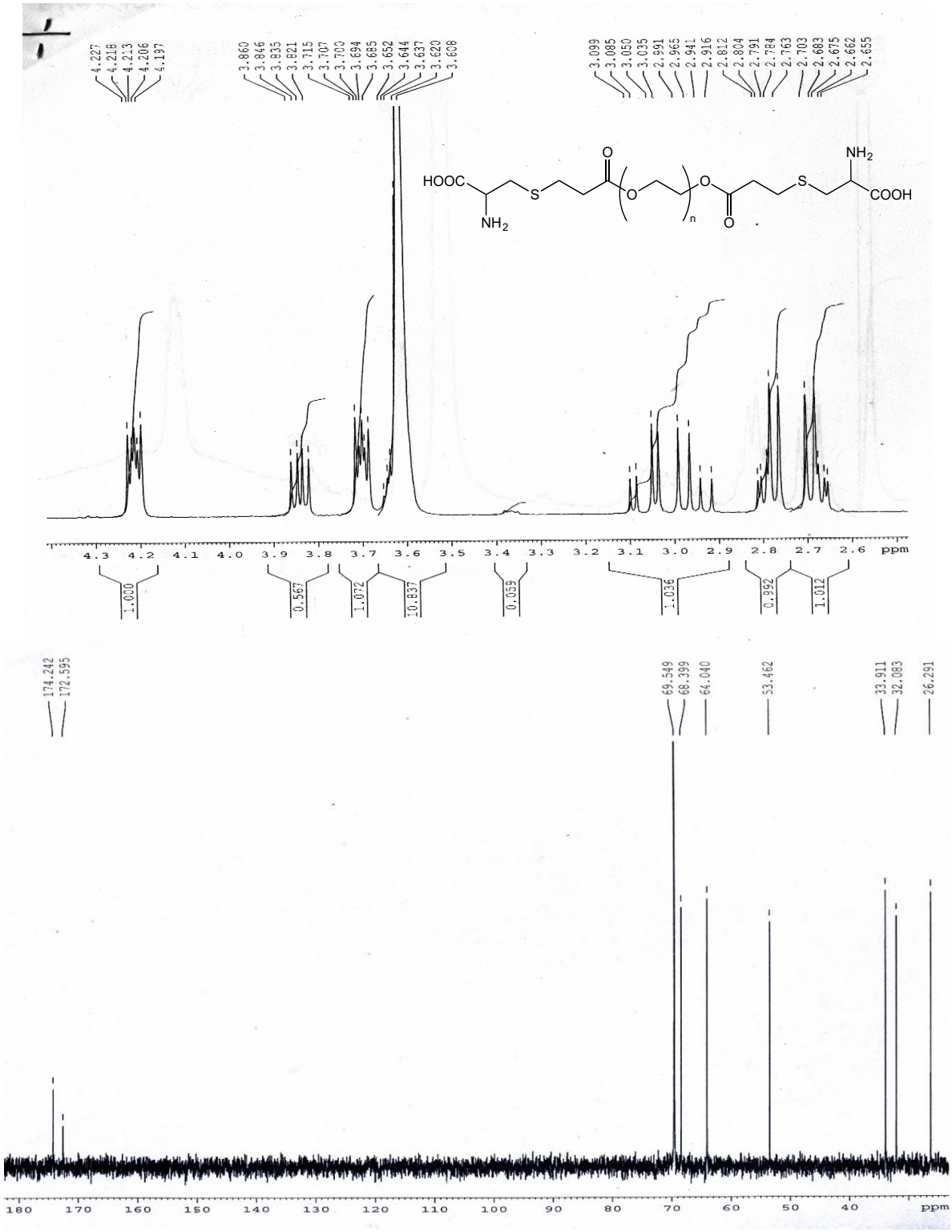

Figure A.11 ^{1}H NMR (300 MHz, D_2O) and ^{13}C NMR (75 MHz, D_2O) of compound **1j**.

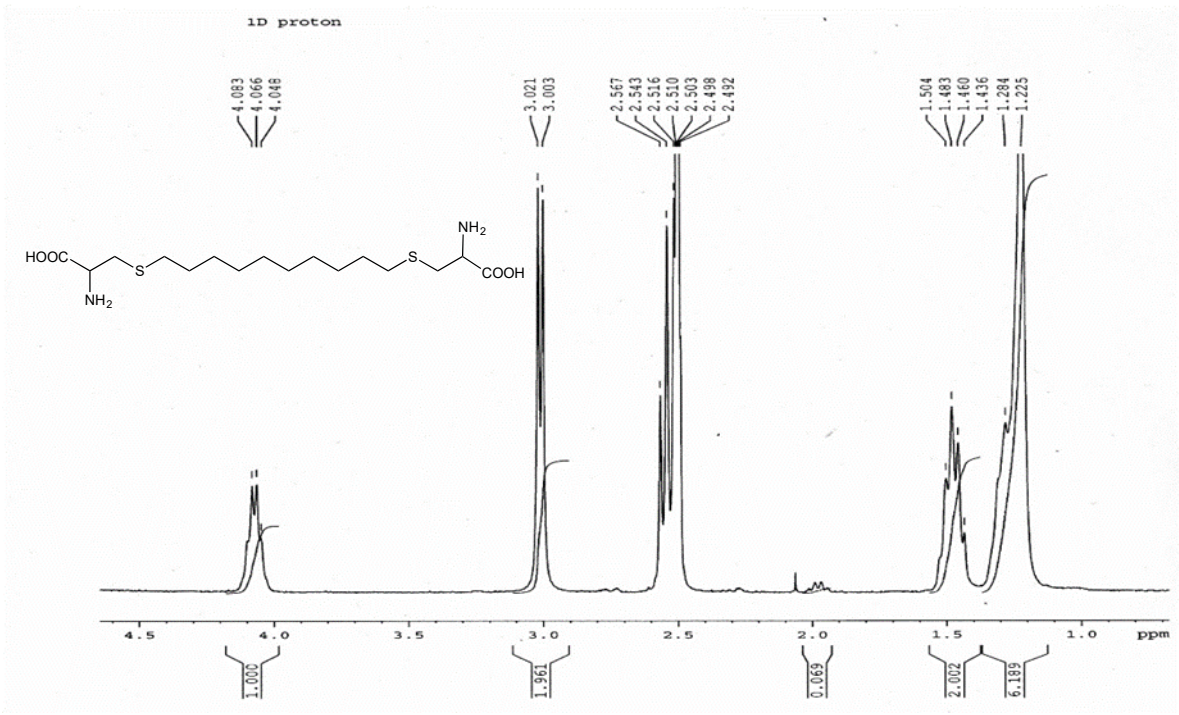

Figure A.12 ^{1}H NMR (300 MHz, DMSO-d_6+HCl) spectrum of compound **1k.**

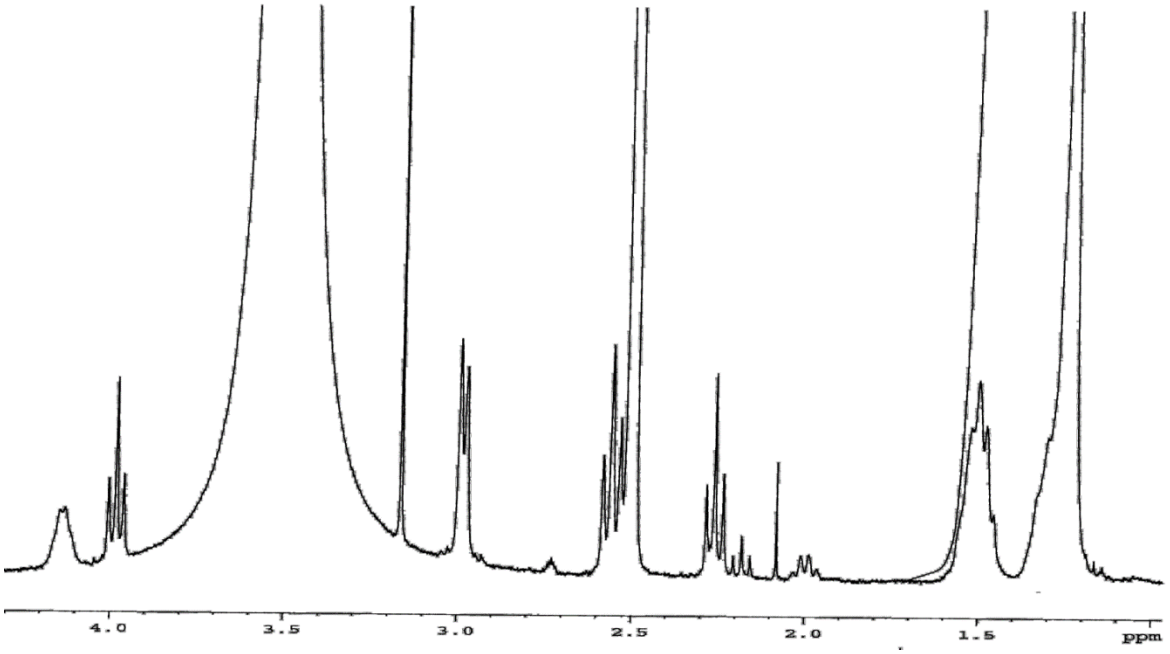

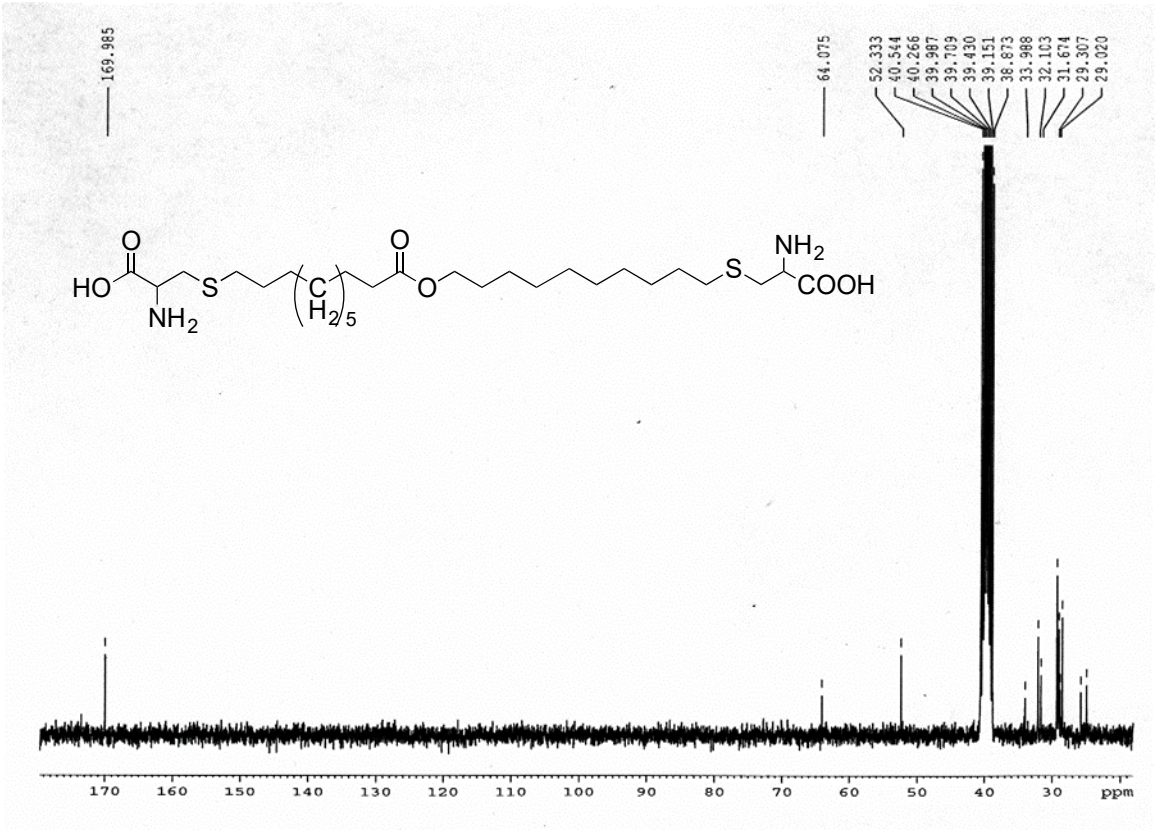

Figure A.13 ^{1}H NMR (300 MHz, DMSO-d_6) and ^{13}C NMR (75 MHz, DMSO-d_6) spectra of compound **1l.**

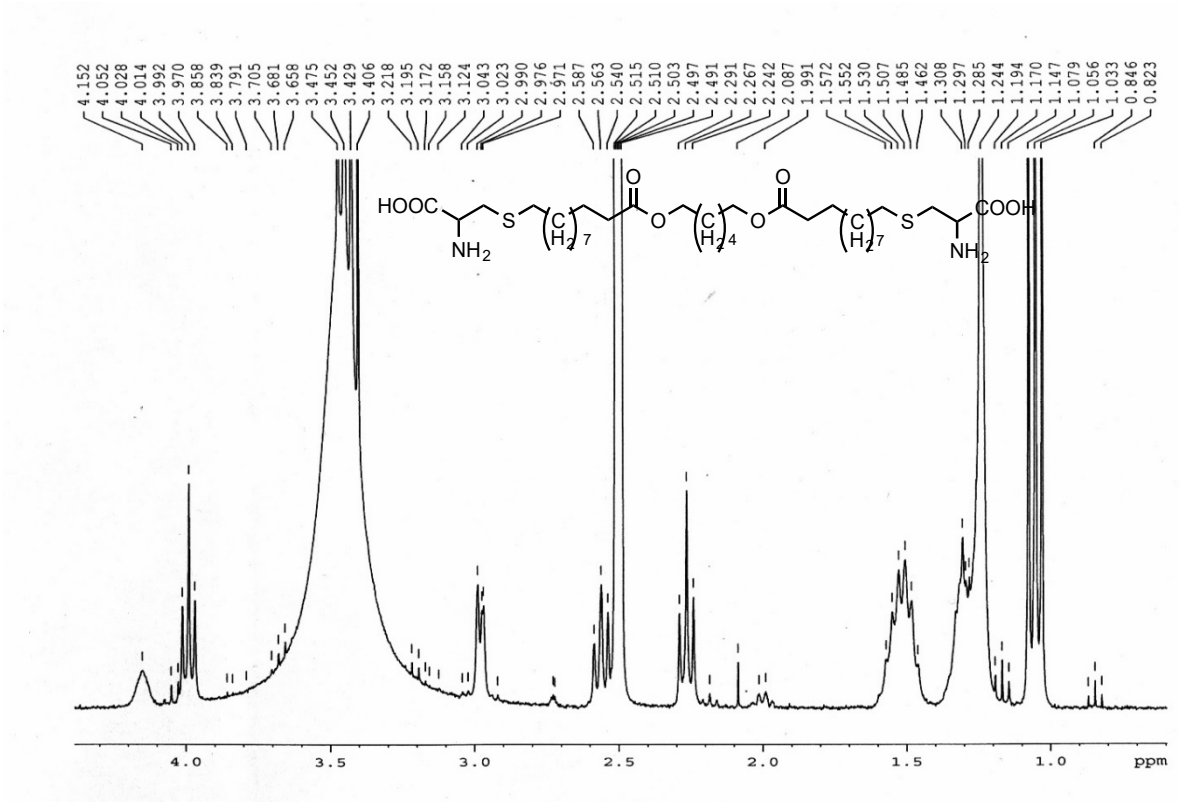

Figure A.14 ^{1}H NMR (300 MHz, DMSO-d_6) spectrum of compound **1m.**

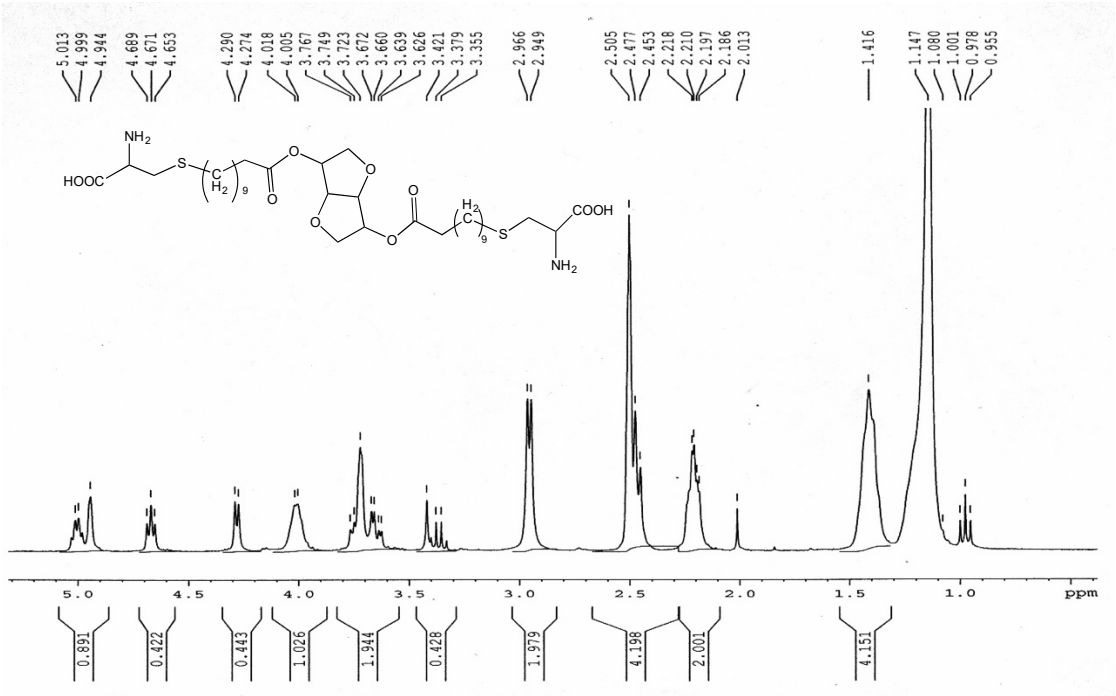

Figure A.15 ^{1}H NMR (300 MHz, DMSO-d_6) spectrum of compound **1n.**

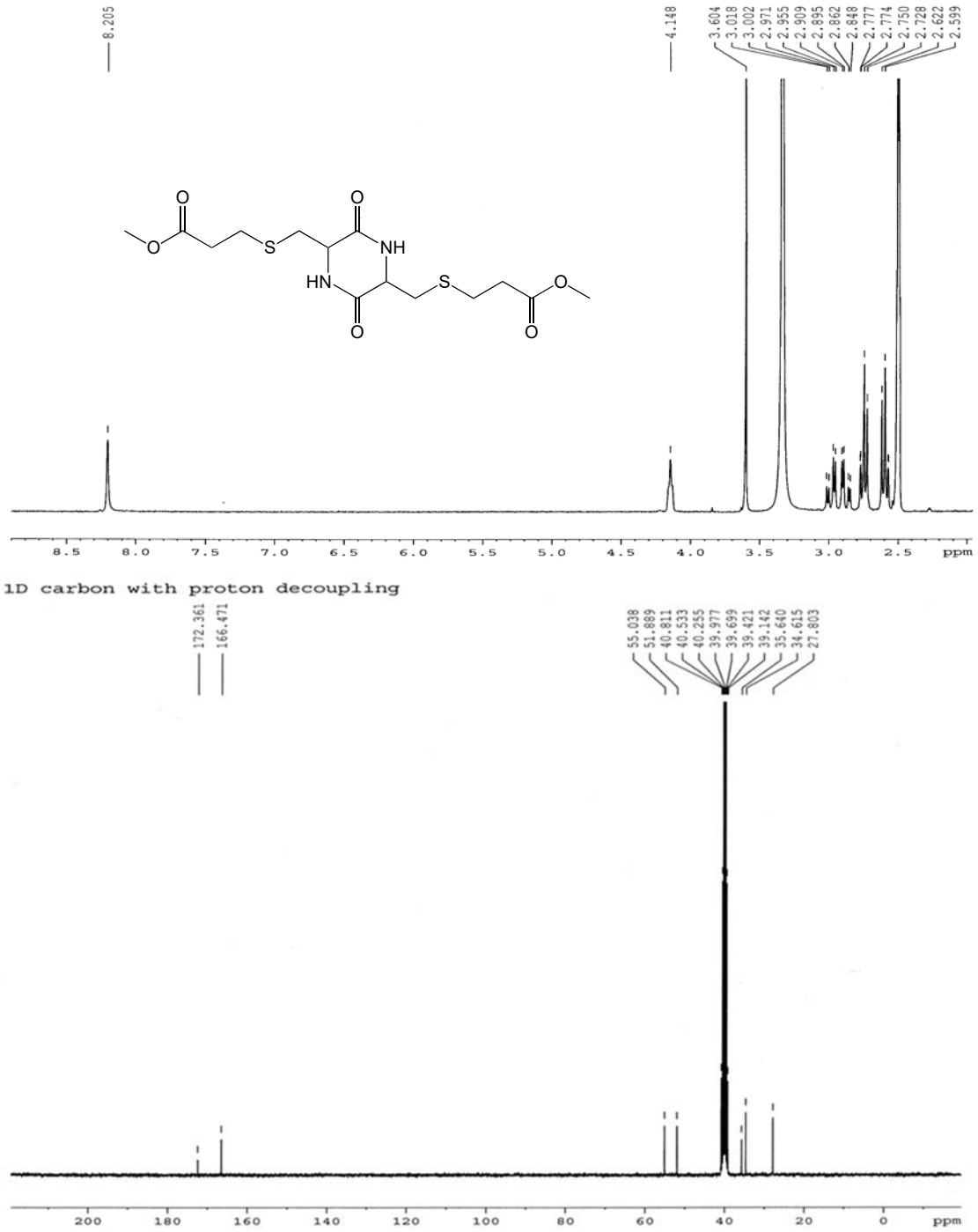

Figure A.16 ^{1}H NMR (300 MHz, DMSO-d_6) and ^{13}C NMR (75 MHz, DMSO-d_6) spectra of cis-**2a.**

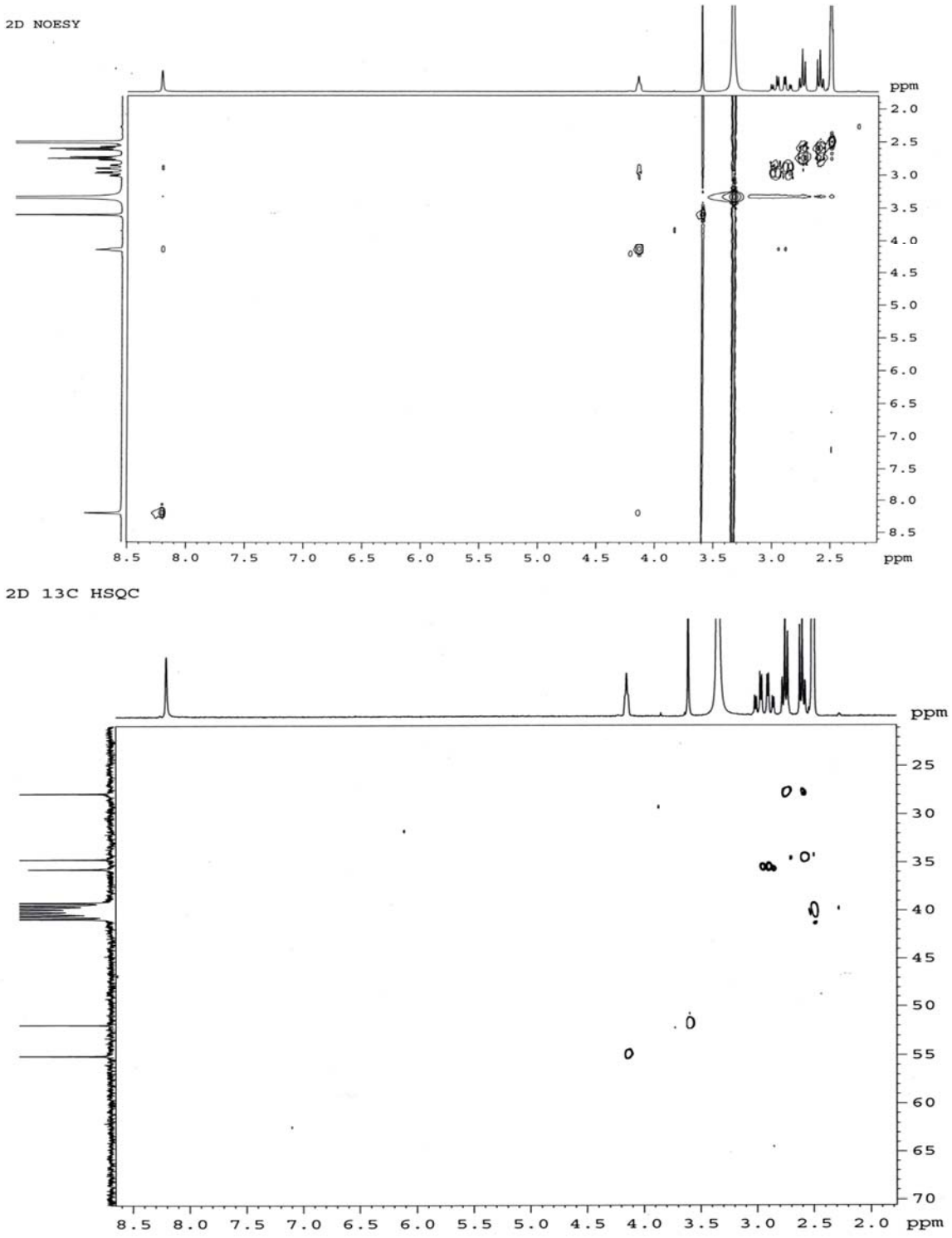

Figure A.17 NOESY and HSQC (DMSO-d_6) spectra of cis-**2a.**

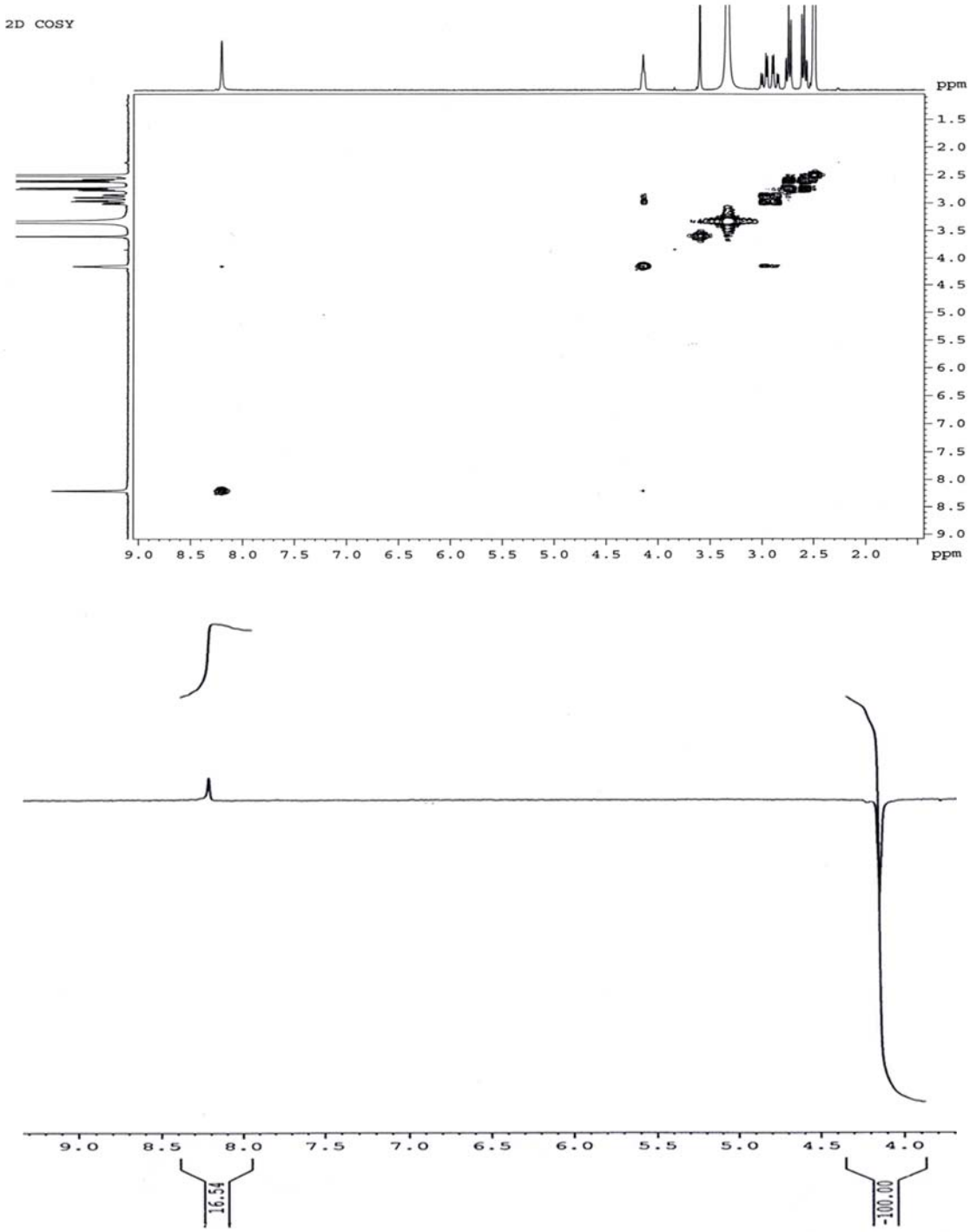

Figure A.18 COSY and 1D NOE difference (DMSO-d_6) spectra of cis-**2a.**

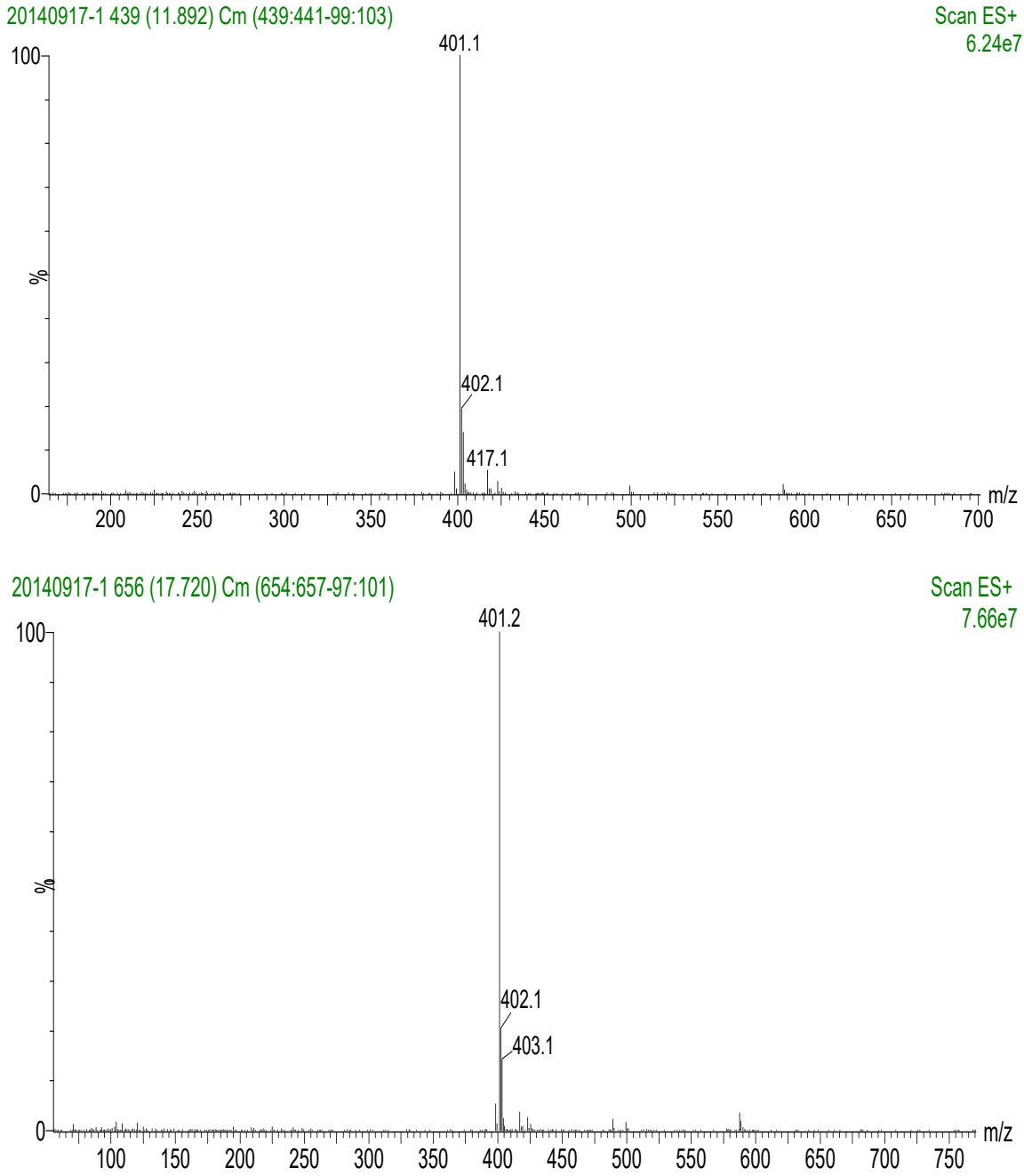

Figure A.19 Mass spectra of cis-**2a** (top) and trans-**2a.**

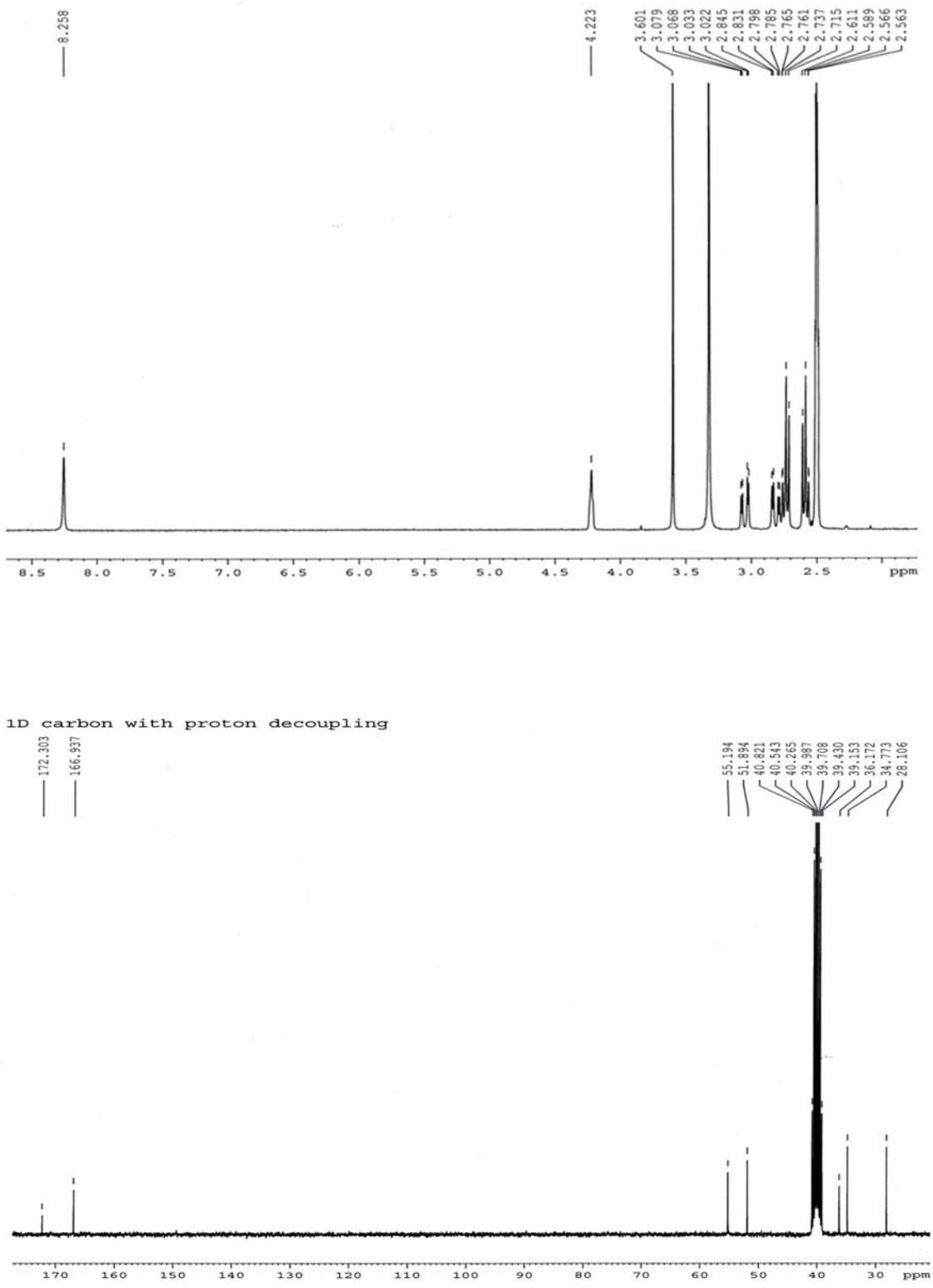

Figure A.20 ^{1}H NMR (300 MHz, DMSO-d_6) and ^{13}C NMR (75 MHz, DMSO-d_6) spectra of trans-**2a.**

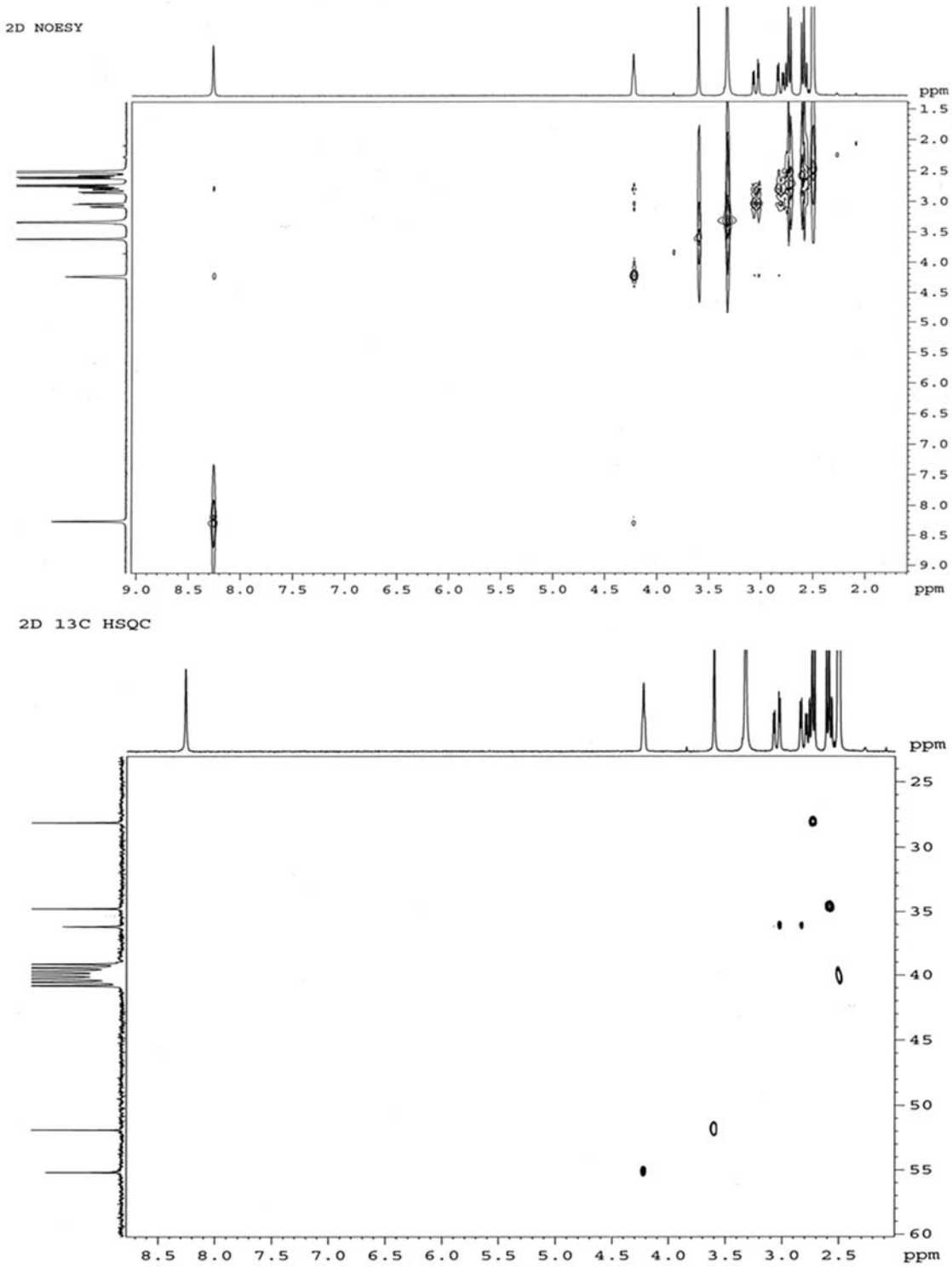

Figure A.21 NOESY and HSQC (DMSO-d_6) spectra of trans-**2a.**

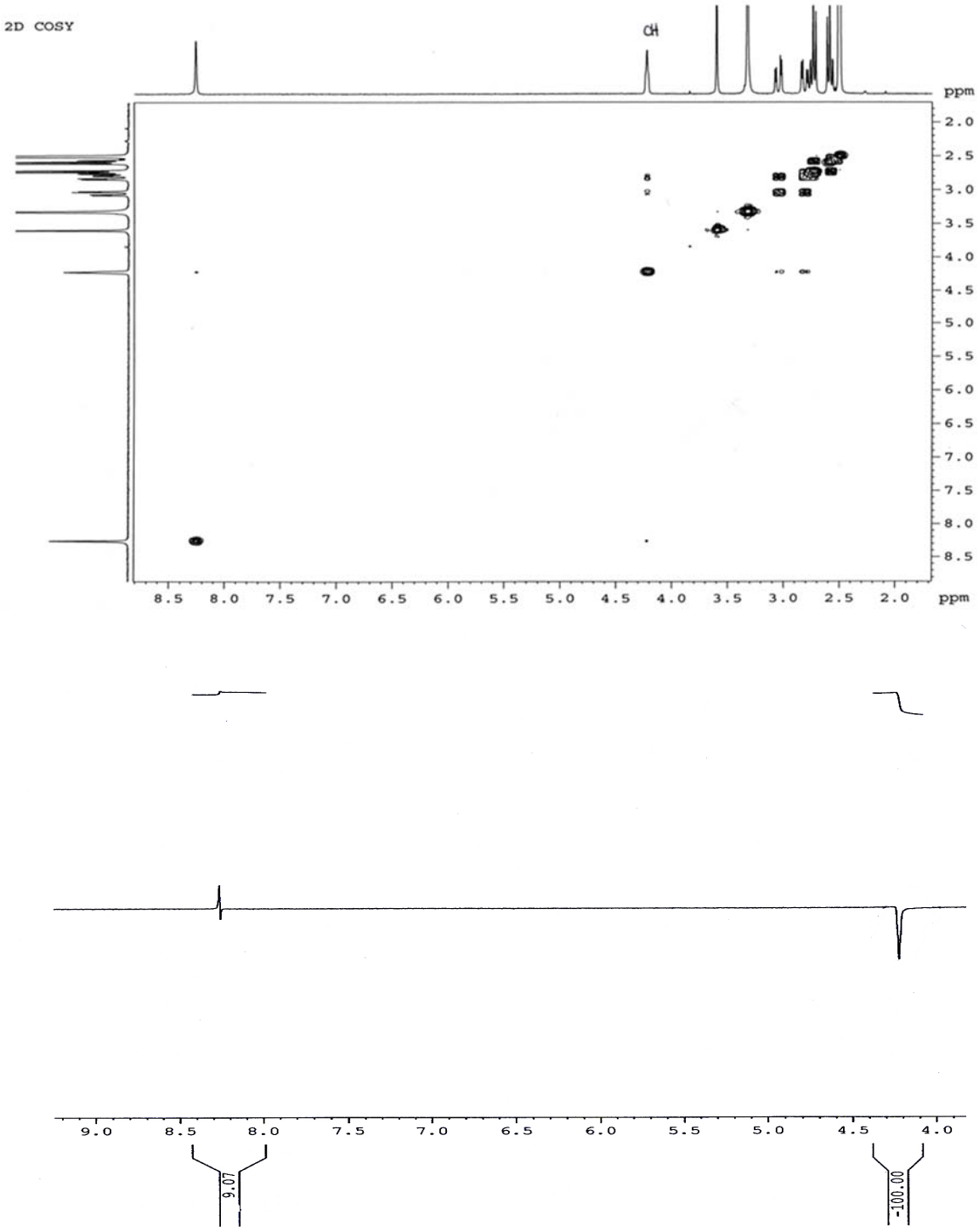

Figure A.22 COSY and 1D NOE difference (DMSO-d_6) spectra of trans-**2a.**

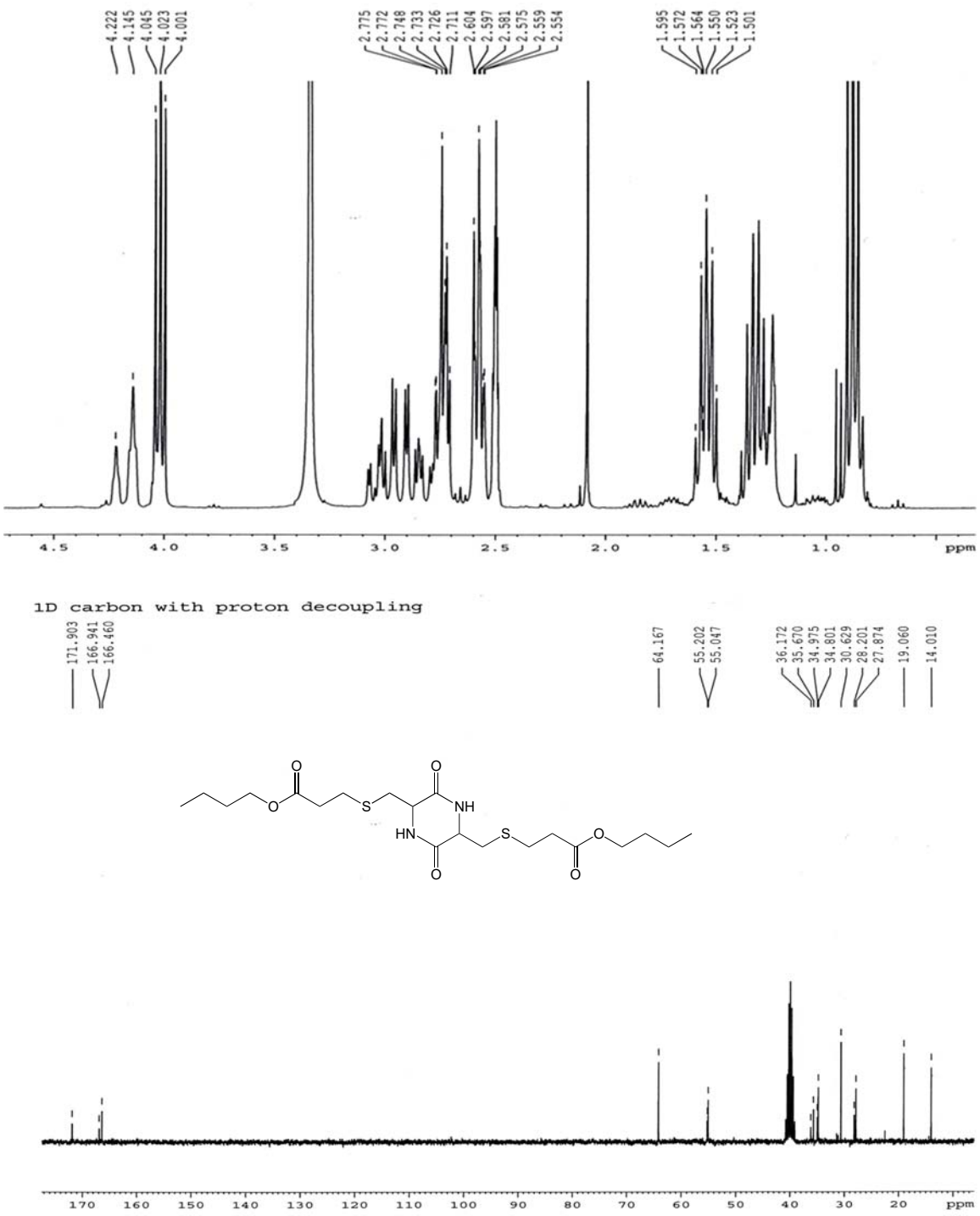

Figure A.23 ^{1}H NMR (300 MHz, DMSO-d_6) and ^{13}C NMR (75 MHz, DMSO-d_6) spectra of compound **2b.**

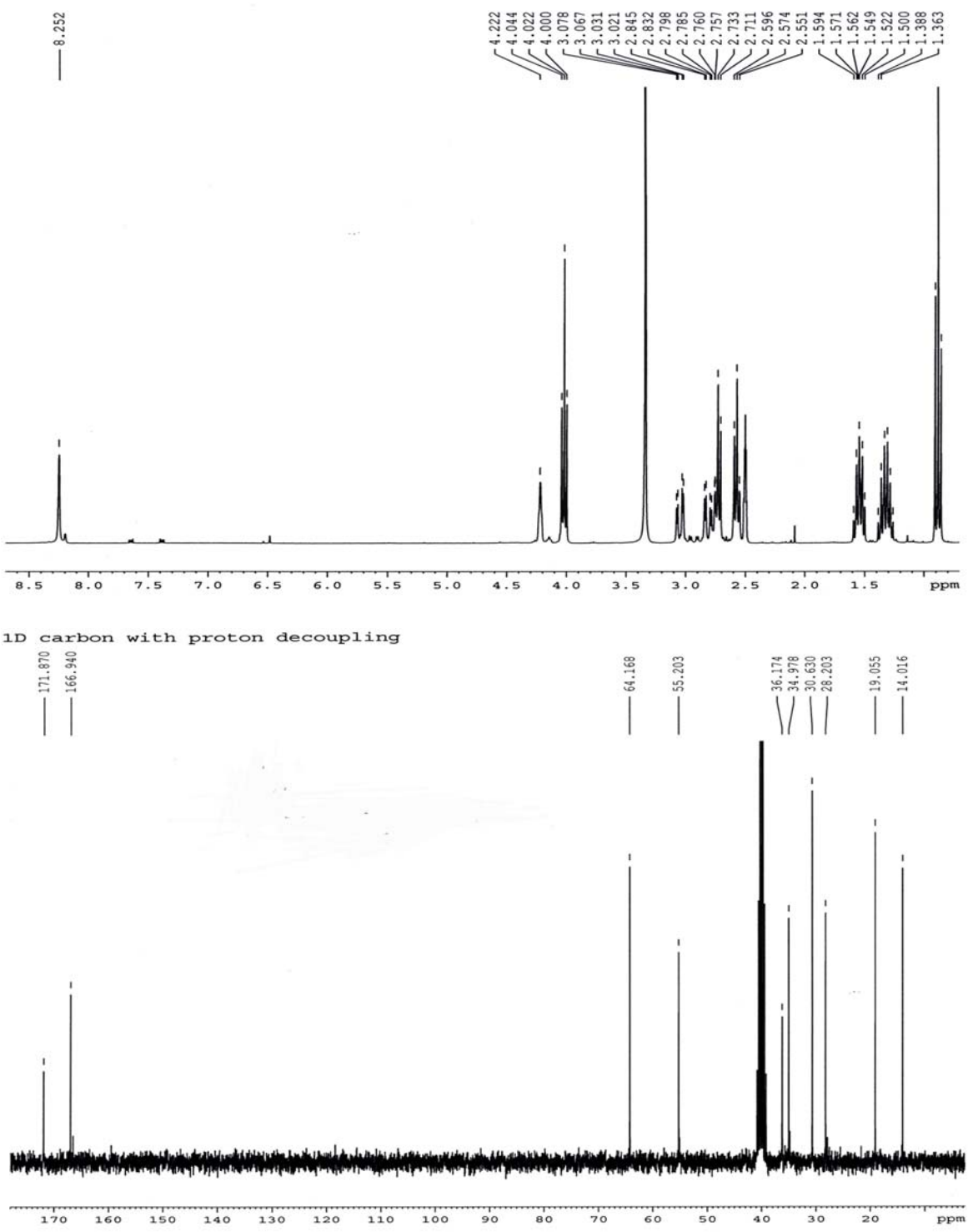

Figure A.24 ^{1}H NMR (300 MHz, DMSO-d$_6$) and ^{13}C NMR (75 MHz, DMSO-d$_6$) spectra of trans-**2b**.

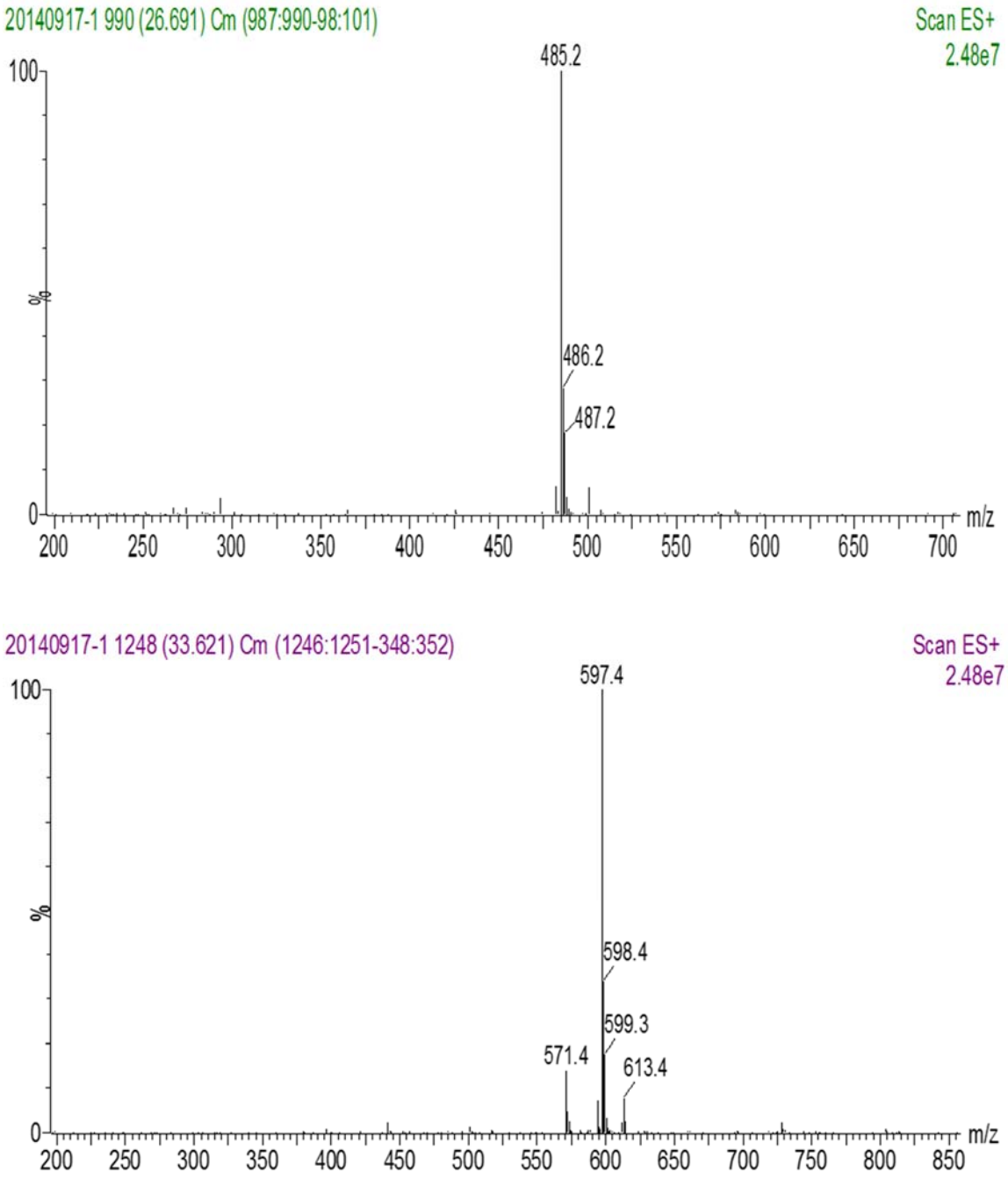

Figure A.25 Mass spectra of compounds **2b** and **2c.**

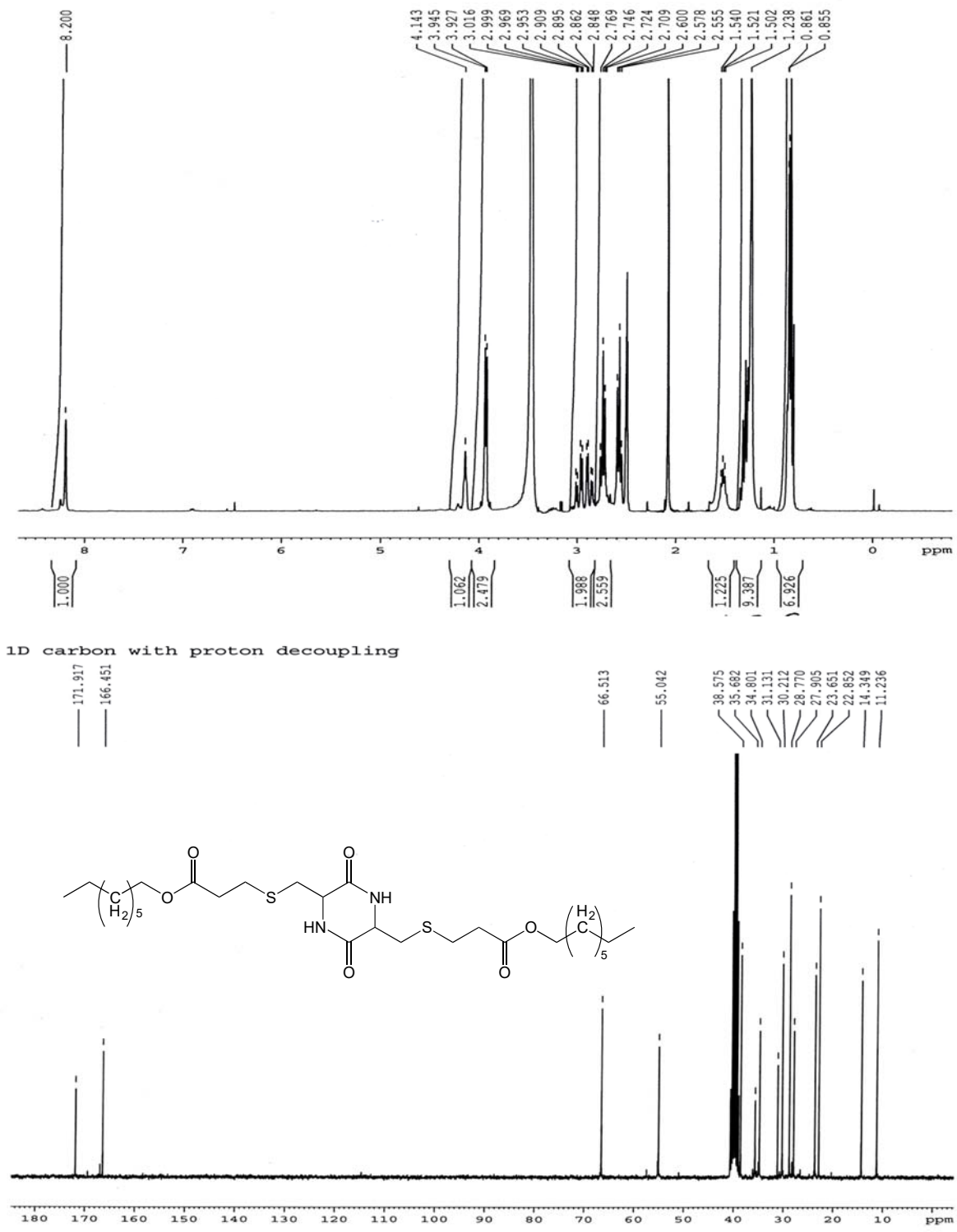

Figure A.26 ^{1}H NMR (300 MHz, DMSO-d$_6$) and ^{13}C NMR (75 MHz, DMSO-d$_6$) spectra of compound **2c**.

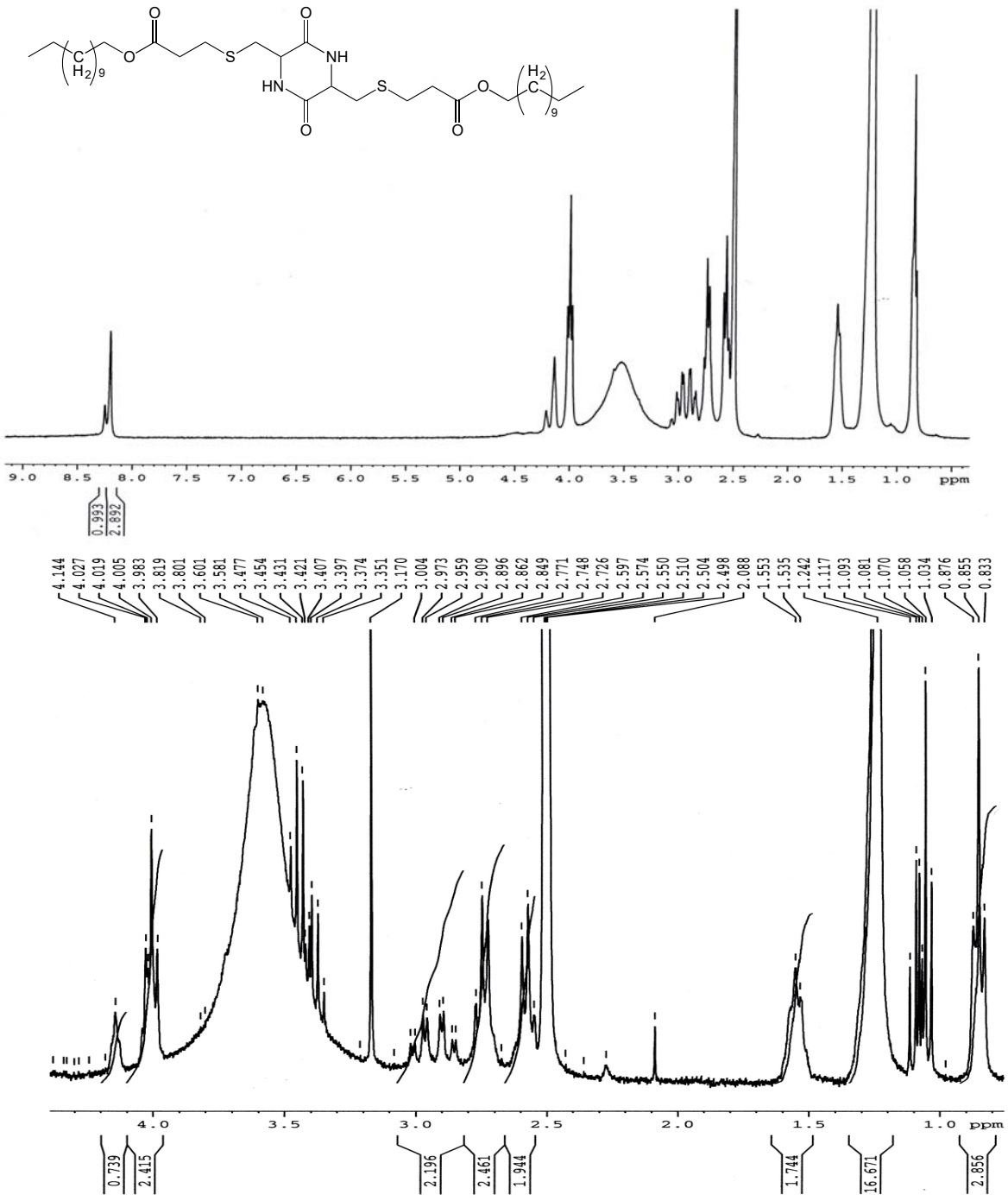

Figure A.27 ^{1}H NMR (300 MHz, DMSO-d_6) spectra of mixture **2d** and cis-**2d**.

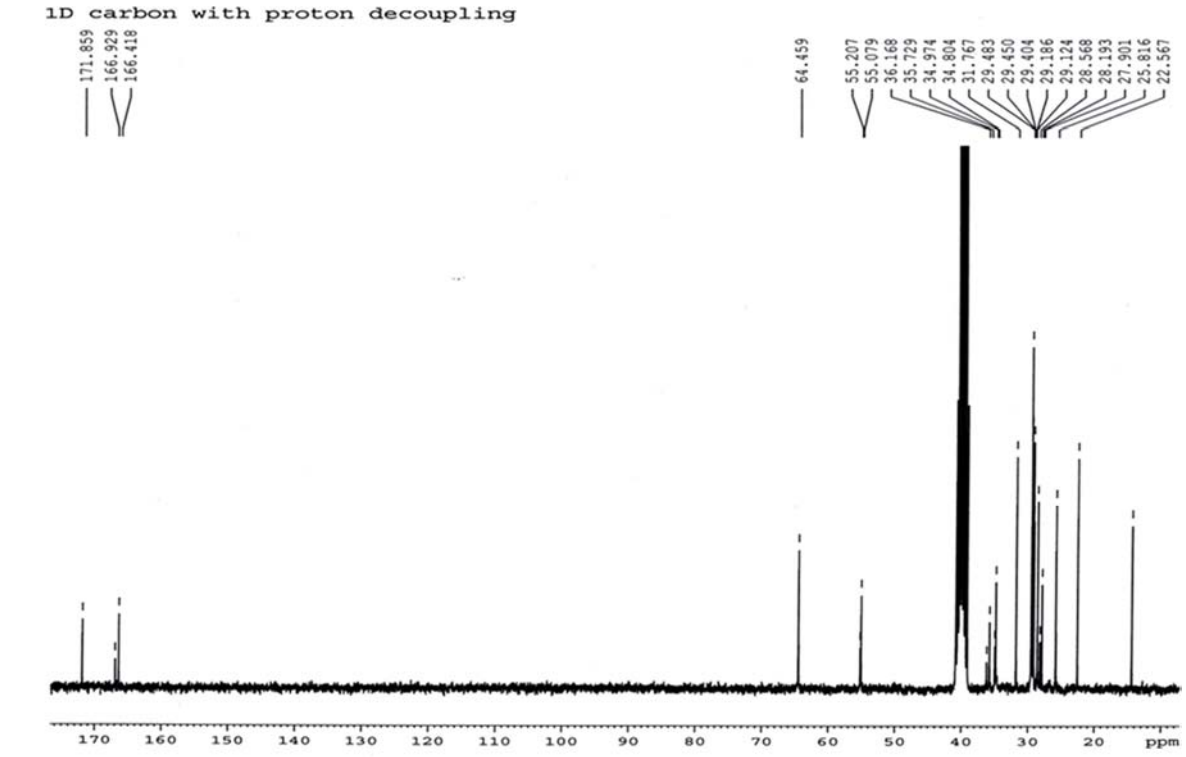

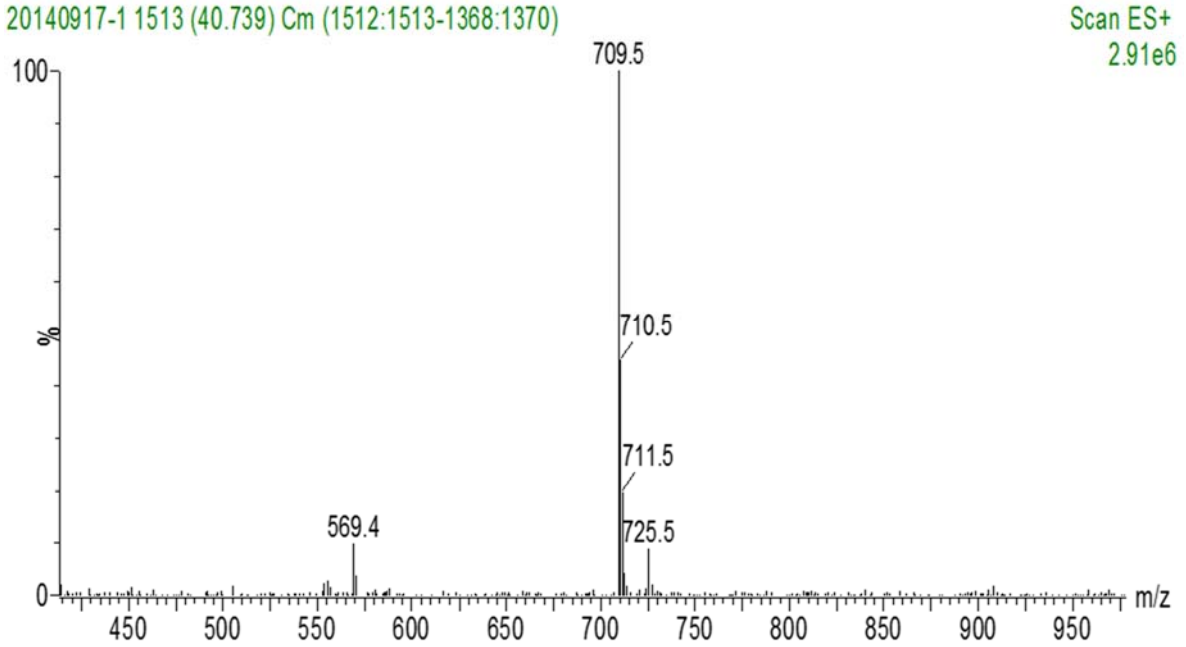

Figure A.28 ^{13}C NMR (75 MHz, DMSO-d_6) and mass spectra of compound **2d**.

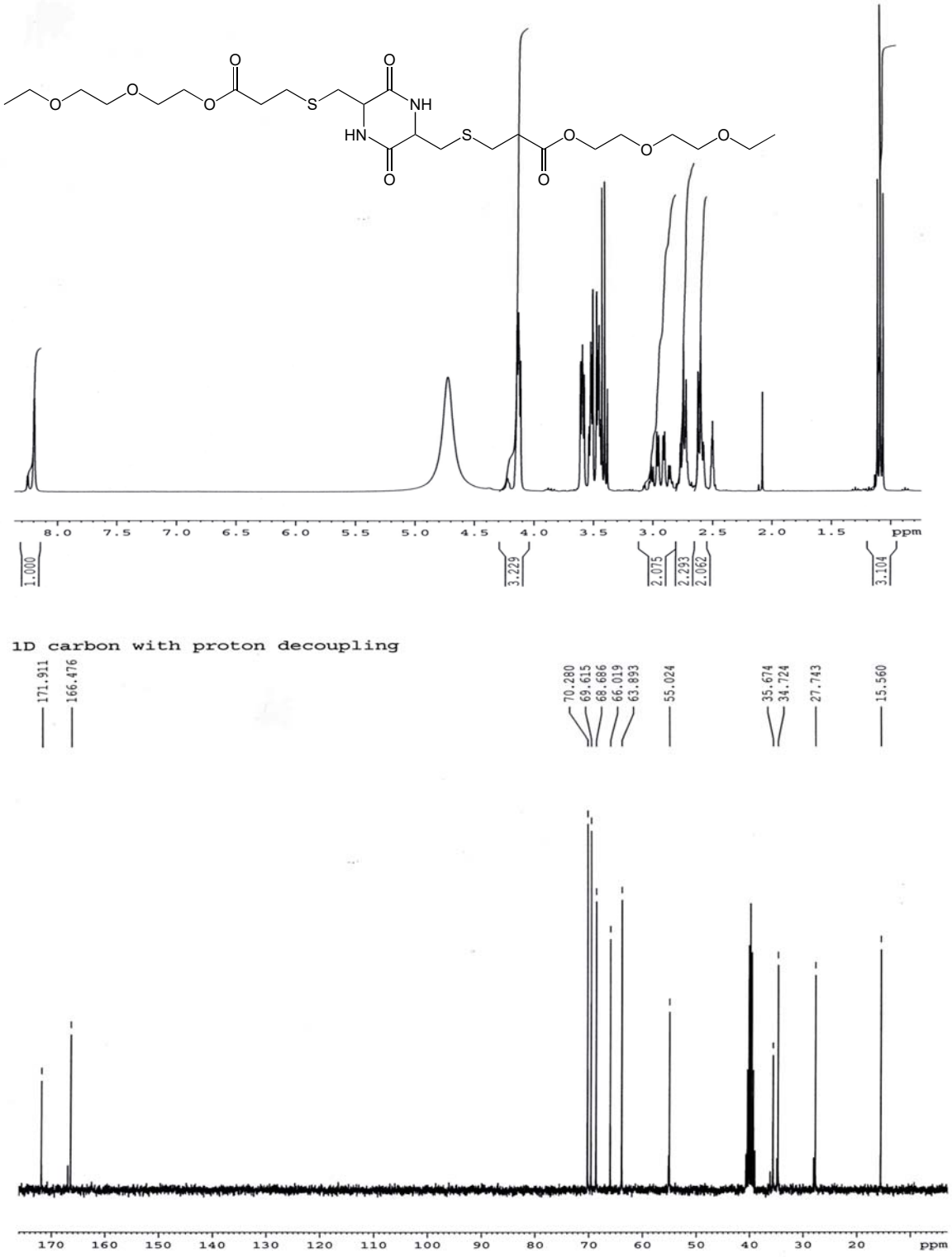

Figure A.29 ^{1}H NMR (300 MHz, DMSO-d_6) and ^{13}C NMR (75 MHz, DMSO-d_6) spectra of cis-**2e**.

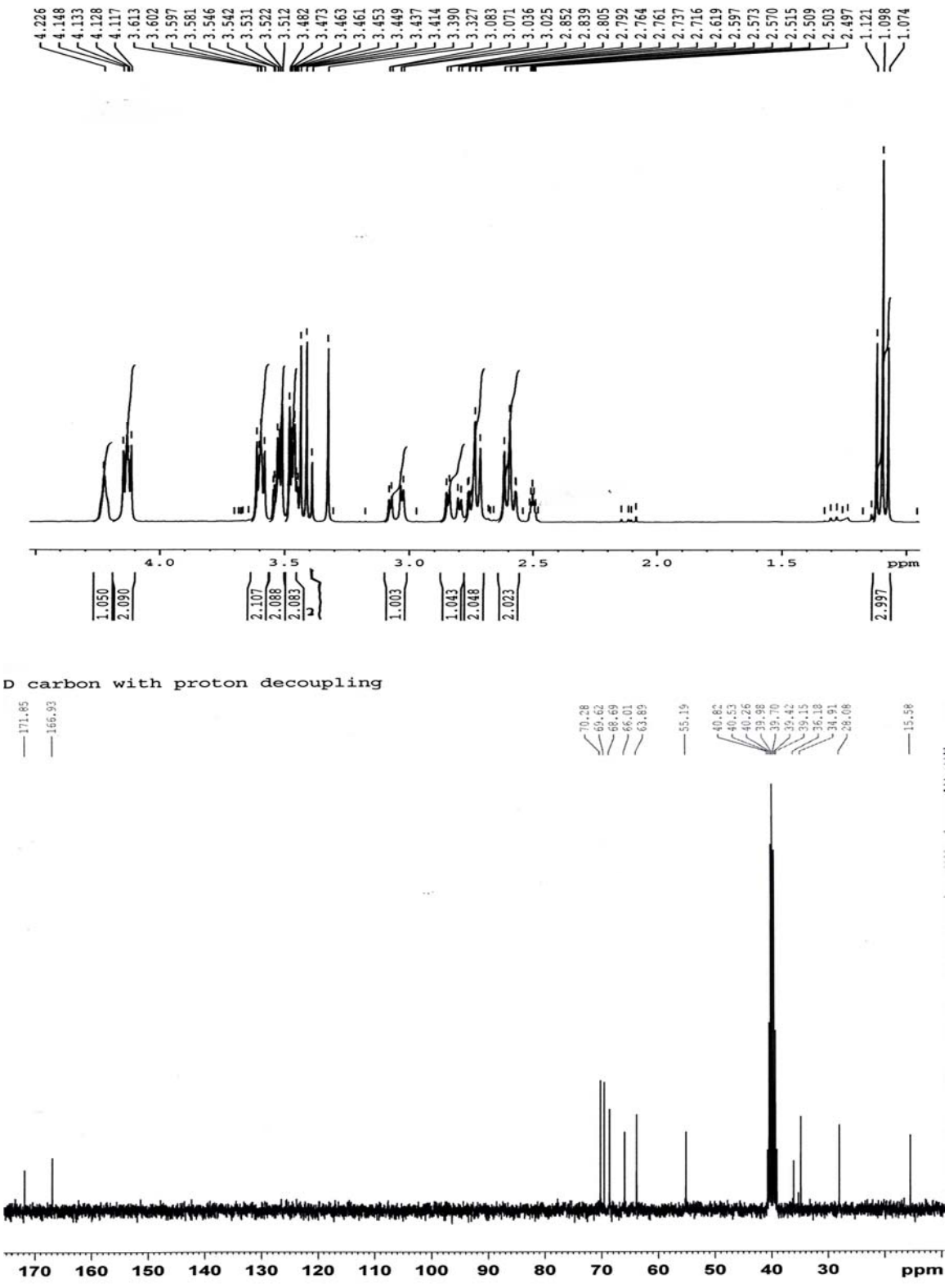

Figure A.30 ^{1}H NMR (300 MHz, DMSO-d_6) and ^{13}C NMR (75 MHz, DMSO-d_6) spectra of trans-**2e**.

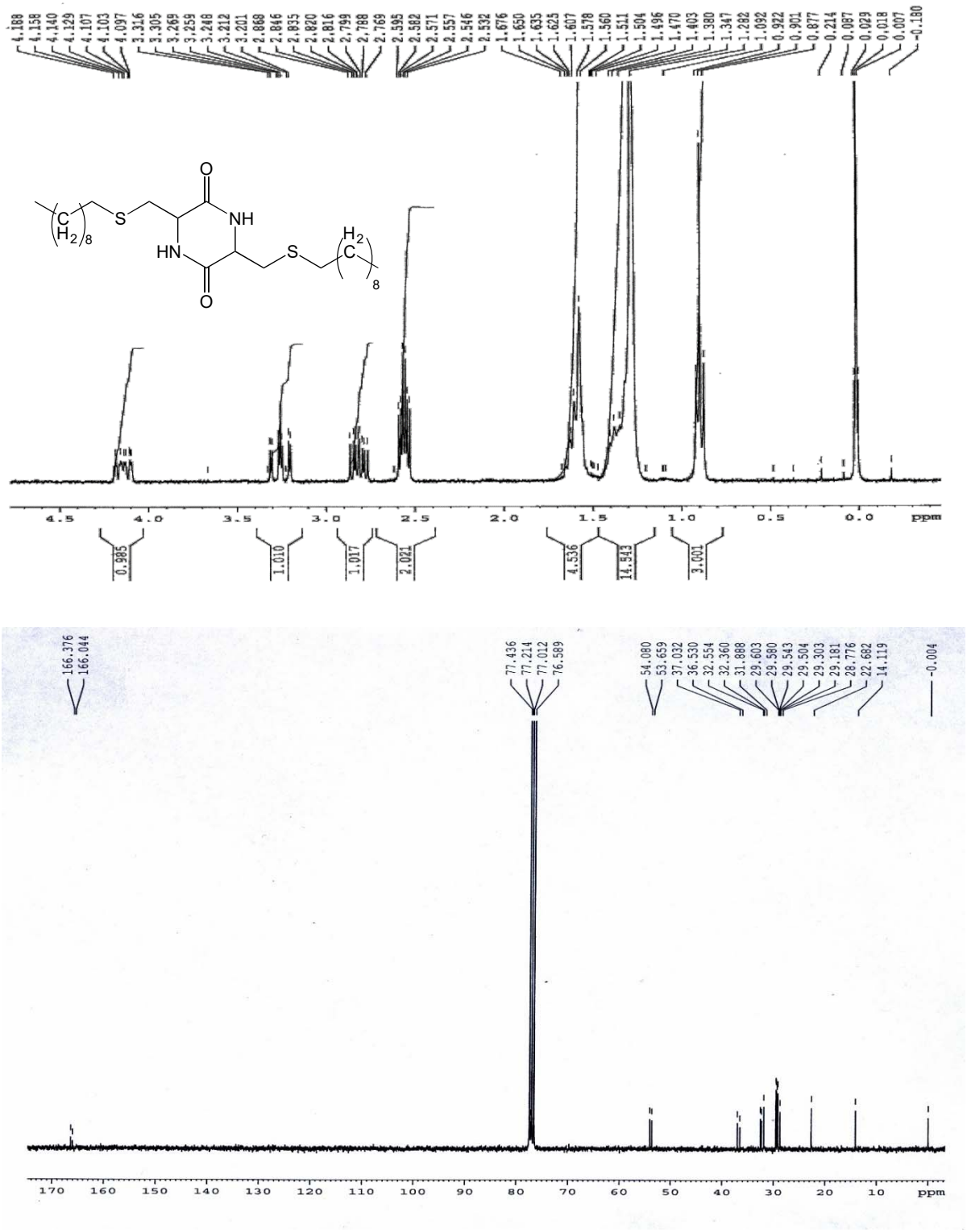

Figure A.31 ^{1}H NMR (300 MHz, $CDCl_3$) and ^{13}C NMR (75 MHz, $CDCl_3$) spectra of compound **2f**.

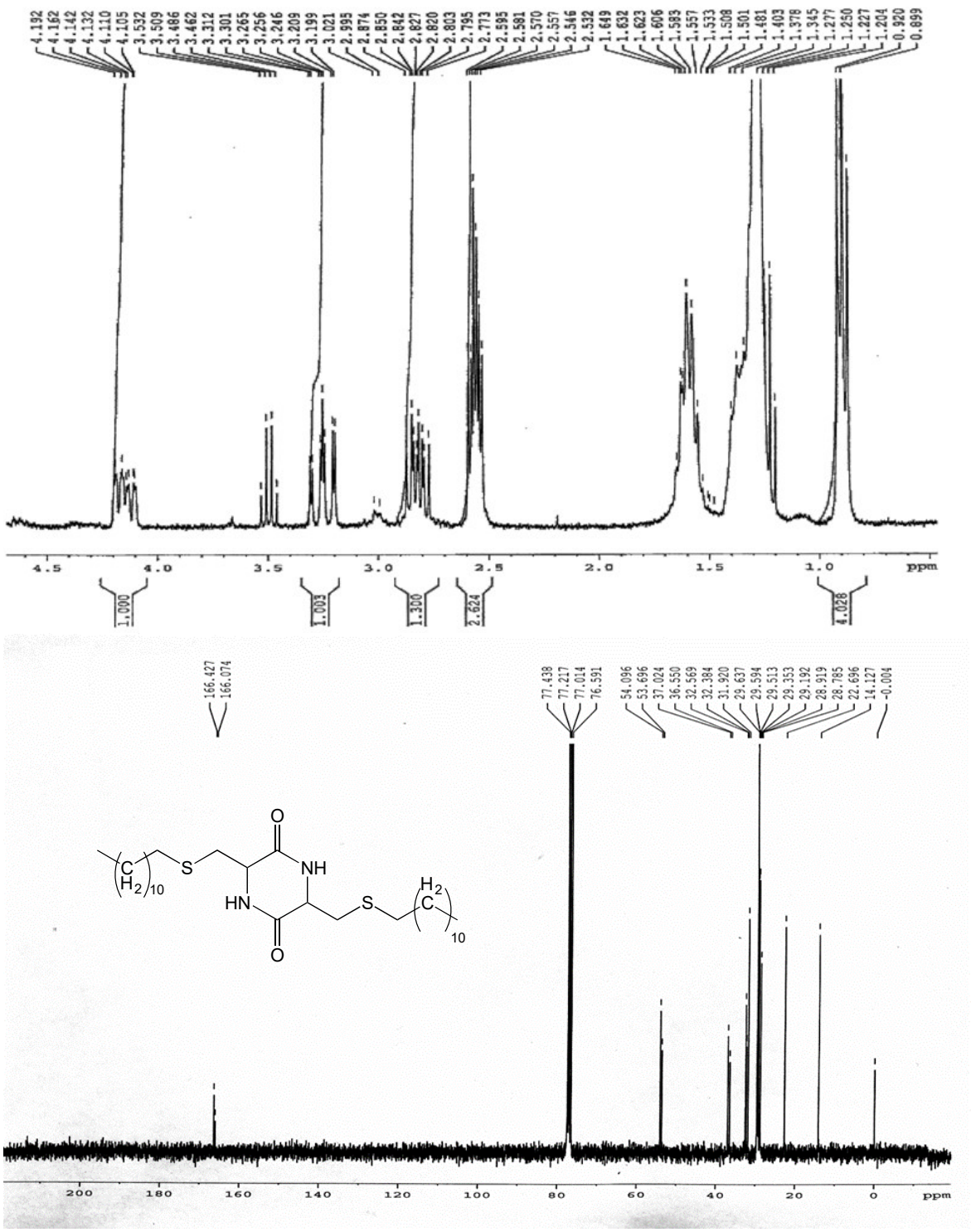

Figure A.32 ^{1}H NMR (300 MHz, $CDCl_3$) and ^{13}C NMR (75 MHz, $CDCl_3$) spectra of compound **2g**.

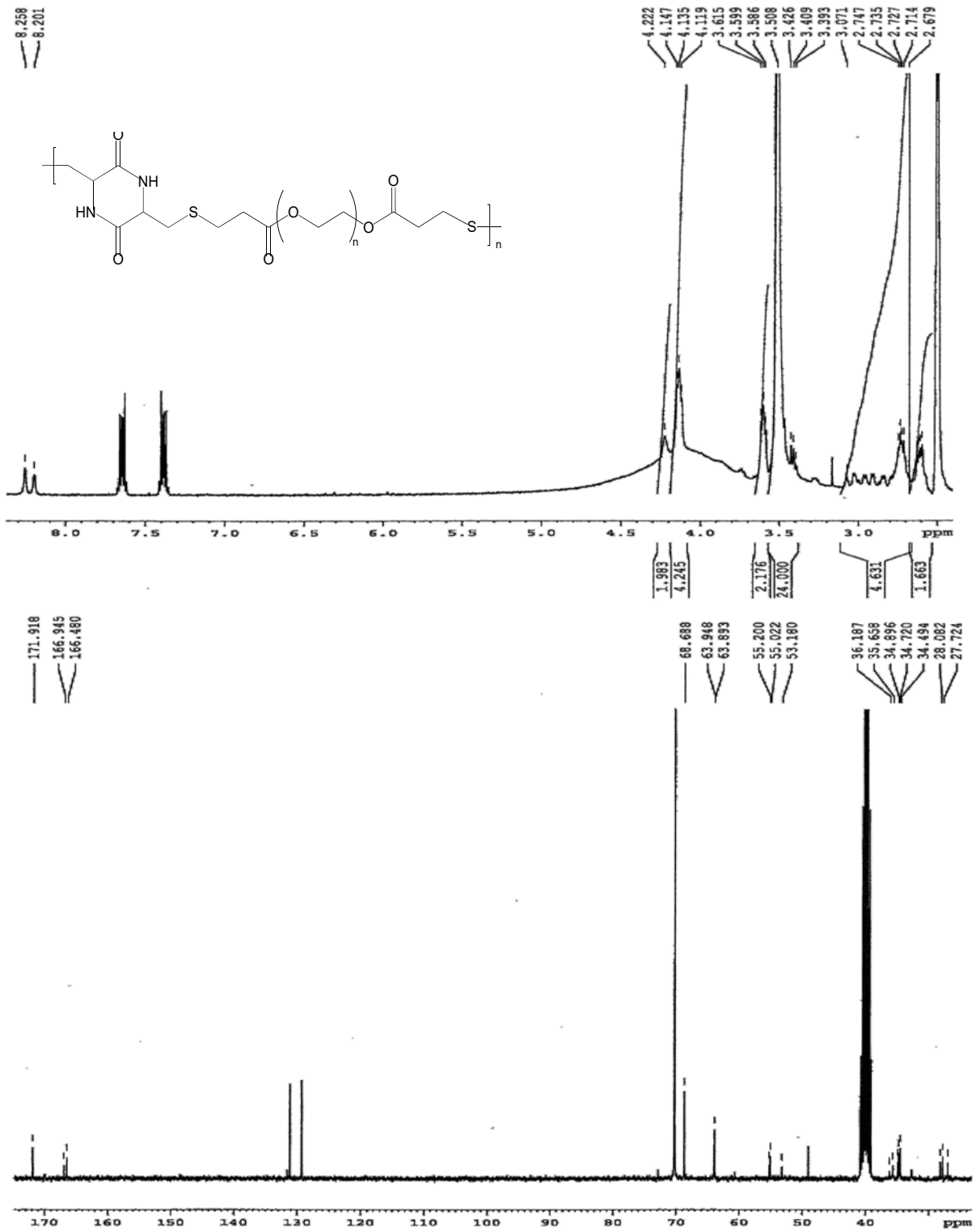

Figure A.33 ^{1}H NMR ((300 MHz, DMSO-d$_6$) and ^{13}C NMR (75 MHz, DMSO-d$_6$) spectra of polymer **2j**.

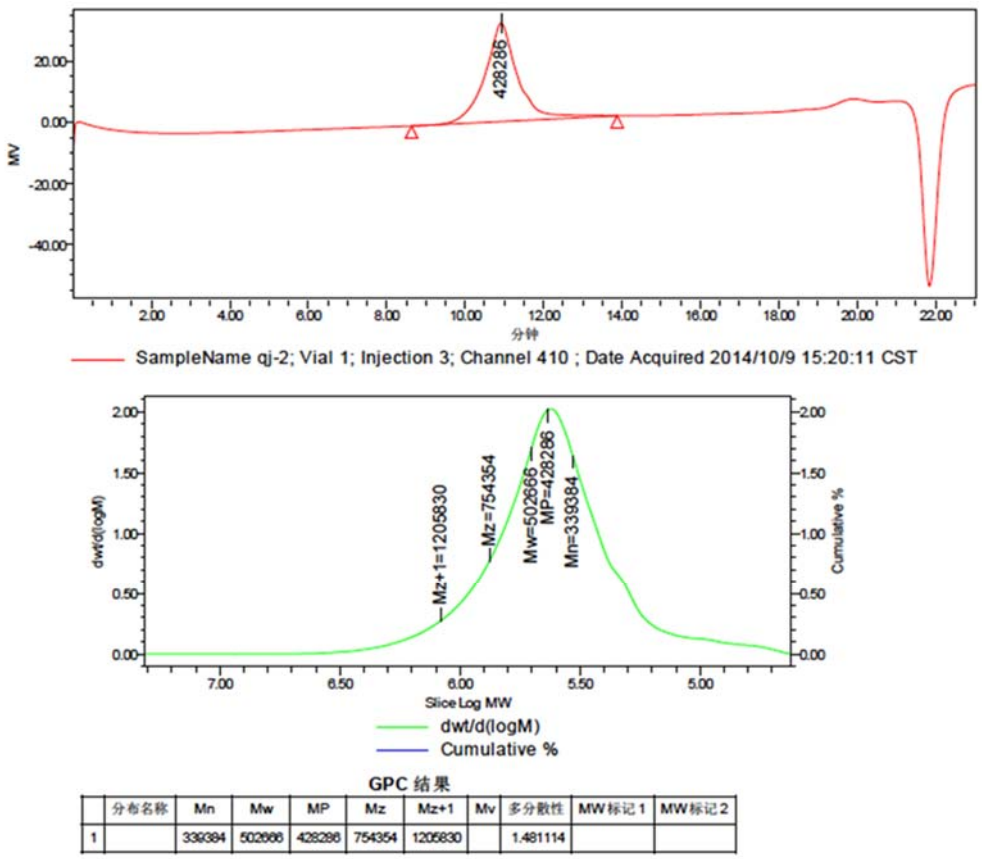

GPC 结果

	分布名称	Mn	Mw	MP	Mz	Mz+1	Mv	多分散性	MW标记 1	MW标记 2
1		339384	502666	428286	754354	1205830		1.481114		

Figure A.34 GPC result of polymer **2j**.

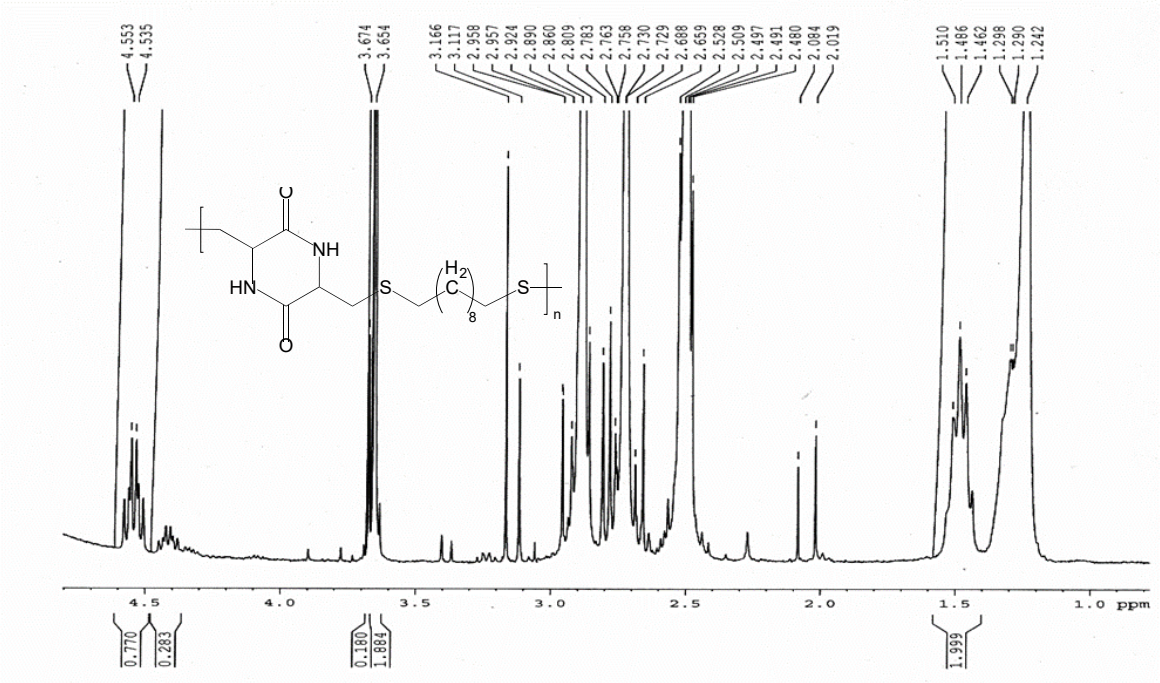

Figure A.35 ^{1}H NMR ((300 MHz, DMSO-d_6) spectrum of oligomer **2k**.

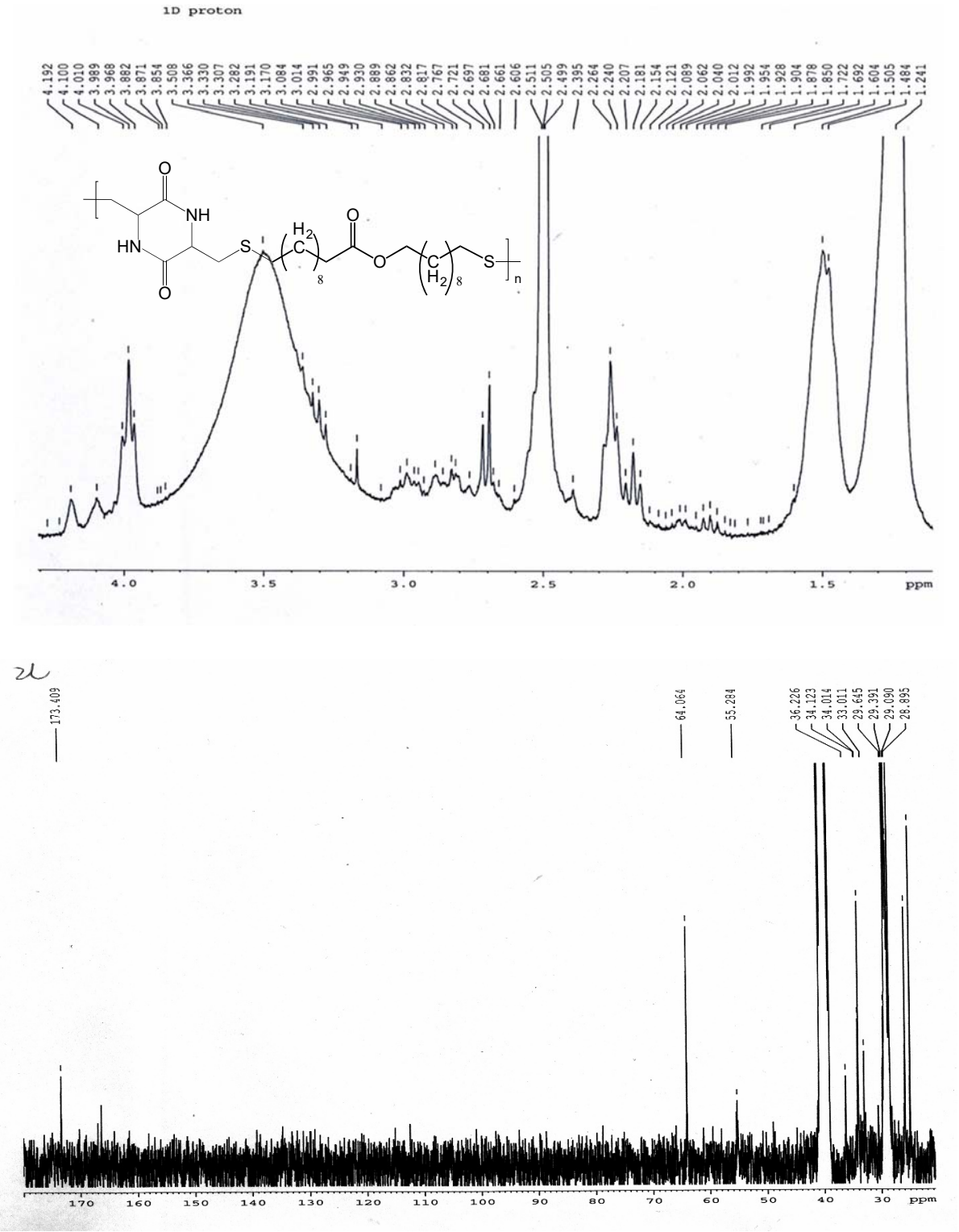

Figure A.36 ^{1}H NMR ((300 MHz, DMSO-d$_6$) and ^{13}C NMR (75 MHz, DMSO-d$_6$) spectra of polymer **2l.**

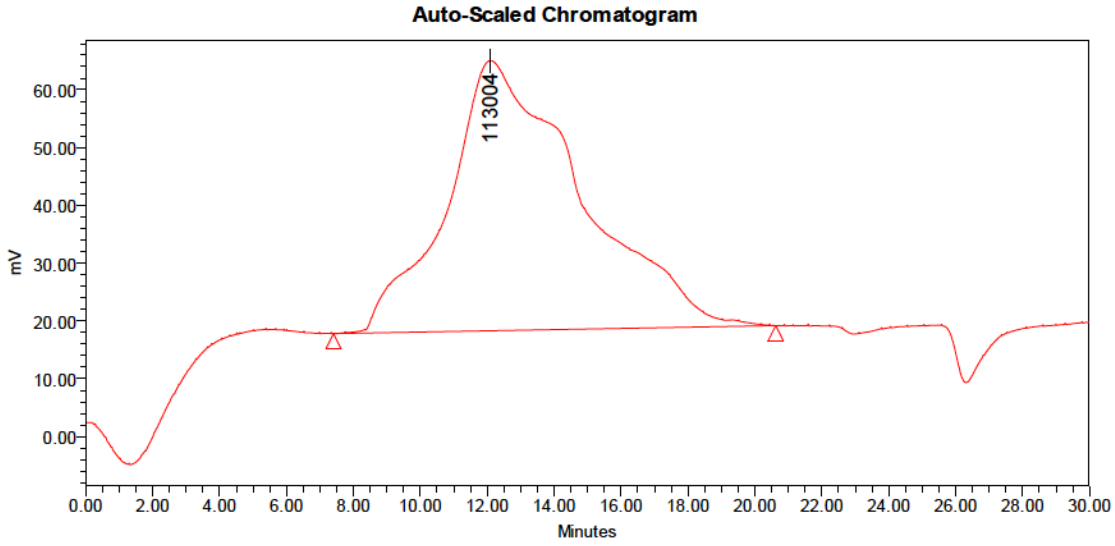

GPC Results

	Dist Name	Mn	Mw	MP	Mz	Mz+1	Mv	Poly dispersity	MW Marker 1	MW Marker 2
1		17811	92108	113004	235056	351076		5.171432		

Figure A.37 GPC trace of polymer **2l**.

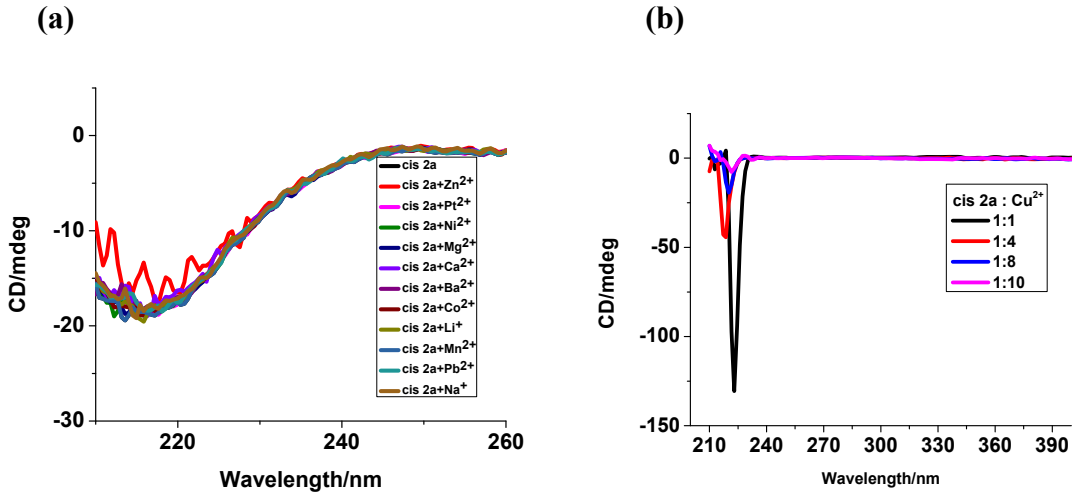

Figure A.38 CD spectra (a) upon addition of different metal ions: Zn^{2+}, Pd^{2+}, Ni^{2+}, Mg^{2+}, Ca^{2+}, Ba^{2+}, Co^{2+}, Li^{+}, Mn^{2+}, Pb^{2+} and Na^{+}, into cis-**2a** at 1:1 molar ratio; (b) upon addition of Cu^{2+} at different molar ratios.

APPENDIX B

Spectra of compounds and polymers in Chapter 3

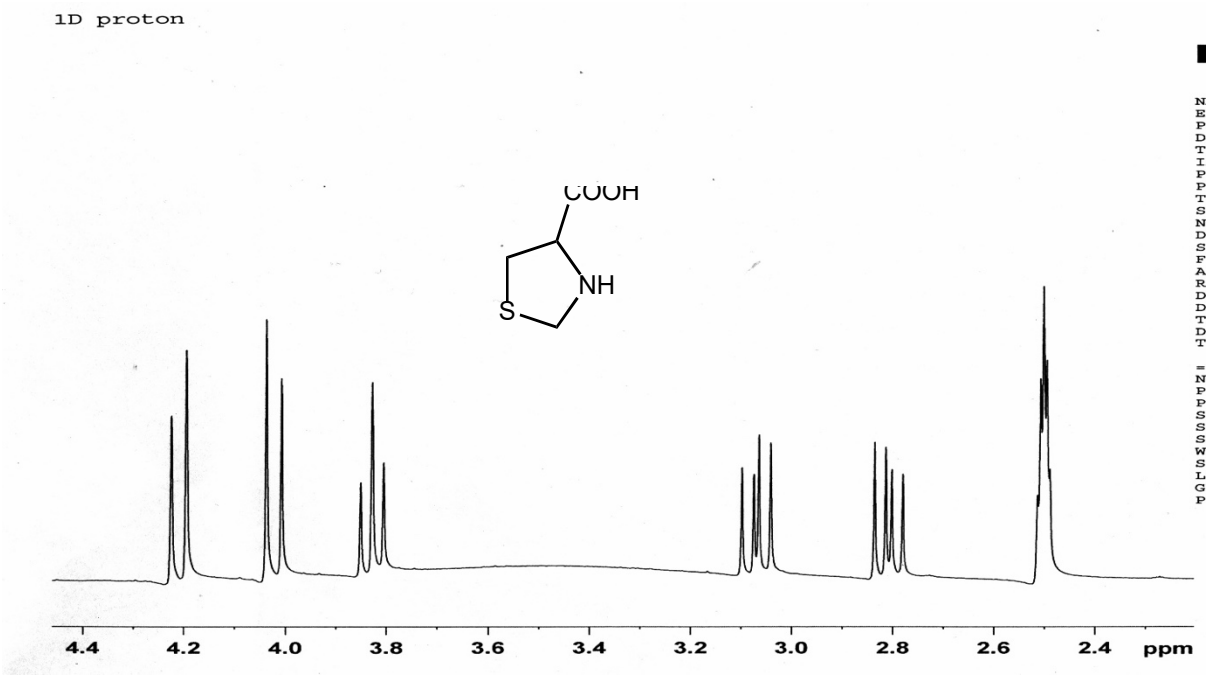

Figure B.1 ^{1}H NMR (300 MHz, DMSO-d_6) spectra of compound **1o.**

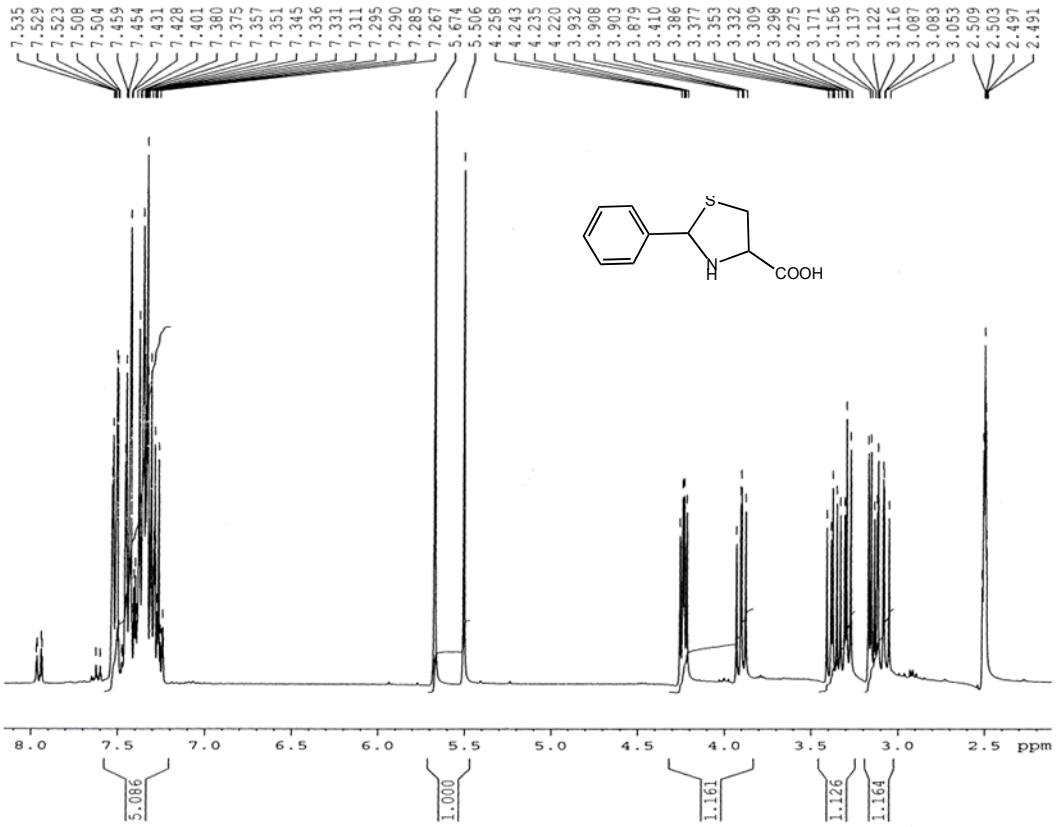

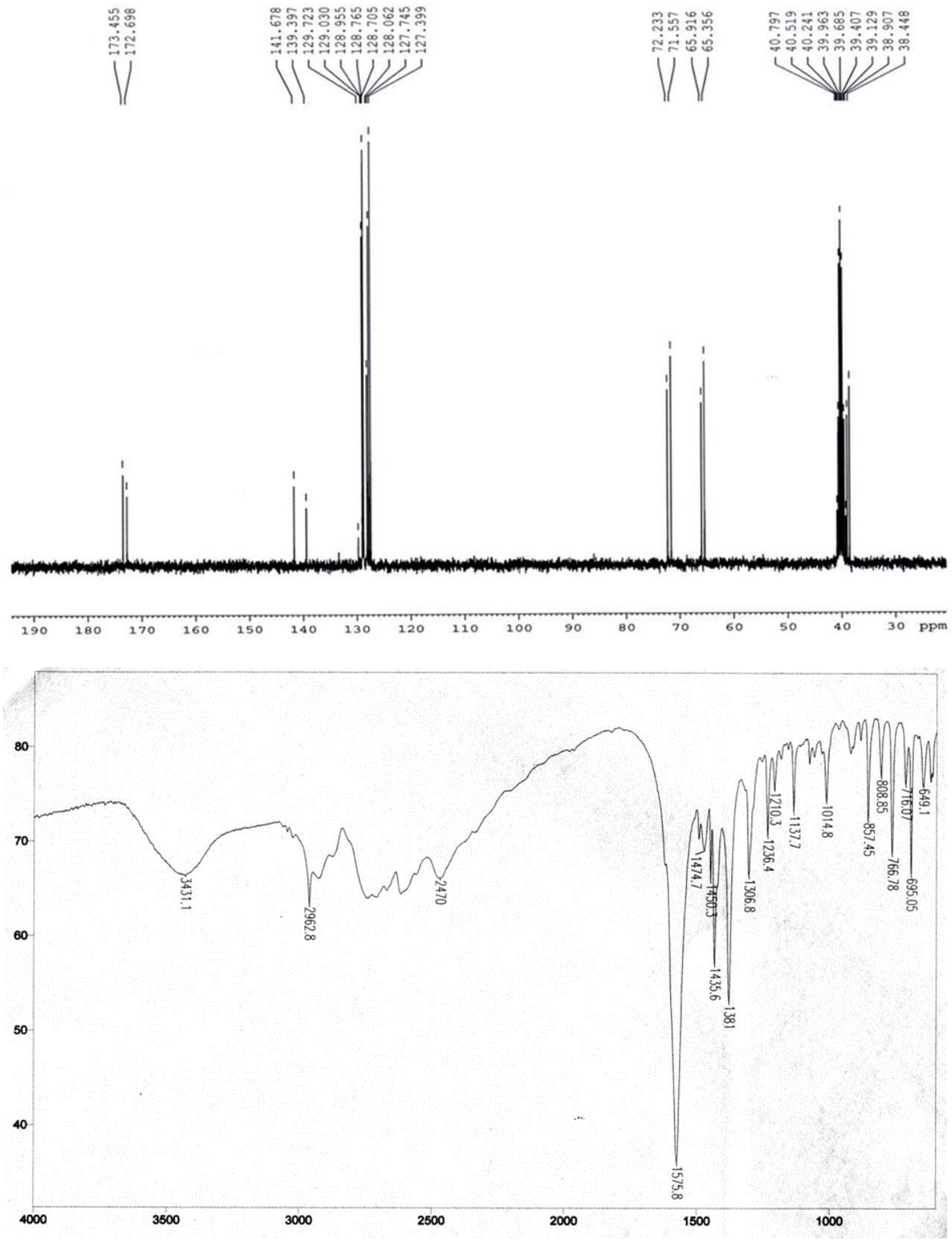

Figure B.2 ^{1}H NMR (300 MHz, DMSO-d_6+HCl), ^{13}C NMR (75 MHz, DMSO-d_6 + HCl) and IR spectra of compound **1p.**

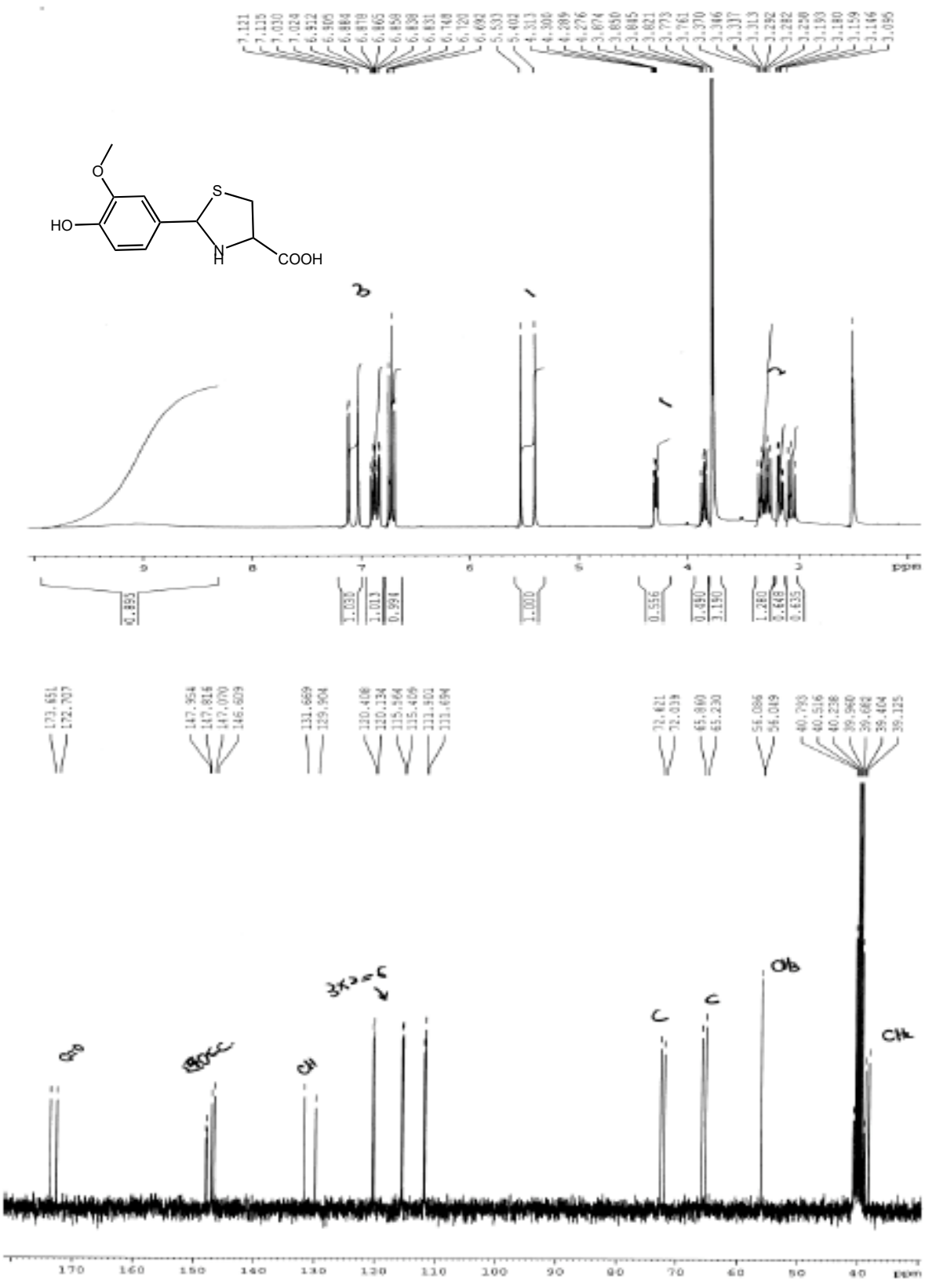

Figure B.3 ^{1}H NMR (300 MHz, DMSO-d_6) and ^{13}C NMR (75 MHz, DMSO-d_6 + HCl) spectra of compound **1q.**

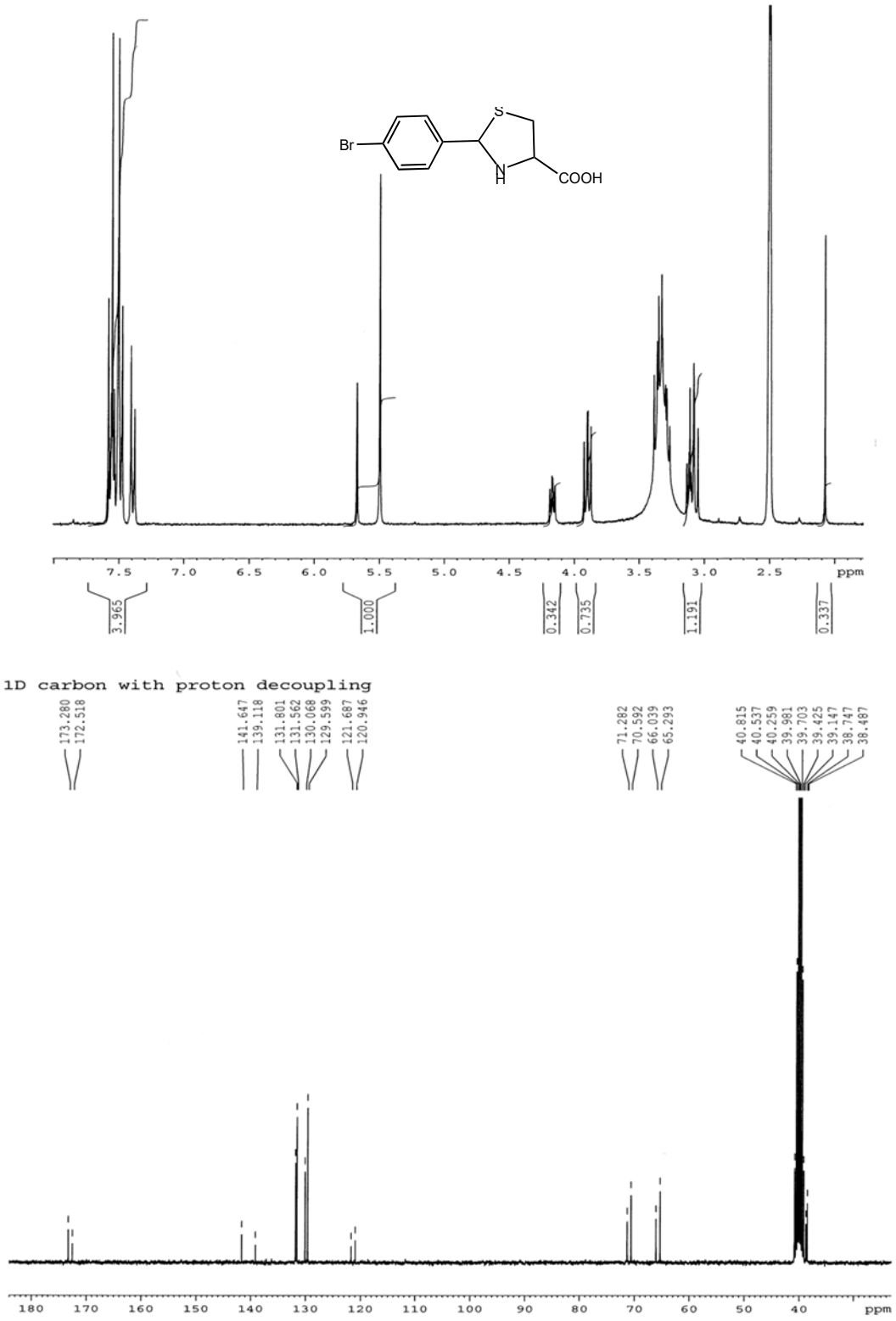

Figure B.4 ^{1}H NMR (300 MHz, DMSO-d_6 + HCl) and ^{13}C NMR (75 MHz, DMSO-d_6 + HCl) spectra of compound **1r.**

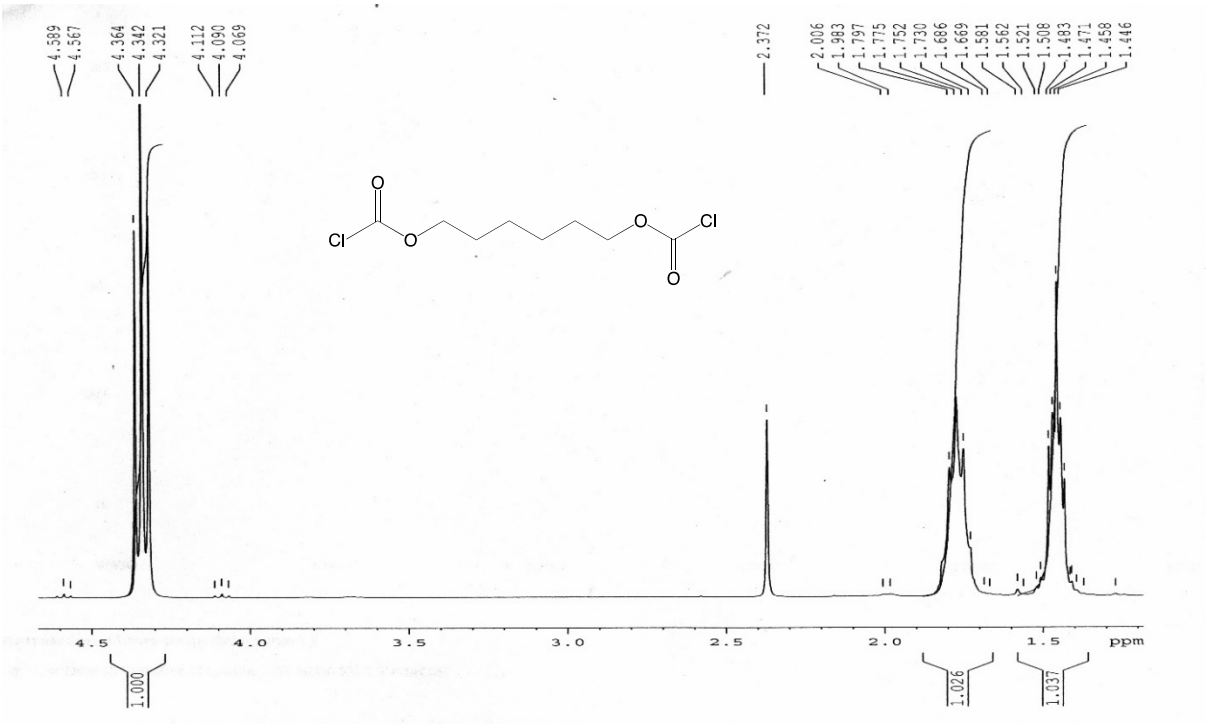

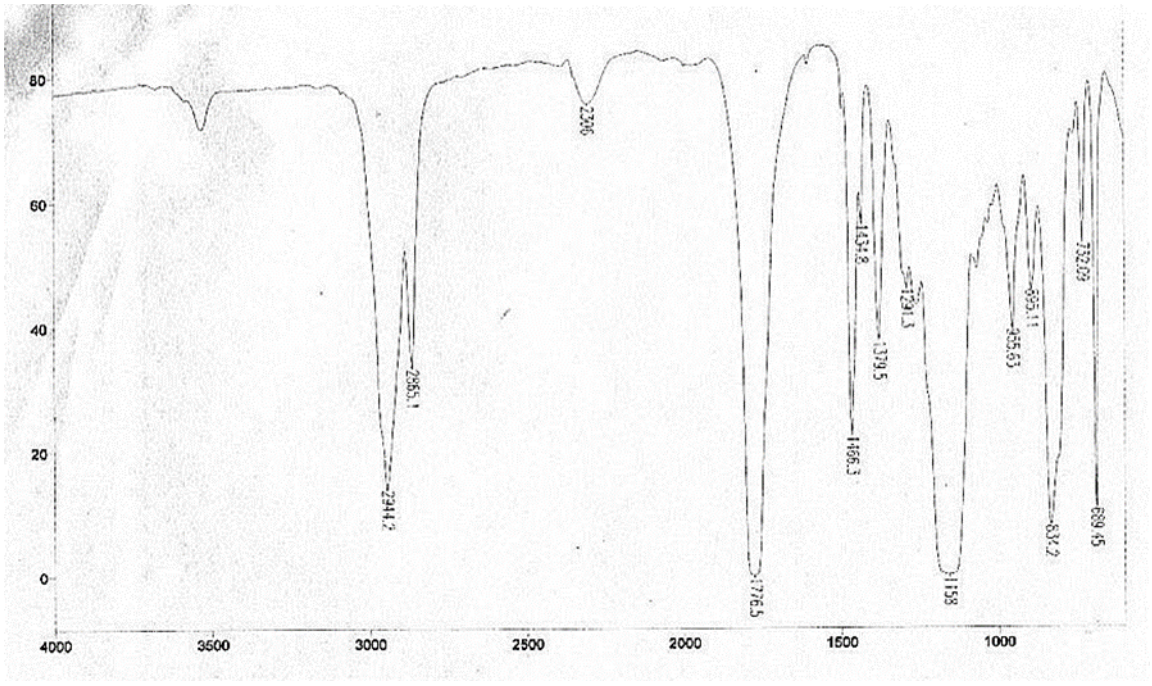

Figure B.5 ^{1}H NMR (300 MHz, $CDCl_3$) and IR spectra of compound **1s.**

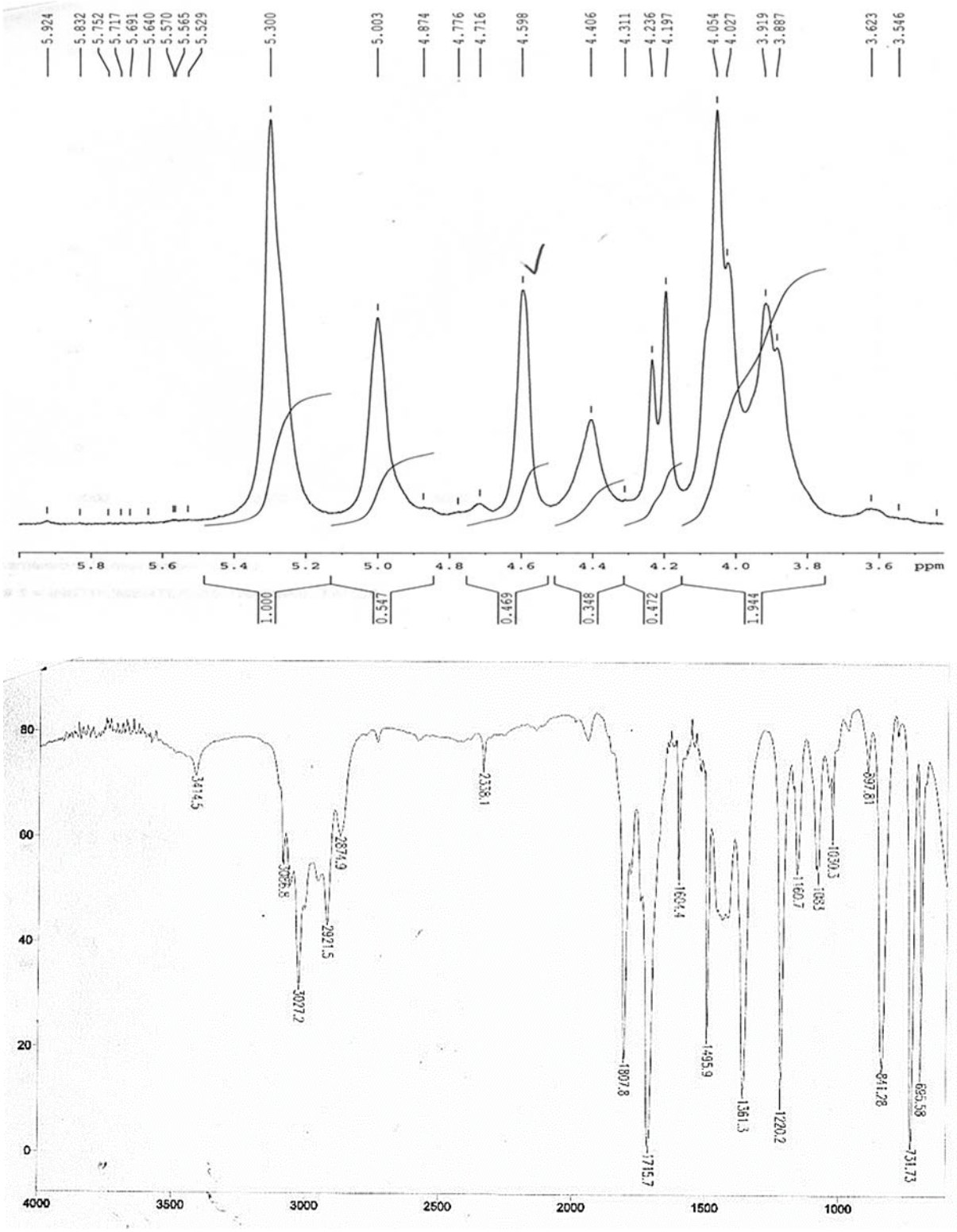

Figure B.6 ^{1}H NMR (300 MHz, $CDCl_3$) and IR spectra of compound **1t.**

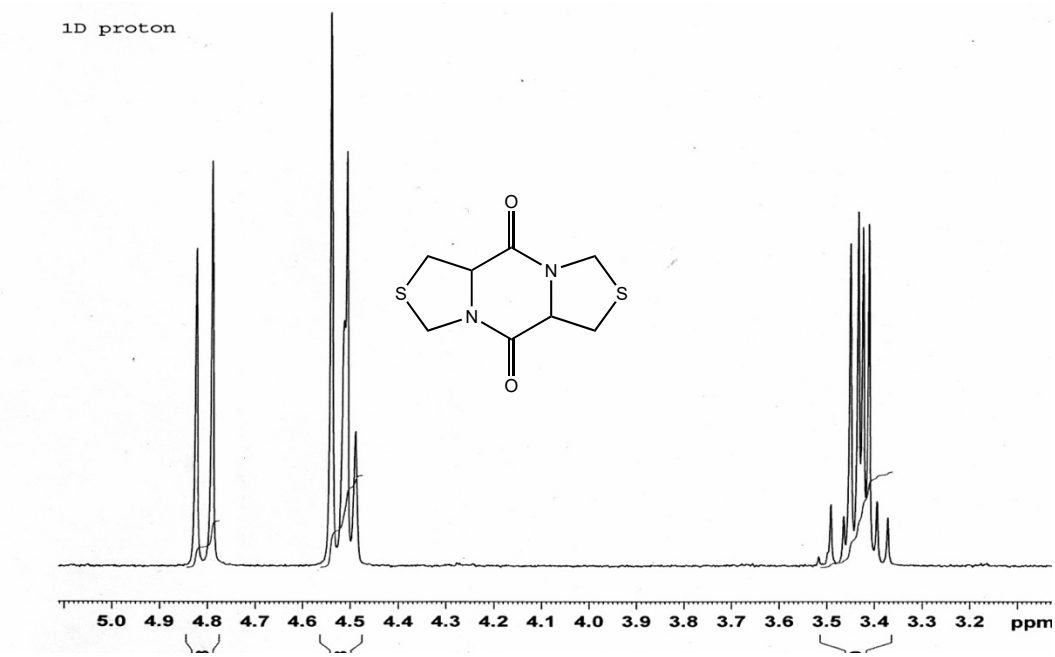

Figure B.7 ^{1}H NMR (300 MHz, $CDCl_3$) spectrum of compound **2o.**

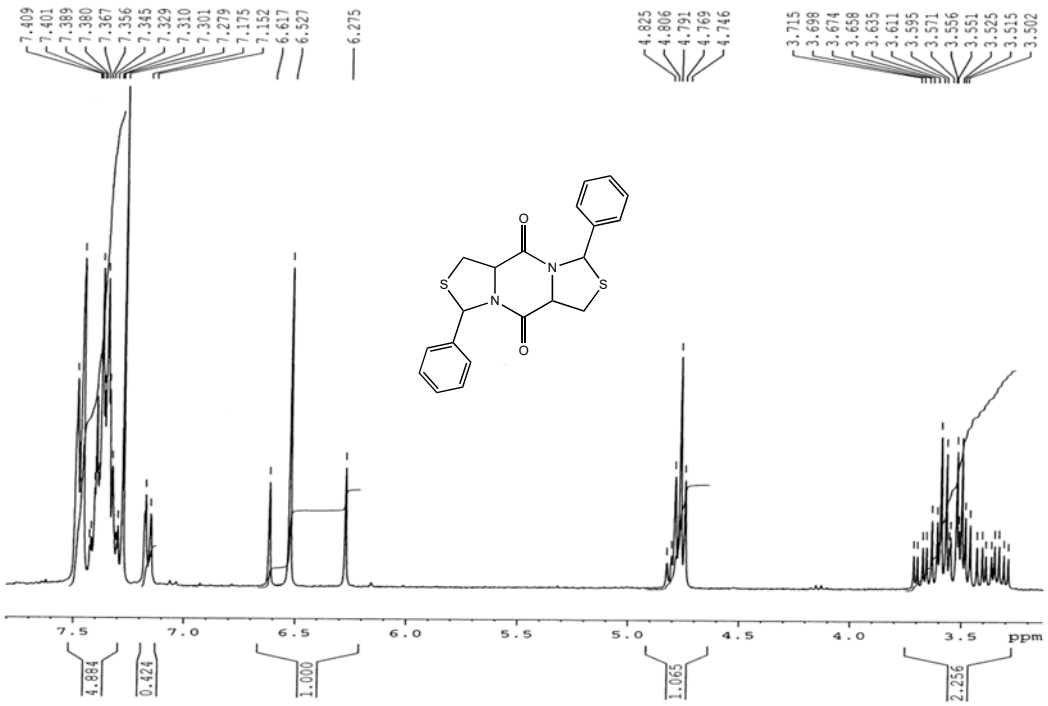

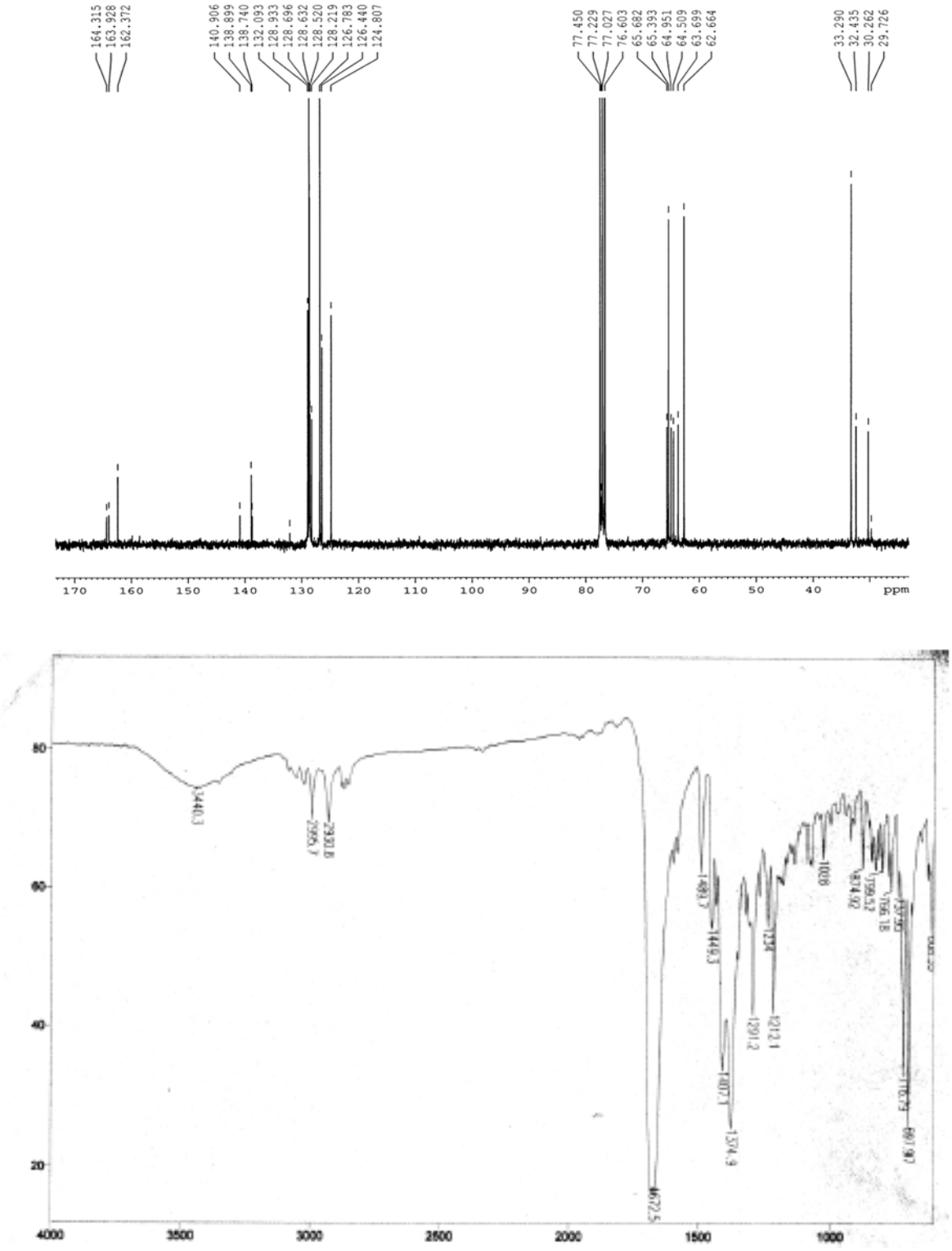

Figure B.8 ^{1}H NMR (300 MHz, $CDCl_3$), ^{13}C NMR (75 MHz, $CDCl_3$) and IR spectra of compound **2p.**

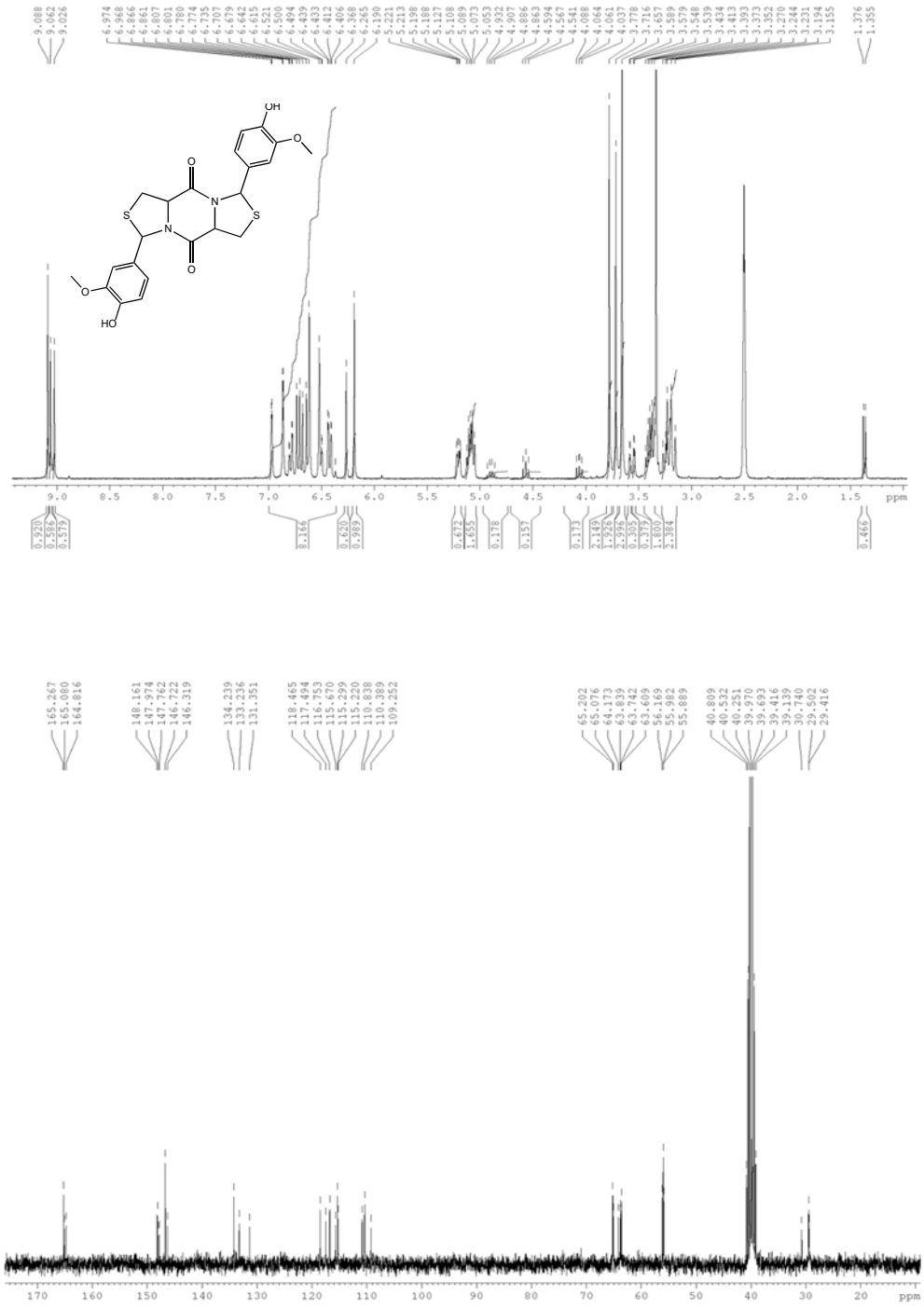

Figure B.9 ^{1}H NMR (300 MHz, DMSO-d$_6$) and ^{13}C NMR (75 MHz, DMSO-d$_6$) spectra of compound **2q.**

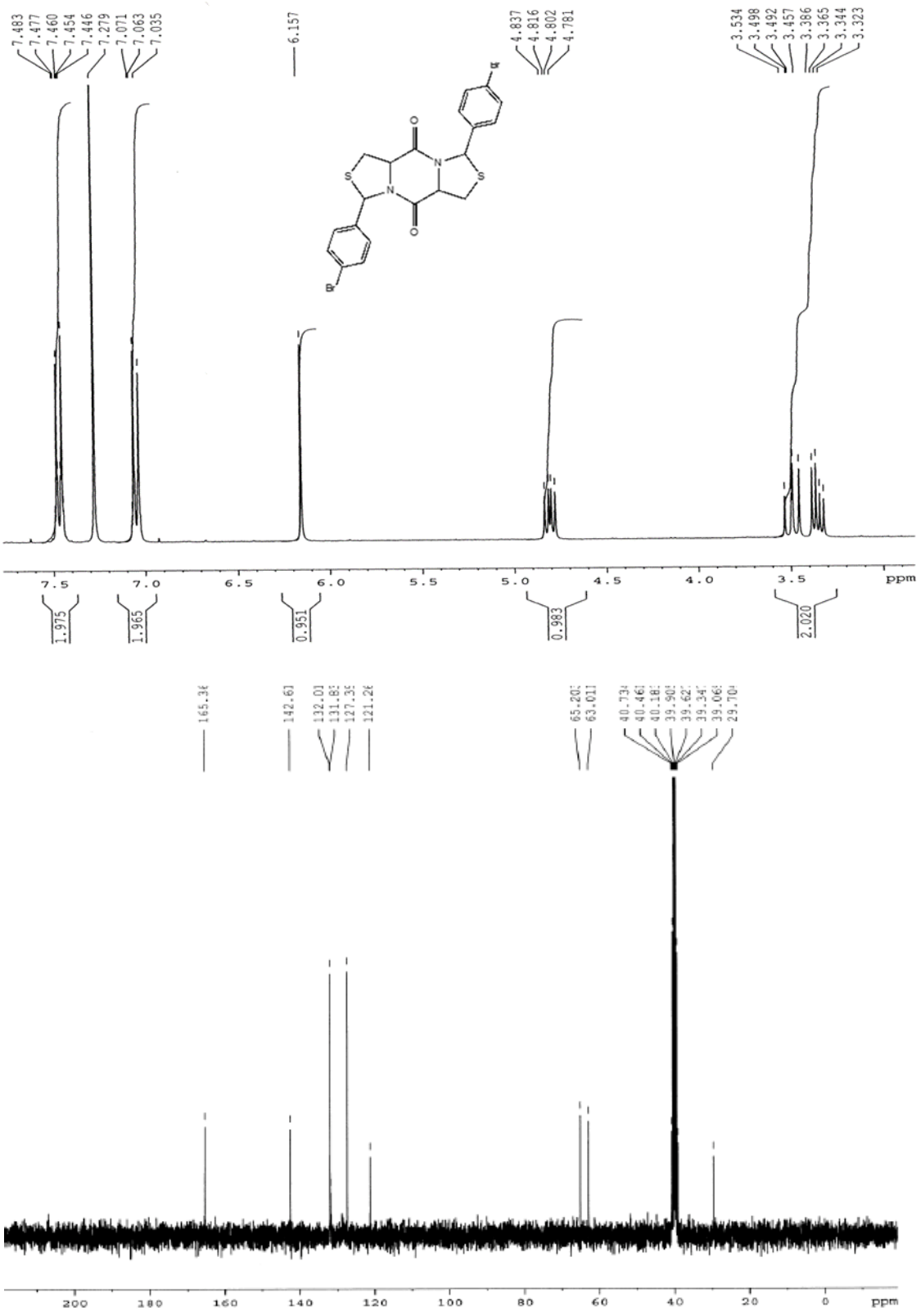

Figure B.10 ^{1}H NMR (300 MHz, $CDCl_3$) and ^{13}C NMR (75 MHz, $CDCl_3$) spectra of compound **2r.**

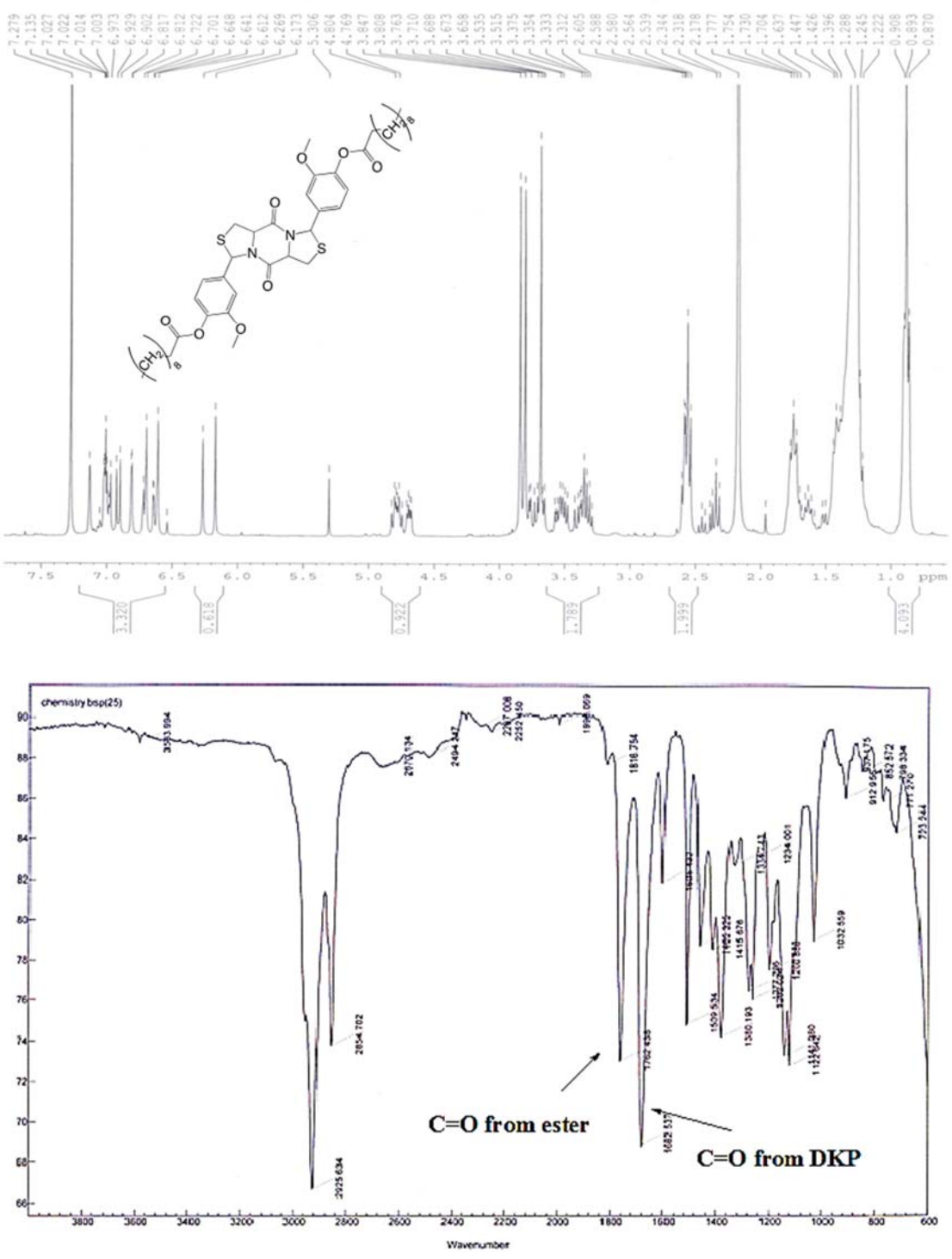

Figure B.11 ^{1}H NMR (300 MHz, $CDCl_3$) and IR spectra of compound **2u.**

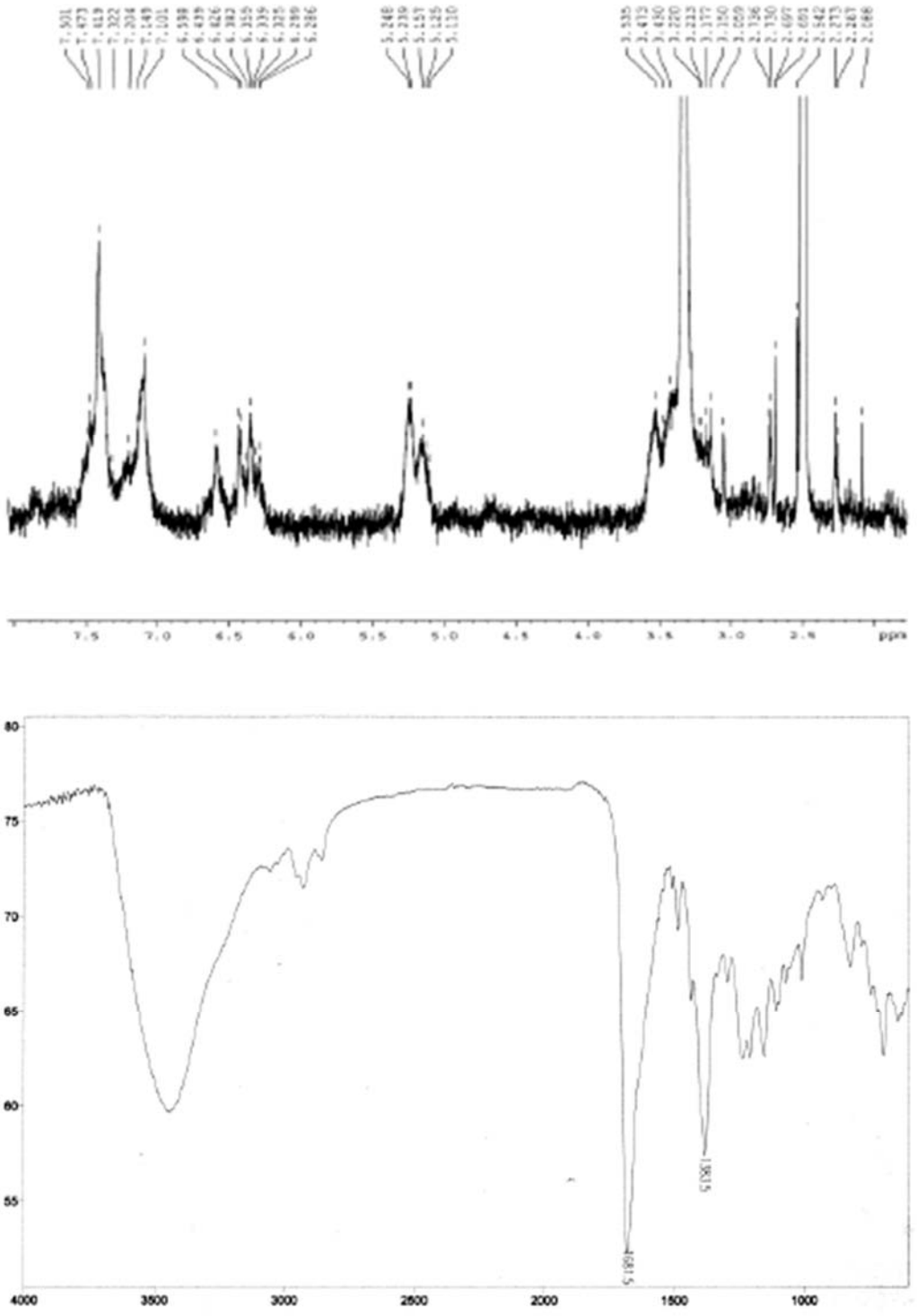

Figure B.12 ^{1}H NMR (300 MHz, DMSO-d_6) and IR spectra of polymer **P1.**

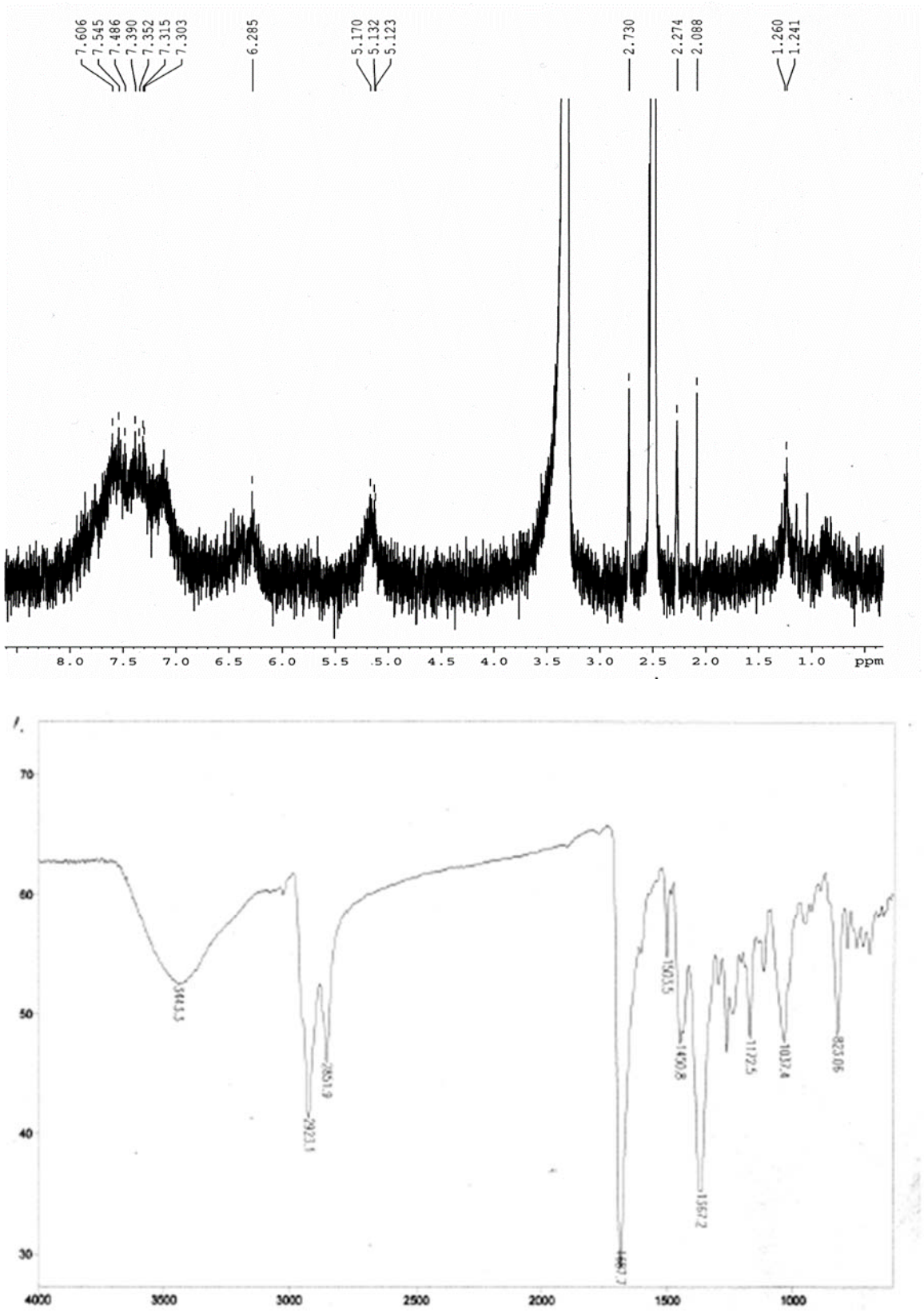

Figure B.13 ^{1}H NMR (300 MHz, DMSO-d_6) and IR spectra of polymer **P2.**

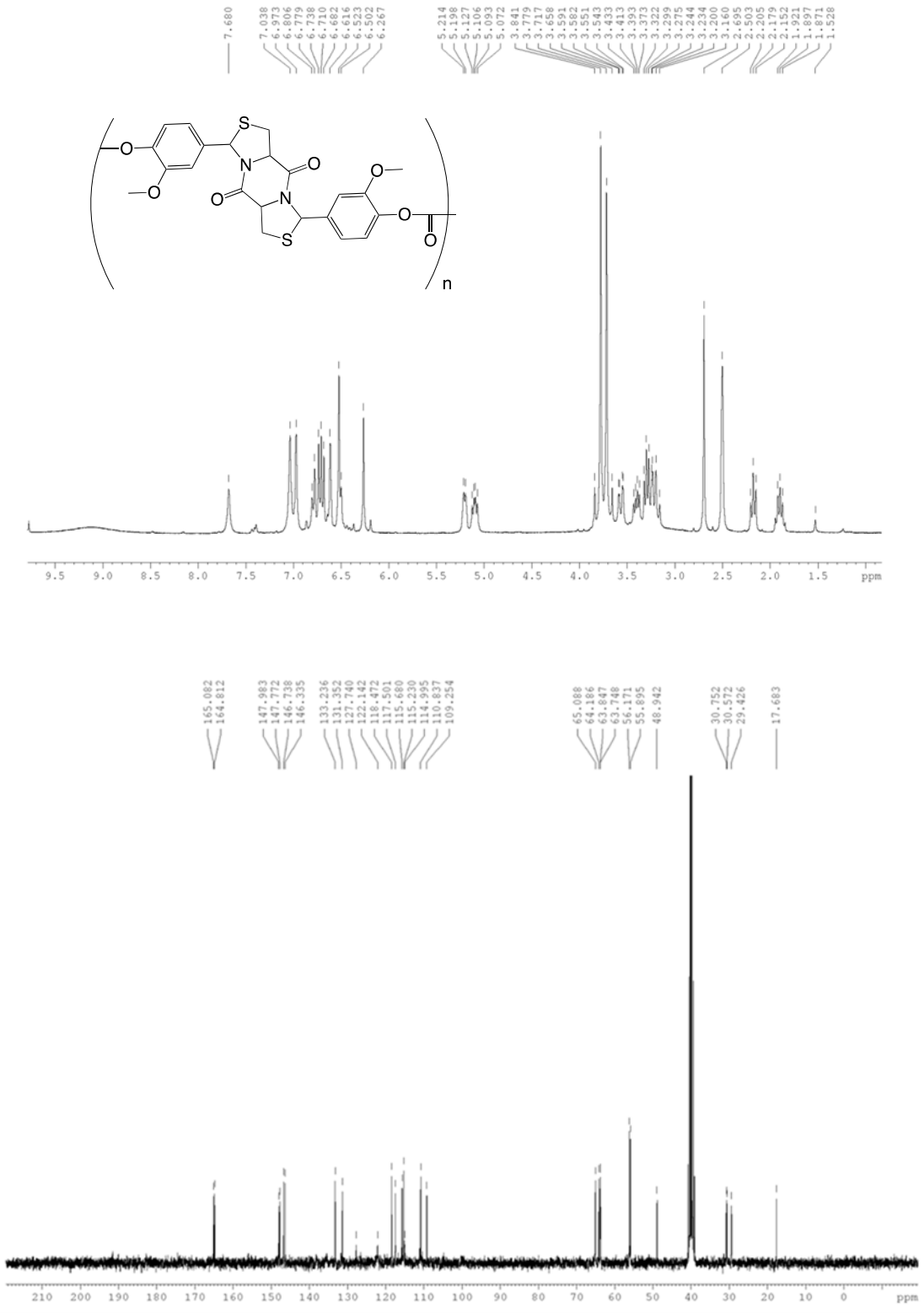

Figure B.14 ^{1}H NMR (300 MHz, DMSO-d_6) and and ^{13}C NMR (75 MHz, DMSO-d_6) spectra of polymer **P3.**

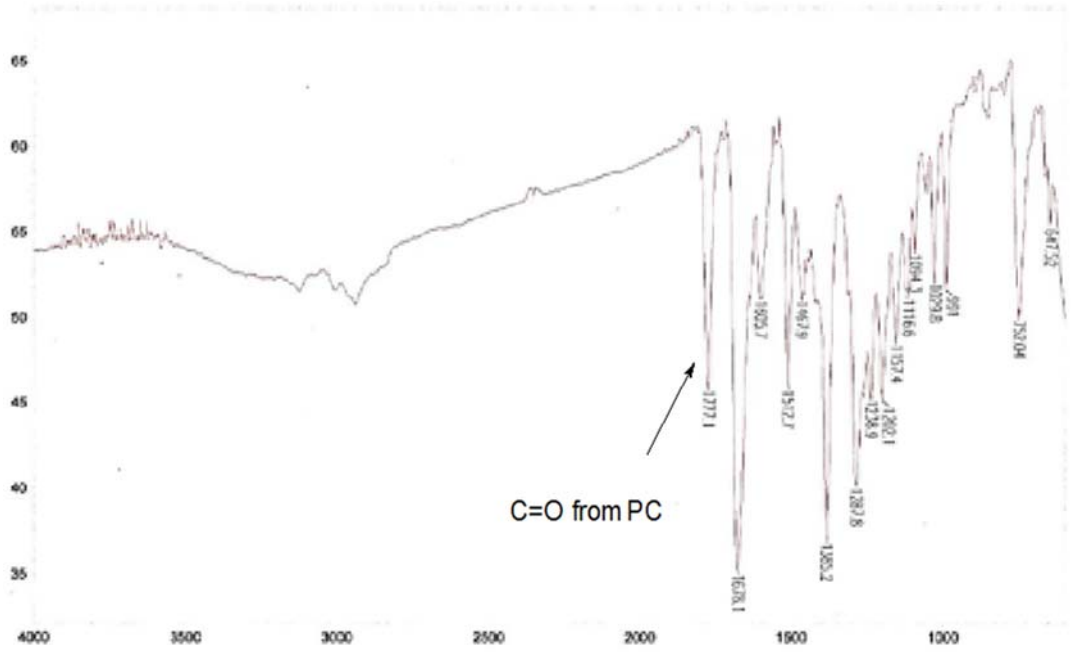

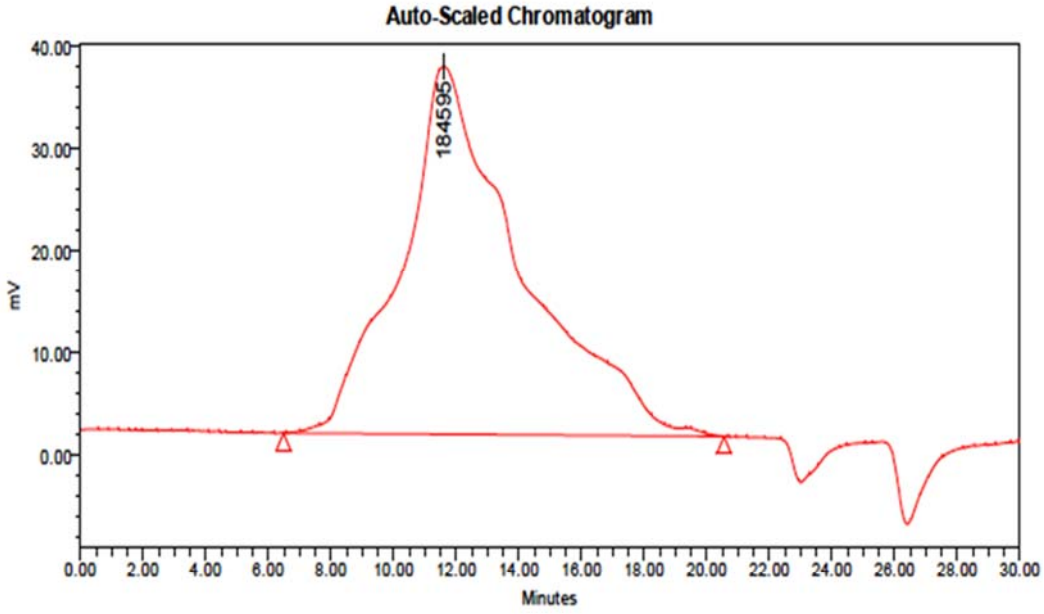

GPC Results

	Dist Name	Mn	Mw	MP	Mz	Mz+1	Mv	Polydispersity	MW Marker 1	MW Marker 2
1		20246	119604	184595	269322	368826		5.907466		

Figure B.15 IR spectrum and GPC result of polymer **P3.**

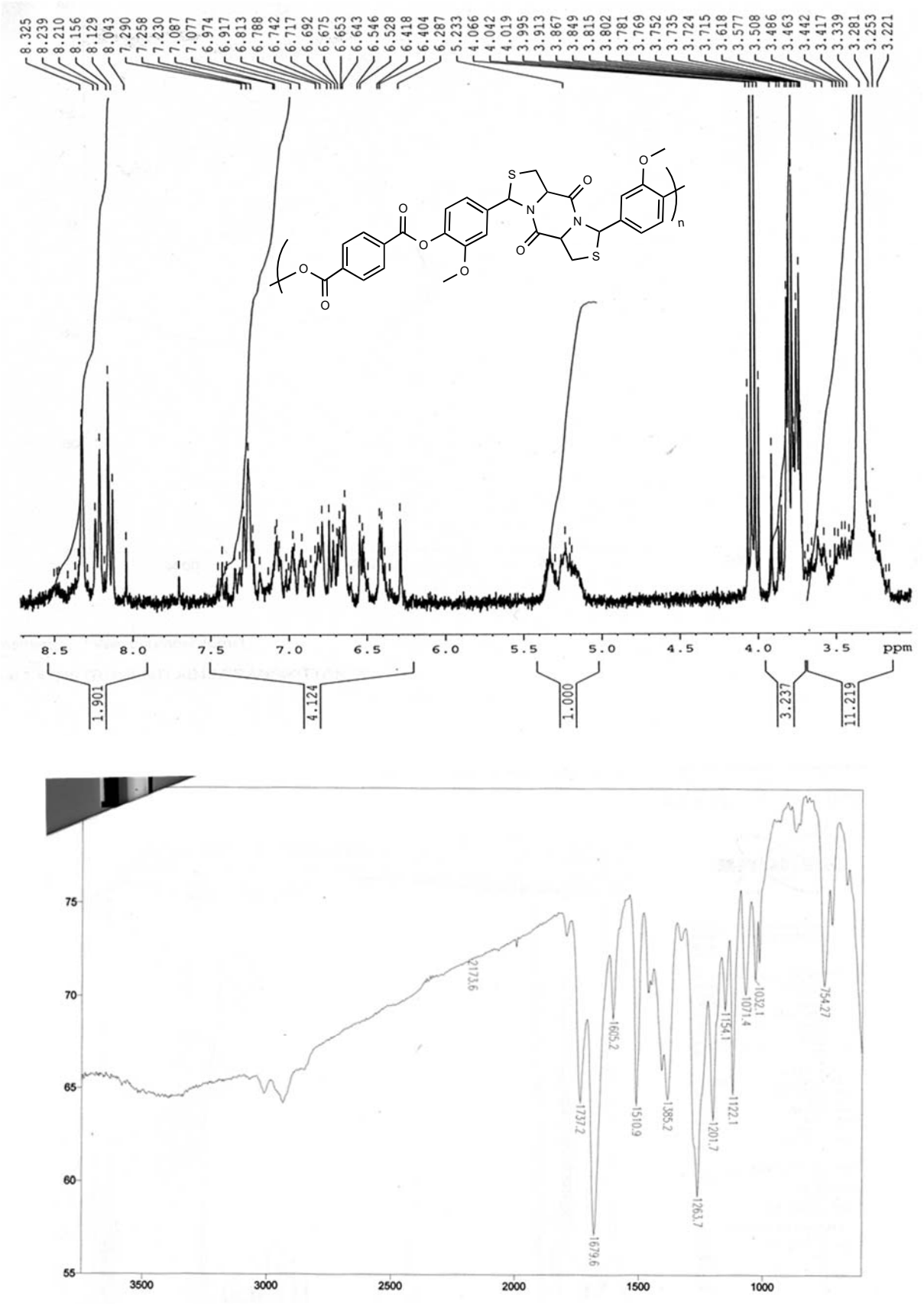

Figure B.16 ^{1}H NMR (300 MHz, DMSO-d$_6$) and IR spectra of polymer **P4.**

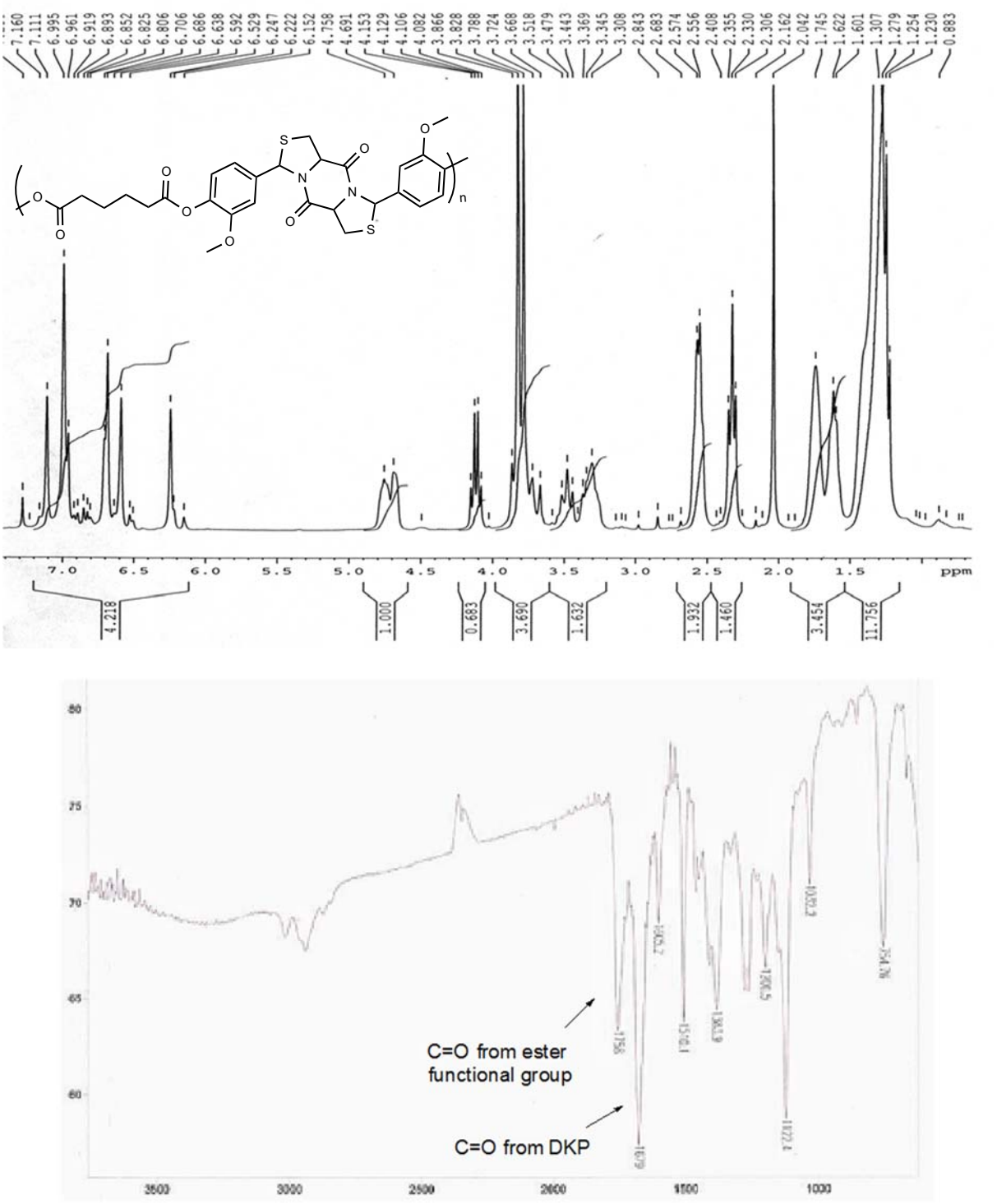

Figure B.17 ^{1}H NMR (300 MHz, $CDCl_3$) and IR spectra of polymer **P5.**

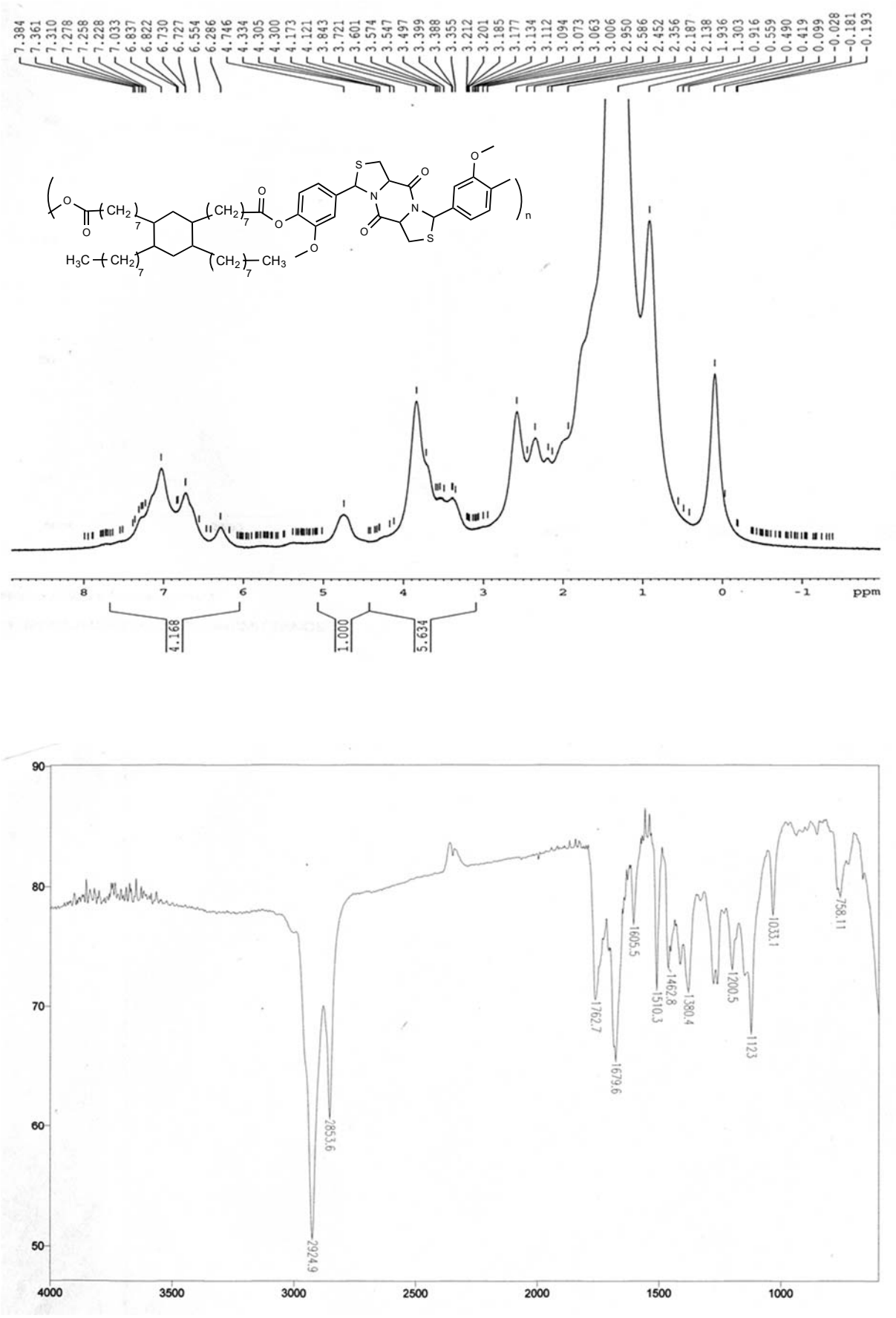

Figure B.18 ^{1}H NMR (300 MHz, $CDCl_3$) and IR spectra of polymer **P6.**

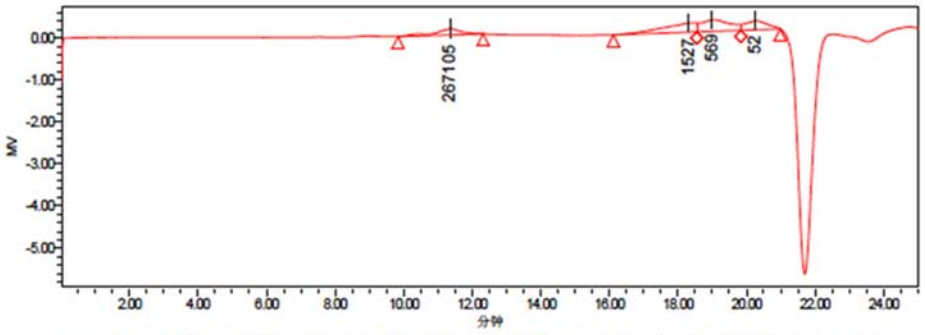

SampleName di-9; Vial 141; Injection 1; Channel 410 ; Date Acquired 2015/4/28 15:19:46 CST

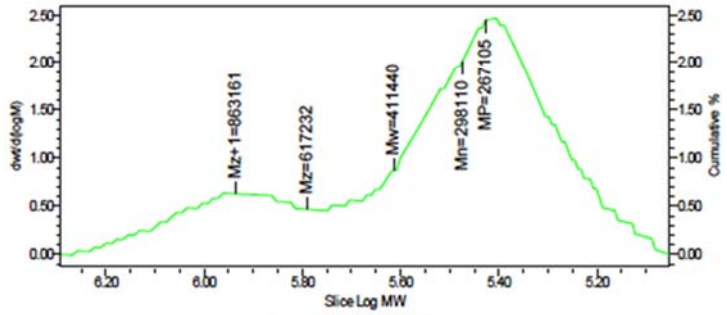

GPC 结果

	分布名称	Mn	Mw	MP	Mz	Mz+1	Mv	多分散性	MW标记 1	MW标记 2
1		298110	411440	267105	617232	863161		1.380162		
2				1527						
3				569						

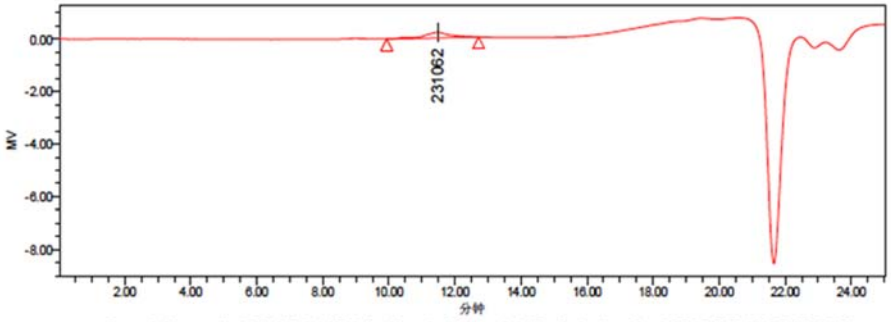

SampleName di-12-3; Vial 147; Injection 1; Channel 410 ; Date Acquired 2015/5/5 10:02:08 CST

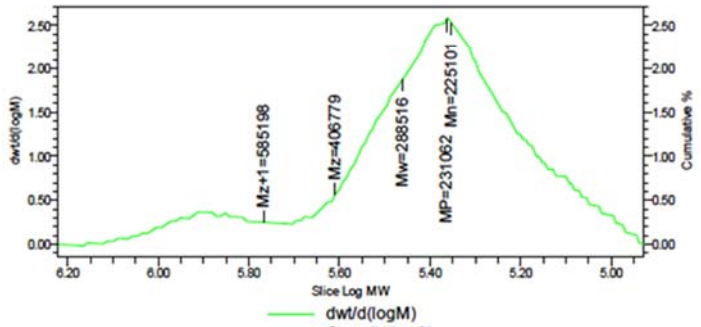

GPC 结果

	分布名称	Mn	Mw	MP	Mz	Mz+1	Mv	多分散性	MW标记 1	MW标记 2
1		225101	288516	231062	406779	585198		1.281717		

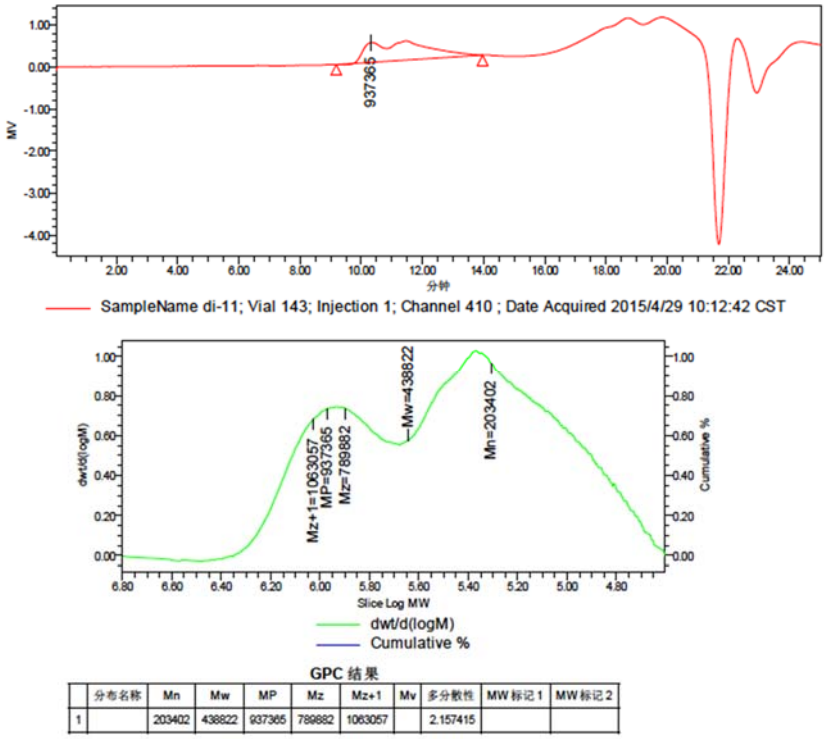

Figure B.19 GPC result of polymer **P4-P6.**

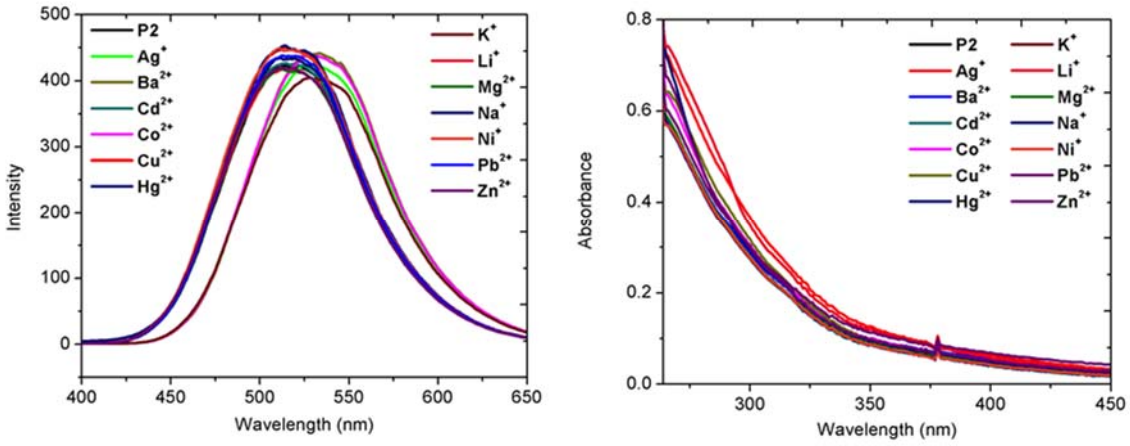

Figure B.20 (a) UV-vis absorption spectra of polymer **P2** with metal ions, (b) PL spectra of polymer **P2** with different metal ions.

APPENDIX C

Spectra of compounds and polymers in Chapter 4

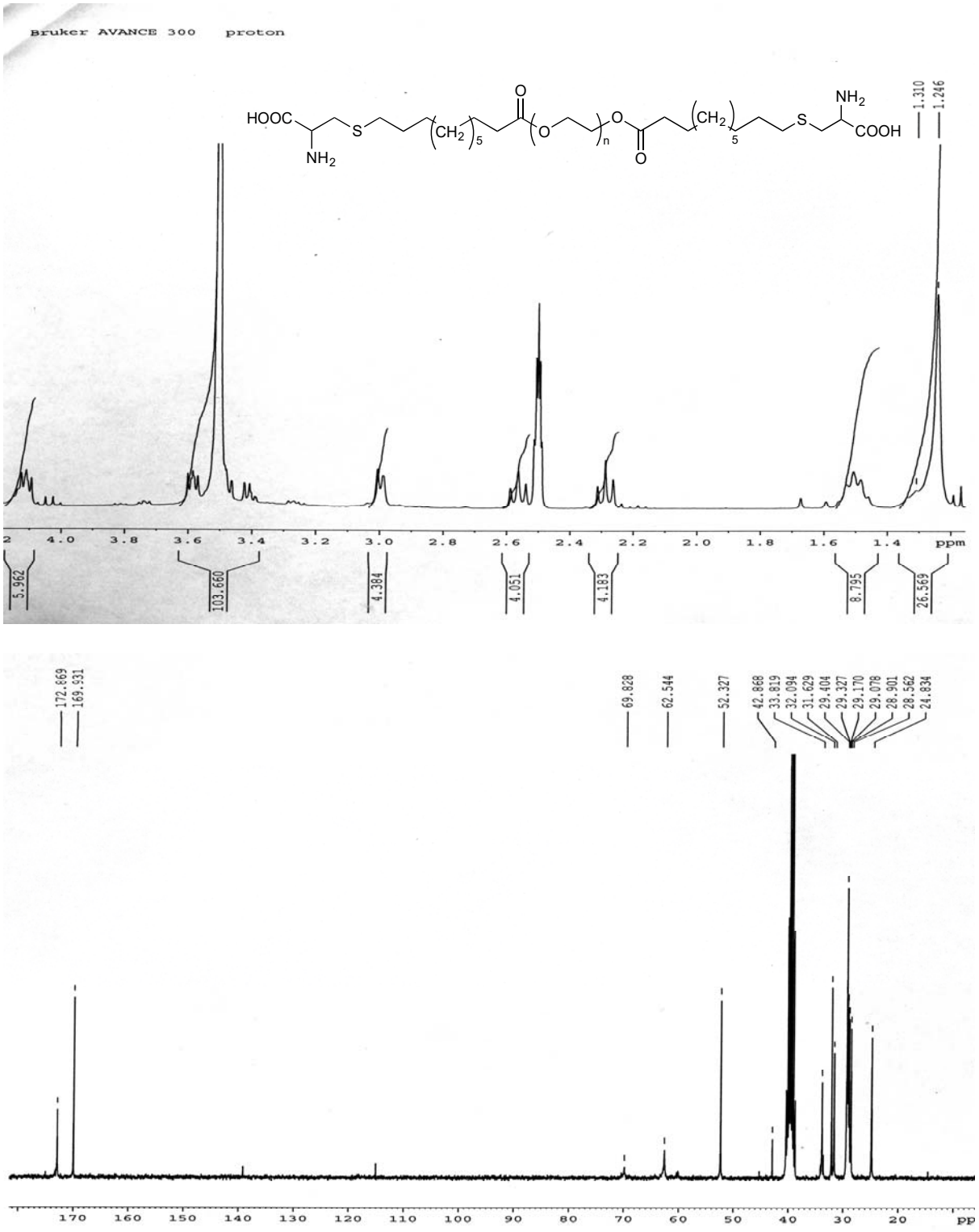

Figure C.1 ^{1}H NMR (300 MHz, DMSO-d_6) and ^{13}C NMR (75 MHz, DMSO-d_6) spectra of compound **Cys1**.

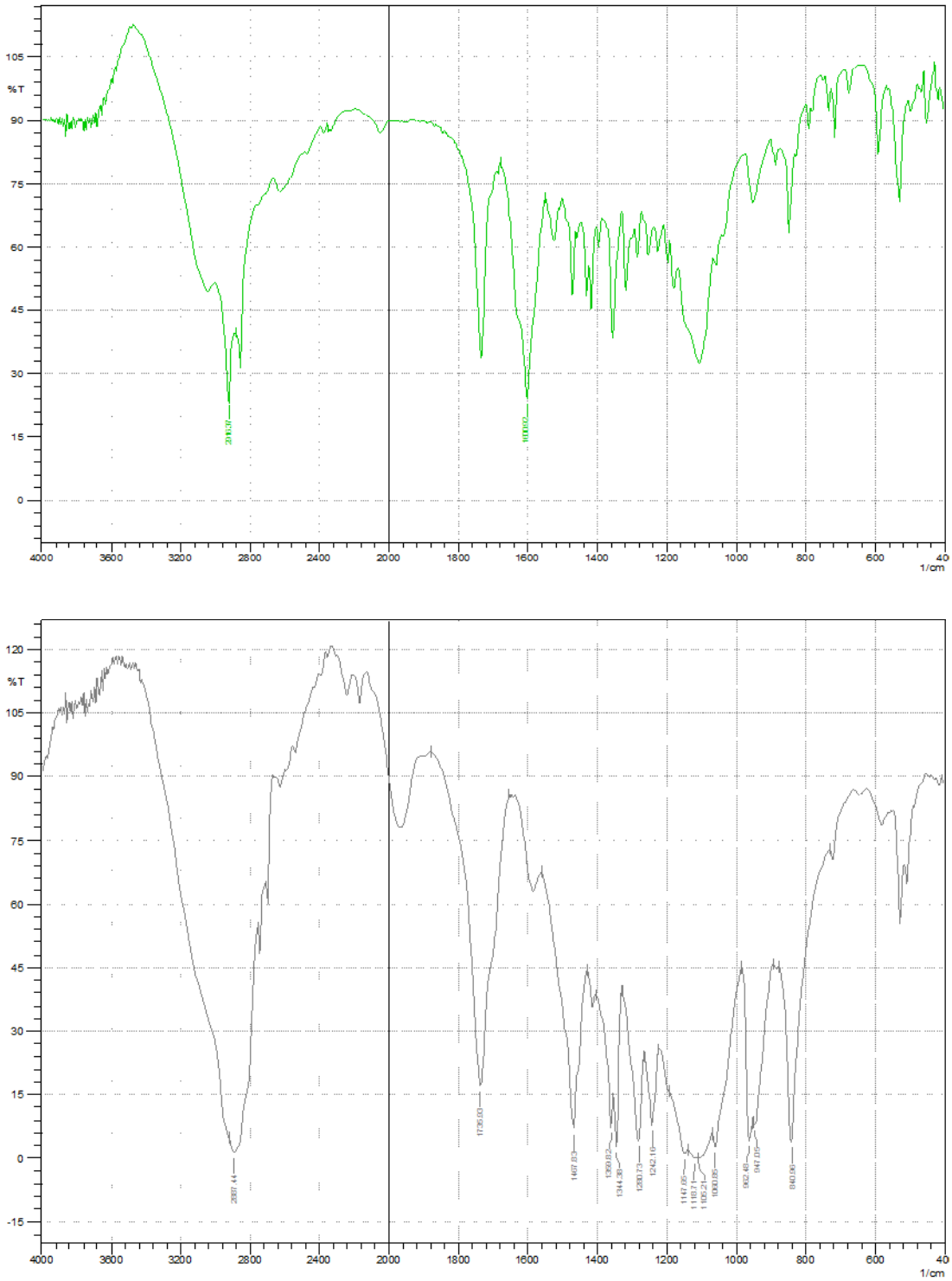

Figure C.2 IR spectra of compounds **Cys1** (top) and **Cys-2** (bottom).

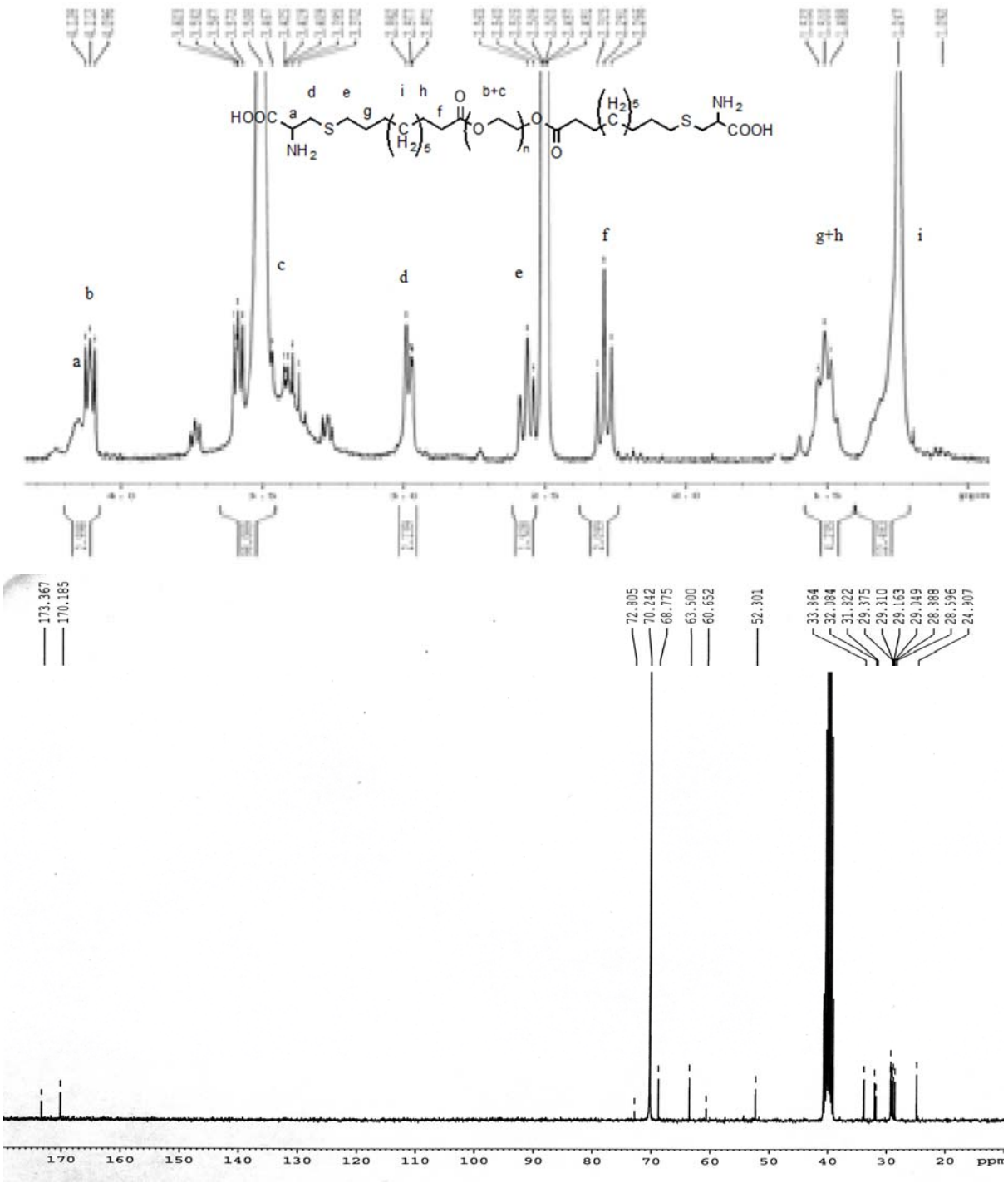

Figure C.3 ^{1}H NMR (300 MHz, DMSO-d$_6$) and ^{13}C NMR (75 MHz, DMSO-d$_6$) spectra of compound **Cys2.**

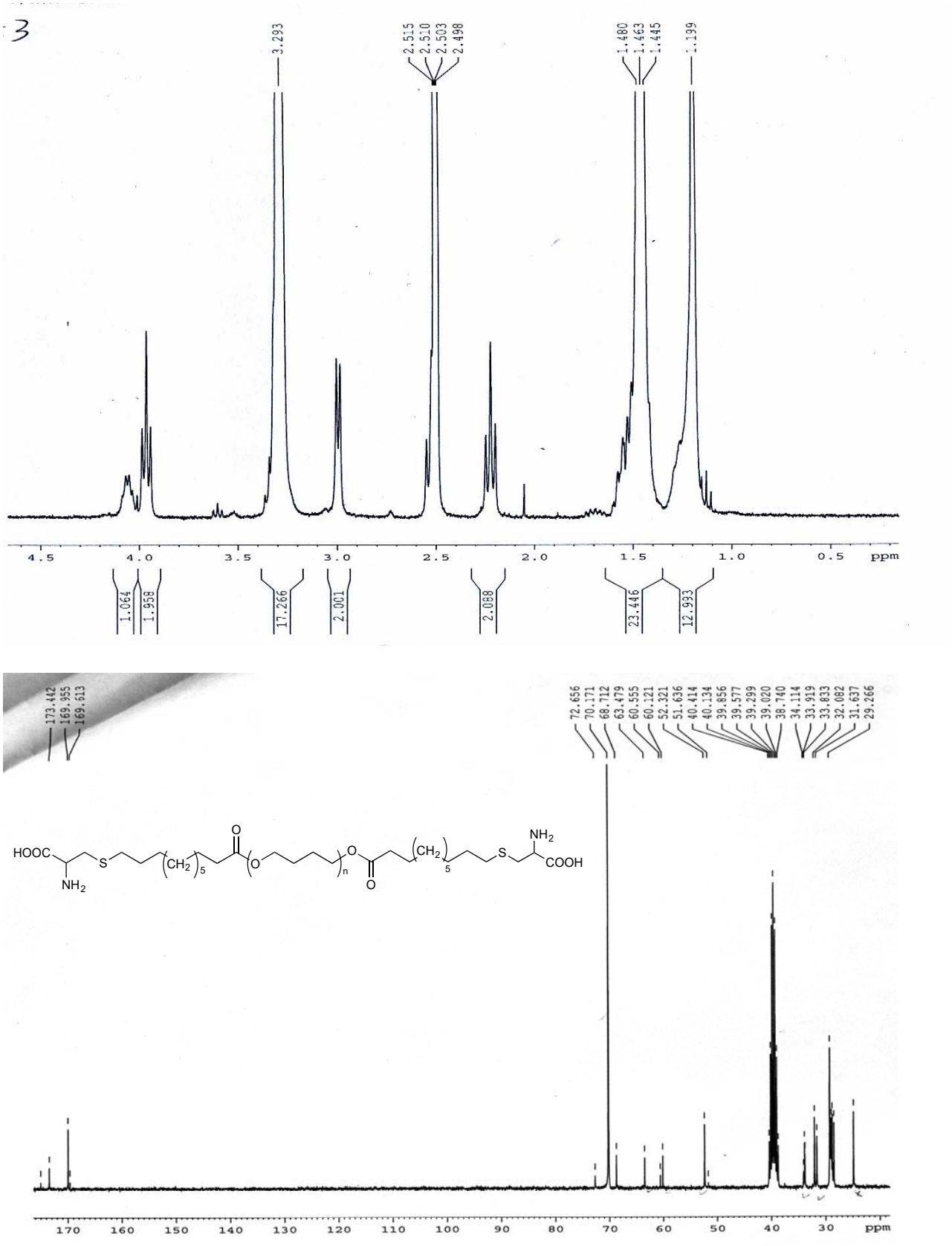

Figure C.4 ^{1}H NMR (300 MHz, DMSO-d_6) and ^{13}C NMR (75 MHz, DMSO-d_6) spectra of compound **Cys3.**

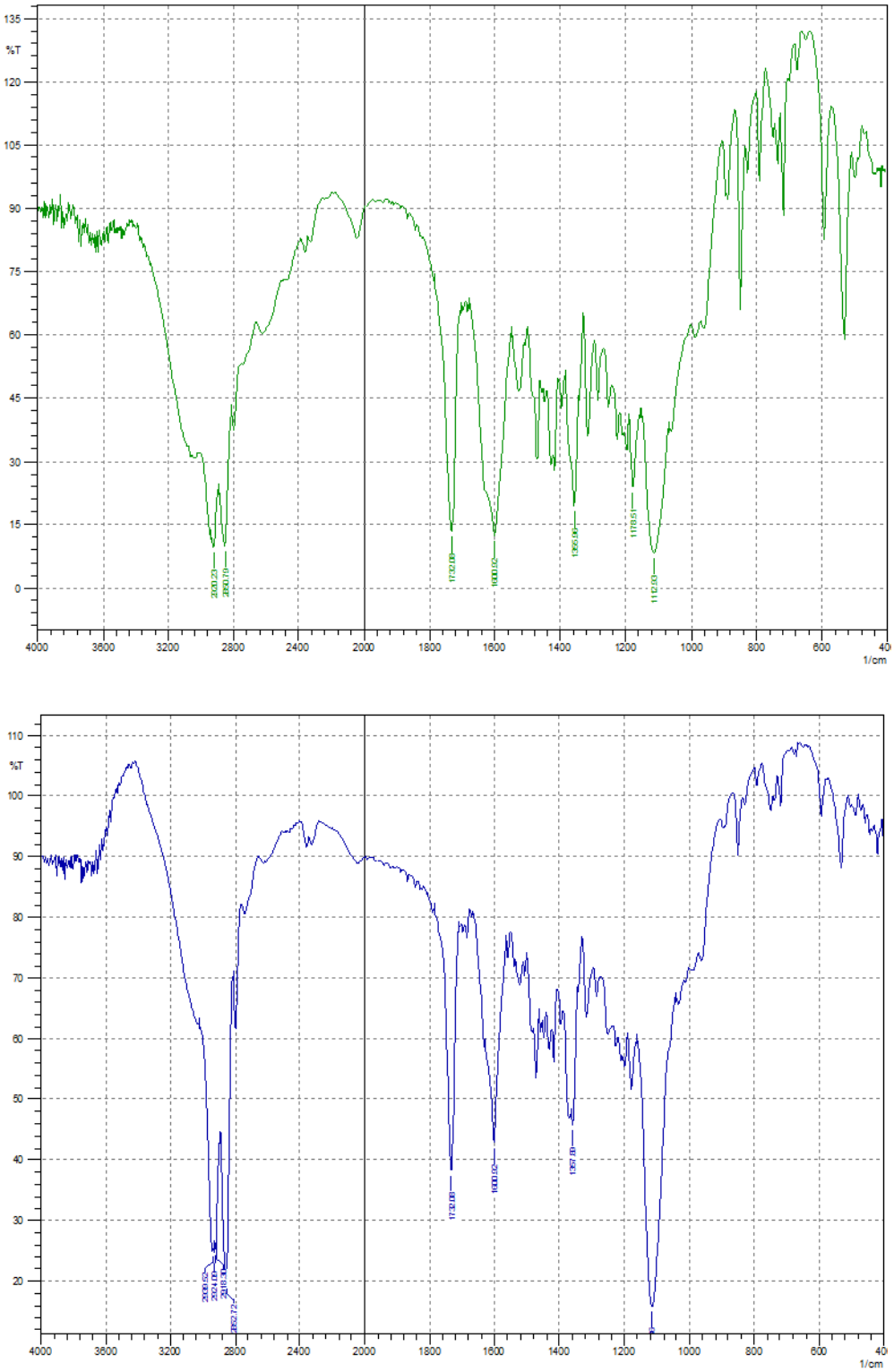

Figure C.5 IR spectra of compound **Cys3** (top) and **Cys4** (bottom).

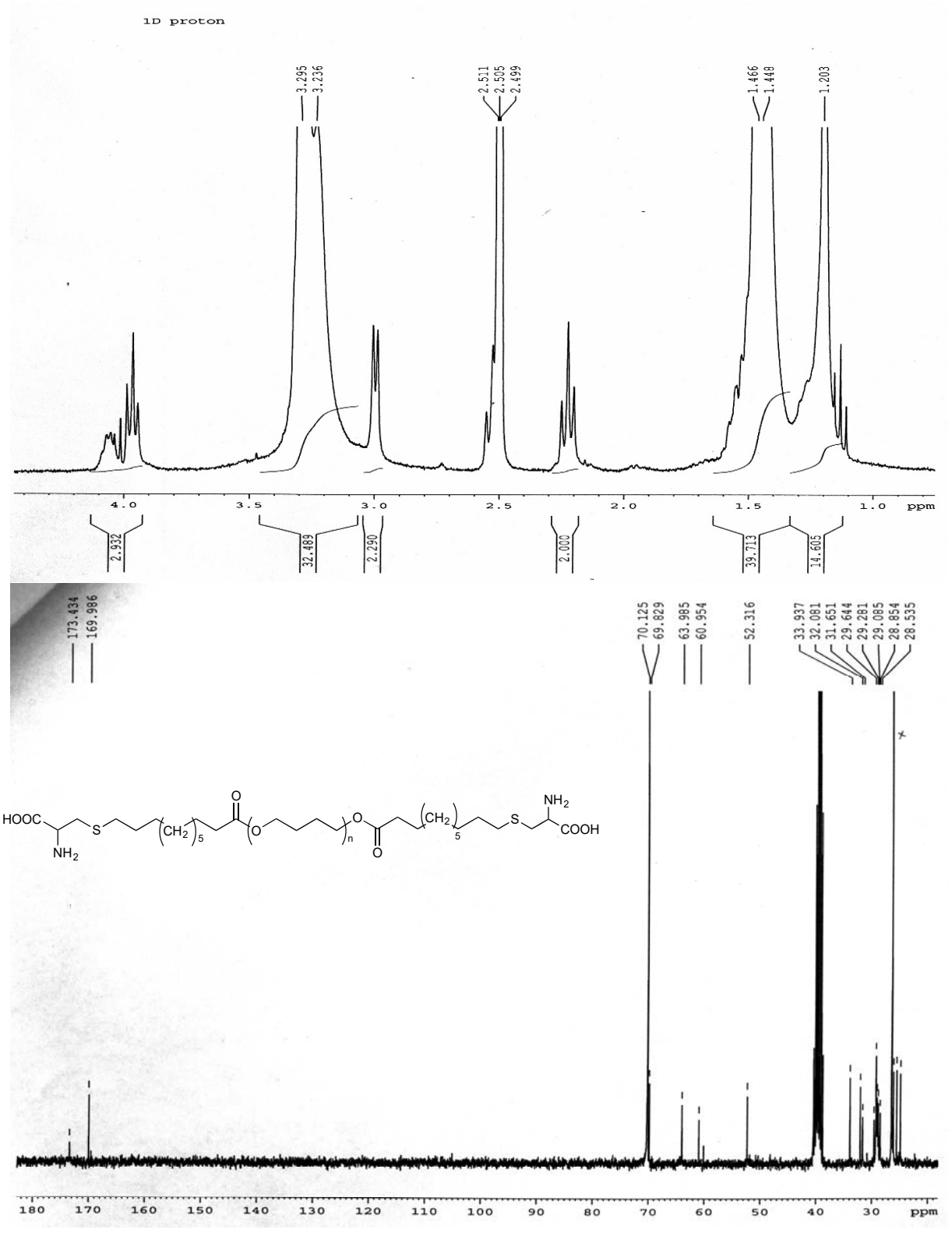

Figure C.6 ^{1}H NMR (300 MHz, DMSO-d$_6$) and ^{13}C NMR (75 MHz, DMSO-d$_6$) spectra of compound **Cys4.**

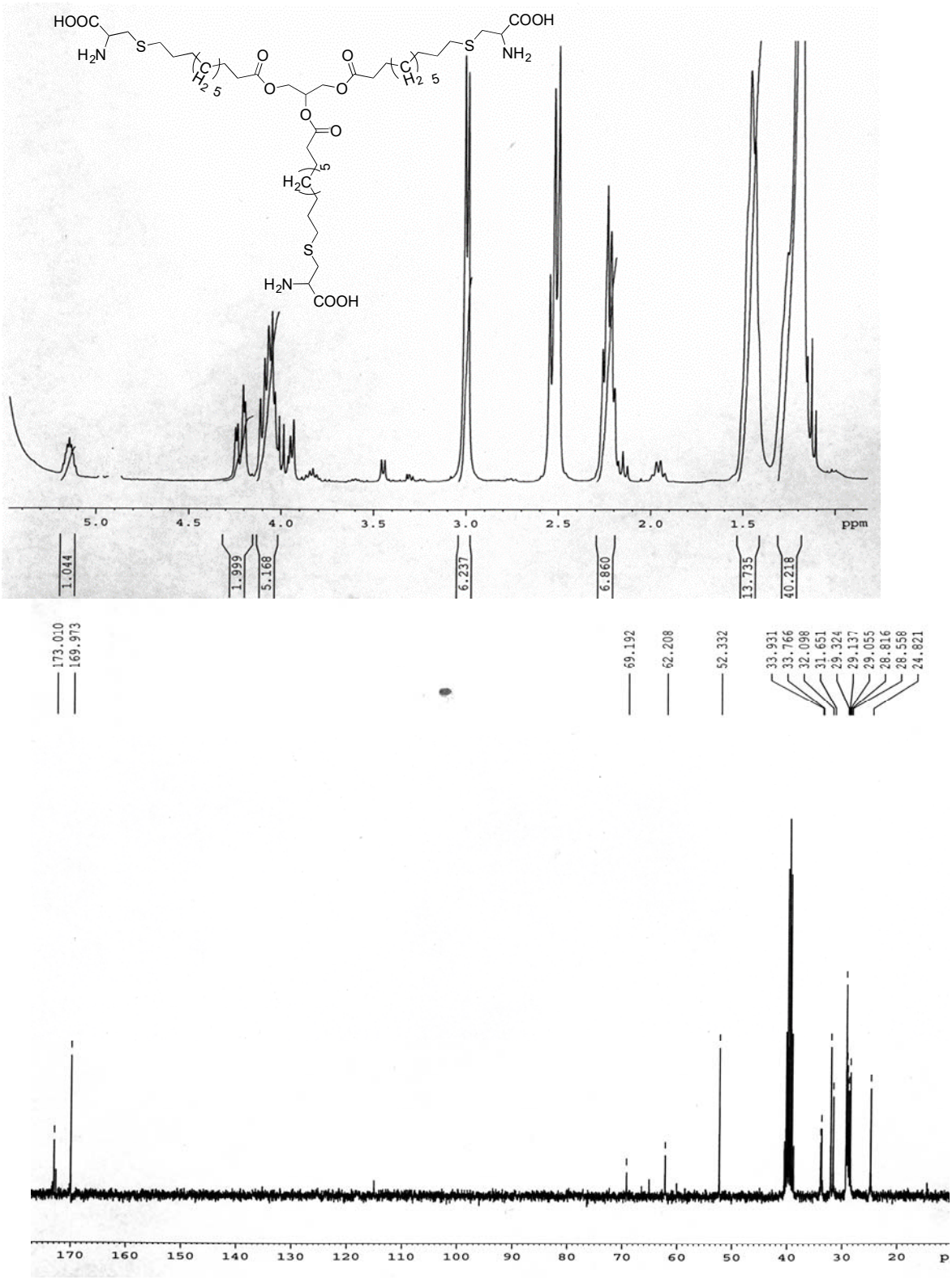

Figure C.7 ^{1}H NMR (300 MHz, DMSO-d$_6$) and ^{13}C NMR (75 MHz, DMSO-d$_6$) spectra of compound **Cys5.**

Figure C.8 IR spectra of compounds **Cys5** (top) and **Cys6** (bottom).

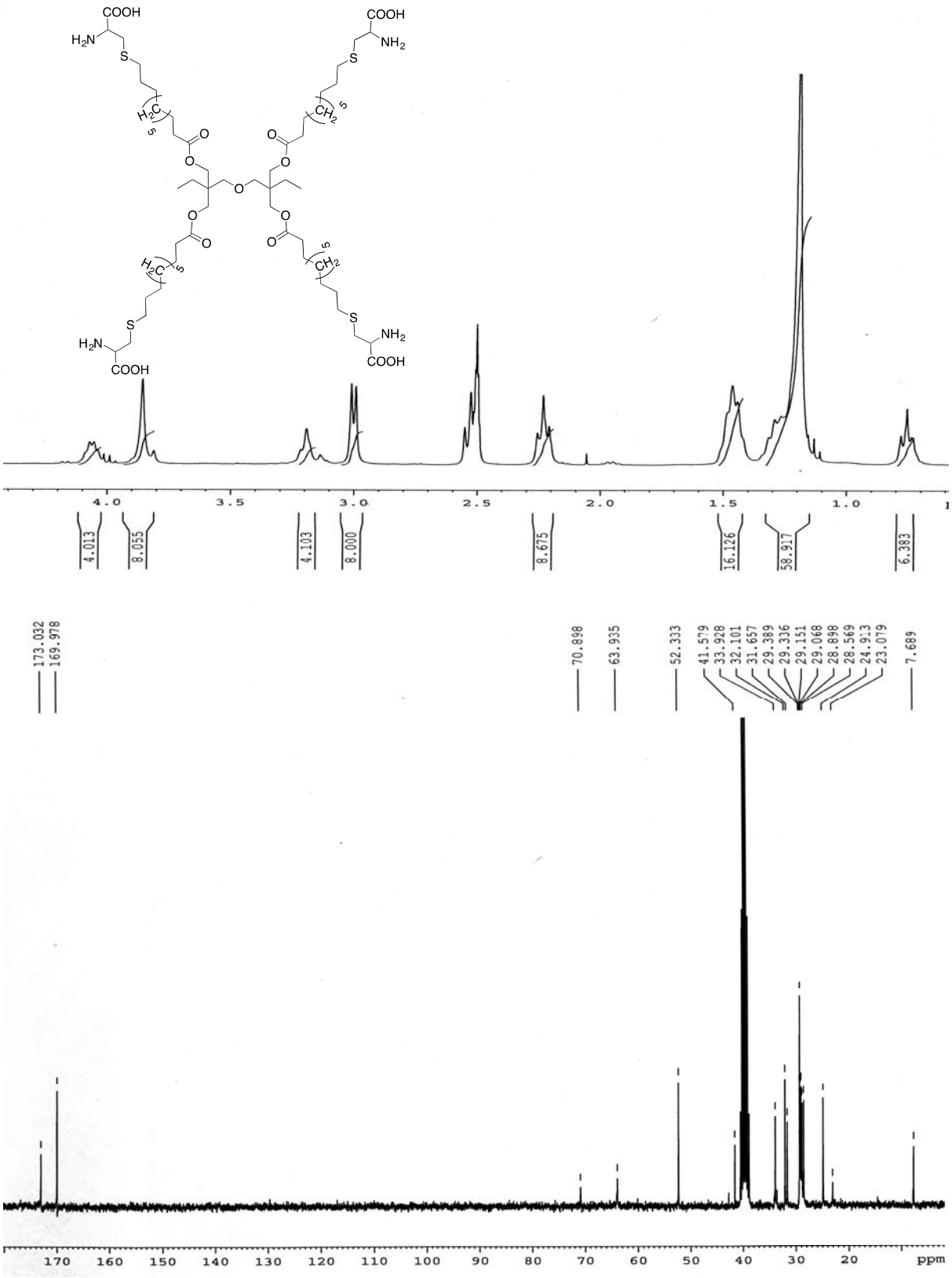

Figure C.9 ^{1}H NMR (300 MHz, DMSO-d$_6$) and ^{13}C NMR (75 MHz, DMSO-d$_6$) spectra of **Cys6.**

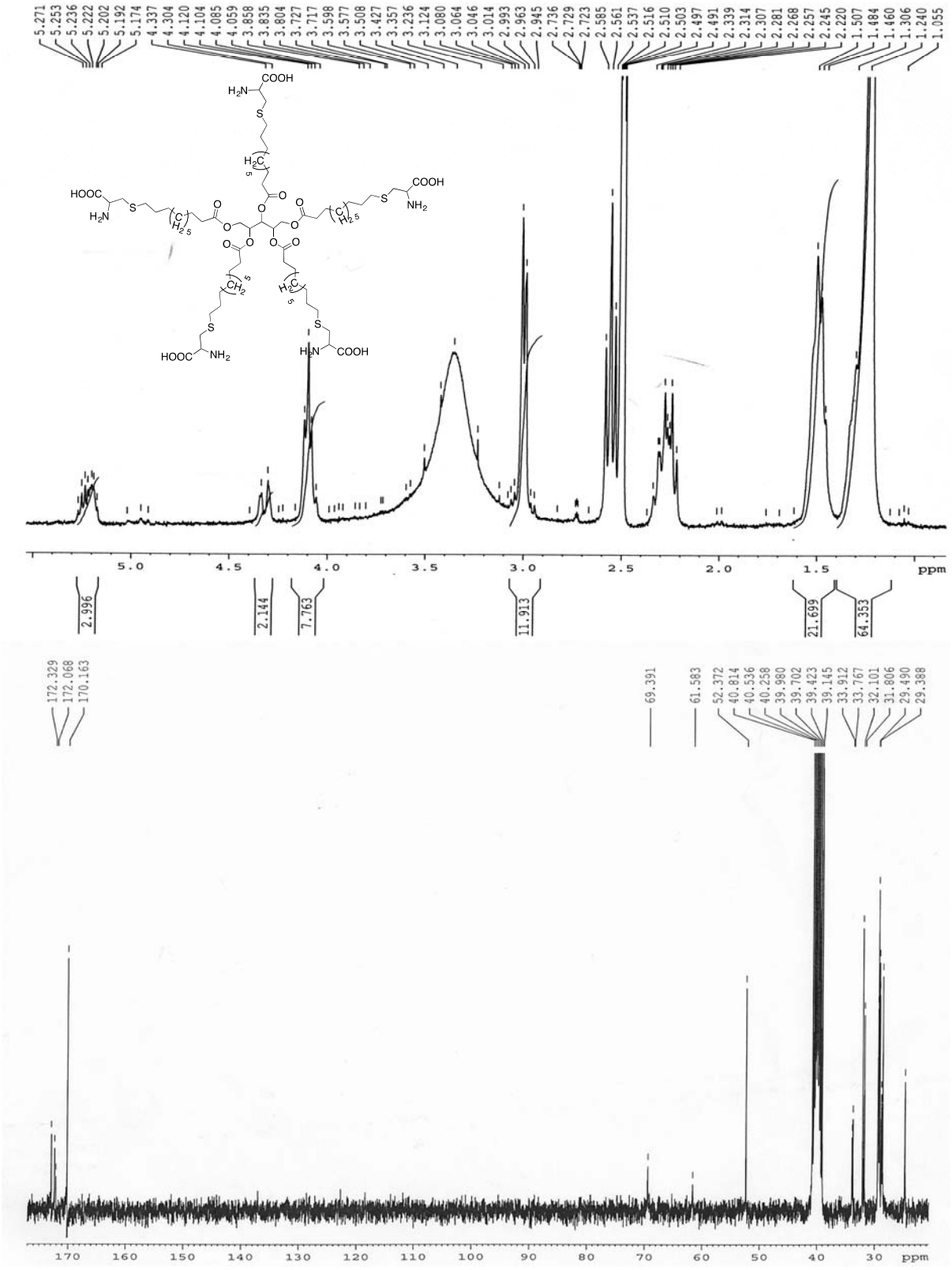

Figure C.10 ^{1}H NMR (300 MHz, DMSO-d_6) and ^{13}C NMR (75 MHz, DMSO-d_6) spectra of **Cys7.**

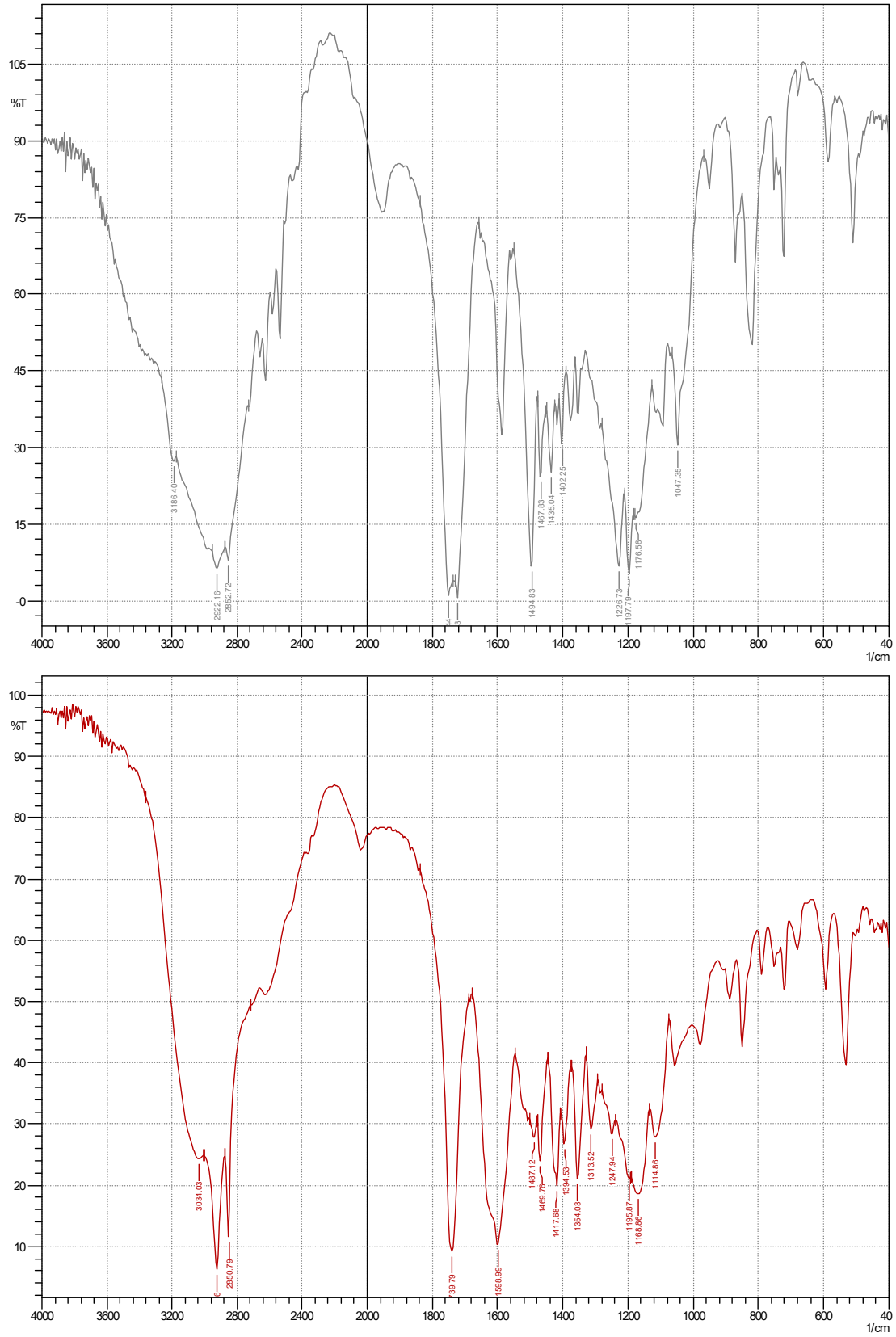

Figure C.11 IR spectra of Cys**7** (top) and **Cys8** (bottom).

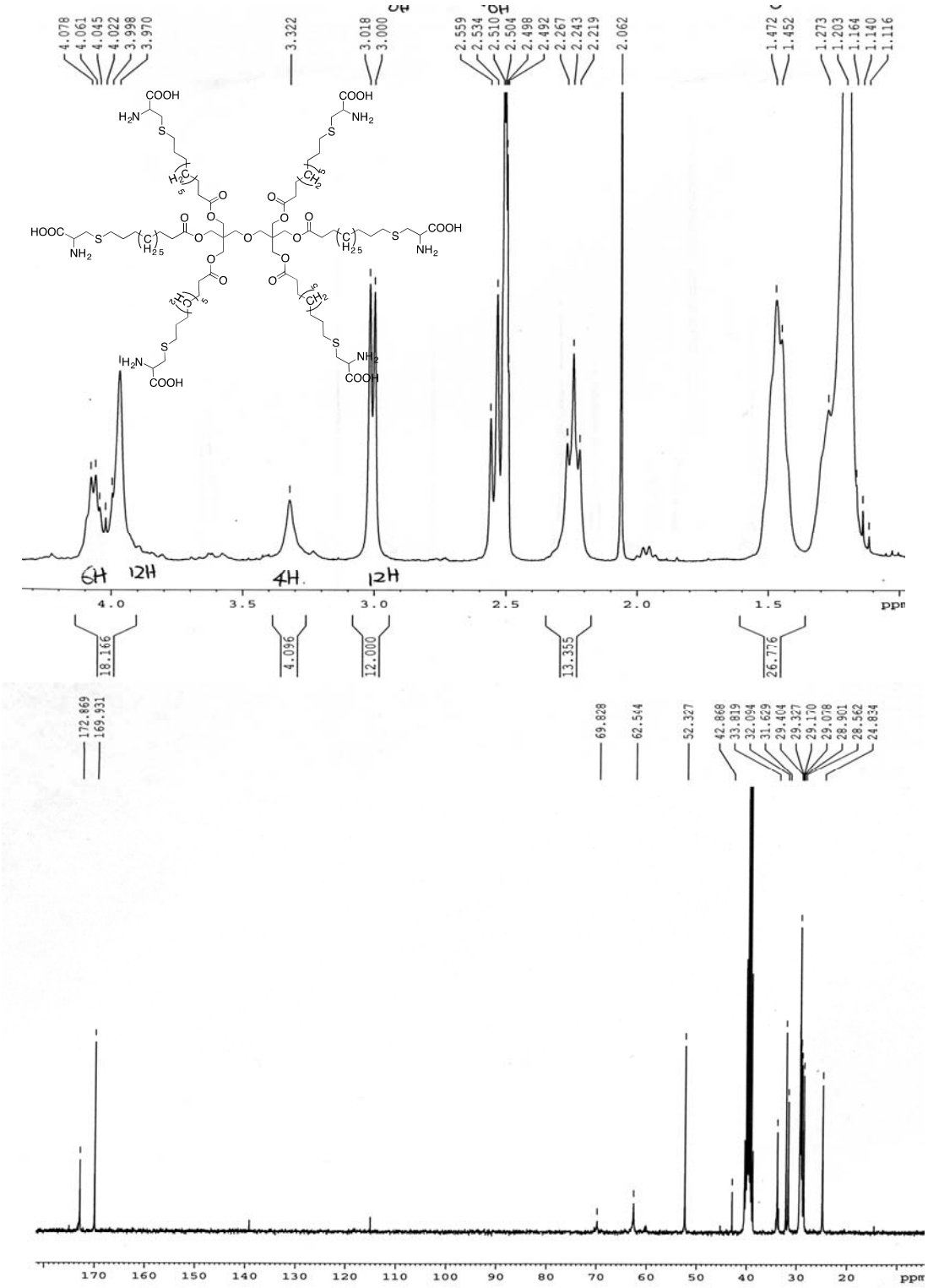

Figure C.12 ^{1}H NMR (300 MHz, DMSO-d_6) and ^{13}C NMR (75 MHz, DMSO-d_6) spectra of compound **Cys8.**

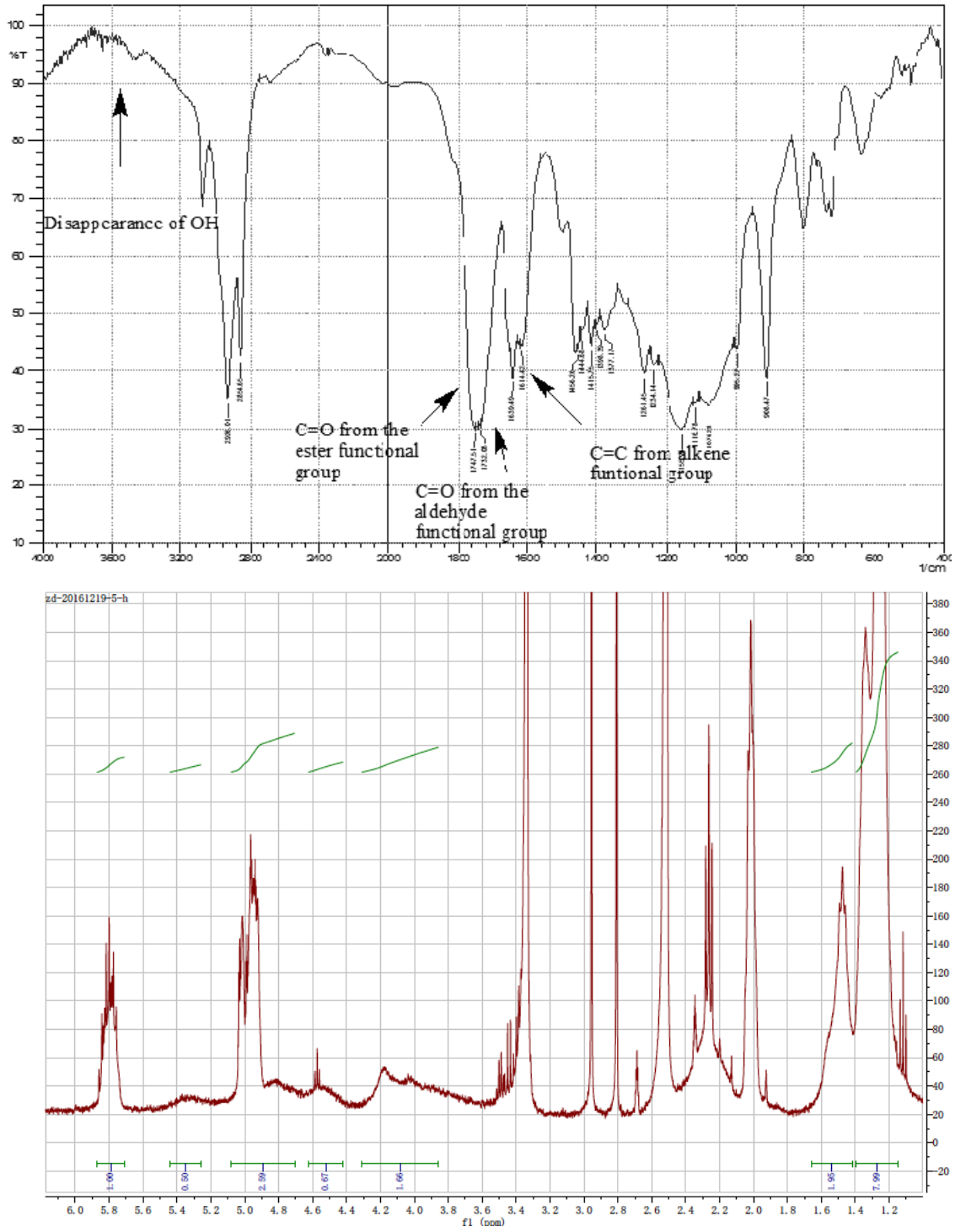

Figure C.13 IR and ^{1}H NMR (300 MHz, DMSO-d$_6$) spectra of compound **1v.**

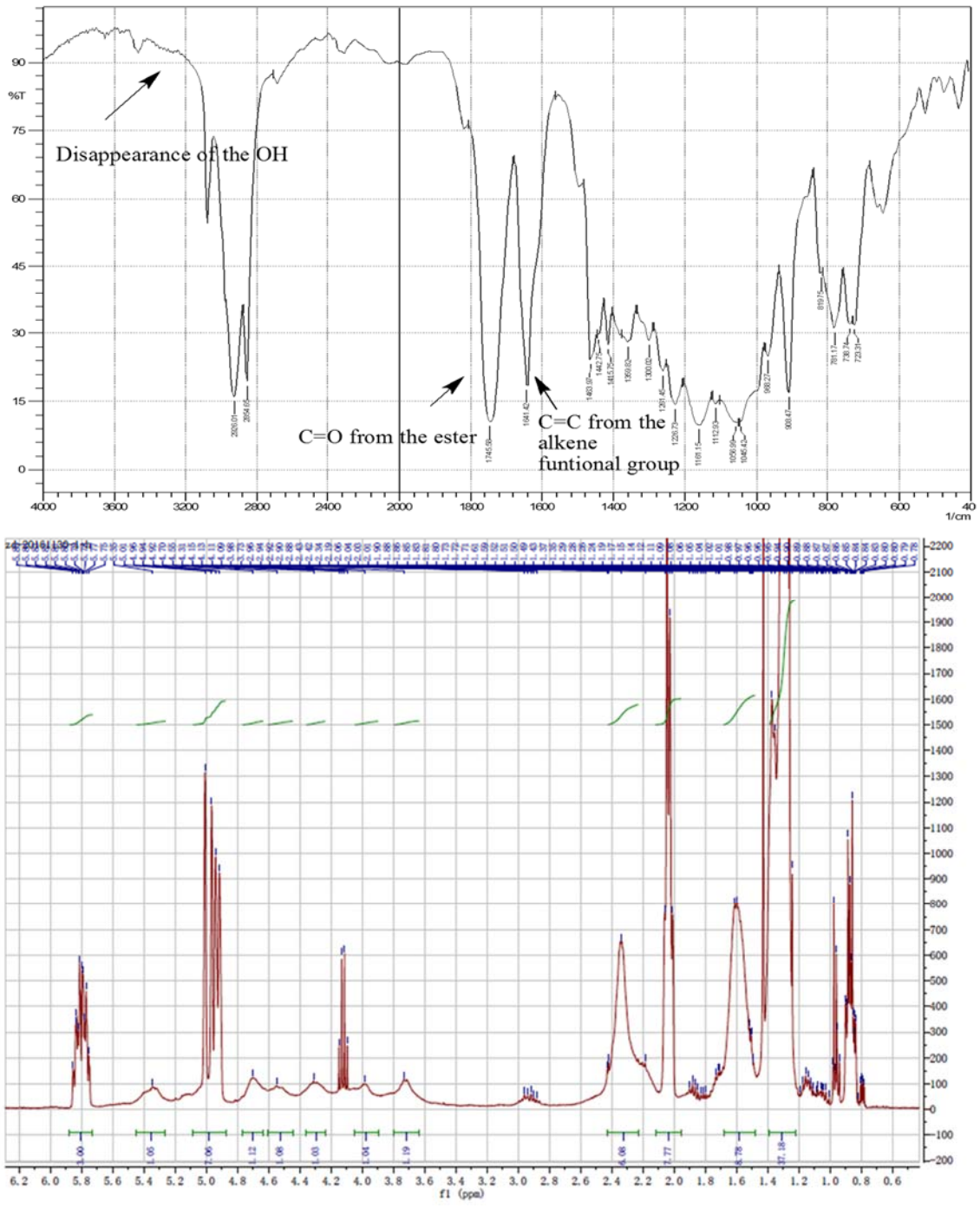

Figure C.14 IR and ^{1}H NMR (300 MHz, DMSO-d_6) spectra of compound **1w.**

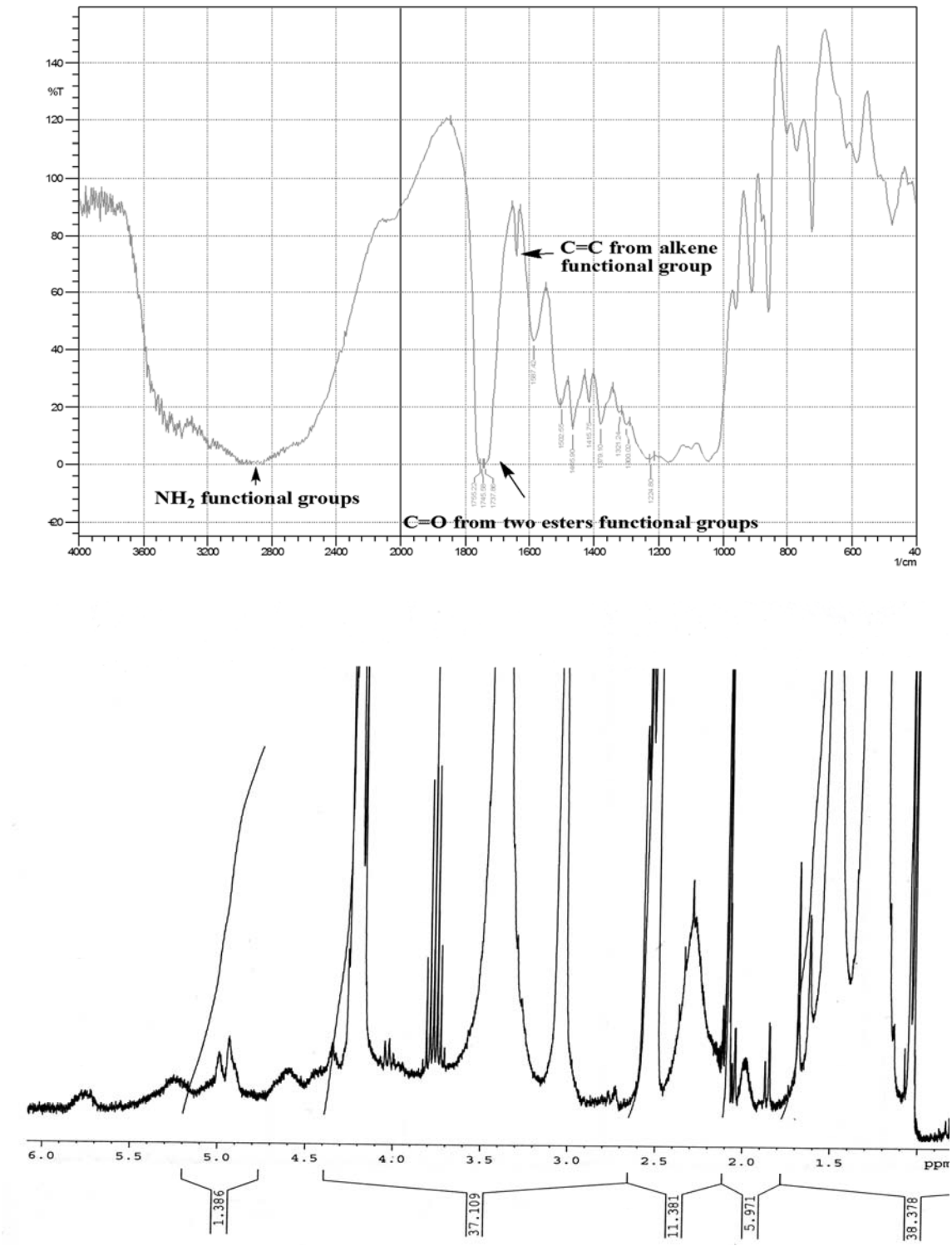

Figure C.15 IR and ^{1}H NMR (300 MHz, DMSO-d_6) spectra of compound **1x.**

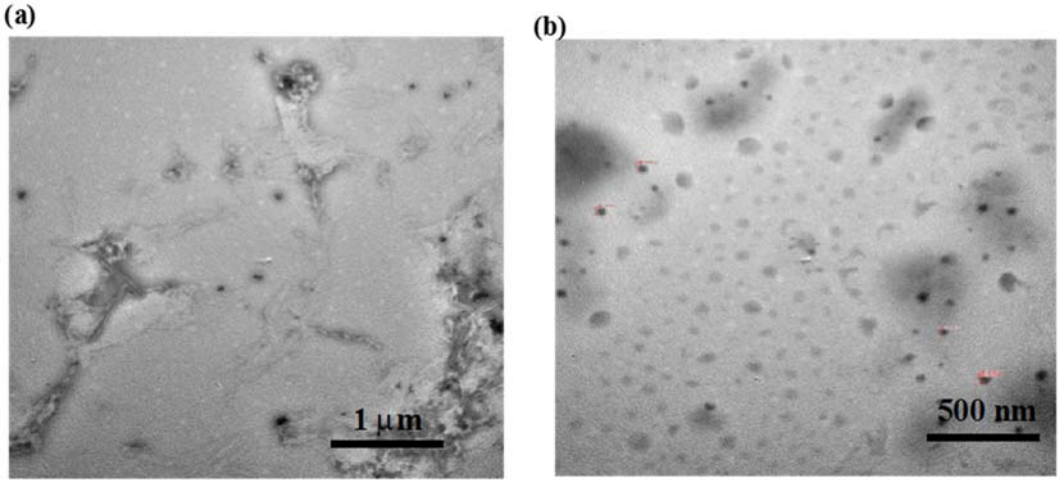

Figure C.16 TEM images of **Cys1** at CAC.

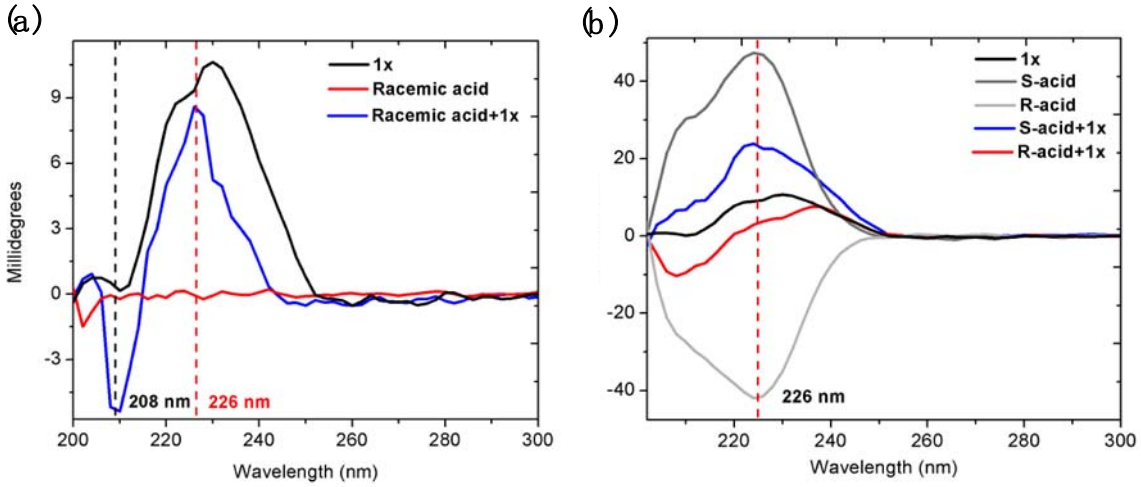

Figure C.17 CD spectra of polyamine **1x** with (a) racemic mandelic acid, (b) mandelic acid enantiomers.